

INVERSE METHODS TO ESTIMATE ANTHOCYANIN DEGRADATION KINETIC
PARAMETERS IN CHERRY POMACE DURING NON-ISOTHERMAL HEATING

By

Ibrahim Greiby

A DISSERTATION

Submitted to
Michigan State University
in partial fulfillment of the requirements
for the degree of

Biosystems Engineering - Doctor of Philosophy

2013

ABSTRACT

INVERSE METHODS TO ESTIMATE ANTHOCYANIN DEGRADATION KINETIC PARAMETERS IN CHERRY POMACE DURING NON-ISOTHERMAL HEATING

By

Ibrahim Greiby

Fruit and vegetables are a rich source of many bio-active compounds from which value-added nutraceuticals can be produced. Anthocyanins (ACY), which are unstable at high temperature ($> 70^{\circ}\text{C}$), are the most abundant flavonoid compound and are used as a natural colorant. ACY have health benefits and can be sourced from inexpensive byproducts, such as cherry pomace. The most common method of using the byproduct is to add it as an ingredient to foods that are thermally processed. To design these processes, the kinetics of ACY degradation must be known as a function of time, temperature, and moisture content. Therefore, the purpose of this work was to estimate color kinetic parameters, and anthocyanin degradation parameters in cherry pomace at different constant moisture contents. To do this, the thermal properties of the pomace had to be estimated first.

The moisture content was kept constant by sealing the cherry pomace in cans. The retention of ACY in the pomace was investigated during heating at two retort temperatures 105 and 126.7°C . Tart cherry pomace was equilibrated to other lower moisture contents (MC) and heated in sealed 54×73 mm cans for different times. ACY retention of 70 MC wet basis (wb) cherry pomace decreased with heating time and ranged from 76 to 10% for 25 and 90 min heating, respectively at 126.7°C , and ranged from 60 to 40 % for 100 and 125 min heating, respectively at 105°C . The total color difference (ΔE) increased with increasing heating time, whereas Browning Index (BI)

exhibited an inverse trend. Correlation between ACY and red color showed a linear relationship at higher moisture content (70 MC, wb) of cherry pomace. Oxygen radical absorbance capacity (ORAC) method showed stability during heating at different times. Differential scanning calorimetry (DSC) was used to measure the specific heat. At °C 25, the measured specific heat was 1671, 2111 and 2943 J kg⁻¹ K⁻¹ for 25, 41 and 70 MC (wb), respectively. Ordinary least squares and sequential estimation methods were used to estimate the thermal and kinetic parameters. Thermal conductivity (W m⁻¹ K⁻¹) was estimated as a linear function of temperature at 25°C (k₁) and 125°C (k₂). The estimated k₁ and k₂ values and standard errors for 70, 41 and 25% MC (wb) were 0.49 +/- 0.00047 and 0.55 +/- 0.00058, 0.20 +/- 0.0015 and 0.39 +/- 0.0012, and 0.15 +/- 0.0034 and 0.28 +/- 0.0037 (W m⁻¹ K⁻¹), respectively. The rate constant and activation energy for 70% MC pomace were estimated as k_{115.8 °C} = 0.0129 ± 0.0013 min⁻¹ and 75.7 ± 10.7 kJ/mol, respectively. The model fit well as shown by a RMSE of approximately 9% of initial ACY concentration (about 65 mg/kg db) and relative error less than 24% for the three MCs.

There was no significant effect of moisture content on the reaction rate constant. Empirical correlations for ACY degradation with red color, thermal properties and kinetic parameters were established. These results can be useful for processors desiring to use cherry pomace to make value-added by-products at elevated temperatures. Examples include extruded snacks and breakfast cereals, dried and powdered products such as drink mixes, and baked goods such as breads, confectionaries, and candies. These products are all heated at temperatures above 100°C, where ACY degrade.

DEDICATION

I dedicate this work to my father, Greiby Emhemed (May Allah have mercy on him), to my mother, Aisha Abdu-Allah (May Allah give here a long life) for their love, support, and prayers.

ACKNOWLEDGEMENTS

(الشكر والتقدير)

بسم الله الرحمن الرحيم (In the name of Allah, the Most Gracious, the Most Merciful)

My deep appreciation and heartfelt gratitude to my advisor, Dr. Kirk D. Dolan, for the patience, guidance, knowledge and mentorship he provided to me throughout my Ph.D. program. His consistent support and encouragement made my degree completion possible. I would also like to thank my committee members, Dr. James Steffe, Dr. Bradley Marks and Dr. Maurice Bennink for the friendly guidance, helpful suggestions, and the general collegiality that each of them offered to me.

I sincerely thank Dr. Neil Wright, Department of Mechanical Engineering, for allowing me to work in his lab for specific heat measurements needed for my research. My great thanks to Dr. James Beck, Department of Mechanical Engineering, for all the time he gave me for data analysis by teaching the use of his software (Prop1D). My high appreciation goes to Dr. Muhammad Siddiq, Department of Food Science, for all his guidance in chemical analyses, color measurements and scientific writing.

In a similar vein, I'd like to recognize: Mr. Steve Marquie for all his great help regarding establishing all software for data collection; Mr. Phill Hill, for his help with maintaining the steam retort, other equipment, and thermocouples modification.

My special thanks go to my friends and lab mates: Dharmendra Mishra, for all his help and guidance for MATLAB coding; Dr. Rabiha Sulaiman, for her support and care all the time, who is now a faculty in University Putra Malaysia, she is the one who helped and persuaded me to come to MSU in the first place. My best wishes and thanks to all my friends: Shantanu Kelkar, Sunisa Roidoung, Ahmad Rady, Hayati Samsudin, George Nyombaire, and Muhammad Eldosari for their support and camaraderie.

Special thanks to my lovely country (Libya) for the scholarship and my liability to be back and work hard to help building the country as free and progressive country.

My appreciation and thanks goes to all staff in Department of Biosystems & Agricultural Engineering, Department of Food Science & Human Nutrition, Graduate School and OISS for their support and resources during a hard time.

Last but not least, my sincere appreciation is due to my wife for the parenting (sons, Asem & Ala, and daughter, Farah) and the bearing of household burdens while I pursued my degree. Without her support and caring this work would not have been possible. To my brothers and sisters for their care, support and encouragement.

TABLE OF CONTENTS

LIST OF TABLES.....	x
LIST OF FIGURES.....	xii
KEY TO SYMBOLS.....	xvi
CHAPTER 1	1
INTRODUCTION.....	1
1.1 Overview of the Dissertation	2
1.2 Statement of the Problem.....	4
1.3 Significance of the Study.....	6
1.4 Objective of the Study	6
CHAPTER 2	8
LITERATURE REVIEW.....	8
2.1 Heat transfer theory	9
2.2 Cylindrical coordinates:	10
2.3 Heat transfer boundary conditions:	11
2.3.1 Convection heat transfer function of time:	11
2.3.2 Surface temperature as function of time (T_s) :.....	13
2.4 Thermal conductivity k (T) (linear with T):	14
2.4.1 Thermal properties of foods:	15
2.4.2 Isothermal and non-isothermal Processing	19
2.5 Cherry Pomace’s Anthocyanins	22
2.5.1 Cherry pomace.....	22
2.5.2 Anthocyanins in Nature	23
2.5.3 Structure of Anthocyanins:	23
2.5.4 Stability of Anthocyanins	24
2.5.4.1 Effect of pH on ACY Stability	25
2.5.4.2 Effect of Temperature on Anthocyanins Stability	26
2.5.5 Anthocyanins Antioxidant Capacity	28
2.6 Kinetics And Mechanism of Degradation of Anthocyanins In Foods	30
2.6.1 Kinetics Mechanism:	30
2.6.2 Anthocyanins Degradation Model:	32
REFERENCES.....	35
CHAPTER 3	45
OBJECTIVE ONE.....	45
Effect of Non-Isothermal Heat Processing and Moisture Content on the Anthocyanin Degradation and Color Kinetics of Cherry Pomace.....	45
Abstract.....	46
3.1 Introduction	47
3.2 Materials and Methods	49

3.2.1 Pomace sample preparation	49
3.2.2 Measurement of visual color	50
3.2.3 Anthocyanins extraction	51
3.2.4 Monomeric anthocyanin content determination	52
3.2.5 Antioxidant Capacity	52
3.2.6 Color kinetics.....	53
3.3 Results and Discussion	54
3.3.1 Anthocyanin (ACY) degradation.....	54
3.3.2 Antioxidant Capacity	55
3.3.3 Instrumental Color Changes.....	56
3.4 Kinetics of color degradation	59
3.5 Correlation between red color and anthocyanins	62
3.6 Conclusions.....	64
APPENDICES	65
Appendix A.1 Experimental design and preliminary data	66
Appendix A.2 Oxygen Radical Absorbance Capacity (ORAC) Fluorescein Method	74
REFERENCES.....	76
CHAPTER 4	80
OBJECTIVE TWO.....	80
Estimation of Temperature-Dependent Thermal Properties of Cherry Pomace at Different Moisture Contents During Non-Isothermal Heating	80
Abstract.....	81
4.1 Introduction	82
4.2. Materials and methods	85
4.2.1 Sample preparation.....	85
4.2.2 Measurement of bulk density and specific heat.....	86
4.2.3 Thermal Processing	88
4.2.3.1 Heat Transfer and governing equations	88
4.2.4 Experimental design.....	89
4.2.5 Thermal parameter estimation	91
4.2.5.1 Sensitivity Coefficients.....	91
4.2.5.2 Ordinary Least Squares (OLS) Procedure.....	92
4.2.5.3 Sequential Estimation Procedure	93
4.3 Results and discussion.....	94
4.3.1 Bulk density and Specific heat determination results:	94
4.3.2 Thermal Parameter Estimation Using Ordinary Least Squares.....	97
4.3.3 Thermal Parameter Estimation Using the Sequential Procedure	100
4.4 Model validation	104
4.5 Conclusions.....	106
APPENDICES	107
Appendix B.1 Experimental design and preliminary data	108
Appendix B.2 Thermal properties determination (DSC)	115
Appendix B.3 MATLAB syntax	120
B.3.1 Script file for nlinfit method.....	120

B.3.2 Function file (center can temperature prediction by Comsol).....	123
B.3.3 Script file for sequential parameter estimation method	128
REFERENCES.....	132
CHAPTER 5	137
OBJECTIVE THREE	137
Inverse Methods to Estimate Anthocyanin Degradation Kinetic Parameters in Cherry Pomace During Non-Isothermal Heating.....	137
Abstract.....	138
5.1 Introduction	139
5.2 Materials and Methods	141
5.2.1 Pomace sample preparation	141
5.2.2 Anthocyanins extraction	143
5.2.3 Monomeric anthocyanin content determination	144
5.2.4 Mathematical Modeling	144
5.2.4.1 Estimation the kinetic parameters.....	144
5.2.4.2 Arrhenius Reference Temperature	148
5.2.4.3 Moisture content Constant.....	148
5.2.5 Parameter Estimation Techniques	149
5.2.5.1 Sensitivity Coefficient Plot	149
5.2.5.2 Ordinary Least Squares (OLS) Estimation Procedure	150
5.2.5.3 Sequential Estimation Procedure	150
5.3 Results and discussion.....	152
5.3.1 Anthocyanin (ACY) degradation.....	152
5.3.2 Reference Temperature Plot.....	154
5.3.3 Scaled Sensitivity Coefficient Plot	155
5.3.4 Parameter Estimation using Ordinary Least Squares	156
5.3.4.1 Moisture content constant estimation	163
5.3.5 Sequential Parameter Estimation.....	163
5.4 Conclusions.....	165
APPENDICES	166
Appendix C.1 Experimental design and preliminary data.....	167
Appendix C.2 Predicted Temperatures data by Comsol software	172
Appendix C.3 MATLAB syntaxes	188
C.3.1 Script file for reference temperature determination.....	188
C.3.2 Function file-1 and 2	188
C.3.3 Script file scaled sensitivity coefficients	191
C.3.4 Script file for nlinfit method	193
C.3.5 Script file for sequential parameter estimation method	197
REFERENCES.....	204
CHAPTER 6	209
Overall Conclusions and Recommendations.....	209
6.1 Summary and Conclusions	210
6.2 Recommendations for Future Research.....	212

LIST OF TABLES

Table 2.1 Six Common Anthocyanidins.....	24
Table 3.1 Hunter color <i>L</i> , <i>a</i> , <i>b</i> values, hue angle and chroma of cherry pomace after heat treatment at 126.7 °C.....	58
Table 3.2 The estimated kinetic parameters and the statistical values of zero-order and first-order models for Hunter color <i>L</i> , <i>a</i> , <i>b</i> values and total color change (ΔE) for various processing times of cherry pomace at three moisture contents (wb) at 126.7 °C.....	61
Table 3.3 Coefficients of equations (3.7) and (3.8) for correlation between Hunter color <i>a</i> values and anthocyanins content	63
Table A.1 Cherry pomace 's anthocyanins concentration (mg/kg,db) after retorting process at different times	69
Table A.2 Raw data (sample) of retorting process of cherry pomace in a rotary steam retort at 126.7 °C	69
Table A.3 The average total antioxidant values of cherry pomace (treated 25%MC and untreated 70% MC,41%MC ,wb) retorted at 126.7 °C)(values for 5 replicates).....	75
Table 4.1 Thermal properties of cherry pomace at three moisture contents over temperature range 25-126.7 °C.....	97
Table 4.2 Estimation of thermal conductivity parameters for cherry pomace (90 min retorting) at T1=25 °C and T2= 125 °C.	98
Table 4.3 A comparative literature review of thermal conductivity values of some food products	102
Table 4.4: comparative of thermal conductivity values of Cherry pomace by this study with Choi and Okos empirical equations	103
Table 4.5 Estimation of thermal conductivity (k(t)) parameters for cherry pomace (90 min retorting): OLS vs.Prop1D method	105
Table B.1 Cherry pomace 's bulk density at different Moisture contents	109
Table B.2 Can Steel (202×214) exact diminutions & (Steel properties (Singh, 2001).	110
Table B.3 Example Specific heat's (Cp) Excel sheet calculation steps for 70% moisture content (wb) Cherry pomace using DSC method	116

Table B.4 Thermal properties estimation at two temperatures (25, 126) of cherry pomace $J\ kg^{-1}\ K^{-1}$	119
Table 5.1 Cherry pomace ACY concentration after retorting at two different temperatures for different times	153
Table 5.2 Kinetic parameter estimates of ACY degradation in cherry pomace at three constant moisture contents after retorting processing.....	157
Table 5.3 Summary of published kinetic parameters of anthocyanin degradation by thermal treatments	159
Table 5.4 Correlation matrices Table of the kinetics parameters of Eq.(5.11).....	160
Table C.1 Absorbance versus Retorting time of Cherry pomace ACY's extractions at three constant moisture content heated at $126.7^{\circ}C$	169
Table C.2 Cherry pomace's ACY concentration after retorting at two different temperatures for different times	170
Table C.3 Part of predicted temperatures ($^{\circ}C$) data at 15 gauss points (Pts) in the can for Cherry pomace (70% MC, wb) at $126.7^{\circ}C$ Retort Temperature).....	172
Table C.4 Part of predicted temperatures ($^{\circ}C$) data at 15 gauss points (Pts) in the can for Cherry pomace (70% MC, wb) ($105^{\circ}C$ Retort Temp).....	178

LIST OF FIGURES

Figure 1.1 Flow chart of experimental plan of cherry pomace retorting and estimation of kinetic parameters of anthocyanin degradation under the process.....	5
Figure 2.1 Cylindrical coordinates heat transfer by conduction	10
Figure 2.2 Anthocyanin ground structure, flavylium (2-phenylchromenylium)	24
Figure 2.3 pH equilibrium forms of anthocyanins	26
Figure 2.4 Formation of radicals through the addition of AAPH	29
Figure 2.5 Possible thermal degradation mechanism of two common ACYs	31
Figure 3.1 Can-center temperature profile of cherry pomace in a rotary steam retort at 126.7 °C for 40 min after 8 min come-up-time. (RT=Retort temperature; MC-70, MC-41, and MC-25 represent cherry pomace with 70, 41, and 25% moisture (wet basis) , respectively).	50
Figure 3.2 Degradation of cherry pomace anthocyanin (ACY) after non-isothermal treatment in a retort at 126.7 °C. (MC-70, MC-41, and MC-25 represent cherry pomace with 70, 41, and 25% moisture (wb), respectively)	55
Figure 3.3 The average total antioxidant values of the cherry pomace (70 and 41%MC not heated) and 25% MC (wb) after different heating times	56
Figure 3.4 Total color difference (ΔE) and browning index (BI) of cherry pomace after retorting at 126.7 °C. (MC-70, MC-41, and MC-25 represent the moisture content % (wb), respectively). Means with different letters (a–c) at one heating time and (A–D) at different heating times, are significantly different ($p \leq 0.05$).....	59
Figure 3.5 Correlation between Hunter color <i>a</i> values and anthocyanins content of cherry pomace after thermal processing at 126.7 °C. Data three replicate. (MC-70, MC-41, and MC-25 represent cherry pomace with 70, 41, and 25% moisture (wb), respectively)	63
Figure A.1 Process experimental design for ACY and pomace’s color degradation	66
Figure A.2 Plots of retorting process of cherry pomace in a rotary steam retort at 126.7 °C for 25, 40, 60 and 90 min after 10 min come-up-time. (Rt=Retort temperature; MC-70, MC-41, and MC-25 represent cherry pomace with 70, 41, and 25% moisture (wb) , respectively).	67

Figure A.3 Typical Antioxidant Standard Curve (Trolox calibration curve) for ORAC value estimation	74
Figure A.4 Diagram of Antioxidant activity determination expressed as the net area under the curve (AUC). (http://www.biotek.com , accessed on Feb 2013).....	74
Figure 4.1 Geometry diagram (by Comsol) of the can with thermocouples, Left: surface TC taped on the can. Right: cutaway schematic of half-can sliced axially	86
Figure 4.2 Thermal curves from specific heat estimation using DSC method (MC-70) :.....	87
Figure 4.3 Meshing and center temperature profile by Comsol software. “The text in this figure is not meant to be readable but is for visual reference only”.....	89
Figure 4.4 Experimental design of retorting the cherry pomace (three constant moisture content, wb).....	90
Figure 4.5 Temperature profiles for center of cherry pomace at three constant moisture content (wb), for surface temperature of the can, and steam temperature in a steam retort at 126.7 °C for 90 min.	91
Figure 4.6 Specific heat of cherry pomace at three moisture contents (wb)	95
Figure 4.7 Scaled sensitivity coefficients of thermal conductivity of cherry pomace (70% MC,wb) during 90 min of retorting.....	98
Figure 4.8 Time-temperature plot of observed and predicted center temperature of the cans of cherry pomace (70%MC) heated at 126.7°C for 90 min	99
Figure 4.9 Residual plot of Predicted Temperature at the center of two cans of cherry pomace (70%MC) heated at for 90 min.....	100
Figure 4.10 Sequential estimation of thermal conductivity (k_1) =0.489 (W/m °C) of Cherry pomace (70% MC, wb) at 90 min of retorting. T_1 =25 °C.	101
Figure 4.11 Sequential estimation of thermal conductivity (k_2) =0.581 (W/m °C) of Cherry pomace (70% MC, wb) at 90 min of retorting. T_2 =125 °C	101
Figure 4.12 Temperature vs. time profile at three location of cherry pomace (70%, wb) in the steel can after retorting at 126.7°C for about 20 min)	105
Figure B.1 Process experimental design for thermal properties estimation.....	108
Figure B.2 Cherry pomace ‘s Bulk density at different Moisture contents	110

Figure B.3 Gen5 Software view for temperature vs time data collection during retorting. “The text in this figure is not meant to be readable but is for visual reference only”	111
Figure B.4 Images of Comsol simulation Steps of Can Heating. “The text in this figure is not meant to be readable but is for visual reference only”	112
Figure B.5 Steps Cherry pomace’s thermal properties measurement using DSC. “The text on the images is not meant to be readable but is for visual reference only”	115
Figure B.6 Sapphire Specific heat capacity	115
Figure 5.1 Can-center temperature profile of cherry pomace in a rotary steam retort at 126.7 °C for 90 min after 10 min come-up-time. (Rt=Retort temperature; MC-70, MC-41, and MC-25 represent cherry pomace with 70, 41, and 25% moisture (wb), respectively)	143
Figure 5.2 Location of the 15 Gauss-Legendre points in the half-can based on axisymmetric heating	145
Figure 5.3 Correlation coefficient of parameters kr and E_a as a function of the reference temperature Tr (for ACY degradation under retorting process)	154
Figure 5.4 Scaled sensitivity coefficient plots of the three parameters at retort temperatures 105°C and 127°C, using initial parameter values of $E_a = 45\text{kJ/mol}$,	156
Figure 5.5 Plot of observed and predicted with confidence intervals of ACY values in cherry pomace (MC-70, wb) after retorting at 126.7°C and 105°C for different times. Prediction bands for 105°C are not shown, for clarity	161
Figure 5.6 Residual scatter plot of mass average of ACY in cherry pomace (MC-70) heated at retort temperatures(126.7°C &105°C)	162
Figure 5.7 Plots of frequency versus difference between observed and predicted ACY in cherry pomace (MC-70)	162
Figure 5.8 Sequentially estimated parameter of activation energy (E_a)	164
Figure 5.9 Sequentially estimated parameter of reaction rate ($kr_{115.8^\circ\text{C}}$) (min^{-1})	164
Figure 5.10 Sequentially estimated parameter of Initial concentration (C_0)	165
Figure C.1 Process experimental design for kinetic parameter estimation	167
Figure C.2 Can-center temperature profile of cherry pomace in a retort at 105 °C for 100 min (A) and 125 min (B) (TRt=Retort temperature, Ts= can surface	

temperature; 70%, 41%, and 25% MC represent the pomace with 70, 41, and 25% moisture (wb), respectively).	168
Figure C.3 Absorbance versus Retorting time of Cherry pomace ACY's extractions at three constant moisture content (wb) heated at 126.7°C	169
Figure C.4 Slope method for estimate the moisture constant (b) for the retorted cherry pomace samples ACY concentration	170
Figure C.5 Plot of gauss points in the can with cherry pomace 70% MC (wb), predicted by Comsol. "The text in this figure is not meant to be readable but is for visual reference only"	171

KEY TO SYMBOLS

Letters:

- b Moisture Parameter(MC^{-1})
- C_0 Initial Anthocyanins (ACY) concentration, dry basis, (mg/kg)
- $C(t)$ anthocyanins concentration at time, min, (mg/kg)
- C_p specific heat (J/kg.K)
- C_{p_s} specific heat of sample ($J g^{-1} \text{ } ^\circ C^{-1}$)
- $C_{p_{st}}$ sapphire's specific heat ($J g^{-1} \text{ } ^\circ C^{-1}$)
- \bar{c}_{obs} experimental estimated values of ACY (mg/kg)
- \bar{c}_{pred} predicted values of ACY (mg/kg) from eq. (2.39)
- d_c characteristic dimension (radius of the cylinder) for Fourier number.
- D diameter of the cylinder (m)
- E_a activation energy (J/mol)
- g acceleration of gravity (m/s^2)
- H length of the cylinder, m
- H_r heating rate (10 $^\circ C/min$)
- H_s heat flow of sample (mJ/s)
- H_{st} heat flow of Sapphire (mJ/s)
- $h(t)$ heat transfer coefficient as function of time ($W m^{-2} K^{-1}$)

h_{fg} latent heat of condensation in (J/kg) at $T_{\text{saturated}}$
 k thermal conductivity ($\text{W m}^{-1}\text{K}^{-1}$)
 k_r first-order degradation rate at reference temperature T_r (Min^{-1})
 $k(T)$ thermal conductivity Function of temperature ($\text{W m}^{-1}\text{K}^{-1}$)
 k_s calibration constant (dimensionless)
 k_1 thermal conductivity at T_1 ($\text{W m}^{-1}\text{K}^{-1}$)
 k_2 thermal conductivity at T_2 ($\text{W m}^{-1}\text{K}^{-1}$)
 MC Moisture content wet basis (decimal)
 MC_r Reference moisture content wet basis (decimal)
 n number of data
 p number of parameters
 r radial coordinate of the cylinder (m)
 R' radius of the cylinder (m)
 R Gas constant (3.418 J/mole K)
 t time, s
 t_x total process time (sec)
 t_f end of process time, (sec)
 T temperature of the sample as function of time ($^{\circ}\text{C}$)
 T_i initial temperature of the sample ($^{\circ}\text{C}$)
 T_1 particular value of T (low value $^{\circ}\text{C}$)

T₂ particular value of T (high value °C)

T_{obs} measured temperatures at can's center (°C)

T_{prd} predicted temperatures for the center of the can (°C)

T_r reference temperature (°K)

T_{Rt} retort temperature (°C)

T_s surface temperature on the can (°C)

W_{st} sapphire weight (mg)

W_s sample weight (mg)

x thickness (m)

X' scaled Sensitivity coefficient

z axial coordinate of the can (m)

Greek letters:

ρC_p Volumetric heat capacity (J/m³.K)

ρ Density (kg/m³)

ρ_l Density of liquid (kg/m³)

ρ_v Density of vapor (kg/m³)

μ viscosity of liquid (Pa.s)

ΔT is (T_{Rt} - T_s)

α Thermal diffusivity (m²/s)

Ø Angular geometry for the can

β parameter

Ψ(t) time-temperature history for Eq. (2.28)

Dimensionless groups:

Bi	Biot number	$\frac{h \times r}{k} =$	$\frac{\text{Internal diffusive resistance}}{\text{Surface Convective resistance}}$
Fo	Fourier number	$\frac{\alpha t}{d c^2} =$	$\frac{\text{Heat conduction}}{\text{Heat storage}}$
Nu	Nusselt number	$\frac{h D}{k_f} =$	$\frac{\text{Surface Convective resistance}}{\text{Convective resistance}}$
Pr	Prandtl number	$\frac{\mu C p}{k} = \frac{\mu}{\alpha \rho} =$	$\frac{\text{Viscous effect}}{\text{Thermal diffusion effect}}$
Re	Reynolds number	$\frac{\rho v D}{\mu} =$	$\frac{\text{Inertia force}}{\text{Viscous force}}$

CHAPTER 1
INTRODUCTION

1.1 Overview of the Dissertation

Anthocyanins (ACY) are the most abundant flavonoid constituents of fruits and vegetables. They are responsible for the wide array of colors present in flowers, petals, leaves, fruits and vegetables and are a sub-group within the flavonoids characterized by a C6-C3-C6-skeleton (Zhang et al., 2004). The red color of cherries is due to several water-soluble anthocyanin pigments. Pelargonidin, cyanidin, peonidin, delphinidin, petunidin, and malvidin are the six common anthocyanidins found in nature. These pigments are not very stable chemically and may degrade during thermal processing (>70°C) which can affect color quality and nutritional components. ACY have antioxidant effects, which play an important role in the prevention of neuronal and cardiovascular illnesses, cancer and diabetes, among others. There are several studies focusing on the effect of ACY in cancer treatments, human nutrition and its biological activity, (Bohm et al., 1998); Konczak and Zhang (2004); (Lule and Xia, 2005).

Thermal processing of foods involves heating to temperature from 50 to 150 °C. Anthocyanin stability is not only a function of final processing temperature but also of other properties (intrinsic) like pH, storage temperature, product moisture content, chemical structure of the ACY and their initial concentration, light, oxygen, presence of enzymes, proteins and metallic ions Patras et al. (2010). There are many studies examining these factors individually or a combination of one or more of them on degradation of food components. There is limited information available on the effect of high temperature processing at different moisture contents on the stability of these pigments in solid food products. Cherry pomace, left over after cherry juice processing, is a good source of ACY and hence can be used as an ingredient in the food industry.

The temperature history of most food products during processing is non-isothermal. However, kinetic parameters for liquid or high-moisture foods at temperatures below 100°C have typically been estimated using numerous isothermal experiments and two-step linear regression. Because such high-moisture products can usually approach the isothermal temperatures rapidly (< 1 min), with negligible temperature gradient, the kinetic results have been useful for predicting commercial processes.

For Low- or intermediate-moisture solid foods at temperatures > 100°C, the experimental procedure becomes technically difficult to perform, due to the following:

1. The sample container must be pressurized;
2. It becomes more difficult to attain isothermal conditions within a reasonable experimental time, because of the decreased thermal diffusivity;
3. Temperature gradients within the sample become significant;
4. Even if an isothermal temperature is eventually approximated, by that time, the nutrient degradation may be very large, rendering the experiment useless;
5. Non-isothermal estimated kinetic parameters may be significantly different from isothermal estimates. Examples include thermal denaturation $D_{71^\circ\text{C}}$ parameter for lactoperoxidase and the z value for beta-lactoglobulin (Claeys et al., 2001); rate constants and activation energies for zero- and first-order models for broccoli color, vitamin C content, and drip loss during frozen storage (Goncalves et al., 2011a); activation energies for fractional conversion models of pumpkin texture, color, and vitamin C during frozen storage (Goncalves et al., 2011b); and inactivation parameters D and z for *B. stearothermophilus* heated between 115 and 125°C (Periago et al., 1998).

To deal with the low moisture situation, non-isothermal experiments are recommended. The advantages include:

1. Difficulties # 2-5 above can be eliminated by using non-isothermal experiments and analysis.
2. Because the parameters can be estimated from a single set of non-isothermal experiments, the number of trials is significantly reduced compared to that for isothermal methods, thereby saving time, cost, and effort.
3. The sample size can be large (>50g), allowing more accuracy in the measured nutrient concentration;
4. The non-isothermal estimated parameters will be closer to those under actual commercial conditions, and will have significantly increased accuracy;

Anthocyanins (ACY) are routinely processed in low-moisture solid foods under high temperature and high pressure, such as in extruded foods, confectionaries, powders, and baked goods. To design, simulate, and optimize nutrient retention, the ACY degradation kinetics must be known. However, systematic methods to estimate the kinetic degradation parameters in these foods do not exist. Therefore, this research is focused on developing just such a method.

1.2 Statement of the Problem

The research was in two main parts. The sequences of the experimental and analysis steps are given below:

Collect time and temperature at center of the cans of cherry pomace at three constant moisture contents. ACY and color degradation measurements.

Estimate the cherry pomace specific heat at each MC by the DSC method as a function of temperature. Use MATLAB with Comsol for the experimental data in (step 1 & 2) to estimate the thermal conductivity (k_1 & k_2) at each MC at two arbitrary temperatures (T_1 & T_2). Use MATLAB with Comsol to estimate the kinetic degradation parameters for ACY degradation inside the sealed cans after non-isothermal heating at two different temperatures. Experimental steps were summarized in Figure 1.1

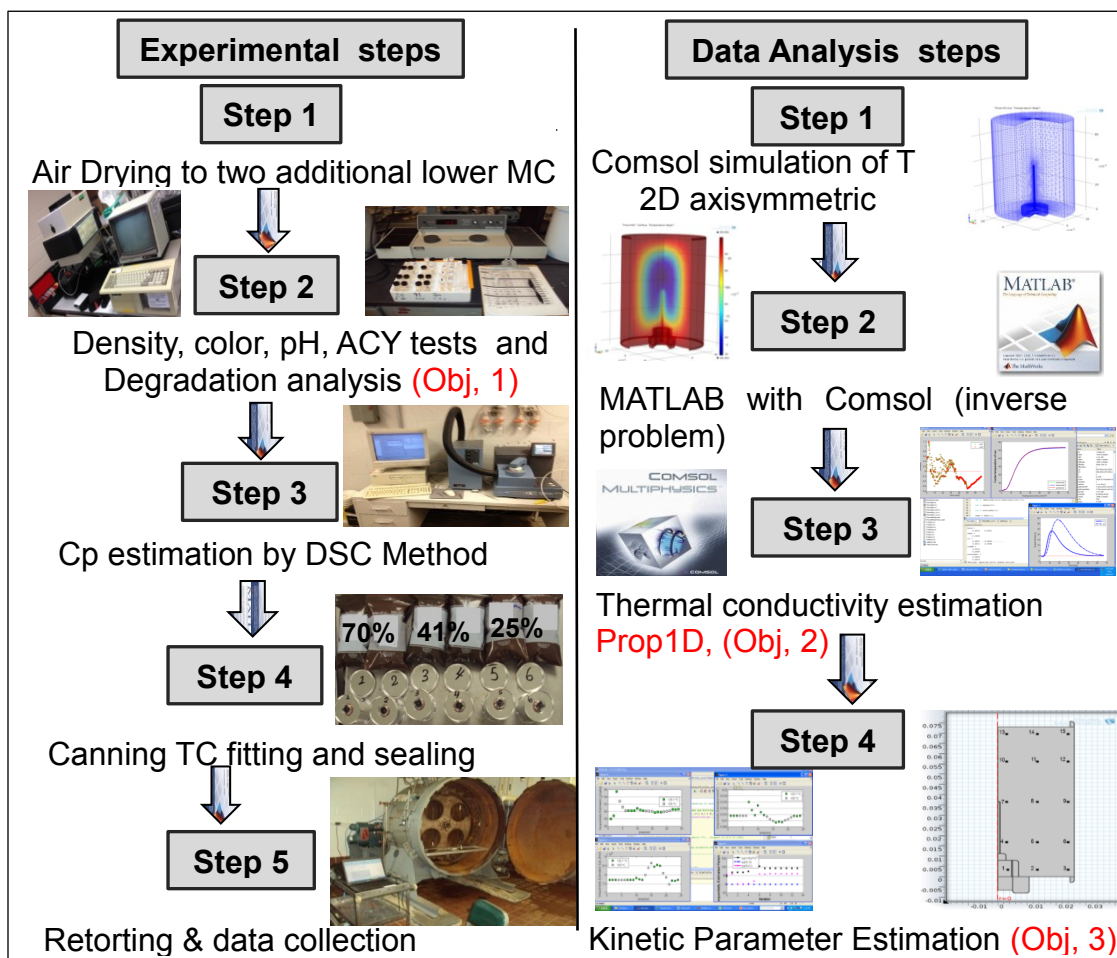


Figure 1.1 Flow chart of experimental plan of cherry pomace retorting and estimation of kinetic parameters of anthocyanin degradation under the process.

“For interpretation of the references to color in this and all other figures, the reader is referred to the electronic version of this dissertation.”

1.3 Significance of the Study

1. A new method to estimate non-isothermal parameters in solid foods during dynamic heating $> 100^{\circ}\text{C}$ was proposed and carried out.
2. Temperature-dependent thermal conductivity and specific heat of a solid food were estimated for a large temperature range, $25\text{-}130^{\circ}\text{C}$.
3. Estimation of kinetic parameters could be used, for example, to predict the anthocyanin retention during drying, where temperature is simultaneously increasing with decreasing moisture content.
4. This method may apply analogously to estimate microbial inactivation or growth parameters in low-moisture foods.

Processors want to dry fruit pomace rapidly but still maintain maximum nutraceutical content to make a high-value by-product ingredient such as anthocyanin-rich powder. ACY degrade more rapidly with temperature (T) and moisture content (MC). Knowledge of the rates of degradation of anthocyanin with T & MC will allow design of optimum drying processes, including tray drying, spray drying, drum drying, extrusion and other processes. The non-isothermal methods used in the study may serve as a standard for other researches studying drying at temperatures $> 100^{\circ}\text{C}$.

1.4 Objective of the Study

In this study, the effect of moisture content (MC) on degradation of ACY during non-isothermal processing of cherry pomace was determined. The specific objectives were to:

1. Determine the effect of non-isothermal heating and moisture content on the anthocyanin retention, color changes, color kinetics and the total antioxidant capacity of cherry pomace
2. To estimate the temperature-dependent thermal properties (specific heat and conductivity) of cherry pomace during non-isothermal heating at temperatures up to 130°C
3. To estimate the kinetic parameters of ACY degradation in cherry pomace for different constant moisture contents.

This dissertation is composed of various sections as follows :

Chapter 2 contains the literature review. The remaining chapters of the dissertation consist primarily of three journal articles: Chapter 3, 4, and 5, based on each objective studied, respectively. The final section of this dissertation (Chapter 6) gives the overall conclusions and recommendations from the research.

CHAPTER 2
LITERATURE REVIEW

2.1 Heat transfer theory

In this section the theory of heat transfer during the retorting process will be reviewed. The thermophysical parameters during heat conduction, heating or cooling have been estimated by different methods. The inverse method is one solution method (Bairi et al., 2007; da Silva et al., 2011; da Silva et al., 2010; Fernandes et al., 2010; Mariani et al., 2008; Mariani et al., 2009; Simpson and Cortes, 2004). Some researchers neglected the convective fluxes in thick creams and purees and used only conduction theory (Betta et al., 2009; Mariani et al., 2009). In our study, the following equations will be used to describe the heat transfer. The fundamental equation of conduction heat transfer in a solid is Fourier's equation (Bird et al., 1960; Datta, 2002a)

$$\rho C_p(T) \frac{\partial T}{\partial t} = -\nabla q + Q \quad (2.1)$$

Where the left term of the equation (2.1) represent the stored energy and the right term ($-\nabla q$) is rate of energy input per unit volume by conduction, and (Q) generation of the energy. Each term has the units (W/m^3). Conduction heat transfer depends on three physical parameters: density (ρ), thermal conductivity (k) and specific heat (C_p). The heat flux q (W/m^2) is given by:

$$q = -k(T) \nabla T \quad (2.2)$$

Substituting Eq. (2.2) into Eq. (2.1) we obtain:

$$\rho C_p(T) \frac{\partial T}{\partial t} = \nabla (k(T) \nabla T) + Q \quad (2.3)$$

Most common geometries used for kinetic studies are the finite plate; the specific forms of Eq. (2.3) below for cylindrical coordinates in the following section. Thermal properties

k and C_p as functions of temperature were estimated, but not of direction (the product is isotropic).

2.2 Cylindrical coordinates:

In general, the rate of heat transfer (steady state conduction) is expressed by Fourier's law for one-dimensional Eq. (2.4) (Datta, 2002a; Geankoplis, 2003; Sawaf et al., 1995) is:

$$q_x = -k(T) \frac{dT}{dx} \quad (2.4)$$

For this study, heat changes with time (transient heat transfer) during the retorting process for food materials inside a can (Cylindrical coordinates), there are three spatial coordinates of the system $T(r, \phi, z, t)$ as shown in Figure 2.1.

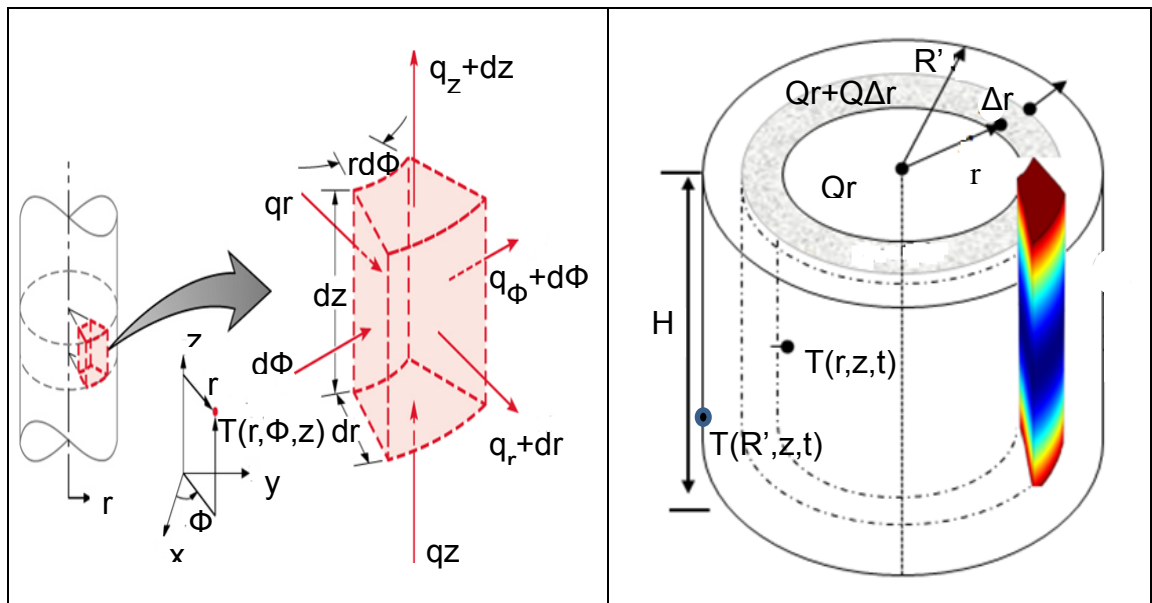


Figure 2.1 Cylindrical coordinates heat transfer by conduction

The components of energy flux ($q, \text{W/m}^3$) for the cylindrical geometry are summarized in the equation for cylindrical coordinates as follows (Bairi et al., 2007; Bird et al., 1960)

$$\frac{1}{r} \frac{\partial}{\partial r} \left(k(T) r \frac{\partial T}{\partial r} \right) + \frac{1}{r^2} \frac{\partial}{\partial \phi} \left(k(T) \frac{\partial T}{\partial \phi} \right) + \frac{\partial}{\partial z} \left(k(T) \frac{\partial T}{\partial z} \right) + Q_{gin} = \rho C_p(T) \frac{\partial T}{\partial t} \quad (2.5)$$

For the case of a can being heated in steam, the conditions are transient with no heat generation. Because the boundary conditions are identical around the circumference of the can, the problem is considered 2D (axial and radial) (Bairi et al., 2007).

Because heat transfer through ϕ direction goes to zero, and there is no heat generation during the process, and thermal conductivity and specific heat are temperature dependent properties, then equation (2.5) is written as follows: (Banga et al., 1993; Betta et al., 2009; Telejko, 2004; Varga and Oliveira, 2000):

$$\frac{1}{r} \frac{\partial}{\partial r} \left(k(T) r \frac{\partial T}{\partial r} \right) + \frac{\partial}{\partial z} \left(k(T) \frac{\partial T}{\partial z} \right) = \rho C_p(T) \frac{\partial T}{\partial t} \quad (2.6)$$

Initial condition;

$$T(r, z, 0) = T_i \quad [t=0, 0 \leq r \leq R', 0 \leq z \leq H] \quad (2.7)$$

Symmetry conditions: at $r = 0$

$$-k \frac{\partial T}{\partial r} = 0 \quad (2.8)$$

2.3 Heat transfer boundary conditions:

Heat transfer boundary conditions for the can (axisymmetric body) in the retort will be based on one of two following conditions types (Naveh et al., 1983):

2.3.1 Convection heat transfer function of time:

Boundary conditions (1):

$$\text{With } T = T_{Rt}(t) \quad [0 < t \leq t_x, r = R', z = 0, z = H]$$

$$-k(T) \frac{\partial T}{\partial r} = h(t) \times (T(R, z, t) - T_{Rt}(t)) \quad (2.9)$$

$$-k(T) \frac{\partial T}{\partial z} = h(t) \times (T(r, H, t) - T_{Rt}(t)) \quad (2.10)$$

Where: $T_{\infty}(t)$ is the time- varying steam temperature. The convection heat transfer is a function of time. The transient heat transfer for equation (2.6) was solved by the finite-element method using Comsol with MATLAB software.

Heat transfer resistance along the heat flow direction is represented by the Nusselt number equation (2.11):

$$Nu = \frac{hL}{k_{fluid}} = \frac{\frac{L}{k_{fluid}}}{\frac{1}{h}} = \frac{\text{Conduction resistance}}{\text{Convection resistance}} \quad (2.11)$$

The analytical solution of heat transfer coefficient depends on the relative internal and external heat transfer resistance (a lumped parameter analysis), which represented by Biot number as follows Eq. (2.12) :

$$Bi = \frac{hR}{k} \quad (2.12)$$

Biot number >40 indicates that external resistance is negligible and Biot number <0.2 indicates that internal resistance is negligible, while Biot number between 0.2 and 40 indicates that both internal and external resistance to heat transfer is important (Rahman, 1995b) .

For negligible internal resistance ($Bi < 0.2$) the following Eq.(2.13) was used to estimate heat transfer coefficients (h), (Singh and heldman, 2001):

$$\ln \left[\frac{T - TRt}{Ti - TRt} \right] = - \left[\frac{hAs}{\rho V C p} \right] t \quad (2.13)$$

For film condensation and Biot number between 0.2 and 40, internal resistance not negligible, an empirical correlation (Nusselt number as a function of Re and Pr numbers) recommended for vertical surface in laminar flow is : (Aston and Kirch, 2012; Atayilmaz, 2011; Chand and Vir, 1979; Geankoplis, 2003; Lienhard, 2006; Naveh et al., 1983; Reymond et al., 2008).

$$N_{Nu} = \frac{hL}{k} = 0.725 \left(\frac{\rho_1(\rho_1 - \rho_v)g \cdot h_{fg} \cdot D^3}{\mu \cdot k \cdot \Delta T} \right)^{1/4} \quad (2.14)$$

The heat flux at the solid surface in the selected direction is equal to the heat convection at the same surface.

$$ACY_t / ACY_0 = 0.0005 \times \exp \left[7.63 \times (a/a_0) \right] \quad R^2=0.89 \quad (2.15)$$

The heat transfer coefficient was estimated experimentally using Eq. (2.14). With given initial and boundary condition (Eqs.(2.7) to (2.10)) and solved per the inverse method with assuming 1D at the initial part of each experiment using finite-difference software (IHCP1D Software, Beck Engineering Consultants Company, www. BeckEng.com).

2.3.2 Surface temperature as function of time (T_s) :

Obtaining temperature profile throughout the surface of the can will be a surface boundary condition for Eq.(2.5) (Naveh et al., 1983; Welti-Chanes et al., 2003).

Initial and boundary conditions throughout the can surface at time, zero, or function of time, could be defined by following equations

$$T(r, z, 0) = f(r, z), \text{ at } t=0 \quad (2.16)$$

$$T(r, z, t) = T_s(r, z, t), \text{ } r=R' \text{ and } z=0 \text{ and } z=H \quad (2.17)$$

Surface temperature was measured with a surface thermocouple placed on the can surface during the process. Data of time and temperature were collected and fed in Comsol software as Heat source boundary condition for predicting can center temperature for each moisture contents of the pomace.

2.4 Thermal conductivity $k(T)$ (linear with T):

Many researchers have expressed thermal conductivity in foods as a linear or quadratic function of temperature (Rahman, 1995a). In this study, we also used a linear model for thermal conductivity (Mishra et al., 2011):

$$k(T) = \left(\frac{(T_2 - T)}{(T_2 - T_1)} \times k_1 + \frac{(T - T_1)}{(T_2 - T_1)} \times k_2 \right) \quad (2.18)$$

The form of Eq. (2.18) is in terms of two thermal conductivities, k_1 ($W \text{ m}^{-1} \text{ K}^{-1}$) is k at T_1 , and k_2 ($W \text{ m}^{-1} \text{ K}^{-1}$) is k at T_2 . The advantage of this form compared to a slope-intercept form is that the two parameters, k_1 and k_2 , have the same units and have easily understood physical meaning. Comparing eq. (2.18) to $k(T) = mT+b$, It is more difficult to understand estimating a slope (m) and an intercept (b) of thermal conductivity vs. temperature. Furthermore, the scaled sensitivity coefficients for k_1 and k_2 in Eq. (2.18) are even larger and more uncorrelated than those for the slope-intercept form, potentially allowing better estimation.

2.4.1 Thermal properties of foods:

Thermal conductivity (k) and specific heat capacity (C_p) are important thermal properties of a material considered during heat transfer. Thermal conductivity describes the heat transfer for a given temperature gradient. It quantifies the steady-state rate of heat transfer at the applied direction of a temperature gradient and it is introduced by Fourier's law of heat conduction (Eq.(2.4)) (Rahman et al., 1997).

Many studies have been done on this subject for estimating these properties for different kinds of food materials. Some studies used measured temperature profiles for estimation of the thermophysical properties in inverse heat conduction problems (Beck and Woodbury, 1998; Yang, 1998).

Estimation of thermal conductivity is classified by two methods: steady and transient state heat transfer methods. Steady-state methods require long times, and moisture content changing with time introduces significant error (Dutta et al., 1988).

The transient method (line source method) is more suitable for biological materials: estimation of thermal conductivity is based on the relationship between the sample temperature and heating time (Yang et al., 2002). However, this method is suitable only for nearly isothermal conditions at temperatures below 100°C.

Appropriate software based on least square optimization of the finite difference solution of Fourier's equation have been developed for thermal diffusivity estimation via heat penetration data from different heat treatments. (Betta et al., 2009).

The probe method is the most widely used method for thermal conductivity estimation. The basic theory for this method is that the temperature rise at a point close to a line heat source inside a sample, and thermal conductivity could be

calculated from the following equation (Baghekhandan et al., 1981; Buhri and Singh, 1993; Choi and Okos, 1983; Sweat, 1975):

$$k = \frac{Q \ln \left[\frac{(t_2 - t_0)}{(t_1 - t_0)} \right]}{4 \pi (t_2 - t_0)} \quad (2.19)$$

Use of $T(t) = (Q/(4 \times \pi \times k)) \times \ln(t)$ shows that this equation is only for near-isothermal conditions at $\leq 80^\circ\text{C}$ because moisture will begin to evaporate above 80°C . A plot of $(T_2 - T_0)$ versus the logarithm of time $(t_2 - t_0)$ is linear until heat penetrates into the sample, where the slope is used for thermal conductivity estimation.

Equation (2.19) was applied for measuring thermal conductivity under high pressure (400MPa) for canned tomato paste and apple (Denys and Hendrickx, 1999; Shariaty-Niassar et al., 2000)

Equations (quadratic models) were developed for predicting thermal conductivity of a meat with a given water content and temperature at different ranges (Sweat, 1975).

Thermal conductivity of carrot and potato (solid food) were measured as well using the probe method at a temperature range $30 - 130^\circ\text{C}$, correlation equation was established for predicting the thermal conductivity (Gratzek and Toledo, 1993). The thermal conductivity of porous foods, which have complex structure is difficult to predict (Sweat, 1995). Studies on linearly temperature dependent thermal conductivity components $k_x(T)$ and $k_y(T)$ and specific heat $C_p(T)$ of transient heat conduction problem for an orthotropic solid have been done using an inverse analysis as following equations:

$$k_x(T) = k_{x0} + k_{x1}T \quad (2.20)$$

$$k_y(T) = k_{y0} + k_{y1}T \quad (2.21)$$

$$Cp(T) = Cp_0 + C_1 T \quad (2.22)$$

A disadvantage of these models is that the coefficients have different units. The analysis was done based on minimizing the sum of squares function with the Levenberg-Marquardt method (Sawaf et al., 1995). Studies using the inverse method to predict the thermal conductivity and the heat of phase transition and the finite element method are used to solve the heat conduction equation. Cylindrical steel samples were heated, and assumed that the thermal conductivity below 720 °C temperature is a second-degree polynomial Equation, and linear function above 770 °C (Telejko, 2004; Yang, 2000) :

$$k(T) = b_1 + b_2 T + b_3 T^2 \quad (2.23)$$

$$k(T) = b_4 + b_5 T \quad (2.24)$$

A quadratic model (Eq.(2.25)) for Thermal conductivity of Tofu as function of temperature and moisture content (M) was established at temperature range (5-80°C) moisture content (0.3-0.7 w b) using probe method (Baik and Mittal, 2003).

$$k = 0.2112 + 8.943 \times 10^{-4} M T + 0.3077 M^2 \quad (2.25)$$

Thermal properties of borage seeds were determined using the line heat source, at temperature range of 6 to 20°C and moisture content range from 1.2 to 30 % .Specific heat was measured by differential scanning calorimetric (DSC) and ranged from 0.77 to 1.99 kJ kg⁻¹K⁻¹. Thermal conductivity increased with moisture content and contributed the most to the uncertainty of thermal diffusivity. A quadratic equation was established for estimating these thermal properties (Yang et al., 2002). Simple linear polynomial models were established in a study on fruit juices, showing that specific heat and

thermal conductivity have linear dependency on water content and temperature, while the density was nonlinearly related to water content (Gratao et al., 2005). Simultaneous estimation of volumetric heat capacity and thermal conductivity was established using nonlinear sequential parameter estimation method, transient temperatures measurements for one dimensional conduction food sample were used to conduct the study (Mohamed, 2009)

Studies on millets, grain and flours, showed that specific heat and thermal conductivity are influenced by the moisture content of the materials, where they increased as moisture content increased values of these two thermal properties were different and this difference is due to a change in the grain and flours constituents and proportions (Subramanian and Viswanathan, 2003). Thermal properties of coffee bean powder were determined: specific heat was determined in a temperature range from 50 to 150 °C, thermal conductivity from 20 to 60 °C, bulk density was determined and its change was negligible at temperature of roasting. Linear relationship for specific heat was given as function of temperature, and for density as function of moisture content. (Singh et al., 1997)

A proposed parallel model (Eq.(2.26)) for predicting thermal conductivity (k) as a function of material temperature (T) reference temperature (Tr) and moisture content (M) was established through the fitting of compiled literature data for some food products during drying process (Maroulis et al., 2002) .

$$k = \frac{1}{1 + M} k_0 \exp \left[- \frac{E_0}{R} \left(\frac{1}{T} - \frac{1}{T_r} \right) \right] + \frac{M}{1 + M} k_i \exp \left[- \frac{E_i}{R} \left(\frac{1}{T} - \frac{1}{T_r} \right) \right] \quad (2.26)$$

Where: k_0 is the thermal conductivity at moisture $M = 0$ and temperature ($T = T_r = 60^\circ\text{C}$),
 k_r is the thermal conductivity at moisture $M = \infty$ and temperature ($T = T_r = 60^\circ\text{C}$)

A thermal conductivity prediction regression equation was developed for some foodstuffs beef, potato, apple, pears and squid as function of moisture content, porosity and initial thermal conductivity. The correlation coefficient was 0.99. This correlation assumed no effect of the temperature on the thermal conductivity (Rahman, 1992). Quadratic models of Thermal conductivity as function of water contents of potatoes, and apples were established (Mattea et al., 1986; Rahman et al., 1997) .

Literature shows that thermal conductivity data have wide variation because of one or more of the following factors: 1) different experimental method applied, 2) material composition, and 3) difference in the structure of the material. Thermal conductivity depends strongly on temperature, moisture content, and material structure. Thermal conductivity was estimated and presented from literature data (more than 140 articles) for about 100 foodstuffs that vary in moisture contents and temperature (Krokida et al., 2001).

2.4.2 Isothermal and non-isothermal Processing

Many foods which contain anthocyanin (ACY) are thermally processed prior to consumption. This process can greatly influence ACY content in the final product. These pigments are not very stable chemically and may degrade during thermal processing ($>70^\circ\text{C}$) thus affecting color, quality and nutritional components. ACY degradation rate increases as temperature rises during processing and storage (Palamidis and Markakis 1978). Thermal processing of foods involves heating up as high as 150°C , depending on the process. There are many studies examining these

factors individually, or a combination of one or more of them, on degradation of food components. There is limited information available on the effect of high temperature processing at different moisture contents on the stability of these pigments in solid food products. The majority of studies on the degradation kinetics of ACYs have been carried out under isothermal conditions at temperatures below 100°C on high-moisture products. However, ACY degradation in low moisture solids or semi-solid foods such as fruit or berry pomace, grains, and dried vegetables is not isothermal. Therefore kinetic modeling should include time-temperature history (Mishra et al., 2008).

Most processing and cooking operations are not isothermal. Therefore, studies on prediction of pathogen behavior require the examination of the cumulative effect of exposure to varying temperatures throughout the cooking process. Changes in chemical and physical characteristics in foods during heating because of temperature rise might affect different elements in the process. For example the “limiting reaction” at a specific temperature might not be the same at lower or higher temperatures (Peleg et al., 2009).

A study on blackcurrant ACYs degradation in the juice under isothermal and non-isothermal condition (4-140°C) showed that the ACY degradation followed first-order kinetics (Harbourne et al., 2008).

The non-isothermal method gave much smaller relative errors compared with the isothermal method for both the activation energy and the rate constants. Specifically, the activation energies were estimated at 73 ± 2 kJ/mol for an isothermal temperature range of 21-100 °C at six constant temperatures. For the non-isothermal experiments, the estimates were 81.51 ± 0.03 kJ/mol at 110 °C and 91.09 ± 0.03 kJ/mol at 140 °C. In

this case the error in estimation of the activation energy was 2.7% for the isothermal experiments, versus 0.03% for the non-isothermal method, an increased accuracy of 90-fold. Also, the isothermal method requires minimum five constant-temperature runs (~60 data points) to estimate the kinetic parameter with accuracy, while the non-isothermal method required only one run (4-10 data points) (Harbourne et al., 2008). The same study indicated that to estimate ACY degradation at typical food industry sterilization temperatures (>100 °C), using non-isothermal methods at these high temperatures is recommended, because the degradation kinetics cannot be extrapolated without significantly underestimating the ACY degradation (Harbourne et al., 2008).

A study on an inactivation kinetics of alkaline phosphatase and lactoperoxidase and denaturation kinetics of β -lactoglobulin in raw milk under isothermal and dynamic temperature conditions demonstrated that the thermal inactivation of the three previous compounds was accurately described by the first-order model. Isothermal parameters predicted non-isothermal results well for alkaline phosphatase and lactoperoxidase, but not for β -lactoglobulin (Claeys et al., 2001). More accurate parameter results were obtained using the global nonlinear regression rather than the two-step linear regression (Claeys et al., 2001).

In summary, there has been a lot of research on isothermal methods for inactivation of organisms and some on degradation kinetics of nutrients and nutraceutical compounds. Processing liquids at temperatures above 100 °C for short times requires the use of non-isothermal methods to estimate degradation kinetics parameters. Processing lower-moisture solids at temperatures above 100°C for any

length of time requires non-isothermal methods because of the changing temperature gradient within the sample. For isothermal processes, the come-up time for heating and come-down time for cooling must be negligible comparing with the longer holding heating time. In non-isothermal processes, the sample temperature during the entire process is included in the model. As shown from some literature, that accuracy in non-isothermal processing is higher comparing with isothermal processing. The number of experiments needed to estimate the kinetic parameters or inactivation parameters is fewer than those for the non-isothermal process.

2.5 Cherry Pomace's Anthocyanins

2.5.1 Cherry pomace

Cherry (*Prunus cerasus* L.) pomace is the solid waste or by-product of cherry juice processing and consists of cherry skin and seeds. It accounts for over 90% of dry matter with high quantity of lignin, cellulose, and dry fiber components (Nawirska A. , 2005). Study on tart cherry indicated that Balaton contains about six times more ACY than does Montmorency has (Wang et al., 1997). Cherries are known to contain substantial quantities of ACY (Wang et al., 1999), which are mainly concentrated in the skins (Chaovanalikit and Wrolstad, 2004; Tomas-Barberan et al., 2001) and constitute a major portion of bioactive compounds in the pomace. Cherry pomace, an otherwise waste material, could be processed into value-added ingredients for use in different food products as colorant and/or nutraceuticals. For example, addition of tart cherry tissue to cooked beef patties has been shown to inhibit lipid and cholesterol oxidation (Britt et al., 1998). Cherry pomace powder or extract may also be added to breakfast

cereals, snacks, drink mixes, confectionaries, breads or other baked goods, or used as a slow-release antioxidant in the packaging films.

2. 5.2 Anthocyanins in Nature

Anthocyanins are natural colorants that provide bright red to purple color in foods. Researches on ACY have increased because of their possible role in reducing the risk of coronary heart disease, cancer and stroke (McGhie and Walton, 2007; Wrolstad, 2004). ACY have antioxidant and anti-inflammatory effects, which play an important role in the prevention of neuronal and cardiovascular illnesses, cancer and diabetes, among others. There are several studies focusing on the effect of ACY in cancer treatments, human nutrition and its biological activity (Bohm et al., 1998; Konczak and Zhang, 2004; Lule and Xia, 2005; Simunic et al., 2005; Zafra-Stone et al., 2007)

2.5.3 Structure of Anthocyanins:

ACY are the most abundant flavonoid constituents of fruits and vegetables. They are responsible for the wide array of colors present in flowers, petals, leaves, fruits and vegetables and are a sub-group within the flavanoids characterized by a C6-C3-C6-skeleton, Figure 2.2. ACY are glycosylated anthocyanidins; sugars are attached to the 3-hydroxyl position of the anthocyanidin (sometimes to the 5 or 7 position of flavinium ion,). Variations in chemical structure (Figure 2.2) are mainly due to differences in the number of hydroxyl groups in the molecule, degree of methylation of these OH groups (Table 2.1). They are responsible for the color ranges of fruits and vegetables from red at pH values below 4, to colorless at pH 4-4.5 and to blue at pH 7 and above. The red color of cherries is due to several water-soluble anthocyanin pigments. Pelargonidin,

cyanidin, peonidin, delphinidin, petunidin, and malvidin are the six common anthocyanidins found in nature (Francis, 1989).

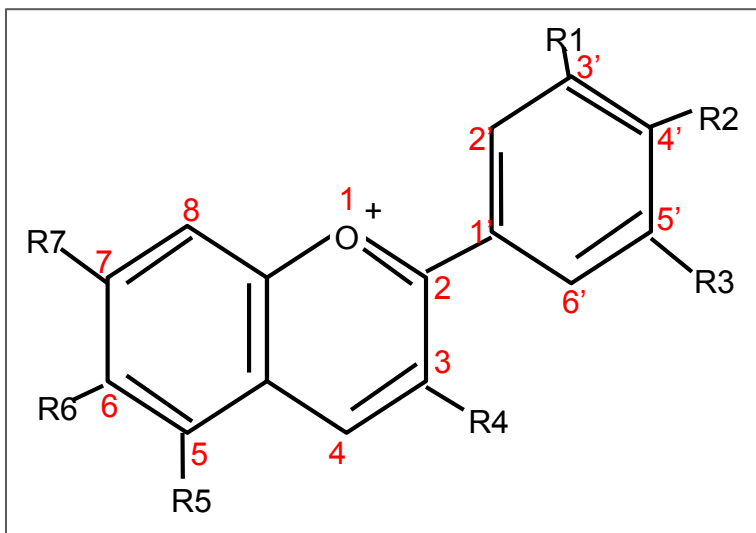


Figure 2.2 Anthocyanin ground structure, flavylum (2-phenylchromenylium)

Table 2.1 Six Common Anthocyanidins

Anthocyanidin	R ₁	R ₂	R ₃	R ₄	R ₅	R ₆	R ₇
Cyanidin	-OH	-OH	-H	-OH	-OH	-H	-OH
Delphinidin	-OH	-OH	-OH	-OH	-OH	-H	-OH
Pelargonidin	-H	-OH	-H	-OH	-OH	-H	-OH
Malvidin	-OCH ₃	-OH	-OCH ₃	-OH	-OH	-H	-OH
Peonidin	-OCH ₃	-OH	-H	-OH	-OH	-H	-OH
Petunidin	-OH	-OH	-OCH ₃	-OH	-OH	-H	-OH

2.5.4 Stability of Anthocyanins

Anthocyanin stability is the main focus in many studies. This stability is not only a function of final processing temperature but also of other properties (intrinsic) like pH, storage temperature, product moisture content, chemical structure of the ACY and its

initial concentration, light, oxygen, presence of enzymes, proteins and metallic ions (Patras et al., 2010). Anthocyanin pigments readily degrade during thermal processing, which has a dramatic impact on color and affects nutritional properties (Jimenez et al., 2010). Anthocyanin stability of black carrots was studied at various solid contents and pHs during both heating, 70–90 °C, and storage at 4–37 °C, degradation of monomeric ACY increased with increasing solid content during heating, while it decreased during storage (Ahmed et al., 2004; Kirca et al., 2007). The degradation kinetics of ACY in blood orange juice was studied (Kirca and Cemeroglu, 2003) and the activation energies for solid content of 11.2 to 69 °Brix were found to be 73.2 to 89.5 kJ/mole. Thermal and moisture effects on grape anthocyanin degradation were investigated using solid media to simulate processing at temperatures above 100 °C (Lai et al., 2009). Anthocyanin degradation followed a pseudo first-order reaction with moisture ACY degrading more rapidly with increasing temperature and moisture. The thermal degradation of ACY has been studied in red cabbage (Dyrby et al., 2001), raspberries (Ochoa et al., 1999), pomegranate, grapes (Marti et al., 2002), plum puree (Ahmed and others 2004), blackberries (Wang and Xu, 2007), and blueberry (Kechinski et al., 2010). Anthocyanin pigments readily degrade during thermal processing, which has a dramatic impact on color and affects nutritional properties

2.5.4.1 Effect of pH on ACY Stability

ACY are more stable in acidic solutions than alkaline solutions, at different pH values the ionic nature of ACY changes by changing in molecule structure, which results in different colors in the solutions (Brouillard, 1982). In acidic solutions, ACY exist in the four different equilibrium species: the quinoidal base, the flavylum cation,

the carbinol or pseudobase (hemiketal) and the chalcone (Figure 2.3). At very acidic conditions, the flavylium cation AH^+ is predominant and appears as the red color. As the flavylium is hydrated by nucleophilic attack of water, the carbinol or pseudobase is formed. In the carbinol form, the anthocyanin appears as colorless due to pH increase (Socaciu, 2008). Hence, ACY are more stable in low pH. Metal ions, heat, pH values > 4, sulfites and oxygen are some factors that can accelerate anthocyanin breakdown. (Garzon and Wrolstad, 2002)

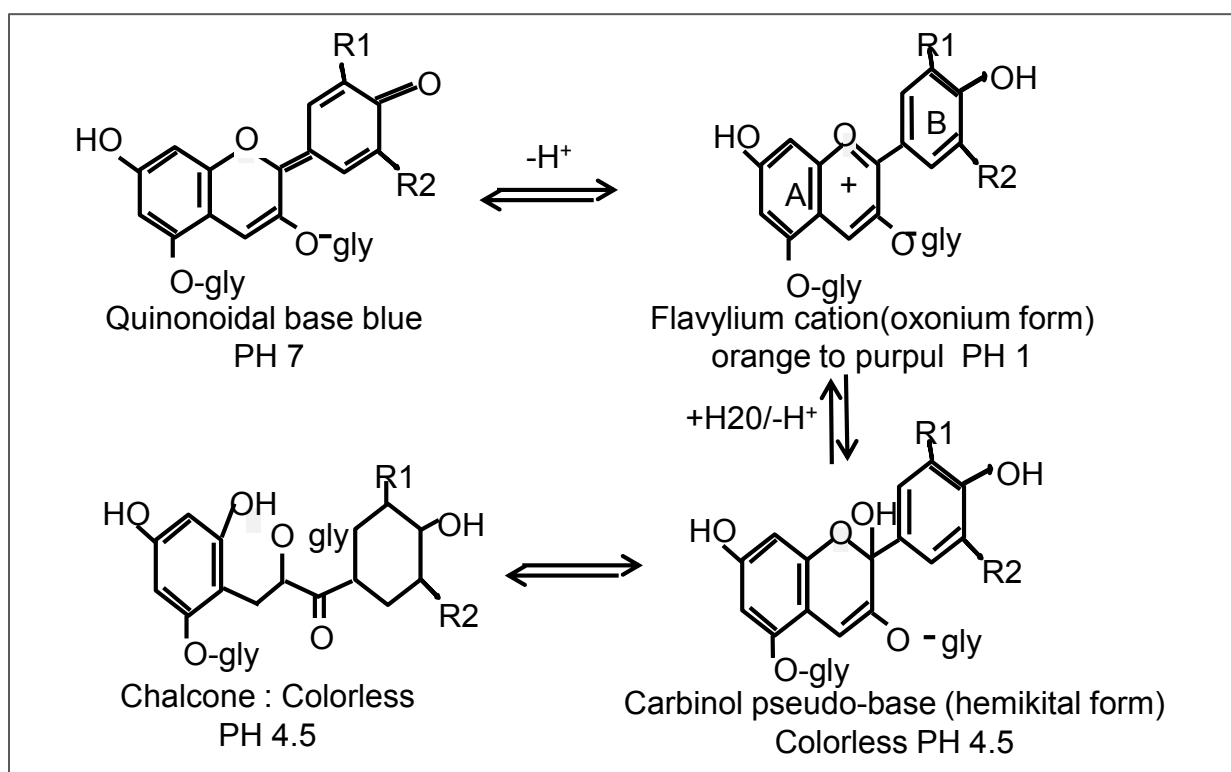


Figure 2.3 pH equilibrium forms of anthocyanins

2.5.4.2 Effect of Temperature on Anthocyanins Stability

Many foods which contain ACY are thermally processed prior to consumption and this process can greatly influence anthocyanin content in the final product. These pigments are not very stable chemically and may degrade during thermal processing

(>70°C) which can affect color quality and nutritional components. Anthocyanin degradation rate increases as temperature rises during processing and storage (Palamidis and Markakis 1978).

Thermal and storage stabilities at different temperature range (5-37, 60-90) on ACY degradation in blackberry juice and concentrate was studied, results indicated that thermal degradation followed first-order reaction kinetics and juice at higher soluble solids (higher activation energy) degraded more rapidly comparing with lower soluble solids contents, which have lower activation energy comparing higher soluble solids juice (Wang and Xu, 2007). There is limited information available on the effect of high temperature processing at different moisture contents on the stability of these pigments in solid food products. The majority of studies on the degradation kinetics of ACY have been carried out under isothermal conditions at temperatures below 100°C on high-moisture products. However, anthocyanin degradation in low moisture solid or semi-solid foods such as fruit or berry pomace, grains, and dried vegetables is not isothermal. Therefore kinetic modeling should include time-temperature history (Mishra et al., 2008). Thermal processing easily degrades the ACY pigments, which has a dramatic impact on color and affects nutritional properties (Jimenez et al., 2010). Havlikova and Mikova (1985) showed that there was lower stability of ACY at pH 1.8 comparing with other pH (2 to 4) values in elderberry concentrate when it was heated at 70-100°C. Based on many studies the thermal stability of ACY depends on the pH value only under aerobic conditions, while under anaerobic conditions (negligible oxygen concentration) the stability is not influenced by pH in range 2-4. This fact might explain the stability of ACY above 70°C, where the anaerobic conditions established (Havlikova

and Mikova, 1985). Commercial sources of ACY (strawberry, elderberry, and black carrot) were investigated; ACY isolates were heated at 95 °C, at pH 1. Total anthocyanin content lightness, and Chroma, but not hue angle, were appropriate parameters to monitor anthocyanin loss on a statistically significant level (Sadilova et al., 2006). Thermal stability and composition of ACY were evaluated for purple corn extracts (Zhao et al., 2008), thermal degradation kinetics of ACY from purple corn cob were studied at selected temperatures (70 °C, 80 °C and 90 °C) at pH 4.0 (Chen et al., 2008).

2.5.5 Anthocyanins Antioxidant Capacity

Tart cherries are rich in ACY and retain high antioxidant activity. Study on Michigan tart cherry for evaluating different quality showed that it has high oxygen radical absorbing capacity (ORAC) of Balaton 145% as compared to Montmorency 100% (Siddiq et al., 2011). A study has shown that the ACY, acting primarily as antioxidants, have anti-inflammatory, anti-carcinogenic, and anti-aging properties (Blando et al., 2004). The development of a fluorescent probe (ORAC_{FL}) method is attributed to Glazer (1990), Ghiselli et al. (1995) and Cao and others (1993) and is classified as a Hydrogen Atom Transfer Assay (HAT). In HAT reactions, the antioxidant will quench free radicals through the donation of a hydrogen atom. The ORAC_{FL} method measures the ability of the antioxidant to search for peroxy radicals using a fluorescent probe (fluorescein sodium salt) for detection. The peroxy radicals will oxidize the fluorescent probe causing a decrease in the intensity of the fluorescence that can be quantified over time using a fluorometer. Antioxidants in the system will reduce the peroxy radicals stopping the loss of intensity in the fluorescence. The

interface between the antioxidants, free radicals, and the fluorescent probe is illustrated in Figure 2.4 (Ou et al., 2001; Zulueta et al., 2009).

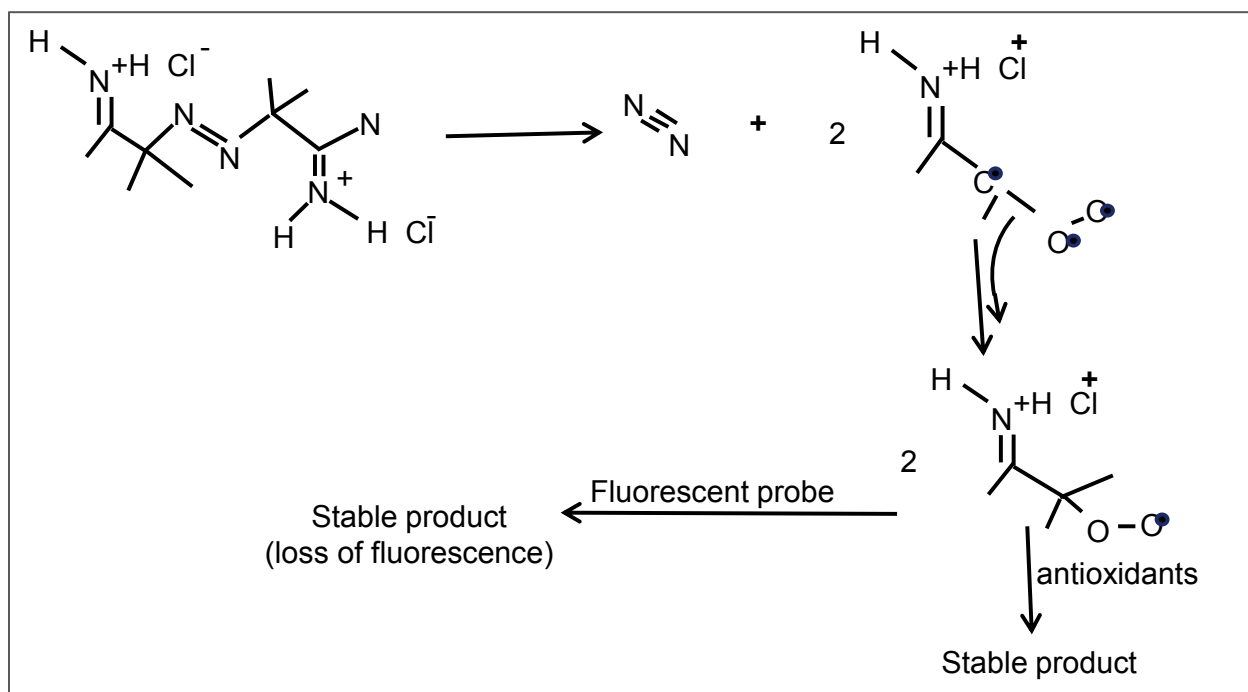


Figure 2.4 Formation of radicals through the addition of AAPH

To build a decay curve for each sample and a blank sample, the relative fluorescence intensity will be measured over time. The area under the curve (AUC) is calculated using the following trapezoidal equation, normalized by dividing by the initial fluorescence value:

$$AUC = \left(\frac{R1}{2} + R2 + R3 + \dots + \frac{Rn}{2} \right) \Delta t$$

Where: R1 is the fluorescence measurement at the initial time of the oxidation reaction, Rn is the final fluorescence measurement, and Δt is the difference of time between the two measurements. The antioxidant capacity was determined by calculating the net area under curve as follows Eq:

$$NetAUC = AUC_{sample} - AUC_{Blank}$$

The calculated net AUC of each sample was compared to a standard calibration curve, which was constructed by plotting the net AUC of a compound called Trolox (6-hydroxy-2, 5, 7, 8-tetramethylchroman-2-carboxylic acid) against five standard concentrations in micromoles of Trolox. Therefore the ORAC value of a sample is expressed as micromoles of Trolox equivalents per gram or liter of sample ($\mu\text{mol TE/g}$ or $\mu\text{mol TE/L}$).

2.6 Kinetics And Mechanism of Degradation of Anthocyanins In Foods

2.6.1 Kinetics Mechanism:

Kinetic models are often used for an objective, fast and economic assessment of food safety. Kinetic modeling may also be employed to predict the influence of processing on critical quality indicators. Knowledge of degradation kinetics, including reaction order, rate constant and activation energy, is vital to simulate and predict food quality loss during storage as well as during thermal process treatments. One of the important factors to be considered in food processing is the loss of nutrients. Therefore, kinetic studies are needed to minimize the undesired change and to optimize quality of specific foods. Anthocyanin degradation under non-isothermal heating is reported to follow first order kinetics (Ahmed et al., 2004; Markakis et al., 1957). Equations (2.25) and (2.26) are for ACY kinetic degradation and by adding constant of moisture content (MC) as a new parameter for estimation (b) the following equations will result:

$$C(t) = C_0 e^{\left[-k_r \psi(t) e^{(b(MC - MC_r))} \right]} \quad (2.27)$$

$$\psi(t) = \int_0^t e^{\left[\frac{-Ea}{R} \left(\frac{1}{T(r,z,t)} - \frac{1}{T_r} \right) \right]} dt \quad (2.28)$$

Thermal degradation of ACY can result in a variety of species depending upon the severity and nature of heating. Figure 2.4 shows the degradation of ACY and formation of various intermediate compounds (Patras et al., 2010).

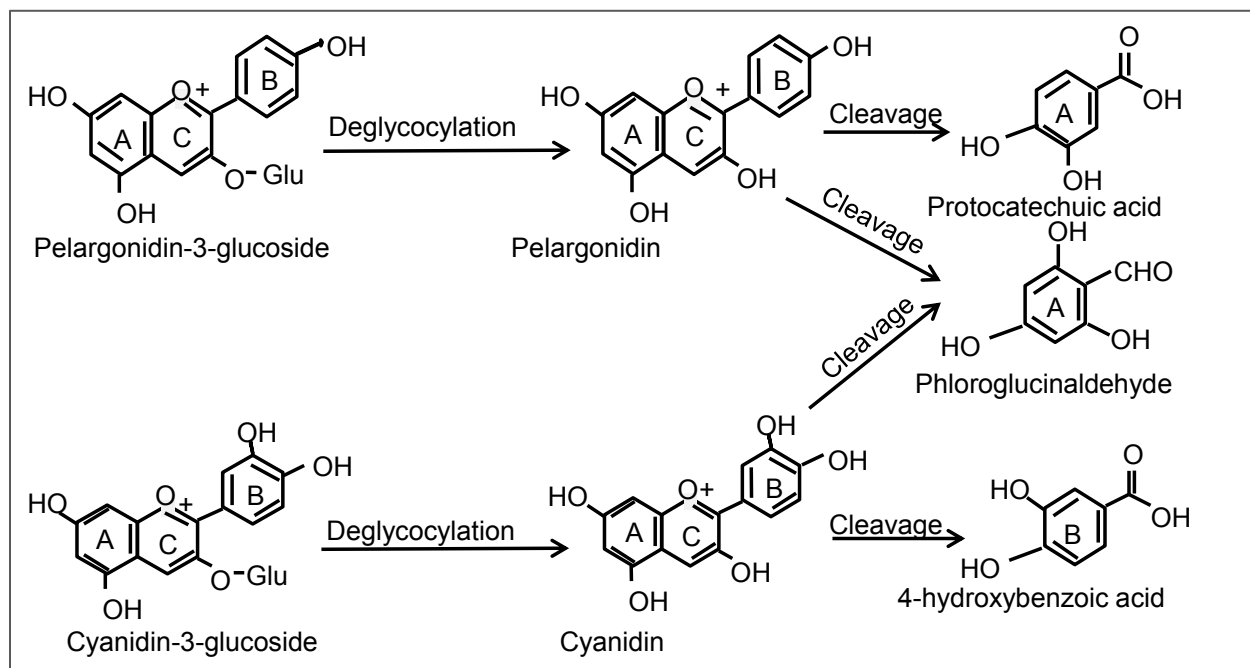


Figure 2.5 Possible thermal degradation mechanism of two common ACYs (Patras et al., 2010)

Recently, (Harbourne et al., 2008; Mishra et al., 2008) studied thermal degradation of ACY of grape pomace, (Harbourne and others 2008) studied blackcurrant ACY in a model juice under non-isothermal conditions. Prior to this study (Dolan, 2003) proposed a one-step kinetic model for determining kinetic parameters for non-isothermal food process Equations (2.29) and (2.30). This model was employed by (Harbourne et al., 2008) for non-isothermal processing of model blackcurrant juice.

$$C_t = C_0 \times \exp(-kr \times \psi(t)) \quad (2.29)$$

$$\psi(t) = \int_0^t e^{\left[\frac{-Ea}{R} \left(\frac{1}{T(r,z,t)} - \frac{1}{Tr} \right) \right]} dt \quad (2.30)$$

Recently, (Jimenez et al., 2010) studied Blackberry juice heated at a high temperature in a hermetically sealed cell. Statistical analysis demonstrated that when the temperature range (100-180°C) was divided into two sub ranges (100-140 and 140-180 °C) for anthocyanin degradation, reaction kinetics were well represented by two sequential first-order reactions. The non-isothermal method developed allows estimating kinetic parameters and thereby generating temperature profiles of heat processes that would help preserve the nutritional properties of foods during high-temperature processes. In summary, for components in low moisture and high temperature processed semi-solid foods such as pastries, baked goods, breads and extruded snacks there are no established experimental procedures and statistical analysis method of kinetic parameters. Also there is lack of nonlinear regression techniques for analysis of food that is processed under unsteady-state conditions of heating.

2.6.2 Anthocyanins Degradation Model:

In this study the reaction is following a first order reaction as following equation:

$$\frac{dC}{dt} = -kC \quad (2.31)$$

Integration of equation (2.31) with integration limits gives:

$$\int_{C_0}^{C(t)} \frac{dC}{C} = \int_0^t -k dt \quad (2.32)$$

When k is function of temperature and moisture content, Eq. (2.32) is written as follows:

$$C(t) - C_0 = \int_0^t \frac{dC}{dt} = \int_0^t -k(T, MC) dt \quad (2.33)$$

Where $k(T, MC)$ is the reaction rate, which follows Arrhenius temperature dependence, and includes the moisture content term:

$$k(T, MC) = -k_r \exp \left[\frac{-Ea}{R} \left(\frac{1}{T(r, z, t)} - \frac{1}{T_r} \right) + b(MC - MC_r) \right] \quad (2.34)$$

k_r is the rate constant at reference temperature (T_r) and at reference moisture content (MC_r). Substituting Eq. (2.34) in Eq.(2.33) yields:

$$\ln C(t) - \ln C_0 = -k_r \int_0^t e^{\left[\frac{-Ea}{R} \left(\frac{1}{T(r, z, t)} - \frac{1}{T_r} \right) + b(MC - MC_r) \right]} dt \quad (2.35)$$

Let the time temperature history equal $\Psi(t)$:

$$\Psi(t) = \int_0^t e^{\left[\frac{-Ea}{R} \left(\frac{1}{T(r, z, t)} - \frac{1}{T_r} \right) \right]} dt$$

Then by solving for $C(t)$ in Eq. (2.33) ,yields :

$$C(t) = C_0 e^{\left[-k_r \Psi(t) e^{(b(MC - MC_r))} \right]} \quad (2.36)$$

Equation (2.36) will predict the degradation of ACY at any chosen point inside the cylinder during heating for a constant MC and time temperature history $\Psi(t)$. Because ACY concentration cannot be measured at an infinitely small point, we must continue to develop the equation for mass-average ACY concentration, which can be measured

experimentally. To compute mass-average ACY in the can $C(t)$ the point concentration in the can $C(t)$ should be integrated over the can:

$$\psi(t) = \frac{\int_0^H \int_0^{R'} C(t) \times 2\pi r dr dz}{\int_0^H \int_0^{R'} 2\pi r dr dz} \quad (2.37)$$

Substituting $C(t)$ from Eq. (2.36) into Eq. (2.37) yields:

$$\bar{C}(t) = \frac{2\pi C_0 \int_0^H \int_0^{R'} e^{-kr\psi(t)} e^{(b(MC - MC_r))} r dr dz}{2\pi \times \frac{R'^2}{2} \times H} \quad (2.38)$$

Normalizing, $r^*=r/R'$ and $z^*=z/H$, the final form of Eq.(2.38) will be as following :

$$\bar{C}(t) = 2C_0 \int_0^1 \int_0^1 e^{-kr\psi(t)} e^{(b(MC - MC_r))} r^* dr^* dz^* \quad (2.39)$$

Equation (2.39) is the equation will be used in our study for calculation of mass-average ACY concentration as function of moisture content and time-temperature history. The moisture content of the pomace samples is constant during this non-isothermal process. The moisture content parameter b in Eq. (2.39) will be estimated in as function of reaction constant kr . The kinetic parameters (Ea , kr) and initial concentration of ACY (C_0) in Equation (2.39) will be estimated using the inverse problem method by MATLAB with Comsol by running the “nlinfit” code , which estimates the parameters by minimizing the sum of squares using Equation (2.40):

$$SS = \sum_i \left[(\bar{C}_{obs})_i - (\bar{C}_{prd})_i \right]^2 \quad (2.40)$$

REFERENCES

REFERENCES

- Ahmed, J., Shivhare, U.S., Raghavan, G.S.V., (2004). Thermal degradation kinetics of anthocyanin and visual colour of plum puree. *European Food Research and Technology* 218(6), 525-528.
- Aston, J.A.D., Kirch, C., (2012). Detecting and estimating changes in dependent functional data. *Journal of Multivariate Analysis* 109, 204-220.
- Atayilmaz, S.O., (2011). Experimental and numerical study of natural convection heat transfer from horizontal concentric cylinders. *International Journal of Thermal Sciences* 50(8), 1472-1483.
- Baghekhandan, M.S., Choi, Y., Okos, M.R., (1981). Improved line heat-source thermal-conductivity probe. *Journal of Food Science* 46(5), 1430-1432.
- Baik, O.D., Mittal, G.S., (2003). Determination and modeling of thermal properties of tofu. *International Journal of Food Properties* 6(1), 9-24.
- Bairi, A., Laraqi, N., de Maria, J.M.G., (2007). Determination of thermal diffusivity of foods using 1D Fourier cylindrical solution. *Journal of Food Engineering* 78(2), 669-675.
- Banga, J.R., Alonso, A.A., Gallardo, J.M., Perezmartin, R.I., (1993). Mathematical-Modeling and Simulation of the Thermal-Processing of Anisotropic and Nonhomogeneous Conduction-Heated Canned Foods - Application to Canned Tuna. *Journal of Food Engineering* 18(4), 369-387.
- Beck, J.V., Woodbury, K.A., (1998). Inverse problems and parameter estimation: integration of measurements and analysis. *Measurement Science & Technology* 9(6), 839-847.
- Betta, G., Rinaldi, M., Barbanti, D., Massini, R., (2009). A quick method for thermal diffusivity estimation: Application to several foods. *Journal of Food Engineering* 91(1), 34-41.
- Bird, R.B., Stewart, E.W., Lightfoot, E.N., (1960). *Transport Phenomena* . " The Equations of Change for Nonisothermal systems". New York . John Wiley & Sons, pp. 310-351.

- Blando, F., Gerardi, C., Nicoletti, I., (2004). Sour cherry (*Prunus cerasus* L.) anthocyanins as ingredients for functional foods. *Journal of Biomedicine and Biotechnology*(5), 253-258.
- Bohm, H., Boeing, H., Hempel, J., Raab, B., Kroke, A., (1998). Flavonols, flavones and anthocyanins as native antioxidants of food and their possible role in the prevention of chronic diseases. *Zeitschrift Fur Ernährungswissenschaft* 37(2), 147-163.
- Britt, C., Gomaa, E.A., Gray, J.I., Booren, A.M., (1998). Influence of cherry tissue on lipid oxidation and heterocyclic aromatic amine formation in ground beef patties. *Journal of Agricultural and Food Chemistry* 46(12), 4891-4897.
- Brouillard, R., (1982). Chemical Structure of Anthocyanins. *Anthocyanins as Food Colors*. Markakis, P, Ed., . New York, Academic Press Inc, pp. 1-38.
- Buhri, A.B., Singh, R.P., (1993). Measurement of food thermal-conductivity using differential scanning calorimetry. *Journal of Food Science* 58(5), 1145-1147.
- Cao, G.H., Alessio, H.M., Cutler, R.G., (1993). Oxygen-radical absorbency capacity assay for antioxidants. *Free Radical Biology and Medicine* 14(3), 303-311.
- Chand, J., Vir, D., (1979). Natural-convection heat-transfer from horizontal cylinders. *Journal of Chemical Engineering of Japan* 12(3), 242-247.
- Chaovanalikit, A., Wrolstad, R.E., (2004). Total anthocyanins and total phenolics of fresh and processed cherries and their antioxidant properties. *Journal of Food Science* 69(1), C67-C72.
- Chen, C.K., Wu, L.W., Yang, Y.T., (2008). Proposed modification to whole domain function specification method to improve accuracy of its estimations. *Journal of Heat Transfer-Transactions of the ASME* 130(5), 130p..
- Choi, Y., Okos, M.R., (1983). The thermal properties of tomato juice concentrates. *TRANSACTIONS of the ASAE* 26(1), 305-311.
- Claeys, W.L., Ludikhuyze, L.R., Van Loey, A.M., Hendrickx, M.E., (2001). Inactivation kinetics of alkaline phosphatase and lactoperoxidase, and denaturation kinetics of beta-lactoglobulin in raw milk under isothermal and dynamic temperature conditions. *Journal of Dairy Research* 68(1), 95-107.
- da Silva, W.P., Silva, C.M.D.P.S.E., Lins, M.A.A., (2011). Determination of expressions for the thermal diffusivity of canned foodstuffs by the inverse method and

- numerical simulations of heat penetration. *International Journal of Food Science and Technology* 46(4), 811-818.
- da Silva, W.P., Silva, C.M.D.P.S.E., Silva, D.D.P.S.E., Neves, G.D., de Lima, A.G.B., (2010). Mass and heat transfer study in solids of revolution via numerical simulations using finite volume method and generalized coordinates for the Cauchy boundary condition. *International Journal of Heat and Mass Transfer* 53(5-6), 1183-1194.
- Datta, A.K., (2002a). *Biological and bioenvironmental heat and mass transfer*. Boca Raton, Florida: Taylor & Francis. p. 424.
- Denys, S., Hendrickx, M.E., (1999). Measurement of the thermal conductivity of foods at high pressure. *Journal of Food Science* 64(4), 709-713.
- Dolan, K.D., (2003). Estimation of kinetic parameters for nonisothermal food processes. *Journal of Food Science* 68(3), 728-741.
- Dutta, S.K., Nema, V.K., Bhardwaj, R.K., (1988). Thermal-properties of gram. *Journal of Agricultural Engineering Research* 39(4), 269-275.
- Dyrby, M., Westergaard, N., Stapelfeldt, H., (2001). Light and heat sensitivity of red cabbage extract in soft drink model systems. *Food Chemistry* 72(4), 431-437.
- Fernandes, A.P., Sousa, P.F.B., Borges, V.L., Guimaraes, G., (2010). Use of 3D-transient analytical solution based on Green's function to reduce computational time in inverse heat conduction problems. *Applied Mathematical Modelling* 34(12), 4040-4049.
- Francis, F., (1989). Food Colorants: Anthocyanins. *Critical Reviews in Food Science and Nutrition* 28, 273-314.
- Garzon, G.A., Wrolstad, R.E., (2002). Comparison of the stability of pelargonidin-based Anthocyanins in strawberry juice and concentrate. *Journal of Food Science* 67(4), 1288-1299.
- Geankoplis, C.J., (2003). *Transport Processes and Separation process Principles."prinsibles of steady-state heat transfer"*. Pearson Education INC 4th Edition, Chapter 4 . pp 235-344.
- Ghiselli, A., Serafini, M., Maiani, G., Azzini, E., Ferroluzzi, A., (1995). A fluorescence-based method for measuring total plasma antioxidant capability. *Free Radical Biology and Medicine* 18(1), 29-36.

- Glazer, A.N., (1990). Phycoerythrin fluorescence-based assay for reactive oxygen species. *Methods in Enzymology* 186, 161-168.
- Goncalves, E.M., Abreu, M., Brandao, T.R.S., Silva, C.L.M., (2011a). Degradation kinetics of colour, vitamin C and drip loss in frozen broccoli (*Brassica oleracea* L. ssp *Italica*) during storage at isothermal and non-isothermal conditions. *International Journal of Refrigeration-Revue Internationale Du Froid* 34(8), 2136-2144.
- Goncalves, E.M., Pinheiro, J., Abreu, M., Brandao, T.R.S., Silva, C.L.M., (2011b). Kinetics of quality changes of pumpkin (*Curcubita maxima* L.) stored under isothermal and non-isothermal frozen conditions. *Journal of Food Engineering* 106(1), 40-47.
- Gratao, A.C.A., Junior, V.S., Polizelli, M.A., Telis-Romero, J., (2005). Thermal properties of passion fruit juice as affected by temperature and water content. *Journal of Food Process Engineering* 27(6), 413-431.
- Gratzek, J.P., Toledo, R.T., (1993). Solid food thermal-conductivity determination at high-temperatures. *Journal of Food Science* 58(4), 908-913.
- Harbourne, N., Jacquier, J.C., Morgan, D.J., Lyng, J.G., (2008). Determination of the degradation kinetics of anthocyanins in a model juice system using isothermal and non-isothermal methods. *Food Chemistry* 111(1), 204-208.
- Havlikova, L., Mikova, K., (1985). Heat-Stability of anthocyanins. *Zeitschrift Fur Lebensmittel-Untersuchung Und-Forschung* 181(5), 427-432.
- Jimenez, N., Bohuon, P., Lima, J., Dornier, M., Vaillant, F., Perez, M., (2010). Kinetics of anthocyanin degradation and browning in reconstituted blackberry juice treated at high temperatures (100-180 °C). *Journal of Agricultural and Food Chemistry* 58(4), 2314-2322.
- Kechinski, C.P., Guimaraes, P.V.R., Norena, C.P.Z., Tessaro, I.C., Marczak, L.D.F., (2010). Degradation kinetics of anthocyanin in blueberry juice during thermal treatment. *Journal of Food Science* 75(2), C173-C176.
- Kirca, A., Cemeroglu, B., (2003). Degradation kinetics of anthocyanins in blood orange juice and concentrate. *Food Chemistry* 81(4), 583-587.
- Kirca, A., Ozkan, M., Cemeroglu, B., (2007). Effects of temperature, solid content and pH on the stability of black carrot anthocyanins. *Food Chemistry* 101(1), 212-218.

- Konczak, I., Zhang, W., (2004). Anthocyanins - More than nature's colours. *Journal of Biomedicine and Biotechnology*(5), 239-240.
- Krokida, M.K., Panagiotou, N.M., Maroulis, Z.B., Saravacos, G.D., (2001). Thermal conductivity: Literature data compilation for foodstuffs. *International Journal of Food Properties* 4(1), 111-137.
- Lai, K.P.K., Dolan, K.D., Ng, P.K.W., (2009). Inverse method to estimate kinetic degradation parameters of grape anthocyanins in wheat flour under simultaneously changing temperature and moisture. *Journal of Food Science* 74(5), E241-E249.
- Lienhard, J.H., (2006). *A heat transfer textbook*, 3rd ed. Englewood Cliffs, NJ: Prentice-Hall, , p. 439.
- Lule, S.U., Xia, W.S., (2005). Food phenolics, pros and cons: A review. *Food Reviews International* 21(4), 367-388.
- Mariani, V.C., de Lima, A.G.B., Coelho, L.D.S., (2008). Apparent thermal diffusivity estimation of the banana during drying using inverse method. *Journal of Food Engineering* 85(4), 569-579.
- Mariani, V.C., do Amarante, A.C.C., Coelho, L.D., (2009). Estimation of apparent thermal conductivity of carrot puree during freezing using inverse problem. *International Journal of Food Science and Technology* 44(7), 1292-1303.
- Markakis, P., Livingston., G., Fellers., C., (1957). Quantitative aspects of strawberry-pigment degradation. *Food Research* 22, 117-130.
- Maroulis, Z.B., Saravacos, G.D., Krokida, M.K., Panagiotou, N.M., (2002). Thermal conductivity prediction for foodstuffs: Effect of moisture content and temperature. *International Journal of Food Properties* 5(1), 231-245.
- Marti, N., Perez-Vicente, A., Garcia-Viguera, C., (2002). Influence of storage temperature and ascorbic acid addition on pomegranate juice. *Journal of the Science of Food and Agriculture* 82(2), 217-221.
- Mattea, M., Urbicain, M.J., Rotstein, E., (1986). Prediction of thermal-conductivity of vegetable foods by the effective medium theory. *Journal of Food Science* 51(1), 113-&.
- McGhie, T.K., Walton, M.C., (2007). The bioavailability and absorption of anthocyanins: Towards a better understanding. *Molecular Nutrition & Food Research* 51(6), 702-713.

- Mishra, D.K., Dolan, K.D., Yang, L., (2008). Confidence intervals for modeling anthocyanin retention in grape pomace during nonisothermal heating. *Journal of Food Science* 73(1), E9-E15.
- Mishra, D.K., Dolan, K.D., Yang, L., (2011). Bootstrap confidence intervals for the kinetic parameters of degradation of anthocyanins in grape pomace. *Journal of Food Process Engineering* 34(4), 1220-1233.
- Mohamed, I.O., (2009). Simultaneous estimation of thermal conductivity and volumetric heat capacity for solid foods using sequential parameter estimation technique. *Food Research International* 42(2), 231-236.
- Naveh, D., Kopelman, I.J., Pflug, I.J., (1983). The finite-element method in thermal-processing of foods. *Journal of Food Science* 48(4), 1086-1093.
- Nawirska A. , K.M., (2005). Dietary fibre fractions from fruit and vegetable processing waste. *J of Food Chemistry* 91, 221–225.
- Ochoa, M.R., Kessler, A.G., Vullioud, M.B., Lozano, J.E., (1999). Physical and chemical characteristics of raspberry pulp: Storage effect on composition and color. *Food Science and Technology-Lebensmittel-Wissenschaft & Technologie* 32(3), 149-153.
- Ou, B.X., Hampsch-Woodill, M., Prior, R.L., (2001). Development and validation of an improved oxygen radical absorbance capacity assay using fluorescein as the fluorescent probe. *Journal of Agricultural and Food Chemistry* 49(10), 4619-4626.
- Palamidis, N., Markakis , P., (1978). Stability of grape anthocyanin in carbonated beverages. *Semana Vitivinicola* 33, 2637-2639.
- Patras, A., Brunton, N.P., O'Donnell, C., Tiwari, B.K., (2010). Effect of thermal processing on anthocyanin stability in foods; mechanisms and kinetics of degradation. *Trends in Food Science & Technology* 21(1), 3-11.
- Peleg, M., Corradini, M.G., Normand, M.D., (2009). Isothermal and non-isothermal kinetic models of chemical processes in foods governed by competing mechanisms. *Journal of Agricultural and Food Chemistry* 57(16), 7377-7386.
- Periago, P.M., Leontidis, S., Fernandez, P.S., Rodrigo, C., Martinez, A., (1998). Kinetic parameters of *Bacillus stearothermophilus* spores under isothermal and non-isothermal heating conditions. *Food Science and Technology International* 4(6), 443-447.

- Piasecka, M., Maciejewska, B., (2012). The study of boiling heat transfer in vertically and horizontally oriented rectangular minichannels and the solution to the inverse heat transfer problem with the use of the Beck method and Trefftz functions. *Experimental Thermal and Fluid Science* 38, 19-32.
- Rahman, M.S., (1992). Thermal-conductivity of 4 food materials as a single function of porosity and water-content. *Journal of Food Engineering* 15(4), 261-268.
- Rahman, M.S., (1995a). *Food Properties Handbook. "Phase Transitions In Foods"* Boca Raton, FL: CRC Press., pp. 87-173.
- Rahman, M.S., (1995b). *Food Properties Handbook. "Thermal diffusivity of Foods"* Boca Raton, FL: CRC Press., pp. 339-1390.
- Rahman, M.S., Chen, X.D., Perera, C.O., (1997). An improved thermal conductivity prediction model for fruits and vegetables as a function of temperature, water content and porosity. *Journal of Food Engineering* 31(2), 163-170.
- Reymond, O., Murray, D.B., O'Donovan, T.S., (2008). Natural convection heat transfer from two horizontal cylinders. *Experimental Thermal and Fluid Science* 32(8), 1702-1709.
- Sadilova, E., Stintzing, F.C., Carle, R., (2006). Thermal degradation of acylated and nonacylated anthocyanins. *Journal of Food Science* 71(8), C504-C512.
- Sawaf, B., Ozisik, M.N., Jarny, Y., (1995). An inverse analysis to estimate linearly temperature-dependent thermal-conductivity components and heat-capacity of an orthotropic medium. *International Journal of Heat and Mass Transfer* 38(16), 3005-3010.
- Shariaty-Niassar, M., Hozawa, M., Tsukada, T., (2000). Development of probe for thermal conductivity measurement of food materials under heated and pressurized conditions. *Journal of Food Engineering* 43(3), 133-139.
- Siddiq, M., Iezzoni, A., Khan, A., Breen, P., Sebolt, A.M., Dolan, K.D., Ravi, R., (2011). Characterization of new tart cherry (*Prunus cerasus* L.) selections based on fruit quality, Total Anthocyanins, and Antioxidant Capacity. *International Journal of Food Properties* 14(2), 471-480.
- Simpson, R., Cortes, C., (2004). An inverse method to estimate thermophysical properties of foods at freezing temperatures: apparent volumetric specific heat. *Journal of Food Engineering* 64(1), 89-96.

- Simunic, V., Kovac, S., Gaso-Sokac, D., Pfannhauser, W., Murkovic, M., (2005). Determination of anthocyanins in four Croatian cultivars of sour cherries (*Prunus cerasus*). *European Food Research and Technology* 220(5-6), 575-578.
- Singh, P.C., Singh, R.K., Bhamidipati, S., Singh, S.N., Barone, P., (1997). Thermophysical properties of fresh and roasted coffee powders. *Journal of Food Process Engineering* 20(1), 31-50.
- Singh, R.P., heldman, D.R., (2001). Introduction to Food Engineering , 3rd Edition in "Heat Transfer in Food Processing". Academic Press, Inc., New York, NY, pp. 283-296.
- Socaciu, C., (2008). Anthocyanins in Foods. In *Food Colorants Chemical and Functional Properties*. Socaciu, C., Ed.; CRC Press, Taylor and Francis: Boca Raton, FL, pp. 241-256.
- Subramanian, S., Viswanathan, R., (2003). Thermal properties of minor millet grains and flours. *Biosystems Engineering* 84(3), 289-296.
- Sweat, V.E., (1975). Modeling the thermal conductivity of meats. *TRANSACTIONS of the ASAE* 18(3), 564-568.
- Sweat, V.E., (1995). Thermal properties of foods. In *Engineering Properties of Foods* (M.A. Rao and S.S. Rizvi). Marcel Dekker Inc New York, NY., 99-138.
- Telejko, T., (2004). Analysis of an inverse method of simultaneous determination of thermal conductivity and heat of phase transformation in steels. *Journal of Materials Processing Technology* 155, 1317-1323.
- Tomas-Barberan, F.A., Gil, M.I., Cremin, P., Waterhouse, A.L., Hess-Pierce, B., Kader, A.A., (2001). HPLC-DAD-ESIMS analysis of phenolic compounds in nectarines, peaches, and plums. *Journal of Agricultural and Food Chemistry* 49(10), 4748-4760.
- Varga, S., Oliveira, J.C., (2000). Determination of the heat transfer coefficient between bulk medium and packed containers in a batch retort. *Journal of Food Engineering* 44(4), 191-198.
- Wang, H.B., Nair, M.G., Iezzoni, A.F., Strasburg, G.M., Booren, A.M., Gray, J.I., (1997). Quantification and characterization of anthocyanins in Balaton tart cherries. *Journal of Agricultural and Food Chemistry* 45(7), 2556-2560.

- Wang, H.B., Nair, M.G., Strasburg, G.M., Chang, Y.C., Booren, A.M., Gray, J.I., DeWitt, D.L., (1999). Antioxidant and antiinflammatory activities of anthocyanins and their aglycon, cyanidin, from tart cherries. *Journal of Natural Products* 62(5), 294–296.
- Wang, W.D., Xu, S.Y., (2007). Degradation kinetics of anthocyanins in blackberry juice and concentrate. *Journal of Food Engineering* 82(3), 271-275.
- Welti-Chanes, J., Vélez-Ruiz, J.F., Barbosa-Cànovas, G.V., (2003). Transport Phenomena in Food Processing "Thermal Processing of Particulate Foods by Steam Injection. Part 2. Convective Surface Heat Transfer Coefficient for Steam". (CRC Press LLC, Washington,), pp. 331-343.
- Wrolstad, R.E., (2004). Symposium 12: Interaction of natural colors with other ingredients - Anthocyanin pigments - Bioactivity and coloring properties. *Journal of Food Science* 69(5), C419-C421.
- Yang, C.Y., (1998). A linear inverse model for the temperature-dependent thermal conductivity determination in one-dimensional problems. *Applied Mathematical Modelling* 22(1-2), 1-9.
- Yang, C.Y., (2000). Determination of the temperature dependent thermophysical properties from temperature responses measured at medium's boundaries. *International Journal of Heat and Mass Transfer* 43(7), 1261-1270.
- Yang, W., Sokhansanj, S., Tang, J., Winter, P., (2002). Determination of thermal conductivity, specific heat and thermal diffusivity of borage seeds. *Biosystems Engineering* 82(2), 169-176.
- Zafra-Stone, S., Yasmin, T., Bagchi, M., Chatterjee, A., Vinson, J.A., Bagchi, D., (2007). Berry anthocyanins as novel antioxidants in human health and disease prevention. *Molecular Nutrition & Food Research* 51(6), 675-683.
- Zhang, Z., Kou, X.L., Fugal, K., McLaughlin, J., (2004). Comparison of HPLC methods for determination of anthocyanins and anthocyanidins in bilberry extracts. *Journal of Agricultural and Food Chemistry* 52(4), 688-691.
- Zhao, X.Y., Corrales, M., Zhang, C., Hu, X.S., Ma, Y., Tauscher, B., (2008). Composition and thermal Stability of anthocyanins from Chinese purple corn (*Zea mays* L.). *Journal of Agricultural and Food Chemistry* 56(22), 10761-10766.
- Zulueta, A., Esteve, M.J., Frígola, A., (2009). ORAC and TEAC assays comparison to measure the antioxidant capacity of food products. *Food Chemistry* 114(1), 310-316.

CHAPTER 3

OBJECTIVE ONE

Effect of Non-Isothermal Heat Processing and Moisture Content on the Anthocyanin Degradation and Color Kinetics of Cherry Pomace

Abstract

Anthocyanins (ACY) and color changes in cherry pomace under non-isothermal processing were investigated. Pomace at moisture content (MC) levels of 70 (MC-70), 41 (MC-41) and 25% (MC-25) was heated at 127°C in a retort for 25, 40, and 60 min. Total ACY, Hunter color values, total color difference (ΔE), Chroma, hue angle (h°) and browning index (BI) were analyzed. Thermal degradation kinetics for color parameters were determined using zero- and first-order models. ACY degradation increased with heating time and ranged from 34 to 68% for 25 and 60 min heating, respectively. The ΔE increased with increasing heating time, whereas BI exhibited an inverse trend. Except for ΔE for MC-70, the zero-order kinetic model showed better fit ($R^2=0.85-0.97$) to experimental data than did first-order for Hunter color b values and ΔE .

Key words: Anthocyanins, color, degradation, non-isothermal heating.

3.1 Introduction

Consumer interest in nutraceuticals has spurred the food industry to improve nutritional content of foods. Byproducts of fruits and vegetables can be used as low-cost sources of nutraceuticals. An example is cherry pomace, which contains high levels of anthocyanins. Cherry (*Prunus cerasus* L.) pomace is the solid waste or by-product of cherry juice processing and consists of cherry skin and seeds. It accounts for over 90% of dry cherry matter, with high concentration of lignin, cellulose, and dry fiber components (Nawirska A., 2005). Cherries are known to contain substantial quantities of anthocyanins (Wang et al., 1999), which are mainly concentrated in the skins (Chaovanalikit and Wrolstad, 2004; Tomas-Barberan et al., 2001) and constitute a major portion of bioactive compounds in the pomace. Cherry pomace, an otherwise waste material, could be processed into value-added ingredients for use in different food products as colorant and/or functional ingredient. For example, addition of tart cherry tissue to cooked beef patties has been shown to inhibit lipid and cholesterol oxidation (Britt et al., 1998). Cherry pomace powder or extract may also be added to many kinds of foods dried or processed at elevated temperatures. Examples include breakfast cereals, snacks, drink mixes, confectionaries, breads or other baked goods, or used as a slow-release antioxidant in the packaging films.

Anthocyanins are the most abundant flavonoid constituents of fruits and vegetables. They are natural colorants and impart a bright-red to purple color to foods. Anthocyanins are known for their antioxidant activity and anti-inflammatory properties (Wang et al., 1999) and may play a role in prevention of heart disease, cancer and diabetes (Chaovanalikit and Wrolstad, 2004; Konczak and Zhang, 2004). Anthocyanin

stability is of significant importance in processed foods. However, food processing often involves the use of thermal treatments, which are detrimental to stability of anthocyanins; such an effect is a function of processing temperature as well other factors, including pH, and moisture content (Patras et al., 2010).

Anthocyanins are sensitive to temperatures above 70 °C (Markakis et al., 1956). Cemeroglu *et al.*, (Cemeroglu et al., 1994) studied the effect of isothermal treatment on sour cherry juice concentrate and observed that only 30% of the original anthocyanins were retained at 50 °C after 48 hours and less than 10% at 70 °C after 16 hours; the rate of anthocyanin degradation followed first-order kinetics. (Bonerz et al., 2007) studied anthocyanins in cherry juice during storage and observed about 70-75% reduction in their levels during storage at 20°C. Anthocyanins degradation may be modeled using the Arrhenius relationship (Ahmed et al., 2004). (Tsami and Katsioti, 2000) suggested that the color of the dehydrated product can be predicted by controlling the process conditions. Other studies have reported anthocyanin degradation in cherries, cherry juice and jams, but the kinetic parameters have not been estimated (Forni et al., 1993; Kim and Padilla-Zakour, 2004).

The degradation of anthocyanins at elevated temperatures in both solids and liquids has been seldom investigated. Therefore, this paper aims to provide a methodology to determine the degradation of anthocyanins in cherry solids at different constant moisture contents over a large (~100 °C) temperature range, typical of the processes previously mentioned. The methodology includes an example anthocyanin byproduct source (cherry pomace), an example container to maintain constant moisture (a can), and an example heat source to elevated temperatures near 130 °C (steam).

The same methodology could be used for different nutraceutical sources, containers, and heating methods. The results can be used to help design both drying and food production unit operations for value-added foods. It is to be noted that most previous related studies used isothermal conditions to monitor anthocyanin degradation; however, the present study was done under non-isothermal conditions. This study investigated the effect of thermal treatment and moisture content on anthocyanin degradation in cherry pomace and examined the correlations between anthocyanin content and instrumental color.

3.2 Materials and Methods

3.2.1 Pomace sample preparation

Montmorency cherry pomace was obtained from Cherry Growers Inc., (Grawn, Michigan, U.S.A.). The moisture content (MC) of the samples was measured using a Sartorius Moisture Analyzer – MA30 (Sartorius AG, Goettingen, Germany). The initial MC of cherry pomace was 70% (wet basis, control). Two additional samples with MC of 41 and 25% (MC-41 and MC-25) were prepared using a pilot-scale cabinet dryer (Proctor and Schwartz Inc., Philadelphia, Penn, U.S.A.) at $50 \pm 2^\circ\text{C}$. Pomace samples MC-70, MC-41, and MC-25 represent pomace with 70, 41, and 25% MC (wb), respectively. Then each of the three cherry pomace samples were filled and sealed under vacuum (20-mm Hg) in 202 ×214 steel cans (54-mm diameter and 73-mm height) and heated at 126.7°C , for heating time intervals (0, 25, 40 and 60 min) using a rotary steam retort (FMC Steritort Laboratory Sterilizer, Madera, Calif, U.S.A.). Each can was fitted with a needle thermocouple (Ecklund-Harrison Technologies Inc., Fort Myers, Florida, U.S.A.) to measure the center temperature. The time-temperature profile of

retorting process (samples and retort) is shown in Figure 4.1. All experiments were done in duplicate. The complete experimental design is shown in Appendices A (Figure A.1). Plots of all running times are shown in Figure A.2 in Appendices. Example of Raw data for retorting in duplicate for each moisture content showed in Table A.2 in the Appendices.

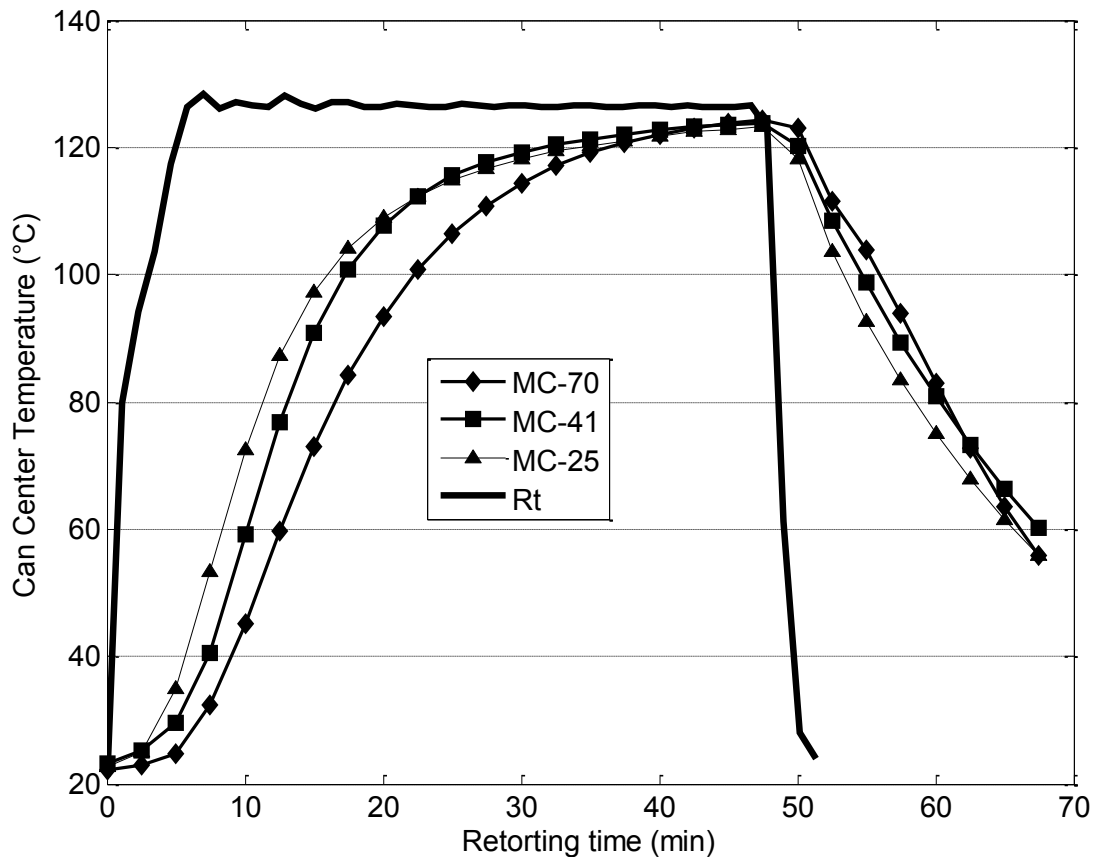


Figure 3.1 Can-center temperature profile of cherry pomace in a rotary steam retort at 126.7 °C for 40 min after 8 min come-up-time. (RT=Retort temperature; MC-70, MC-41, and MC-25 represent cherry pomace with 70, 41, and 25% moisture (wet basis) , respectively).

3.2.2 Measurement of visual color

Hunter color *L* (lightness/darkness), *a* (redness/greenness), and *b* (yellowness/blueness) parameters were determined using a Hunter Color Meter (Model: D25 L

optical sensor, Hunter Associates Lab., Reston, Virginia, U.S.A.). Control samples of cherry pomace and retorted samples were analyzed for color stability at each heating time intervals. The instrument was calibrated using black and white standard calibration tiles. Pomace samples were spread uniformly in a standard sample cup (105 mm diameter) and measurements for L , a , and b values were recorded. The data thus obtained were used to calculate total color difference (ΔE), Chroma, hue angle (h°), and browning index (BI), using the following equations (Maskan, 2001):

$$\text{Total Color Difference } (\Delta E) = \sqrt{(L_0 - L_t)^2 + (a_0 - a_t)^2 + (b_0 - b_t)^2} \quad (3.1)$$

$$\text{Chroma} = \sqrt{a^2 + b^2} \quad (3.2)$$

$$\text{Hue Angle } (h^\circ) = \tan^{-1} \left(\frac{a}{b} \right) \quad (3.3)$$

$$\text{Browning Index (BI)} = \frac{100 (x - 0.31)}{0.17} \quad (3.4)$$

$$\text{Where } x = \frac{(a + 1.75 \times L)}{(5.645L + a - 3.012b)}$$

3.2.3 Anthocyanins extraction

Anthocyanins (ACY) from pomace samples were extracted using the method of Chaovanalikit & Wrolstad (2004), with some modification. Briefly, fresh and heat treated samples of cherry pomace were dried (41 °C) and then ground using a coffee grinder (Krupps, Medford, Mass, U.S.A.) to a coarse-particle size powder. Ground pomace (20 g) was suspended in 80 mL of acetone stock solution (70% aqueous acetone, 0.01% hydrochloric acid, and 30% distilled water). The pomace slurry was stored overnight (–

20°C) in sealed glass jars, wrapped in aluminum foil to protect the sample from light, to achieve an equilibrium state. The slurry was filtered through Whatman no. 4 filter paper (Whatman Inc., Clifton, New Jersey, U.S.A.) using a Buchner funnel (under vacuum), followed by a wash with 50 mL of stock buffer. The filtrate volume was made up to a final volume of 130 mL and mixed with 40 mL of chloroform and stored overnight. The supernatant was collected and used for the determination of monomeric anthocyanin content.

3.2.4 Monomeric anthocyanin content determination

The total monomeric anthocyanin content was determined using the pH differential assay (Rodriguez-Saona et al., 1999). Pomace samples were dissolved in potassium chloride buffer (KCl, 0.025 M, pH 1.0) and sodium acetate ($\text{CH}_3\text{CO}_2\text{Na}_3 \cdot \text{H}_2\text{O}$, 0.4 M, pH 4.5) and allowed to equilibrate, with a predetermined dilution factor. The absorbance of each equilibrated sample of extracted ACY was then measured at 510nm and 700 nm for haze correction, using a Genesys 5 spectrophotometer (Spectronic Instruments, Rochester, NY, USA) and 1 cm path-length cells were used for spectral measurements. ACY contents was calculated, as cyanidin 3-glucoside equivalent (Lee et al., 2005), and reported as mg/100 g (dry-basis).

3.2.5 Antioxidant Capacity

The Oxygen Radical Absorbance Capacity (ORAC) assay using fluorescein as fluorescent probe (ORAC_{FL}) was used to determine the antioxidant capacity (Cao et al., 1993; Huang et al., 2002). The equipment used for this analysis was BioTekFL×800 Multi-Detection Microplate Reader (Biotek Instruments, Winooski, Vermont, USA). The

antioxidant capacity of cherry pomace was determined as Oxygen Radical Absorbance Capacity (ORAC) values. The results are generally expressed as Trolox equivalent (TE) – $\mu\text{m TE/g}$ sample. Plot of the calibration curve (Figure A.3) and AUC (Figure A.4) are shown in Appendices.

3.2.6 Color kinetics

Previous studies have evaluated the kinetics of color degradation in food materials through zero order (Eq.(3.5)) and first order (Eq.(3.6)) models (Maskan, 2001).

$$C_t = C_0 + k_0 t \quad (3.5)$$

$$\ln C_t = \ln C_0 + k_1 t \quad (3.6)$$

Where, C_t is measured value of color at time t , C_0 is initial value of color at time zero, t is heating time (min), k_0 the zero order kinetic constant (min^{-1}) and k_1 the first order kinetic constant (min^{-1}). Color measurements can be used for monitoring color changes in foods, because it is simpler and faster than chemical analysis. Hunter color measurements provided valuable data on describing color degradation during different food processing treatments, such as canned strawberries (Kammerer et al., 2007), mangosteen peel (Chiste et al., 2010), cupuacu puree (Silva and Silva, 1999). The relationship between anthocyanins concentration and the a value, which represents the redness of cherry pomace, was described by Eqs.(3.7) and (3.8) as follows (Bechtold et al., 2007):

$$\text{ACY}_t / \text{ACY}_0 = b_1 (a/a_0) - b_2 \quad (3.7)$$

$$ACY_t / ACY_0 = b_1 \times \exp[b_2 \times (a/a_0)] \quad (3.8)$$

Where: ACY_t is measured value of anthocyanins at time t , ACY_0 is initial value of anthocyanins at time zero, a is the Hunter color a -value at time t , a_0 is the initial (control) Hunter color a -value, and b_1 and b_2 are the parameters to be estimated.

Statistical analysis

All data were analyzed using JMP 9.0 software (SAS Institute, Inc., Cary, North Carolina, U.S.A.). One-way analysis of variance was used to analyze the data. The separation of means or significant difference comparisons were made by Tukey's HSD test ($\alpha=0.05$).

3.3 Results and Discussion

3.3.1 Anthocyanin (ACY) degradation

Initial ACY content in the control cherry pomace (MC-70) was 6.54 mg/100 g (dry-basis). Thermal treatment in the rotary steam retort at 126.7 °C for 60 min degraded the ACY to 2.38 mg/100 g. This process reduced the ACY to 6.21 mg/100 g for MC-41 and 5.84 mg/100g for MC-25 pomace (Figure 4.2). The ACY degradation was significantly ($p \leq 0.05$) higher in the lower-moisture pomace samples (MC-41 and MC-25) than in the control (MC-70) at 25-min heating, whereas no differences were observed for 0, 40, or 60 min heat treatment. Generally, the ACY loss was rapid during the first 25 min of heating, regardless of the moisture content. Heat treatment (60 min) further degraded the ACY to 1.73 mg/100 g in MC-41 and to 1.59 mg/100g in MC-25.

The fate of ACY in cherry pomace has not been studied previously; however, Cemeroglu *et al.*, (1994) observed that at 37 °C, the half-life of ACY drops from 38 to 11

days in cherry juice concentrate. Greater ACY loss was observed with both an increase in thermal treatment time and the moisture content of cherry pomace. Similar observations were reported by (Kirca and Cemeroglu, 2003).

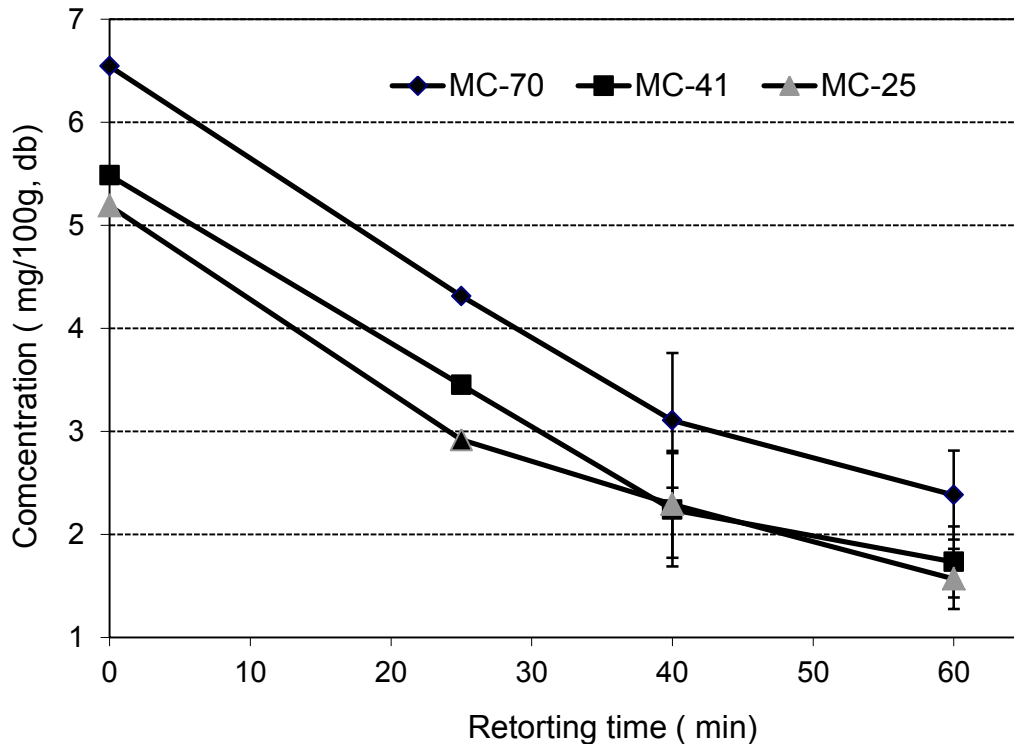


Figure 3.2 Degradation of cherry pomace anthocyanin (ACY) after non-isothermal treatment in a retort at 126.7 °C. (MC-70, MC-41, and MC-25 represent cherry pomace with 70, 41, and 25% moisture (wb), respectively)

3.3.2 Antioxidant Capacity

MC-25 pomace after retorting at 126.7 °C at different times showed no significant difference in ORAC_{FL} values ($p > 0.05$) as showed in Figure 3.3. The average values are about 33.24 ± 0.21 (TE- $\mu\text{m TE/g, db}$) at zero time for MC-25 Pomace and 33.75 ± 3.02 , 33.44 ± 4.13 (TE- $\mu\text{m TE/g, db}$) for 40 and 60 min heating, respectively (Table A.3 Appendix A.2). This result showed kind of stability and a small elevation in the ORAC_{FL}

value, which has an agreement and similarity with a prior study on grape pomace after it was heated for about 60 min with no significant change in ORAC_{FL} values (Mishra et al., 2008). A study on sweet corn showed elevation in antioxidant capacity after processing for 25 min at 115 °C (Dewanto et al., 2002)

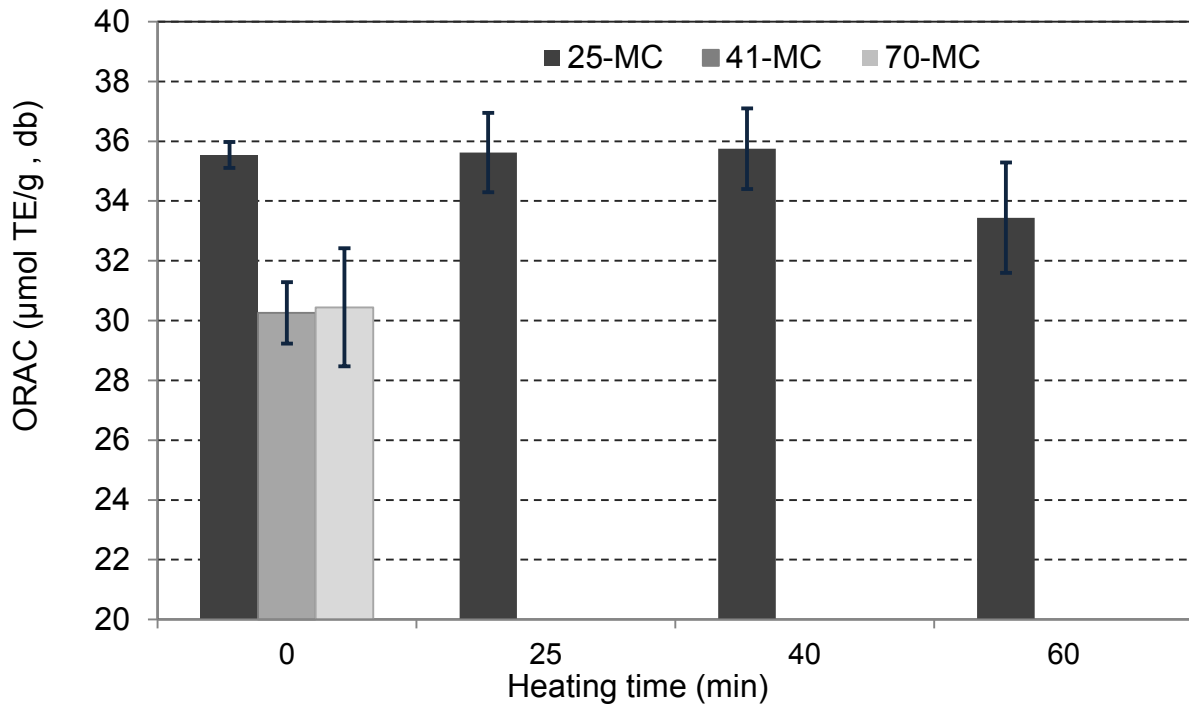


Figure 3.3 The average total antioxidant values of the cherry pomace (70 and 41%MC not heated) and 25% MC (wb) after different heating times

3.3.3 Instrumental Color Changes

Hunter color measurements provided valuable data on describing color degradation during different food processing treatments, in particular non-isothermal processing such as canning of strawberries (Kammerer *et al.*, 2007), mangosteen peel (Chiste *et al.*, 2010), cupuacu puree (Silva & Silva, 1999). Drying of cherry pomace affected the instrumental color values (Table 3.1). MC-25 (wb) pomace was significantly different ($p \leq 0.05$) with respect to decrease in Hunter *L*, *a*, *b* values, hue angle and

chroma when compared with the control (MC-70) and MC-41 pomace samples. The moisture content of cherry pomace did not have a significant ($p \leq 0.05$) effect on the Hunter L values when compared across heating time. However, the cumulative effect of 60 min heat treatment significantly ($p \leq 0.05$) decreased the L value from 16.73 to 14.37 (MC-70), from 16.37 to 12.90 (MC-41), and from 15.07 to 12.93 (MC-25). These decreases in L values (lightness) have been correlated with pigment degradation and may be considered as a measure of browning (Ibarz et al., 1999; Maskan, 2006; Mohammadi et al., 2008). Similarly, a significant decrease in Hunter a value (redness/greenness scale) and b value (yellowness/blueness) was observed with increasing heating time. MC-25 pomace showed the greatest decrease in both Hunter color a and b values after 60 min of heating at 126.7 °C.

Hunter color a and b values were converted to hue angle and chroma, which represent an average person's perception of type and richness of color, respectively (Mcguire, 1992). The significant changes in Hunter color a and b values were not reflected in the hue angle. Cherry pomace had hue angle of 42-48°, which indicated that the pomace had a color between red-purple (0°) and yellow (90°) (Mcguire, 1992). Chroma, which measures the degree of change from gray to chromatic color, decreased by 47% for MC-70, 40% for MC-41 and 50% for MC-25 after 60 min heat treatment. Total color change (ΔE) increased significantly with heating time (Figure 3.3). Browning Index (BI) is a function of L , a and b values as defined in equation (3.4). Therefore, with increasing heat treatment time, Hunter color values decreased and as a result, BI decreased. BI represents the purity of brown color but, it is not an indicator of a darkness of the sample since BI increases with L value at fixed a and b values.

Table 3.1 Hunter color *L*, *a*, *b* values, hue angle and chroma of cherry pomace after heat treatment at 126.7 °C.

	Heating time (min)	MC-70 ¹	MC-41 ²	MC-25 ³
Hunter Color <i>L</i> :	0	16.73 ±0.2Aa	16.37±0.03Aa	15.07±0.03Ab
	25	16.03±0.4ABa	15.50±0.3Ba	15.57±0.1Aa
	40	14.40±0.4Ba	14.73±0.2Ba	14.00±0.2Ba
	60	14.37±0.7Ba	12.90±0.1Ca	12.93±0.2Ca
Hunter Color <i>a</i> :	0	7.93±0.1Aa	6.27±0.1Ab	5.53±0.03Ac
	25	6.90±0.3BAa	6.27±0.03Aba	5.57±0.1Ab
	40	6.17±0.3BCa	6.17±0.1Aa	4.73±0.03Bb
	60	5.70±0.3Ca	4.97±0.03Ba	3.97±0.1Cb
Hunter Color <i>b</i> :	0	7.67±0.1Aa	6.90±0.1Ab	5.70±0.1Ac
	25	6.63±0.2Ba	6.17±0.03Ba	5.47±0.03Ab
	40	5.67±0.2Ca	5.60±0.1Ca	4.70±0.1Bb
	60	5.53±0.3Ca	4.60±0.1Db	3.83±0.1Cc
Hue Angle (h°):	0	44.0±0.32Ac	47.7±0.32 Aa	45.8±0.34 ABb
	25	43.9±0.34 Aab	44.5±0.27 Bb	44.5±0.52 Ba
	40	42.6±0.38 Aab	42.2±0.58 Cb	44.8±0.54 Ba
	60	44.2±0.43 Aa	42.8±0.41 BCa	44.0±0.26 Ba
Chroma:	0	11.0±0.11 Aa	9.3±0.12 Ab	7.9±0.05 Ac
	25	9.6±0.32 Ba	8.8±0.02 Ba	7.8±0.06 Ab
	40	8.4±0.32 BCa	8.3±0.03 Ca	6.7±0.02 Bb
	60	7.9±0.39 Ca	6.8±0.05 Db	5.5±0.11 Cc

^{1,2,3} MC-70, MC-41, and MC-25 represent cherry pomace with 70, 41, and 25% moisture (wb), respectively. Values are means ± SE of 3 replicates. Means with different letters (a–c) in rows and (A–D) in columns are significantly different ($p \leq 0.05$)

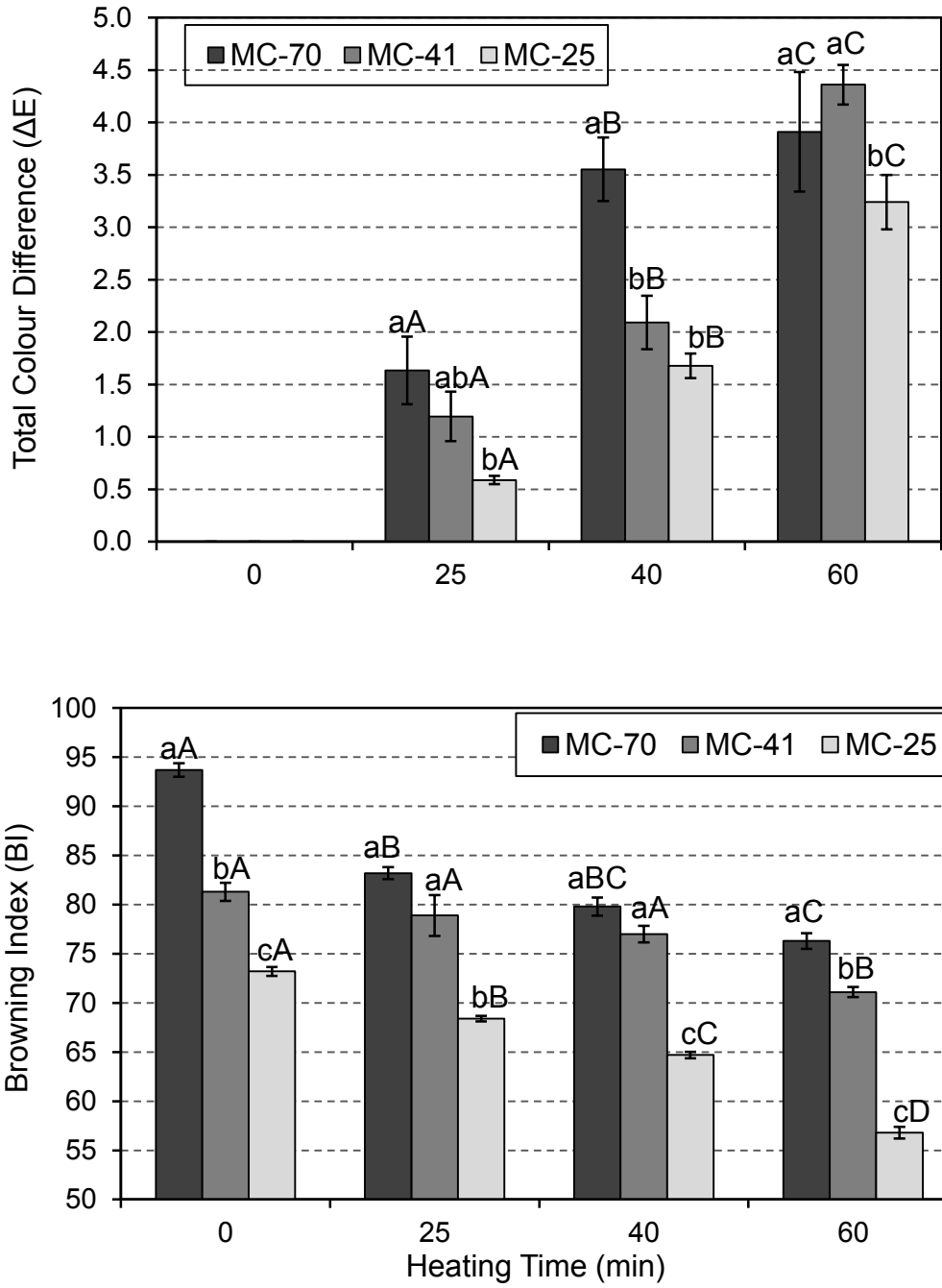


Figure 3.4 Total color difference (ΔE) and browning index (BI) of cherry pomace after retorting at 126.7 °C. (MC-70, MC-41, and MC-25 represent the moisture content % (wb), respectively). Means with different letters (a–c) at one heating time and (A–D) at different heating times, are significantly different ($p \leq 0.05$)

3.4 Kinetics of color degradation

Color values were fitted to equations describing the color change using zero- and first-order kinetics and linear regression analysis. The kinetic parameters estimated

from these data are presented in Table 3.2. Except for ΔE (MC-70), the zeroth-order kinetic model showed slightly better fit to experimental data than first-order for Hunter color b values and ΔE . Generally, the C_0 kinetic parameters of color degradation were larger for MC-70 pomace when compared to that of MC-41 and MC-25 for the zero-order model. However, a mixed trend was observed with the k_0 parameter. For the k_1 parameter, MC-25 pomace had the largest kinetic parameters for Hunter color a , and b values, and ΔE . Overall, Hunter color value b and ΔE showed good fits ($R^2=0.97-0.83$, range) for both zero- and first-order kinetics.

Deterioration of color occurs due to ACY and other pigments' degradation, oxidation of ascorbic acid and non-enzymatic Maillard browning reactions (Abers and Wrolstad, 1979; Barreiro et al., 1997; Skrede, 1985). Abers & Wrolstad (1979) and Skrede (1985) concluded that stable polymeric anthocyanins produced during heat treatment contribute to brown color formation and loss of detectable free anthocyanins measured by the pH differential method. However, Maskan (2006) and Cemeroglu *et al.*, (1994) noted that sugar and its degradation products might accelerate ACY breakdown and enhance non-enzymatic browning during heat processing. Ibarz *et al.*, (1999) suggested that zero-order model corresponded to formation of colored polymers of pigments and was followed by first-order for the degradation of these polymers into non-colored products. It is possible that ACY degradation may have proceeded via the polymer formation followed by degradation route while greater non-enzymatic browning may have occurred in the MC-25 pomace with higher soluble solids and therefore of sugar.

Table 3.2 The estimated kinetic parameters and the statistical values of zero-order and first-order models for Hunter color *L*, *a*, *b* values and total color change (ΔE) for various processing times of cherry pomace at three moisture contents (wb) at 126.7 °C.

	Zero-order Model								
	k0 min ⁻¹			C ₀			R ²		
	MC-70 ¹	MC-41 ²	MC-25 ³	MC-70	MC-41	MC-25	MC-70	MC-41	MC-25
Hunter <i>L</i>	-0.044±0.0108	-0.056±0.0066	-0.0367±0.0095	16.75±0.41	16.65±0.25	15.63±0.36	0.62	0.88	0.60
Hunter <i>a</i>	-0.038±0.0053	-0.012±0.0051	-0.0272±0.0042	7.87±0.20	6.54±0.19	5.81±0.16	0.83	0.61	0.81
Hunter <i>b</i>	-0.038±0.0051	-0.038±0.0019	-0.0317±0.0035	7.55±0.19	7.00±0.08	5.91±0.13	0.85	0.97	0.89
ΔE	0.069±0.0093	0.071±0.0066	0.0543±0.0055	0.10±0.36	-0.31±0.25	-0.32±0.21	0.85	0.92	0.90
	First-order Model								
	k1 min ⁻¹			C ₀			R ²		
	MC-70	MC-41	MC-25	MC-70	MC-41	MC-25	MC-70	MC-41	MC-25
Hunter <i>L</i>	-0.003±0.0007	-0.004±0.0004	-0.0027±0.0005	16.76±0.03	16.72±0.02	15.63±0.02	0.61	0.88	0.68
Hunter <i>a</i>	-0.006±0.0008	-0.004±0.0009	-0.0057±0.0008	7.89±0.03	6.58±0.04	5.86±0.03	0.83	0.61	0.80
Hunter <i>b</i>	-0.006±0.0008	-0.007±0.0005	-0.0067±0.0008	7.57±0.03	7.08±0.02	5.99±0.03	0.83	0.95	0.87
ΔE	0.009±0.001	0.008±0.0008	0.0091±0.0011	1.01±0.04	0.96±0.03	0.93±0.04	0.86	0.91	0.87

^{1,2,3} MC-70, MC-41, and MC-25 represent cherry pomace with 70, 41, and 25% moisture (wb), respectively. Values represent average of triplicate ± standard error.

3.5 Correlation between red color and anthocyanins

Hunter *a* value (redness/greenness) of cherry pomace as well as the ACY content decreased with increasing heating time. This effect was the most significant for the lowest moisture content sample (MC-25) as observed in Table 1 and Figure 3.4. The relationship between ACY and red color degradation was evaluated using regression analysis and Eq. 3.7 and Eq. 3.8, as shown in Figure 3.5. The ACY degradation showed a strong linear correlation, Eq.3.8 ($R^2=0.98$) with red color values for the fresh pomace sample, MC-70 (Table 3.3). Similar observations have been reported with thermal processing of plum puree by (Ahmed et al., 2004). A study on purple corn cob was also established a correlation between Hunter color parameters and contents of ACY and showed that that Hunter color parameters could be used of ACY contents during heating (Chen et al., 2008).

For MC-41 and MC-25 pomace, the correlation was exponential, as shown by Eq. 3.8. Similar correlations for color with ACY concentration in grape pomace were made by Bechtold *et al.*, (2007). Thus, anthocyanin degradation in cherry pomace during non-isothermal processing may be predicted from Hunter color *a* value using a linear relationship in Eq. 3.7 for high moisture samples and a exponential relationship Eq. 3.8 for lower moisture samples.

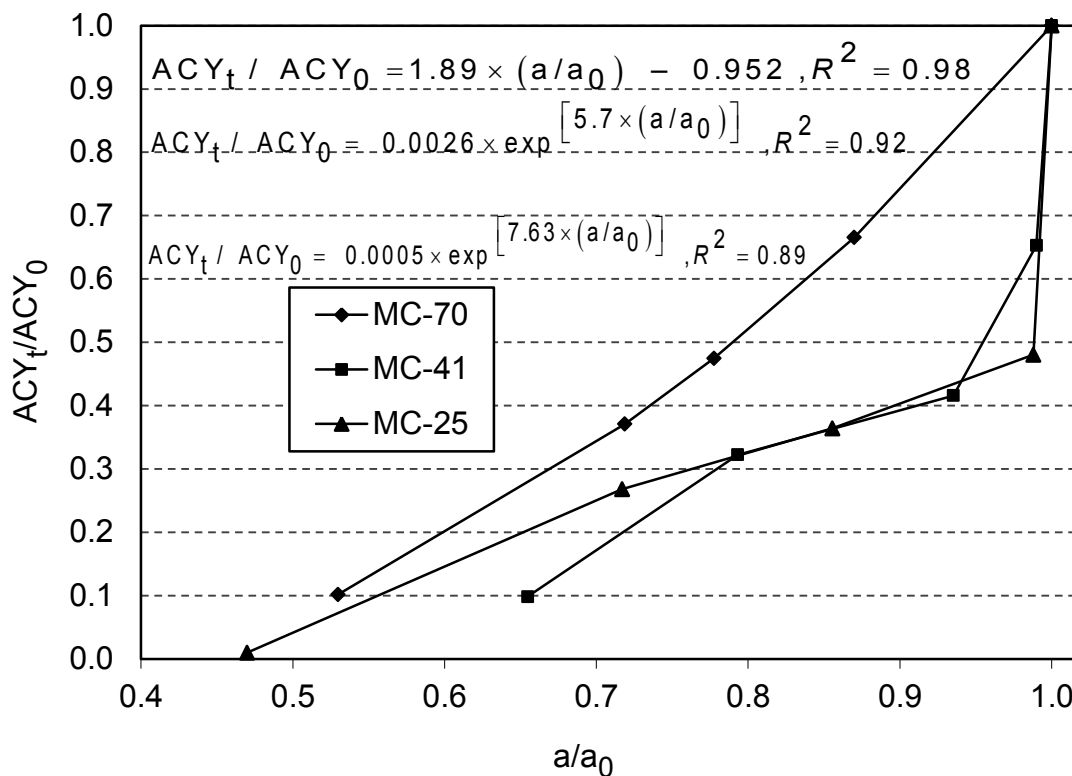


Figure 3.5 Correlation between Hunter color a values and anthocyanins content of cherry pomace after thermal processing at 126.7 °C. Data three replicate. (MC-70, MC-41, and MC-25 represent cherry pomace with 70, 41, and 25% moisture (wb), respectively)

Table 3.3 Coefficients of equations (3.7) and (3.8) for correlation between Hunter color a values and anthocyanins content

Pomace	Equation	b_1	b_2	R^2
MC-70 ¹	(3.7)	1.8929	0.9522	0.98
MC-70 ¹	(3.8)	0.0095	4.837	0.95
MC-41 ²	(3.7)	2.0302	1.2778	0.76
MC-41 ²	(3.8)	0.0026	5.7024	0.92
MC-25 ³	(3.7)	1.4016	0.7053	0.71
MC-25 ³	(3.8)	0.0005	7.636	0.89

^{1,2,3} MC-70, MC-41, and MC-25 represent cherry pomace with 70, 41, and 25% moisture, respectively.

3.6 Conclusions

Cherry pomace is an excellent source of ACY and has potential to be developed into value-added products. This is the first study on cherry pomace that assessed the effect of non-isothermal heat treatment on the free ACY content and color of pomace. Many products such as extruded foods, baked goods and powders are manufactured using processes that use non-isothermal heat treatment. Knowledge of the anthocyanin thermal degradation kinetics will help design such industrial processing of this industrial by-product. Overall, the extent of color degradation increased with heating time. A significant decrease in Hunter color L , a , b and chroma values was observed at each heating time. Loss of color due to heat treatment followed zero-order kinetics. Higher ACY degradation was observed with increasing heating time for all pomace samples at different moisture contents. ACY degradation may be correlated with changes in red color. It showed a linear relationship at higher moisture content (MC-70) of cherry pomace and an exponential relationship at lower moisture content of cherry pomace (MC-41 and MC-25).

APPENDICES

Appendix A.1 Experimental design and preliminary data

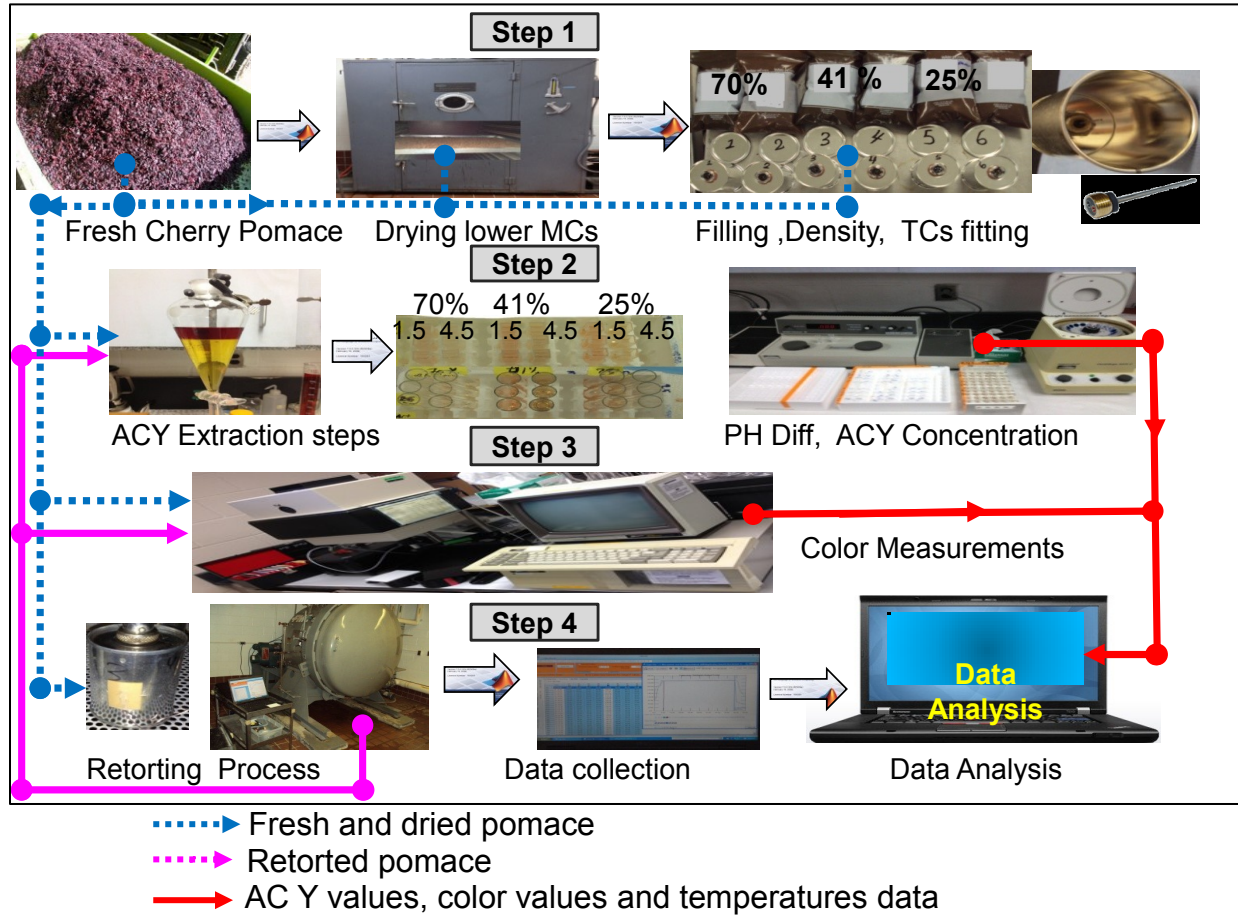


Figure A.1 Process experimental design for ACY and pomace's color degradation

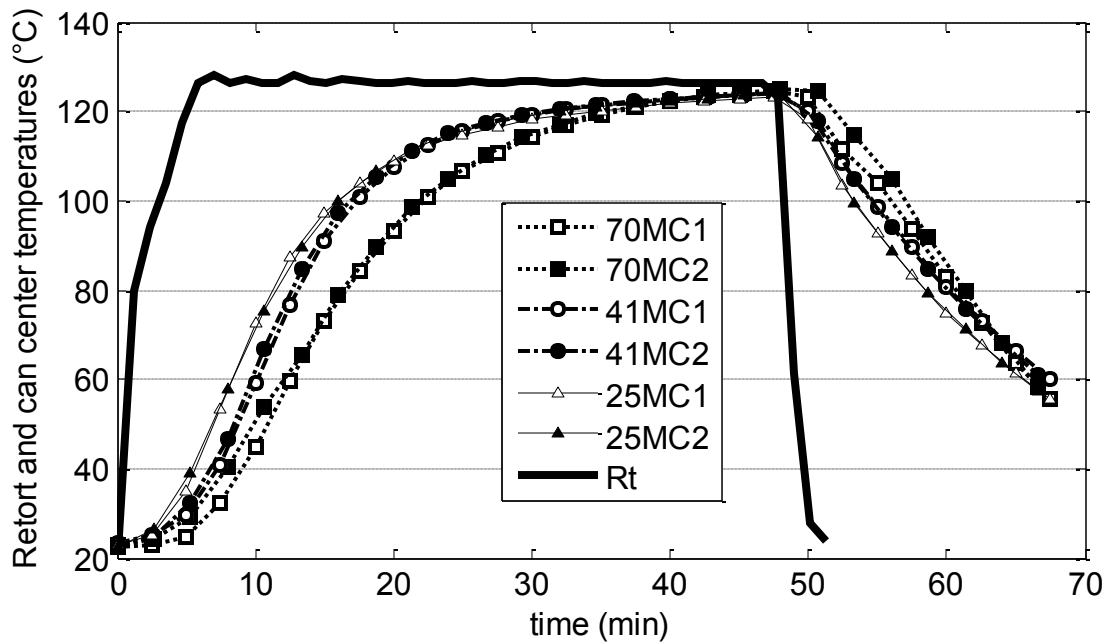
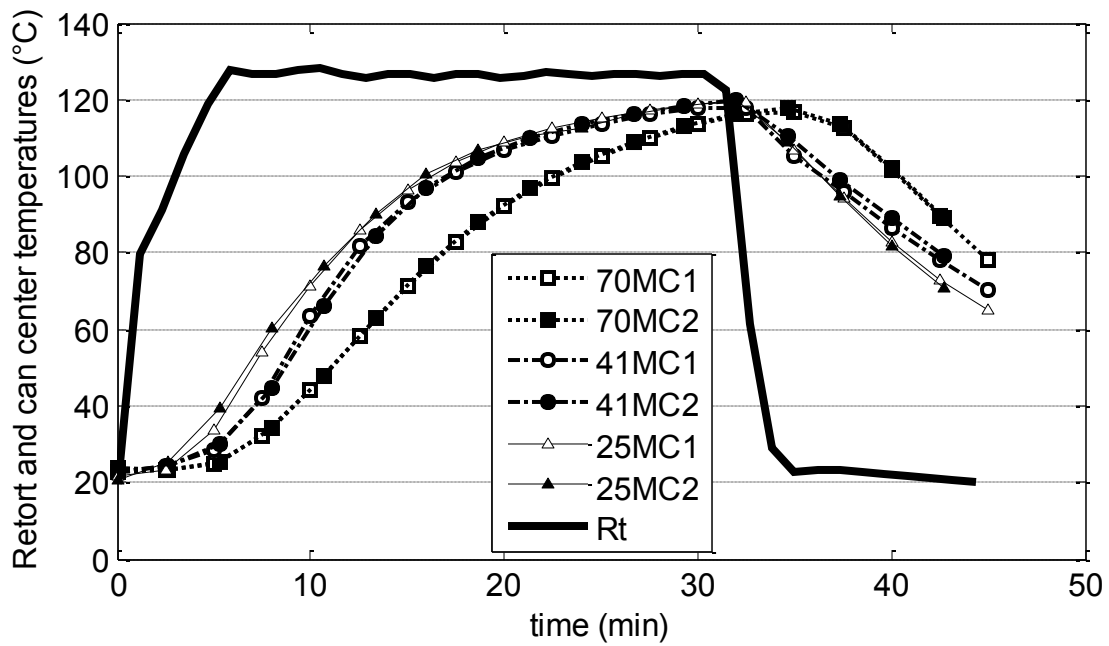


Figure A.2 Plots of retorting process of cherry pomace in a rotary steam retort at 126.7 °C for 25, 40, 60 and 90 min after 10 min come-up-time. (Rt=Retort temperature; MC-70, MC-41, and MC-25 represent cherry pomace with 70, 41, and 25% moisture (wb), respectively).

Figure A.2 (cont'd)

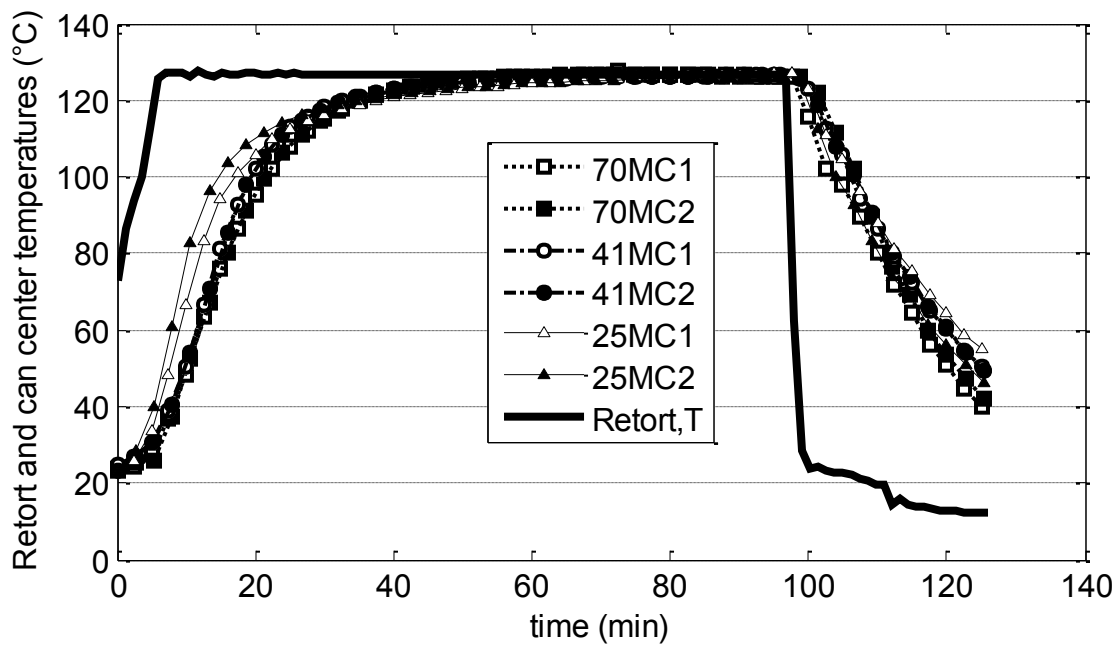
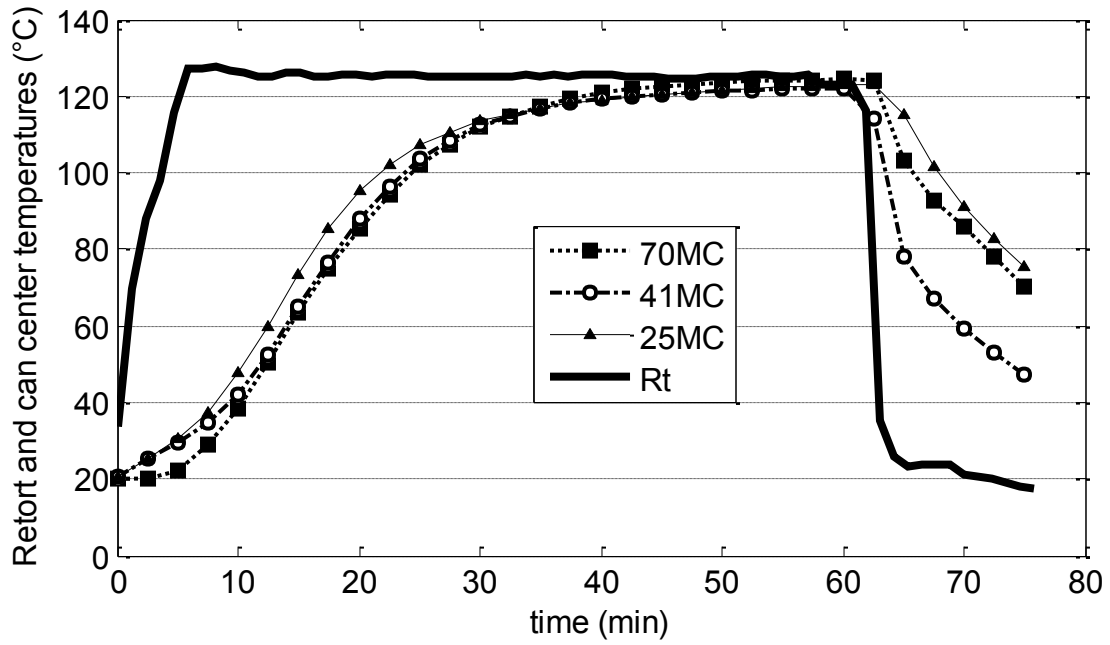


Table A.1 Cherry pomace 's anthocyanins concentration (mg/kg,db) after retorting process at different times

Time (min)	Retorting Temperature 126.7°C		
	Cherry pomace Moisture contents (MC %, wb)		
	70-MC	41-MC	25-MC
0	57.89	44.61	37.27
0	59.70	69.33	57.89
0	78.70	59.79	60.42
25	37.99	40.48	28.22
25	44.32	32.20	31.12
25	47.04	30.82	29.33
40	19.00	22.08	14.47
40	37.99	12.88	28.58
40	36.18	32.20	25.69
60	28.04	17.48	21.35
60	19.00	19.78	17.37
60	24.42	14.72	8.32
90	1.81	5.98	0.00
90	10.85	9.66	0.00
90	7.24	0.00	0.00

Table A.2 Raw data (sample) of retorting process of cherry pomace in a rotary steam retort at 126.7 °C

time(sec)	MC-70	MC-70	MC-41	MC-41	MC-25	MC-25	Ts	TRt
0	23.33	23.64	25.05	23.26	22.66	22.66	23.23	72.76
10	23.47	23.83	24.52	23.32	22.71	22.76	29.40	77.41
20	23.53	23.88	24.62	23.37	22.73	22.82	37.70	73.13
30	23.58	23.86	24.38	23.44	22.79	22.89	48.50	79.52
40	23.65	23.94	24.41	23.59	22.86	23.09	57.00	78.45
50	23.70	24.02	24.47	23.76	22.99	23.28	64.60	83.08
60	23.77	24.12	24.61	23.96	23.18	23.57	71.00	83.66
70	23.82	24.19	24.85	24.25	23.38	23.93	76.60	86.26
80	23.87	24.28	24.99	24.47	23.61	24.29	81.60	86.32
90	23.76	23.83	25.13	24.72	24.12	24.68	85.20	84.14
100	23.86	24.06	25.35	24.97	24.31	25.05	86.00	88.84
110	23.91	24.17	25.54	25.24	24.56	25.53	91.10	89.11
120	23.97	24.32	25.81	25.48	24.74	26.01	93.00	90.71
130	23.99	24.41	25.98	25.69	25.03	26.43	94.40	90.38

Table A.2 (cont'd)

140	24.19	24.93	26.42	26.19	25.37	27.40	97.00	93.55
150	24.29	25.10	26.73	26.48	25.80	28.00	98.20	94.95
160	24.42	25.27	27.03	26.77	26.19	28.64	99.70	96.35
170	24.57	25.44	27.34	27.07	26.68	29.34	101.20	97.69
180	24.72	25.50	27.61	27.38	27.15	30.03	102.40	98.76
190	24.83	25.56	27.78	27.56	27.43	30.48	103.60	99.30
200	24.97	25.61	27.95	27.76	27.69	30.91	104.50	99.82
210	25.02	25.67	28.04	27.81	27.83	31.07	105.30	99.99
220	25.31	25.72	28.40	28.18	28.56	32.03	105.80	100.82
230	25.38	25.78	28.48	28.27	28.68	32.22	107.20	100.97
240	25.54	25.83	28.74	28.47	29.13	32.74	109.40	102.69
250	25.67	25.89	29.16	28.82	30.18	33.70	111.20	106.60
260	25.91	25.94	29.50	29.09	30.84	34.53	113.00	108.99
270	26.18	26.00	29.82	29.36	31.45	35.34	114.60	111.18
280	26.38	26.1	29.96	29.51	31.84	35.79	116.10	112.42
290	26.68	26.5	30.32	29.83	32.57	36.74	117.60	114.67
300	27.22	27.0	30.81	30.33	33.66	38.11	119.10	117.76
310	27.68	27.4	31.22	30.76	34.45	39.18	120.50	119.68
320	28.16	27.9	31.63	31.15	35.22	40.22	121.90	121.22
330	28.42	28.5	31.89	31.38	35.68	40.79	123.20	122.11
340	28.88	29.0	32.34	31.82	36.59	41.86	124.50	123.69
350	29.34	29.6	32.82	32.23	37.56	42.98	125.70	125.41
360	30.07	30.2	33.51	32.89	39.01	44.83	126.90	127.61
370	30.69	30.7	34.11	33.42	40.08	46.11	126.70	129.18
380	31.03	31.4	34.44	33.73	40.56	46.91	125.20	129.74
390	31.85	32.0	34.91	34.30	41.37	48.30	124.20	126.89
400	33.03	32.7	35.72	35.24	42.78	50.20	124.20	124.48
410	33.71	33.4	36.36	35.93	44.02	51.62	126.00	124.90
420	34.06	34.2	37.00	36.51	45.13	52.92	127.50	127.46
430	34.40	34.9	37.39	36.86	45.63	53.67	126.80	128.76
440	35.09	35.7	37.96	37.41	46.74	55.07	125.70	129.00
450	36.64	36.4	38.85	38.43	48.26	57.07	125.00	126.54
460	37.50	37.2	39.57	39.19	49.52	58.56	125.70	125.59
470	38.04	38.0	40.32	39.89	50.84	59.96	127.60	127.38
480	38.23	38.9	40.74	40.24	51.53	60.77	127.50	128.56
490	38.89	38.03	41.43	40.91	52.71	62.24	126.50	130.03
500	40.03	39.66	42.12	41.69	53.83	63.76	125.70	128.08
510	41.45	41.29	43.27	42.88	55.66	65.88	125.30	126.42
520	41.92	42.68	43.72	43.34	56.47	66.71	126.30	126.18
530	42.79	43.19	44.89	44.45	58.21	68.77	127.60	128.24
540	43.09	43.70	45.34	44.88	58.85	69.54	126.80	129.50
550	44.52	44.21	46.46	46.08	60.67	71.67	126.00	128.01
560	45.14	44.72	46.96	46.59	61.35	72.47	125.40	127.35
570	46.56	45.23	48.27	47.97	63.18	74.52	125.50	126.25

Table A.2 (cont'd)

580	47.03	45.90	48.77	48.48	63.88	75.29	126.80	126.34
590	47.98	46.70	50.09	49.71	65.71	77.15	127.00	128.98
600	48.46	47.50	50.59	50.19	66.39	77.89	126.30	129.18
610	49.99	48.30	51.89	51.56	68.07	79.70	125.60	127.31
620	50.59	49.10	52.46	52.11	68.77	80.41	125.40	126.79
630	51.98	49.90	53.86	53.57	70.48	82.12	126.30	126.19
640	52.42	50.70	54.41	54.11	71.12	82.75	126.90	126.57
650	53.49	51.50	55.81	55.43	72.73	84.29	126.50	128.57
660	54.05	52.30	56.31	56.01	73.34	84.92	125.80	128.07
670	55.61	53.10	57.79	57.49	74.92	86.39	125.40	126.60
680	56.17	53.90	58.33	58.06	75.54	86.92	125.90	126.15
690	57.45	55.00	59.88	59.61	77.09	88.32	126.80	126.65
700	57.81	56.10	60.45	60.13	77.66	88.82	126.50	127.84
710	59.09	57.20	61.86	61.53	79.06	90.03	125.90	128.01
720	59.68	58.30	62.42	62.12	79.55	90.49	125.50	127.31
730	61.23	59.40	63.94	63.72	80.96	91.68	125.60	126.17
740	61.72	60.50	64.51	64.32	81.47	92.11	126.50	126.04
750	63.21	61.60	66.62	66.31	83.31	93.56	126.60	128.07
760	63.41	62.70	66.86	66.55	83.50	93.74	126.10	128.15
770	65.25	63.80	68.66	68.41	85.01	94.93	125.60	126.73
780	65.50	64.90	68.90	68.67	85.22	95.10	125.50	126.49
790	67.08	66.00	70.76	70.54	86.65	96.21	126.20	126.38
800	67.27	67.10	71.03	70.81	86.87	96.38	126.60	126.68
810	67.72	68.20	71.74	71.47	87.43	96.84	126.20	127.62
820	69.54	69.30	73.69	73.42	88.89	97.96	125.70	126.99
830	69.78	70.40	73.93	73.68	89.05	98.08	125.60	126.78
840	70.54	70.87	74.72	74.51	89.60	98.52	125.90	126.24
850	71.29	71.37	75.74	75.56	90.61	99.07	126.40	126.19
860	72.63	72.44	77.64	77.34	91.97	99.97	126.20	127.68
870	72.86	72.71	77.87	77.56	92.13	100.07	125.80	127.56
880	73.62	73.41	78.57	78.31	92.62	100.44	125.60	127.11
890	74.56	74.51	79.56	79.33	93.28	100.88	125.80	126.40
900	76.06	75.71	81.44	81.18	94.49	101.72	126.30	126.76
910	76.46	76.19	82.04	81.75	94.89	101.97	126.20	127.43
920	76.68	76.57	82.30	82.01	94.99	102.06	125.90	127.51
930	77.55	77.49	83.17	82.89	95.53	102.48	125.70	127.26
940	78.48	78.43	84.10	83.82	96.12	102.91	125.80	126.66
950	79.57	79.54	85.36	85.15	96.82	103.41	126.10	126.34
960	79.95	79.97	85.86	85.62	97.13	103.63	126.30	126.57
970	80.49	80.28	86.65	86.35	97.64	103.94	126.10	127.38
980	82.08	82.06	88.28	87.98	98.62	104.62	125.80	126.86
990	82.63	82.64	88.82	88.58	98.89	104.85	125.70	126.54
1000	82.85	82.84	89.08	88.86	99.04	104.94	125.90	126.44
1010	83.56	83.48	89.89	89.71	99.49	105.26	126.20	126.49
1020	84.81	84.80	91.36	91.12	100.26	105.87	126.20	127.48

Table A.2 (cont'd)

1030	85.33	85.33	91.83	91.59	100.56	106.06	126.00	127.18
1040	85.61	85.59	92.09	91.87	100.70	106.19	125.80	127.03
1050	86.38	86.38	92.86	92.72	101.14	106.49	125.90	126.60
1060	87.61	87.89	94.26	94.10	101.72	106.99	126.10	126.87
1070	87.93	88.03	94.69	94.53	101.99	107.16	126.10	127.27
1080	88.14	88.33	94.91	94.74	102.12	107.28	126.00	127.39
1090	88.82	89.01	95.52	95.36	102.46	107.51	125.90	127.13
1100	90.14	90.37	96.87	96.78	103.18	108.01	125.90	126.52
1110	90.83	90.98	97.62	97.53	103.64	108.31	126.00	126.92
1120	91.15	91.39	98.04	97.93	103.84	108.51	126.10	127.23
1130	91.25	91.44	98.16	98.03	103.89	108.51	126.00	127.22
1140	91.78	91.94	98.62	98.52	104.20	108.73	125.90	127.12
1150	92.44	92.67	99.23	99.14	104.52	108.97	125.90	126.81
1160	92.99	93.31	99.82	99.72	104.84	109.19	126.00	126.63
1170	94.01	94.31	100.89	100.78	105.43	109.62	126.00	127.03
1180	94.68	94.88	101.51	101.41	105.81	109.89	125.90	127.08
1190	94.87	95.11	101.69	101.59	105.93	109.98	125.90	127.02
1200	95.09	95.22	101.89	101.79	106.01	110.04	125.90	126.85
1210	95.64	95.83	102.44	102.32	106.29	110.24	126.30	126.68
1220	96.18	96.42	102.99	102.87	106.64	110.49	126.30	126.71
1230	97.07	97.13	103.87	103.71	107.11	110.86	126.30	127.06
1240	97.73	98.01	104.49	104.33	107.48	111.11	126.20	126.88
1250	98.36	98.55	105.08	104.88	107.79	111.36	126.20	126.70
1260	98.47	98.68	105.18	104.99	107.88	111.38	126.20	126.72
1270	98.57	98.82	105.27	105.08	107.93	111.43	126.40	126.76
1280	98.99	99.27	105.67	105.47	108.17	111.57	126.40	126.89
1290	99.47	99.81	106.12	105.89	108.43	111.77	126.30	126.91
1300	100.38	100.62	106.88	106.66	108.87	112.09	126.20	126.83
1310	100.94	101.22	107.40	107.14	109.20	112.34	126.20	126.73
1320	101.02	101.31	107.46	107.20	109.21	112.34	126.20	126.73
1330	101.42	101.69	107.82	107.55	109.46	112.48	126.50	126.86
1340	101.60	101.91	107.99	107.73	109.54	112.59	126.40	127.02
1350	102.03	102.32	108.35	108.07	109.74	112.75	126.20	126.96
1360	102.47	102.71	108.71	108.43	109.96	112.93	126.10	126.80
1370	103.26	103.55	109.37	109.07	110.38	113.21	126.20	126.79
1380	103.75	104.04	109.74	109.48	110.61	113.39	126.30	126.98
1390	103.99	104.18	109.98	109.67	110.74	113.51	126.30	126.97
1400	104.10	104.40	110.07	109.78	110.86	113.56	126.20	126.99
1410	104.46	104.67	110.34	110.05	110.97	113.68	126.20	126.88
1420	104.82	104.96	110.62	110.31	111.17	113.82	126.20	126.72
1430	105.19	105.35	110.92	110.60	111.34	113.98	126.20	126.75
1440	105.87	106.11	111.46	111.14	111.69	114.22	126.20	126.97
1450	106.32	106.52	111.79	111.49	111.94	114.40	126.20	126.79
1460	106.56	106.76	111.97	111.67	112.01	114.48	126.40	126.69
1470	106.64	106.86	112.03	111.72	112.07	114.50	126.20	126.68

Table A.2 (cont'd)

1480	106.93	107.14	112.26	111.94	112.27	114.63	126.20	126.69
1490	107.21	107.47	112.49	112.18	112.36	114.73	126.10	126.87
1500	107.90	108.13	113.00	112.70	112.69	115.00	126.20	126.86
1510	108.31	108.54	113.29	113.01	112.92	115.15	126.30	126.69
1520	108.69	108.93	113.58	113.28	113.10	115.30	126.20	126.79
1530	108.73	108.96	113.61	113.33	113.11	115.30	126.10	126.86
1540	108.86	109.07	113.71	113.42	113.17	115.37	126.10	126.95
1550	109.11	109.37	113.89	113.61	113.32	115.47	126.20	126.99
1560	109.42	109.68	114.11	113.83	113.41	115.57	126.20	126.87
1570	109.72	110.00	114.31	114.04	113.61	115.68	126.20	126.71
1580	110.01	110.30	114.52	114.26	113.71	115.81	126.20	126.68
1590	110.49	110.65	114.93	114.66	114.04	116.01	126.10	126.98
1600	110.85	110.98	115.16	114.90	114.18	116.14	126.20	126.86
1610	111.18	111.27	115.38	115.14	114.37	116.28	126.10	126.69
1620	111.23	111.33	115.44	115.17	114.39	116.31	126.30	126.69
1630	111.29	111.41	115.48	115.22	114.39	116.33	126.30	126.67
1640	111.55	111.78	115.67	115.42	114.55	116.42	126.20	126.77
1650	111.81	111.89	115.83	115.61	114.65	116.53	126.10	127.01
1660	112.05	112.12	116.00	115.76	114.78	116.62	126.10	126.88
1670	112.57	112.64	116.35	116.13	115.02	116.82	126.20	126.67
1680	112.86	112.94	116.57	116.33	115.21	116.93	126.20	126.76
1690	113.12	113.20	116.74	116.52	115.33	117.03	126.20	126.96
1700	113.28	113.37	116.86	116.63	115.42	117.11	126.20	126.96
1710	113.34	113.42	116.87	116.67	115.44	117.11	126.10	126.91
1720	113.48	113.55	116.97	116.76	115.50	117.17	126.10	126.82
1730	113.71	113.79	117.12	116.92	115.64	117.28	126.30	126.70
1740	113.94	114.01	117.29	117.08	115.74	117.38	126.20	126.66
1750	114.15	114.23	117.42	117.24	115.87	117.47	126.10	126.81
1760	114.57	114.64	117.68	117.51	116.04	117.61	126.10	126.88
1770	114.82	114.89	117.86	117.69	116.18	117.71	126.10	126.68
1780	115.09	115.14	118.03	117.85	116.25	117.81	126.20	126.65
1790	115.23	115.29	118.11	117.94	116.33	117.87	126.20	126.77
1800	115.27	115.33	118.15	117.97	116.36	117.88	126.10	126.78
1810	115.37	115.44	118.22	118.05	116.41	117.92	126.20	126.92
1820	115.57	115.63	118.36	118.18	116.51	118.01	126.10	126.80
1830	115.77	115.83	118.48	118.32	116.62	118.09	126.10	126.70
1840	115.97	116.03	118.60	118.46	116.73	118.18	126.30	126.66
1850	116.29	116.36	118.82	118.67	116.88	118.31	126.20	126.85

Appendix A.2 Oxygen Radical Absorbance Capacity (ORAC) Fluorescein Method

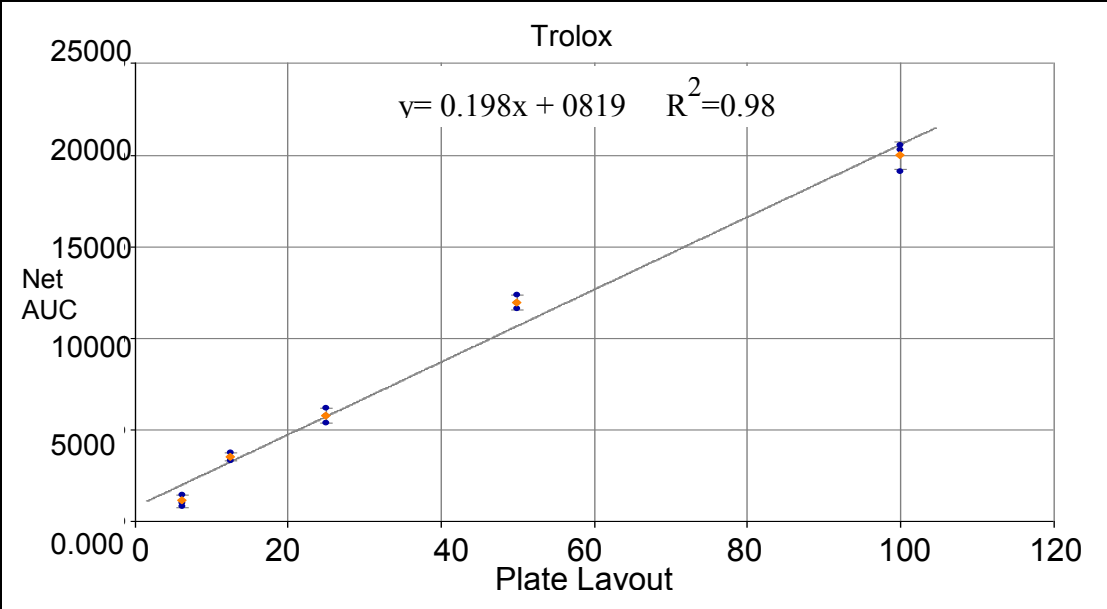


Figure A.3 Typical Antioxidant Standard Curve (Trolox calibration curve) for ORAC value estimation

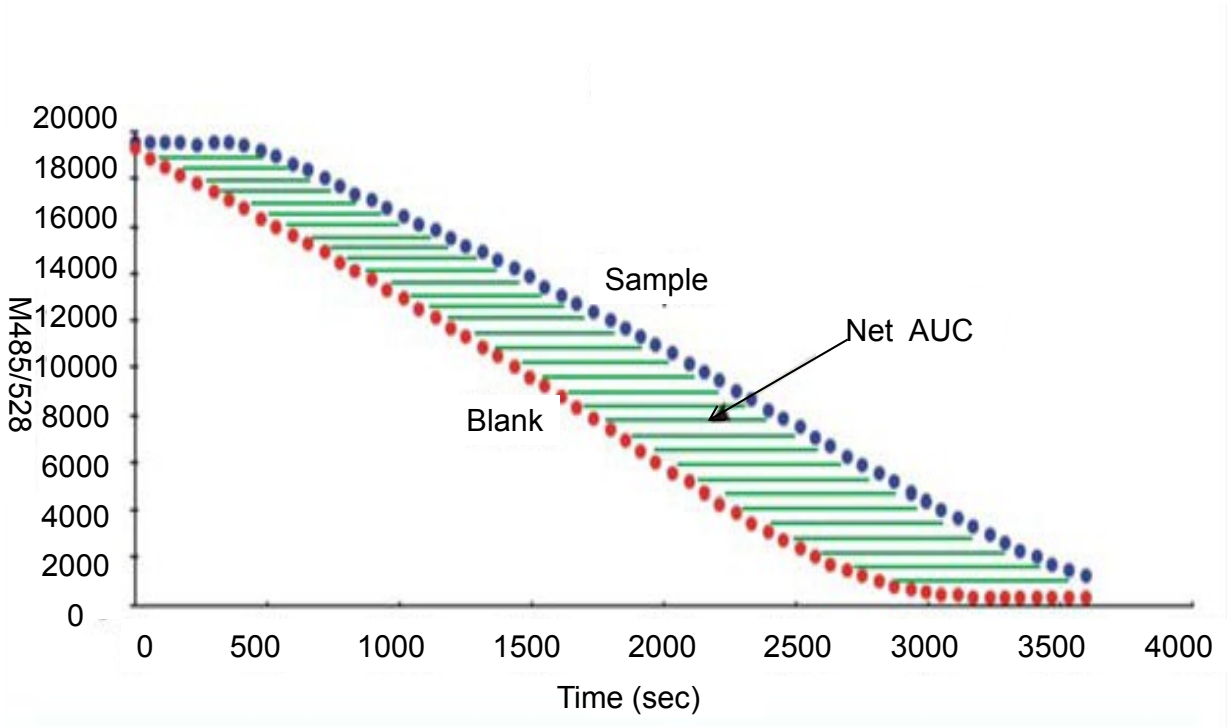


Figure A.4 Diagram of Antioxidant activity determination expressed as the net area under the curve (AUC). (<http://www.biotek.com> , accessed on Feb 2013)

Table A.3 The average total antioxidant values of cherry pomace (treated 25%MC and untreated 70% MC,41%MC ,wb) retorted at 126.7 °C)(values for 5 replicates)

Retorting time (min)	ORAC ($\mu\text{mol TE/g pomace ,db}$)		
	25%	41%	70%
0	35.24 \pm 1.21	30.44 \pm 4.42	30.26 \pm 2.51
25	35.62 \pm 3.25	NA	NA
40	35.75 \pm 3.02	NA	NA
60	33.44 \pm 4.13	NA	NA

REFERENCES

REFERENCES

- Abers, J.E., Wrolstad, R.E., (1979). Causative factors of color deterioration in strawberry preserves during processing and storage. *Journal of Food Science* 44(1), 75-&.
- Ahmed, J., Shivhare, U.S., Raghavan, G.S.V., (2004). Thermal degradation kinetics of anthocyanin and visual colour of plum puree. *European Food Research and Technology* 218(6), 525-528.
- Barreiro, J.A., Milano, M., Sandoval, A.J., (1997). Kinetics of colour change of double concentrated tomato paste during thermal treatment. *Journal of Food Engineering* 33(3-4), 359-371.
- Bechtold, T., Mahmud-Ali, A., Mussak, R., (2007). Anthocyanin dyes extracted from grape pomace for the purpose of textile dyeing. *Journal of the Science of Food and Agriculture* 87(14), 2589-2595.
- Bonerz, D., Wurth, K., Dietrich, H., Will, F., (2007). Analytical characterization and the impact of ageing on anthocyanin composition and degradation in juices from five sour cherry cultivars. *European Food Research and Technology* 224(3), 355-364.
- Britt, C., Gomaa, E.A., Gray, J.I., Booren, A.M., (1998). Influence of cherry tissue on lipid oxidation and heterocyclic aromatic amine formation in ground beef patties. *Journal of Agricultural and Food Chemistry* 46(12), 4891-4897.
- Cao, G.H., Alessio, H.M., Cutler, R.G., (1993). Oxygen-Radical Absorbency Capacity Assay for Antioxidants. *Free Radical Biology and Medicine* 14(3), 303-311.
- Cemeroglu, B., Velioglu, S., Isik, S., (1994). Degradation kinetics of anthocyanins in sour cherry juice and concentrate. *Journal of Food Science* 59(6), 1216-1218.
- Chaovanalikit, A., Wrolstad, R.E., (2004). Total anthocyanins and total phenolics of fresh and processed cherries and their antioxidant properties. *Journal of Food Science* 69(1), C67-C72.
- Chiste, R.C., Lopes, A.S., de Faria, L.J.G., (2010). Thermal and light degradation kinetics of anthocyanin extracts from mangosteen peel (*Garcinia mangostana* L.). *International Journal of Food Science and Technology* 45(9), 1902-1908.
- Dewanto, V., Wu, X.Z., Liu, R.H., (2002). Processed sweet corn has higher antioxidant activity. *Journal of Agricultural and Food Chemistry* 50(17), 4959-4964.

- Forni, E., Polesello, A., Torreggiani, D., (1993). Changes in anthocyanins in cherries (*prunus-avium*) during osmodehydration, pasteurization and storage. Food Chemistry 48(3), 295-299.
- Huang, D.J., Ou, B.X., Hampsch-Woodill, M., Flanagan, J.A., Prior, R.L., (2002). High-throughput assay of oxygen radical absorbance capacity (ORAC) using a multichannel liquid handling system coupled with a microplate fluorescence reader in 96-well format. Journal of Agricultural and Food Chemistry 50(16), 4437-4444.
- Ibarz, A., Pagan, J., Garza, S., (1999). Kinetic models for colour changes in pear puree during heating at relatively high temperatures. Journal of Food Engineering 39(4), 415-422.
- Kammerer, D.R., Schillmoller, S., Maier, O., Schieber, A., Carle, R., (2007). Colour stability of canned strawberries using black carrot and elderberry juice concentrates as natural colourants. European Food Research and Technology 224(6), 667-679.
- Kim, D.O., Padilla-Zakour, O.I., (2004). Jam processing effect on phenolics and antioxidant capacity in anthocyanin-rich fruits: Cherry, plum, and raspberry. Journal of Food Science 69(9), S395-S400.
- Kirca, A., Cemeroglu, B., (2003). Degradation kinetics of anthocyanins in blood orange juice and concentrate. Food Chemistry 81(4), 583-587.
- Konczak, I., Zhang, W., (2004). Anthocyanins - more than nature's colours. Journal of Biomedicine and Biotechnology(5), 239-240.
- Lee, J., Durst, R.W., Wrolstad, R.E., (2005). Determination of total monomeric anthocyanin pigment content of fruit juices, beverages, natural colorants, and wines by the pH differential method: Collaborative study. Journal of Aoac International 88(5), 1269-1278.
- Markakis, P., Livingston, G.E., Fellers, C.R., (1956). Quantitative aspects of strawberry pigment degradation. Food Technology 10(12), 31-31.
- Maskan, M., (2001). Kinetics of colour change of kiwifruits during hot air and microwave drying. Journal of Food Engineering 48(2), 169-175.
- Maskan, M., (2006). Production of pomegranate (*Punica granatum L.*) juice concentrate by various heating methods: colour degradation and kinetics. Journal of Food Engineering 72(3), 218-224.

- Mcguire, R.G., (1992). Reporting of objective color measurements. *Hortscience* 27(12), 1254-1255.
- Mishra, D.K., Dolan, K.D., Yang, L., (2008). Confidence intervals for modeling anthocyanin retention in grape pomace during nonisothermal heating. *Journal of Food Science* 73(1), E9-E15.
- Mohammadi, S., R., Z., E.-D., A., K., (2008). Kinetic models for colour changes in kiwifruit slices during hot air drying. *World Journal of Agricultural Sciences* 4 (3), 376-383.
- Nawirska A. , K.M., (2005). Dietary fibre fractions from fruit and vegetable processing waste. *J of Food Chemistry* 91, 221–225.
- Patras, A., Brunton, N.P., O'Donnell, C., Tiwari, B.K., (2010). Effect of thermal processing on anthocyanin stability in foods; mechanisms and kinetics of degradation. *Trends in Food Science & Technology* 21(1), 3-11.
- Rodriguez-Saona, L.E., Wrolstad, R.E., Pereira, C., (1999). Glycoalkaloid content and anthocyanin stability to alkaline treatment of red-fleshed potato extracts. *Journal of Food Science* 64(3), 445-450.
- Silva, F.M., Silva, C.L.M., (1999). Colour changes in thermally processed cupuacu (*Theobroma grandiflorum*) puree: critical times and kinetics modelling. *International Journal of Food Science and Technology* 34(1), 87-94.
- Skrede, G., (1985). Color quality of blackcurrant syrups during storage evaluated by Hunter L'-Value, L'a-value, L'b-value. *Journal of Food Science* 50(2), 514-&.
- Tomas-Barberan, F.A., Gil, M.I., Cremin, P., Waterhouse, A.L., Hess-Pierce, B., Kader, A.A., (2001). HPLC-DAD-ESIMS analysis of phenolic compounds in nectarines, peaches, and plums. *Journal of Agricultural and Food Chemistry* 49(10), 4748-4760.
- Tsami, E., Katsioti, M., (2000). Drying kinetics for some fruits: Predicting of porosity and color during dehydration. *Drying Technology* 18(7), 1559-1581.
- Wang, H.B., Nair, M.G., Strasburg, G.M., Chang, Y.C., Booren, A.M., Gray, J.I., DeWitt, D.L., (1999). Antioxidant and antiinflammatory activities of anthocyanins and their aglycon, cyanidin, from tart cherries (vol 62, pg 296, 1999). *Journal of Natural Products* 62(5), 802-802.

CHAPTER 4

OBJECTIVE TWO

Estimation of Temperature-Dependent Thermal Properties of Cherry Pomace at Different Moisture Contents During Non-Isothermal Heating

Abstract

Fruit and vegetables are a rich source of many bio-active compounds from which value-added nutraceuticals can be produced. To design processes for these solids, thermal properties must be known. Because many of the bio-active compounds, e.g., anthocyanins and phenolics, degrade exponentially faster at elevated temperatures (above 100°C), use of temperature-dependent thermal properties will give more accurate results than those from constant properties. Differential scanning calorimetry (DSC) was used to measure the specific heat of cherry pomace at three constant moisture contents (MC). At 25 °C, the measured specific heat was found to be 1671, 2111 and 2943 J kg⁻¹ K⁻¹ for 70, 41 and 25% moisture content, respectively. Tart cherry pomace was equilibrated to 25, 41, and 70% MC wet basis (wb) and heated in sealed 54× 73 mm cans at 127 °C in a steam retort for 25, 40, 60 and 90 min. Can center temperature was recorded. For the ordinary least squares method, the sum of squares of errors = (center temperature observed – center temperature predicted)² was minimized by nonlinear regression in MATLAB with Comsol. The sequential estimation method was also used to determine how the addition of each datum affected the thermal property estimates during the experiment. Thermal conductivity (W m⁻¹ K⁻¹) was estimated at 25°C (k₁) and 125°C (k₂), using a linear function of temperature. At 90 min heating, the estimated k₁ and k₂ values and standard errors for 70, 41 and 25% MC were 0.49 +/- 0.00047 and 0.55 +/- 0.00058, 0.20 +/- 0.0015 and 0.39 +/- 0.0012 and 0.15 +/- 0.0034 and 0.28 +/- 0.0037 W m⁻¹ K⁻¹, respectively. These results can be useful for processors desiring to use cherry pomace to make value-added by-products

at elevated temperatures common in extrusion, spray-drying and other food drying methods.

4.1 Introduction

Thermal processing of foods involves heating to temperatures typically from 50 to 150 °C. Anthocyanin stability is a main focus in many studies. This stability is not only a function of final processing temperature but also of other properties (intrinsic) like pH, storage temperature, product moisture content, chemical structure of the anthocyanins and its initial concentration, light, oxygen, presence of enzymes, proteins and metallic ions (Patras et al., 2010). There are many studies examining these factors individually or a combination of one or more of them on degradation of food components. There is limited information available on the effect of high temperature processing at different moisture contents on the stability of these pigments in solid food products. A challenge in collecting this information is the confounding decrease in moisture during heating at temperatures greater than 100 °C. A study on the change in physical properties of ground beef during cooking showed that thermal conductivity of ground beef varied between 0.35 and 0.41 W/m °C in temperature range of 5 to 70 °C (Pan and Singh, 2001). Estimation methods for thermal conductivity are classified into two main methods: steady- and transient-state heat transfer methods. Steady-state methods require long times, and moisture content changing with time introduces significant error (Dutta et al., 1988). Many studies have been done on this subject for estimating these properties for different kinds of food materials. Some studies used measured temperature profiles for estimation of the thermophysical properties in inverse heat conduction problems (Beck and Woodbury, 1998; Yang, 1998).

Equations (quadratic models) were developed for predicting thermal conductivity of a meat with a given water content and temperature at different ranges (Rahman, 1992; Sweat, 1975). Thermal conductivity of carrot and potato (solid food) were measured as well, using the probe method at a temperature range 30 -130 °C, a correlation equation based on composition alone was established for predicting the thermal conductivity (Gratzek and Toledo, 1993). The thermal conductivity of porous foods, which have complex structure is difficult to predict (Sweat, 1995).

Thermal properties was determined for borage seeds, Specific heat was measured by differential scanning calorimetric (DSC) and ranged from 0.77 to 1.99 kJ kg⁻¹K⁻¹ and thermal conductivity increased with moisture content and contributed the most to the uncertainty of thermal diffusivity; however quadratic equations were established for estimating these thermal properties (Yang et al., 2002). A study on wheat, corn and rice flour proposed an equation to predict the specific heat of these products as function of temperature, moisture content and protein content. The DSC method was used in this study at a temperature range from 20 to 120 °C and moisture content of 0-70% dry basis and 20 atm pressure (Kaletunc, 2007).

In a study on fruit juices, the specific heat and thermal conductivity of the juices had linear dependency on water content and temperature, while the density was nonlinearly related to water content (Gratao et al., 2005). Mohamed (2009) used transient temperature measurements with known heat flux at boundary for one dimensional conduction solid food sample for estimation of volumetric heat capacity and thermal conductivity simultaneously using a nonlinear sequential parameter estimation method.

Thermal properties of coffee bean powder were determined as functions of temperature and a linear model for specific heat was given as a function of temperature, and for density as a function of moisture content. (Singh et al., 1997). Thermal conductivity of cherry (9 - 60 °Brix) and sweet-cherry (12 - 50 °Brix) juices and other fruits was studied by a coaxial-cylinder technique (steady state) at a temperature range 20 to 120 °C. A prediction model as function of temperature or temperature with concentration was established for predicting thermal conductivity (Magerramov et al., 2006a).

Changes in chemical and physical characteristics in foods during heating (non-isothermal) might affect the level of reactants and product concentrations in the process. Competition between combination and degradation was indicated during the chemical process or reaction that peaks at only high temperature, a model was established with very different reactions in foods, this model can be converted into a dynamic rate reaction for simulating a process under non-isothermal conditions (Peleg et al., 2009).

Cherry pomace, a by-product of juice processing, is a rich source of anthocyanins, a functional food, and hence can be used as an ingredient in the food industry. Examples include cherry powder added as a nutraceutical and colorant to breakfast cereals, snacks, drink mixes and pet foods, and as a slow-release antioxidant in packaging films. In the past decade, health properties of cherries have become more prominent (McCune et al., 2011). Therefore, in this study, the objective was to estimate specific heat and thermal conductivity of cherry pomace at different levels of moisture content as function of temperature during non-isothermal heating.

4.2. Materials and methods

4.2.1 Sample preparation

Tart cherry pomace was obtained from Cherry Growers Inc., (Grawn, MI, USA). The moisture content (MC) of the samples was measured using a Sartorius Moisture Analyzer MA30 (Sartorius AG, Goettingen, Germany). The initial MC of the cherry pomace was 70% (wet basis, control). Two additional samples with lower MC (41 and 25%) were prepared using a pilot-scale cabinet dryer (Proctor and Schwartz Inc. K2395, Philadelphia, PA, USA) at $45 \pm 2^\circ\text{C}$. Pomace samples were identified as MC-70, MC-41, and MC-25 representing pomace with 70, 41, and 25% MC (wet basis), respectively. Each of the three cherry pomace samples were filled in duplicate (total 6 cans) and sealed (Dixie Seamer, Athens, Georgia) under vacuum (20-mm Hg) in 54×73 steel cans (Figure 4.1), the filling was manually by pressing the pomace in each can and recording the weight each time (for density measurements, Table B.1 at Appendix B.1), The pressing of the pomace was an important step to eliminate porosity effect on heat penetration. The pomace at 25%MC was difficult to obtain zero no porosity (the assumption for this study was zero porosity). Then all cans were heated at 126.7°C using a still steam retort (FMC Steritort Laboratory Sterilizer, Madera, CA, USA) for 25, 40, 60 and 90 min. Each can was fitted with a needle-type thermocouple (Ecklund-Harrison Technologies Inc., Fort Myers, FL, USA) to measure the center temperature. All experiments were done in duplicate.

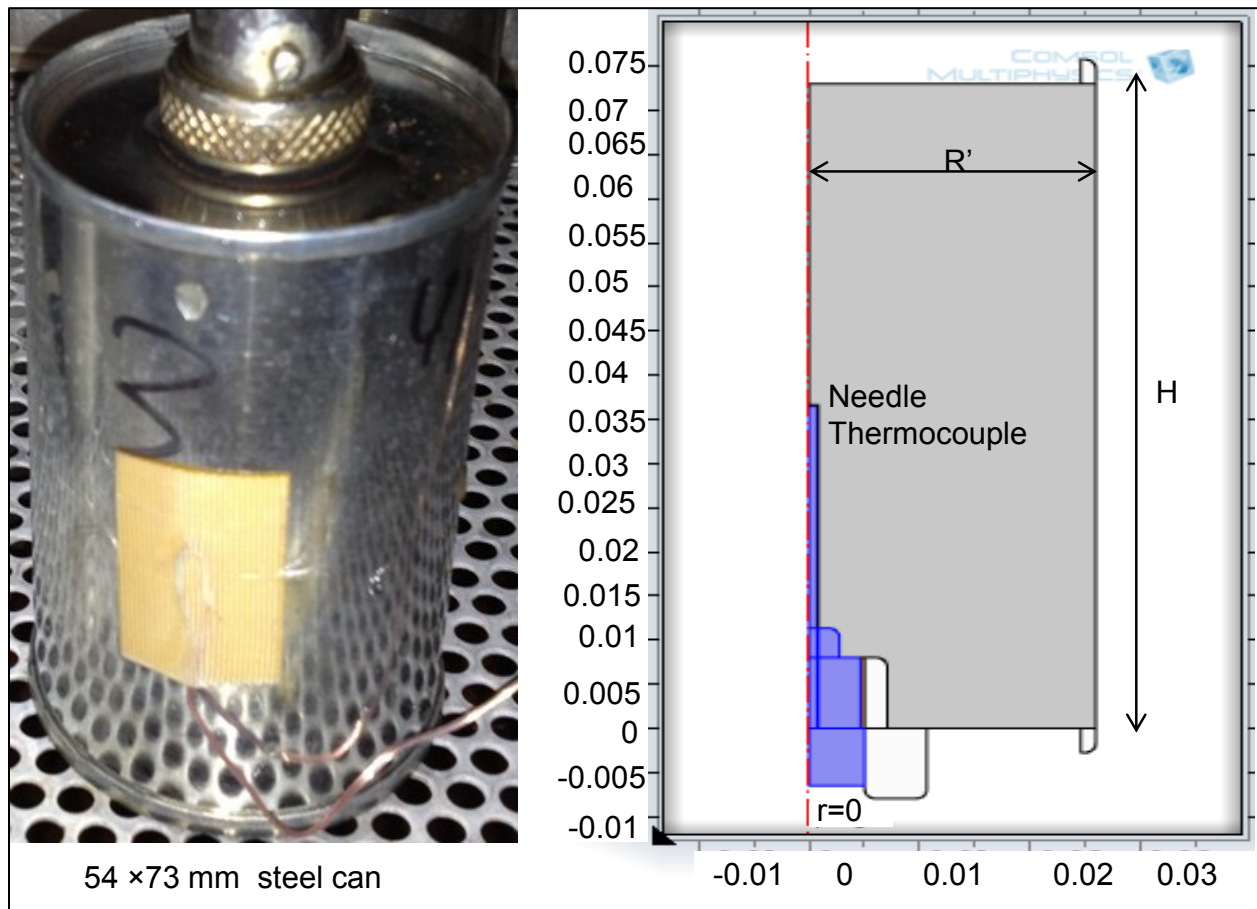


Figure 4.1 Geometry diagram (by Comsol) of the can with thermocouples, Left: surface TC taped on the can. Right: cutaway schematic of half-can sliced axially

4.2.2 Measurement of bulk density and specific heat

The bulk density of cherry pomace was determined by weighing of the pomace in each can, which had effective volume of 136 cm^3 (volume measured by water replacement in the can) (Hsu et al., 1991). Samples at the three different moisture contents were used to determine the bulk density; ten replications were made for each moisture level. Specific heat was measured using the differential scanning calorimetric (DSC) method following a similar procedure to that described by (Gill et al., 2010; Singh et al., 1997; Yang et al., 2002). Samples in triplicate of each moisture content of cherry

pomace were weighed. Each sample for each MC was placed in the hermetically sealed aluminum pans (baseline) and analyzed using the DSC as shown at Figure B.5 at Appendix B.2 . The samples were first cooled from 10°C to -50°C and then heated at a ramp of 10°C/min from 10°C to 130°C with a with a standard material (reference sample sapphire (Archer, 1993)). Example of heat flow curves are shown in Figure (4.2), which for 70% moisture content. Dry nitrogen gas flow was used to minimize the condensation in the cell during the measurements. Specific heat capacity was calculated based on follows:

$$Cps = ks \times \frac{Hs \times 60}{Hr \times Ws} \tag{4.1}$$

Where 60 is the conversion constant (min to second). Table B.3 at Appendix B.2 shows an example of specific heat calculation (MC-70) steps in Excel sheet.

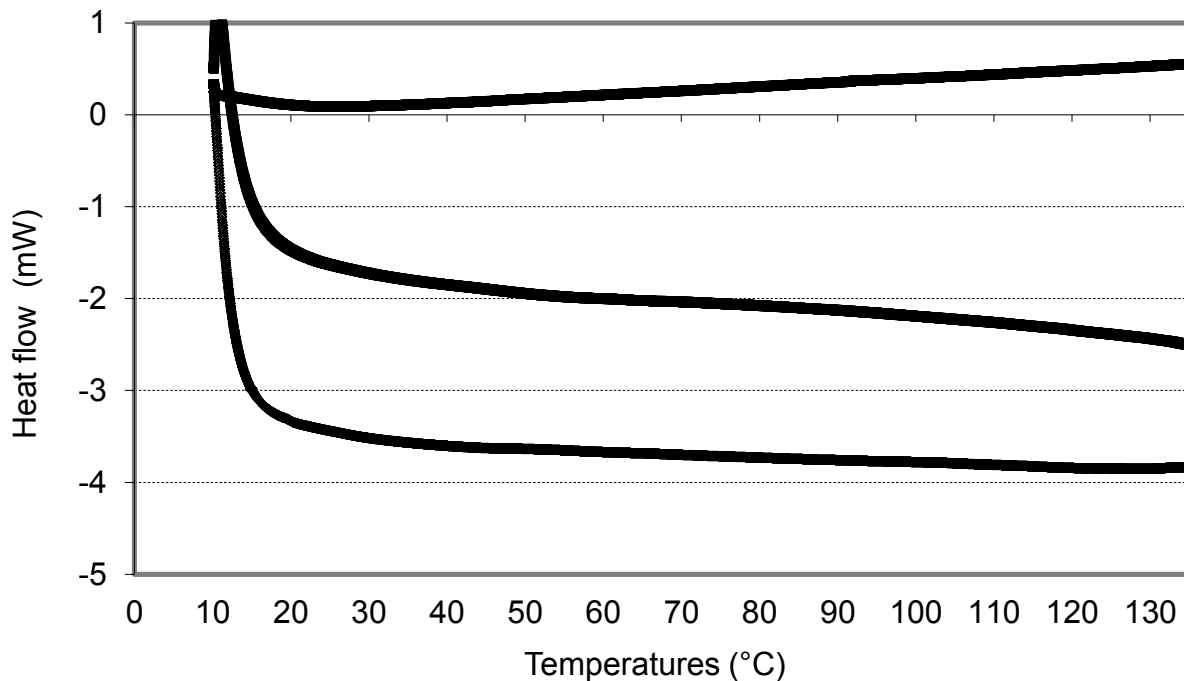


Figure 4.2 Thermal curves from specific heat estimation using DSC method (MC-70) : Lines; 1 =baseline, 2= sample and 3= sapphire

4.2.3 Thermal Processing

4.2.3.1 Heat Transfer and governing equations

For the case of a can being heated is steam, the conditions are transient with no heat generation. Because the boundary conditions are assumed to be nearly identical around the circumference and lids of the can, the problem is considered 2D (axial and radial) (Bairi et al., 2007). Because heat transfer through θ direction goes to zero, and there is no heat generation during the process, and thermal conductivity and specific heat are temperature dependent properties, the equation for cylindrical coordinates (Eq.(4.2)) could be written as follows (Banga et al., 1993; Betta et al., 2009; Telejko, 2004; Varga and Oliveira, 2000)

$$\frac{1}{r} \frac{\partial}{\partial r} \left(k(T) r \frac{\partial T}{\partial r} \right) + \frac{\partial}{\partial z} \left(k(T) \frac{\partial T}{\partial z} \right) = \rho C_p(T) \frac{\partial T}{\partial t} \quad (4.2)$$

Initial condition was uniform temperature throughout the samples:

$$T(r, z, 0) = T_i \quad [t=0, 0 \leq r \leq R', 0 \leq z \leq H] \quad (4.3)$$

Axisymmetric conditions: at $r=0$, axisymmetric

$$-k \frac{\partial T}{\partial r} = 0 \quad (4.4)$$

Boundary conditions (Abdul Ghani and Farid, 2006; Naveh et al., 1983):

$$\text{With } T = T_s(t) \quad [0 < t \leq t_f, r=R', z=0, z=H] \quad (4.5)$$

$$T = T(r, H) = T(R', z) = f(t)$$

Surface temperature was measured with a surface thermocouple taped on the can's surface during the process as showed in Figure 4.1, with the assumption that the temperatures at all surfaces of the can were equal.

Simulation for the can geometry and meshing steps were done using Comsol software Figure 4.3, where the thermocouple materials included in the simulation process. The can materials were neglected because the very thin layer of steel (0.22 mm) and its high thermal diffusivity of the can Table B.2 at Appendix B.1 shows all dimensions of the can and thermal properties of the steel. Because of a this thin layer of the steel (can surfaces) the thermal resistance ($m^2 \cdot ^\circ C / W$), which equal thickness divided by thermal conductivity (Datta, 2002b) , is very small and could be neglected in comparison with cherry pomace thermal resistance in the can. All Comsol simulation is shown in Figure B.4, Appendix B.1.

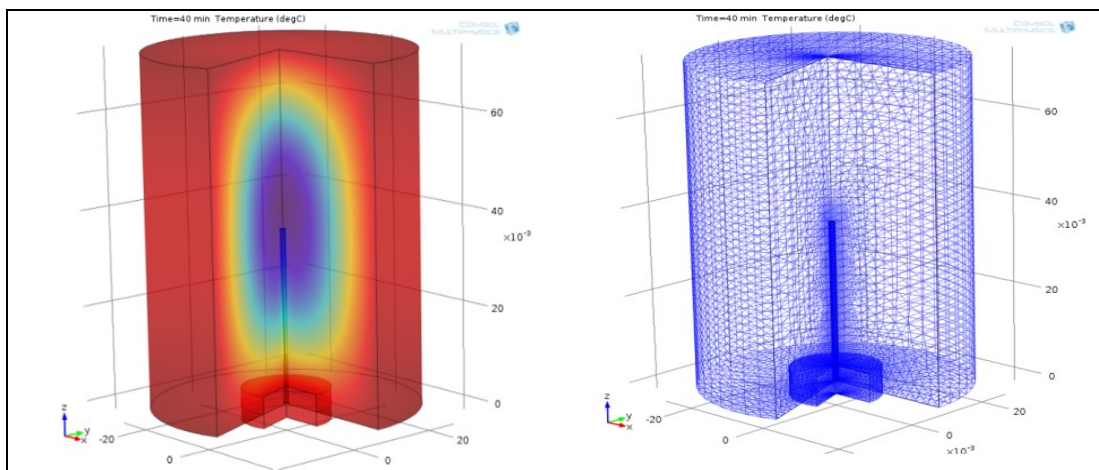


Figure 4.3 Meshing and center temperature profile by Comsol software. “The text in this figure is not meant to be readable but is for visual reference only”.

4.2.4 Experimental design

Cherry pomace samples were heated for 25, 40, 60 and 90 min in cans inside a steam retort in duplicate at 126.7 °C. Figure 4.4 shows the design of the process. Cans were placed stationary on the bottom of the retort on a steel mesh, to allow steam to touch all can surfaces equally. Each can had one sealed fixed needle thermocouple

installed in the end of the can running half-way along the axis, to measure the center temperature. One other 30-gauge flexible thermocouple (The OMEGA Self-Adhesive thermocouples, OMEGA Engineering, INC, Stamford CT, U.S.A) was taped (High performance polyimide film with silicone adhesive) on the surface of one can to record surface temperature. The last thermocouple was placed free in the retort to record the steam temperature during the process. Temperature was recorded every 10 sec using data acquisition system (CALplex) with CALSoft-5 software (TechniCAL, Inc New Orleans, Louisiana). Experimental design is showed in Appendix B.1, Figure B.1.

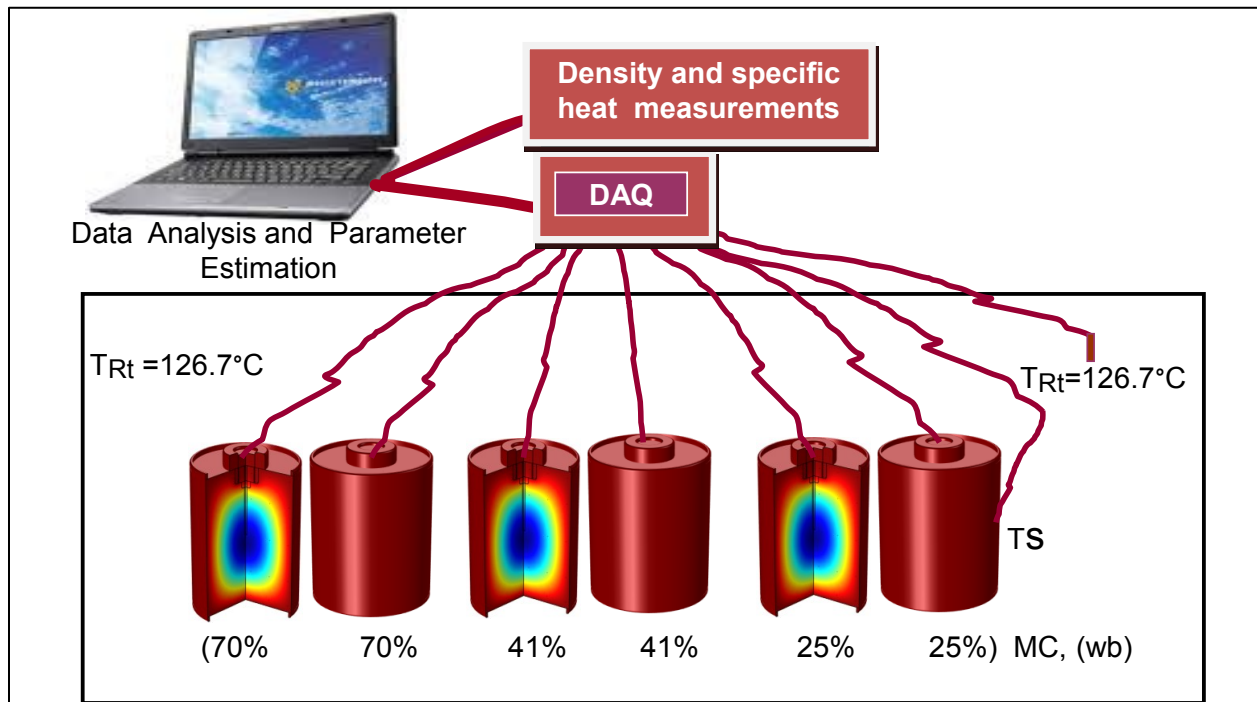


Figure 4.4 Experimental design of retorting the cherry pomace (three constant moisture content, wb)

The time-temperature profiles of retorting process (center, surface and retort temperature) are shown in Figure 4.5 for the 90 min retorting process.

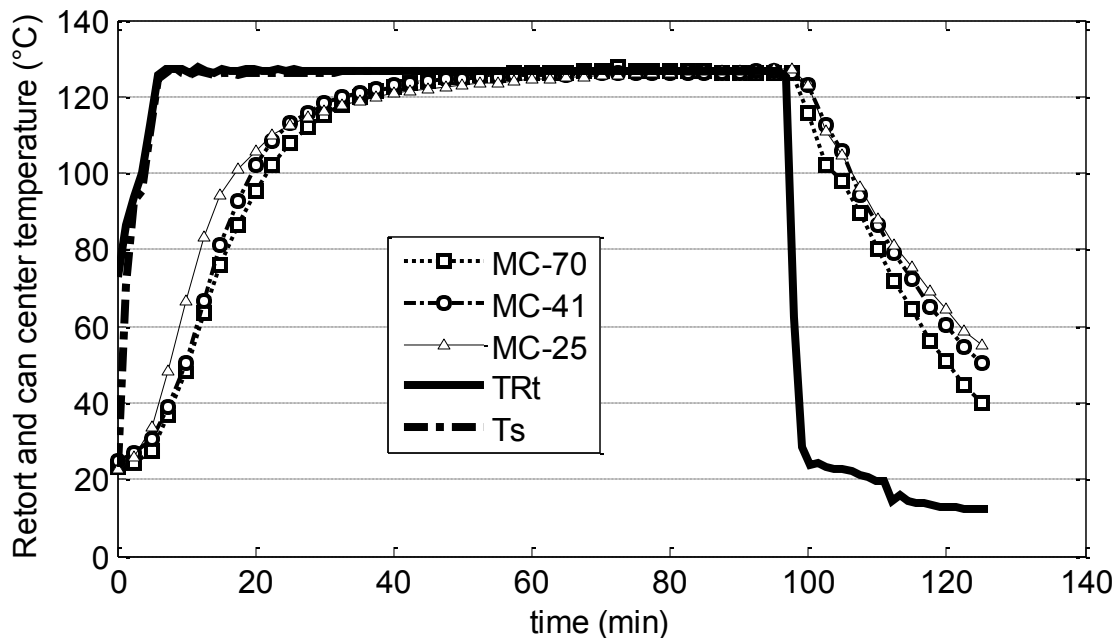


Figure 4.5 Temperature profiles for center of cherry pomace at three constant moisture content (wb), for surface temperature of the can, and steam temperature in a steam retort at 126.7 °C for 90 min.

4.2.5 Thermal parameter estimation

4.2.5.1 Sensitivity Coefficients

The sensitivity coefficient X_{ij} , where i is the time index, and j is the parameter index, indicates how sensitive the dependent variable is to a parameter β_j . X_{ij} was formed by taking the first derivative of the dependent variable with respect to a specific parameter β_j . The scaled sensitivity coefficient (X'_{ij}) was used to compare directly to the dependent variable temperature T . The X' in the model should be large and uncorrelated to be estimated accurately (Beck and Arnold, 1977) “Large” means greater than ~10% of the temperature rise. From the plots of the scaled sensitivity coefficients it could be seen which parameters could be estimated most accurately, and which parameters dominate. In this work we determined the scaled sensitivity coefficient

(X'_{ij}) of parameters (k_1 and k_2) using the forward finite difference method approximation (Beck and Arnold, 1977) for each parameter as presented in Eq.(4.7) The db_j is some relatively small quantity and given as $0.001 \times b_j$. Using MATLAB programming the scaled sensitivity coefficients Eq. (4.7) were computed. For plotting the sensitivity coefficient, the independent variables and approximate value of parameters must be known.

Sensitivity coefficient:

$$\frac{\partial T(i)}{\partial b_i} = X_i = \frac{T(b_1, \dots, b_j, +db_j, \dots, b_p) - T(b_1, \dots, b_j, \dots, b_p)}{\partial b_j} \quad (4.6)$$

Scaled Sensitivity coefficient:

$$X'_{ij} = \beta_j \frac{\partial T(i)}{\partial b_i} = \frac{T(b_1, \dots, b_j, +db_j, \dots, b_p) - T(b_1, \dots, b_j, \dots, b_p)}{0.001} \quad (4.7)$$

The index p in the previous equations is the number of parameters.

4.2.5.2 Ordinary Least Squares (OLS) Procedure

A commercial finite-element software (Comsol), was used to generate predicted center temperatures ($T(t)$ predicted), given the inputs of measured surface temperature T_s , heating time (t) as shown in Figure 4.1, and initial estimate of pomace thermal conductivity k_1 (thermal conductivity at temperature T_1) and k_2 (thermal conductivity at temperature T_2). T_1 and T_2 were arbitrarily chosen temperatures ($T_1 < T_2$) within the temperature range. MATLAB (nlinfit) was used to run nonlinear regression OLS with Comsol. Temperature was inputted from Comsol, changing as the parameters k_1 and k_2 changed by the nonlinear regression routine. When the sum of the squares of errors of $(T(t)_{\text{observed}} - T(t)_{\text{predicted}})^2$ was minimized (SS) given in Eq.(4.8) the final k_1 and k_2

were used as the best-fit values of the pomace thermal properties, giving a linear function $k(T)$ Eq. (4.9) for each constant MC (Mishra et al., 2009). All MATLAB syntax for OLS method is shown in Appendix B.3 at Appendices.

$$SS = \sum_i [(Tobs)_i - (Tpred)_i]^2 \quad (4.8)$$

$$k(T) = \left\{ \frac{(T_2 - T)}{(T_2 - T_1)} \times k_1 + \frac{(T - T_1)}{(T_2 - T_1)} \times k_2 \right\} \quad (4.9)$$

4.2.5.3 Sequential Estimation Procedure

Non-linear Maximum A Posteriori (MAP) sequential estimation procedure given in (Beck and Arnold, 1977 p. 277) was used in this section. The MAP equation is shown in Eqs. (4.10) and (4.11):

$$b_{MAP} = \mu_\beta + P_{MAP} X^T \psi^{-1} (Y - X \mu_\beta) \quad (4.10)$$

$$P_{MAP} = (X^T \psi^{-1} X + V_\beta^{-1})^{-1} \quad (4.11)$$

Where Eqs. (4.10) and (4.11) are in matrix format, where b_{MAP} is the matrix (px1) vector parameter to be estimated; μ_β is matrix (px1) vector with prior information on the parameters; P_{MAP} is the covariance vector matrix of parameters (pxp) which gives information about the variance (on the diagonal) and covariance (correlation between parameter) on off-diagonal elements; X is the sensitivity coefficient matrix (npx); ψ is covariance matrix (nxn) of errors, and Y is the measurement (nx1) vector and V is covariance matrix of μ_β .

Sequential parameter estimation gives more insight into the estimation process. Improvement in the estimation is indicated when estimating the parameters at each data addition (Mohamed, 2009). Under sequential estimation we expect the parameters to approach a constant as the number of observations increases. MATLAB programming was used to conduct the sequential estimation. All MATLAB syntaxes for sequential estimation method is shown in Appendix B.3.

4.2.6 Data analysis

Statistical analyses were performed using MATLAB software. Standard deviations (Zuritz et al.), standard errors (SE) and correlation coefficients were calculated. OLS and sequential estimation were performed using MATLAB software.

4.3 Results and discussion

4.3.1 Bulk density and Specific heat determination results:

Bulk density of cherry pomace increased with increasing moisture contents. The density showed linear correlation with moisture content, which was fitted by following equation:

$$\rho = (10.506 \times MC) + 330.26 \quad R^2 = 0.99 \quad (4.12)$$

Where: MC was in decimal percent, e.g 70, 41 and 25% (wet basis).

A second-order polynomial correlation was used to model the specific heat of cherry pomace as function of temperature (Valentas et al., 1997a) Figure 4.7 shows the results of specific heat as estimated by the DSC method. Table B.3 at Appendices B showed some the values of heat flow (mJ/s) (MC-70) and the estimation steps of the specific heat in triplicate

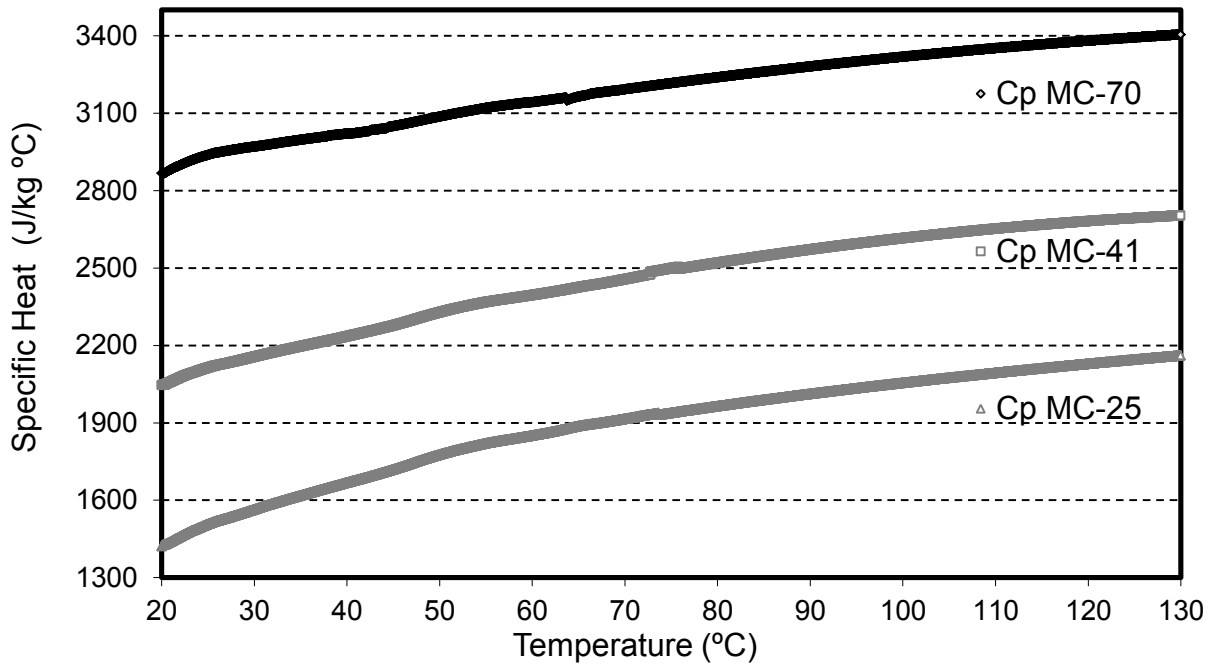


Figure 4.6 Specific heat of cherry pomace at three moisture contents (wb) .

The estimation of specific heat followed a quadratic correlation with correlation coefficient about 0.99 for the three samples of cherry pomace. The equations, which were input to the Comsol software for center temperature prediction, are summarized as following:

$$Cp_{(70MC)} = 2743.3 + 7.9606 \times T - 0.0221 \times T^2 \quad (4.13)$$

$$Cp_{(41MC)} = 1844.4 + 11.373 \times T - 0.0367 \times T^2 \quad (4.14)$$

$$Cp_{(25MC)} = 1209.9 + 13.364 \times T - 0.0479 \times T^2 \quad (4.15)$$

Where: T was in °C. This trend of specific heat with increase in temperature (as shown in Table 4.1) have similarity with some studies like a study on specific heat and thermal conductivity of softwood bark and softwood char particle from about 40 °C to

140 °C, where both specific heat and thermal conductivity increased linearly with temperature (Gupta et al., 2003)

Thermal diffusivity was estimated for the three different moisture contents of cherry pomace using the following equation (Eq.(4.16)):

$$\alpha(T, MC) = \frac{k(T, MC)}{\rho(MC) \times Cp(T, MC)} \quad (4.16)$$

The following Table (4.1) gives values of the specific heat, density, thermal conductivity and the thermal diffusivity values at each moisture content and temperature of 25 to 126.7 °C.

Table 4.1 Thermal properties of cherry pomace at three moisture contents over temperature range 25-126.7 °C

MC (%,wb)	ρ^a (kg/m ³)	Cp-range ^b 25 to 126 °C (J kg ⁻¹ °C ⁻¹)	Cp ^c (J kg ⁻¹ °C ⁻¹)	α (m ² /s)
70	1071 ±1.7	2937 -3395	2943 ± 24 3248 ± 56	(1.547 ± 0.0123)×10 ⁻⁷ (1.611 ± 0.0288)×10 ⁻⁷
41	745 ±2.2	2112-2694	2111 ± 32 2510 ± 55	(1.300 ± 0.0206)×10 ⁻⁷ (2.012 ± 0.0430)×10 ⁻⁷
25	603 ±1.9	1507-2148	1560 ± 34 2153 ± 34	(1.589 ± 0.0329)×10 ⁻⁷ (2.175 ± 0.0303)×10 ⁻⁷

^a is average value of ten replicate(Table B.1 Appendix B.2). ± (Standard error)

^b is average value at each of the two temperature range (9 replicate) by DSC method (Table B.4 Appendix B.2).

^c is average value at each of the two temperature range (9 replicate, Table B.4 Appendix B.2)).

4.3.2 Thermal Parameter Estimation Using Ordinary Least Squares

From the value and the plot of the scaled sensitivity coefficients (Figure 4.7) the parameters in the model Eq. (4.9) are large compared to 100 °C rise and uncorrelated, which means they could be estimated separately and easily.

Using MATLAB (nlinfit) the thermal conductivity was estimated at two different arbitrary temperatures, k_1 and k_2 at $T_1 = 25$ °C and $T_2 = 125$ °C, respectively. Results are summarized in Table 4.2 for heating time =90 min.

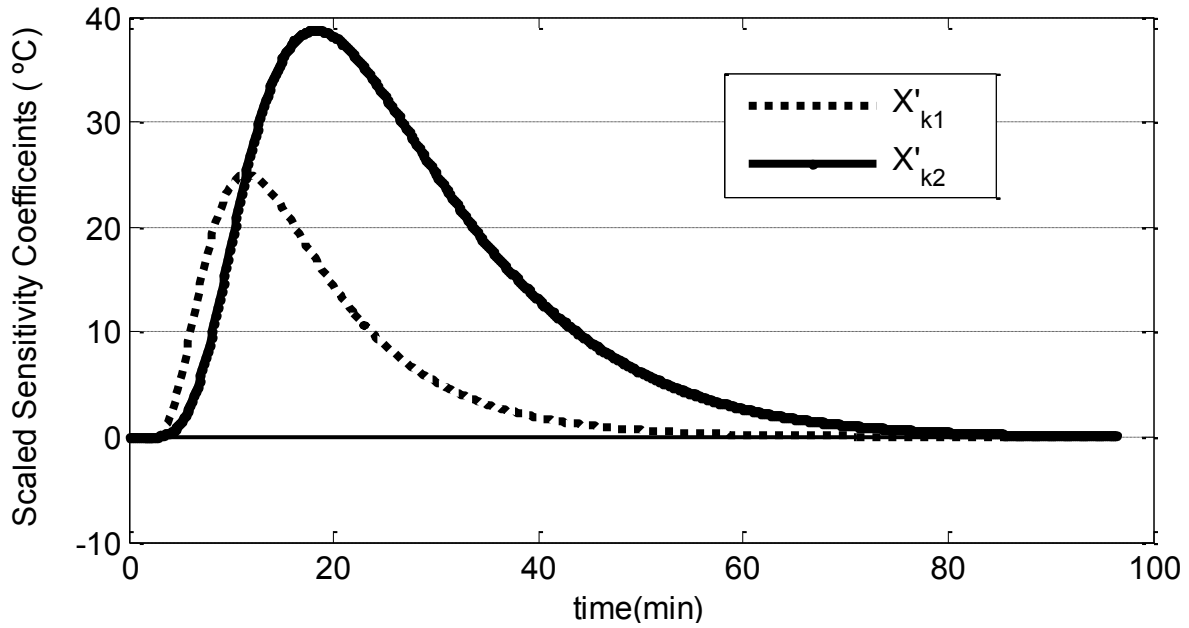


Figure 4.7 Scaled sensitivity coefficients of thermal conductivity of cherry pomace (70% MC,wb) during 90 min of retorting

Table 4.2 Estimation of thermal conductivity parameters for cherry pomace (90 min retorting) at T1=25 °C and T2= 125 °C.

MC (wb)	k W m ⁻¹ °C ⁻¹	Estimate k	Std Err	Correlation Coefficient	Confidence Interval (95%)	RMSE (°C)
70%	k ₁	0.498	0.00047	-0.84	0.4981 0.4981	0.67
	k ₂	0.559	0.00058		0.5590 0.5591	
41%	k ₁	0.204	0.00145	-0.99	0.2043 0.2044	0.95
	k ₂	0.375	0.00124		0.3752 0.3754	
25%	k ₁	0.149	0.0034	-0.92	0.1497 0.1499	4.2
	k ₂	0.282	0.0037		0.2820 0.2824	

Based on data on Table 4.2, thermal conductivity was correlated as function of the three moisture contents and the following Eqs were found:

$$k_1(MC) = 0.008043 \times MC - 0.08096 \quad R^2 = 0.95 \quad (4.17)$$

$$k_2(MC) = 0.00617 \times MC + 0.1252 \quad R^2=0.99 \quad (4.18)$$

The slope in Eq. (4.17) has $p = 0.13$ which means the effect of moisture is not significant but the slope in Eq. (4.18) has $p = 0.014$ which shows a significant effect of moisture contents in cherry pomace on thermal conductivity as a function of temperature. Predicted and observed temperature vs. time data by Comsol (for two cans) was plotted with observed data and showed good fit with very small confidence intervals as shown in Figure 4.8. Residuals for Comsol’s center temperature prediction also showed small values after the first 10 min as shown in Figure 4.9. The residuals were larger during the first 10 min, showing some difficulty in fitting. After the first 10 min, the residuals were additive and variance constant and the mean ≈ 0 , meeting the standard statistical assumptions.

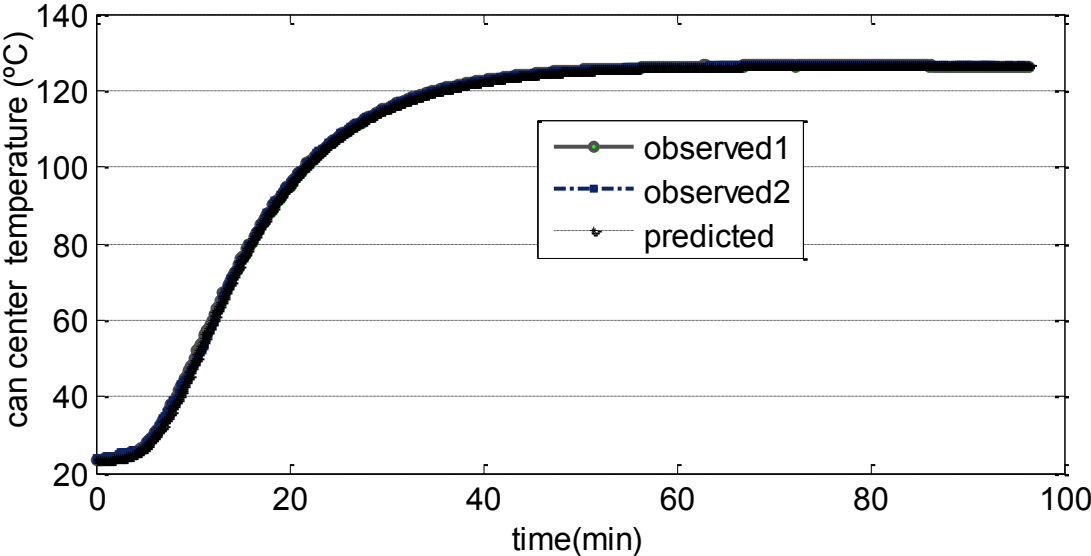


Figure 4.8 Time-temperature plot of observed and predicted center temperature of the cans of cherry pomace (70%MC) heated at 126.7°C for 90 min

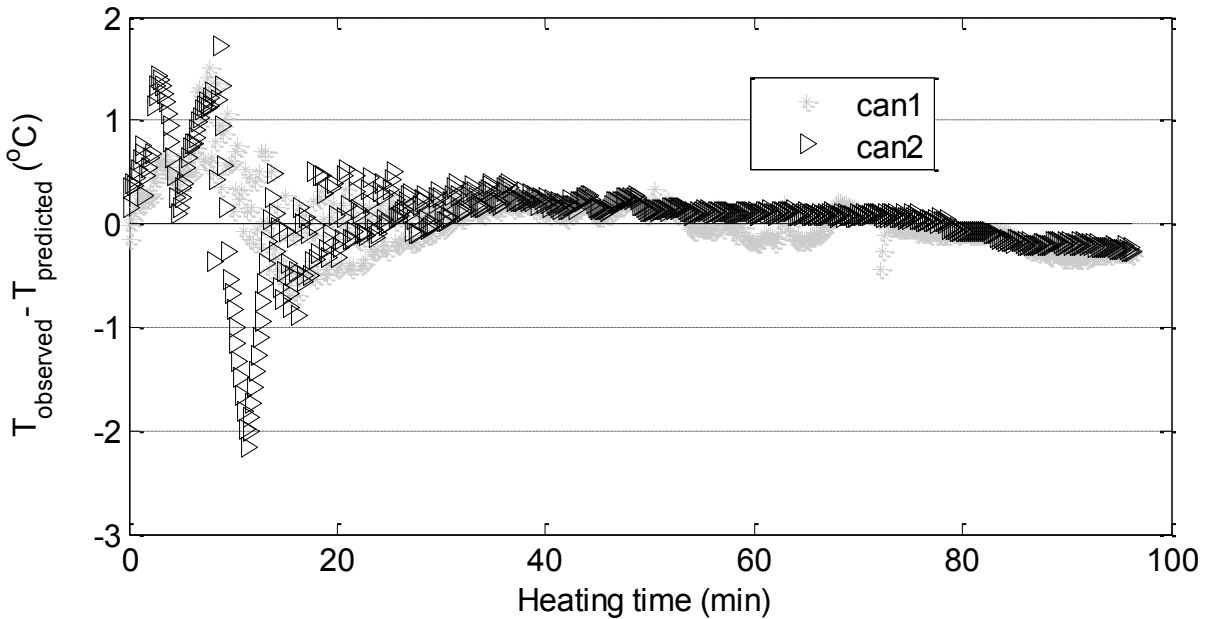


Figure 4.9 Residual plot of Predicted Temperature at the center of two cans of cherry pomace (70%MC) heated at for 90 min

4.3.3 Thermal Parameter Estimation Using the Sequential Procedure

The advantage of sequential estimation is that it gives the big picture on the estimation process. As showed in Figure 4.10 and Figure 4.11 the estimation process of thermal conductivity had steady values after about 200 steps of the process (~17 min). This result is similar with a study on solid foods, where simultaneous estimation of thermal conductivity was performed using sequential parameter estimation (Mohamed, 2009). The final sequential estimation of k_1 and k_2 were identical to those from OLS as shown in Table 2.

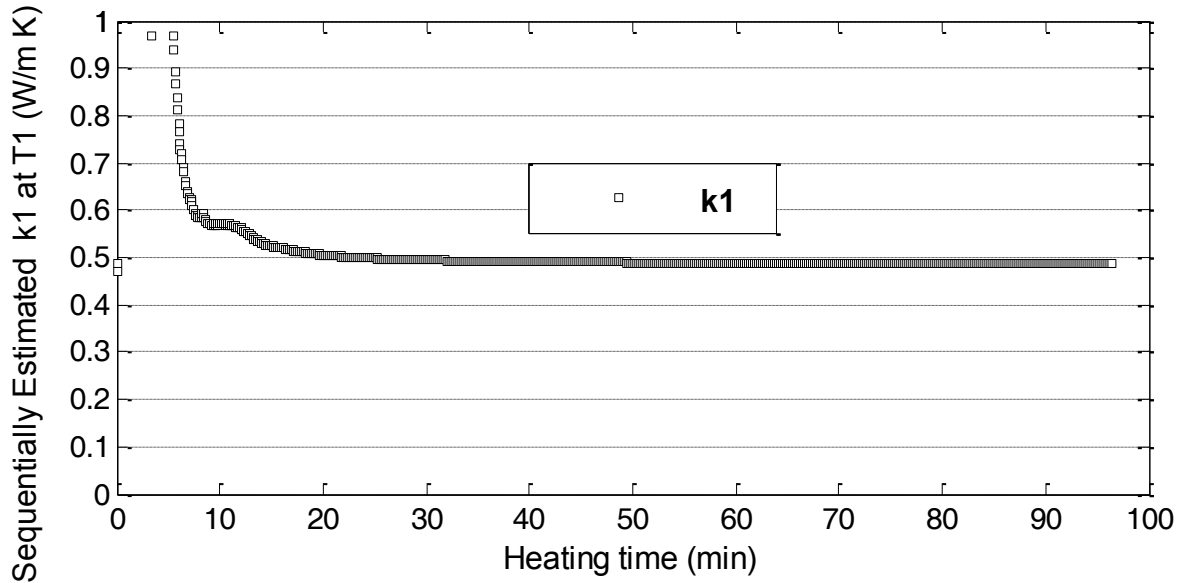


Figure 4.10 Sequential estimation of thermal conductivity (k_1) = 0.489 (W/m °C) of Cherry pomace (70% MC, wb) at 90 min of retorting. $T_1 = 25$ °C.

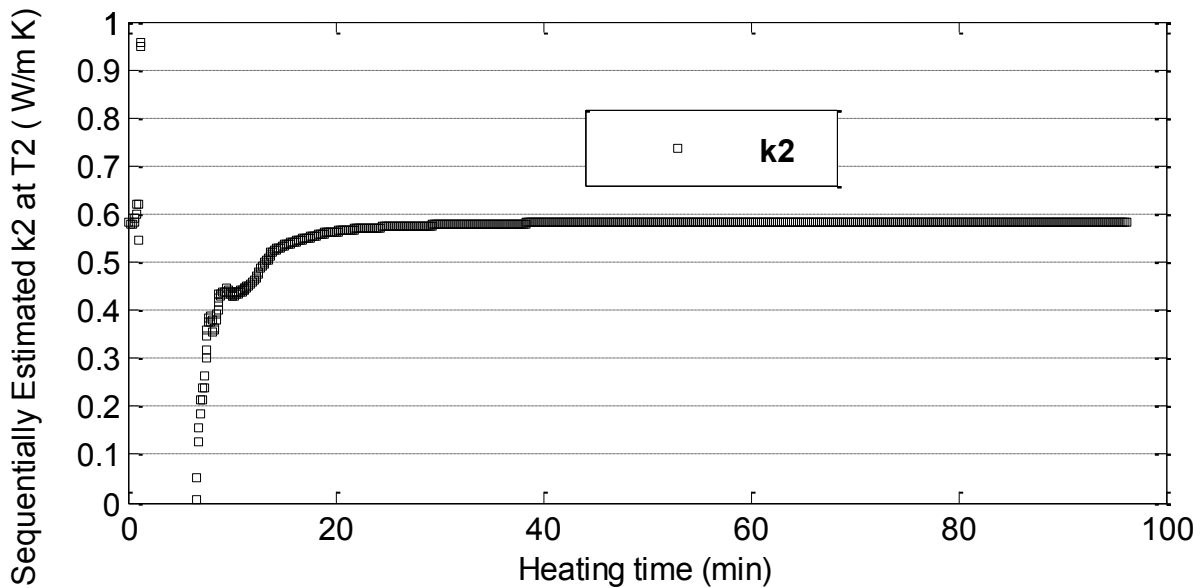


Figure 4.11 Sequential estimation of thermal conductivity (k_2) = 0.581 (W/m °C) of Cherry pomace (70% MC, wb) at 90 min of retorting. $T_2 = 125$ °C

Table 4.3 shows thermal conductivity literature values of some food products, which were estimated under different conditions of temperature and geometry.

Table 4.3 A comparative literature review of thermal conductivity values of some food products

Material	Method	Model's functions	MC (%wb)	Temp, (°C)	Thermal conductivity (W m ⁻¹ K ⁻¹)	Reference
Grape pomace	Nonlinear regression	temperature	42	100	0.50	(Mishra et al., 2008)
Cherry tomato	Probe method	temperature	92	28	0.462	(Sweat and Haugh, 1974)
Potato & Apple	Modified, Fitch method	temperature	fresh	30	0.52 0.43	(Donsi et al., 1996)
Concentrated cherry juice	the coaxial cylinders method	temperature Concentration & combination	°Brix (27)	20-140	0.48-0.56	(Magerramov et al., 2006b)
straw mushroom	Probe method	Temperature MC	(30 to 90%)	50-80	0.212–0.668	(Tansakul and Lumyong, 2008)

Choi and Okos (1986) established empirical equations for thermal conductivity estimation based on the main components of the food materials as a function of temperature. The carbohydrate, fiber and water used for the comparison with this study were the main components for the cherry pomace (McCune et al., 2011). The thermal conductivity of cherry pomace for each moisture content (Table 4.4) was the sum of each component multiplied by its volume fraction (Valentas et al., 1997b).

Table 4.4: comparative of thermal conductivity values of Cherry pomace by this study with Choi and Okos empirical equations .

MC%(wb)	Temperatures (°C)	Choi & Okos (1986)	This study
70	25	0.475	0.498
	126	0.573	0.559
41	25	0.340	0.204
	126	0.419	0.375
25	25	0.265	0.149
	126	0.335	0.282

As showed in Table 4.4 the values at 70%MC were close to those from study. For 41% and 25% the Choi and Okos values were higher than those from this study.

4.4 Model validation

Cherry pomace at the three constant moisture content was filled in the steel cans, which were fitted with three thermocouples, one in the center, the second one in offset (at $R/2$) and the third one on the surface of the can. Figure 4.12 show a plot of the temperatures vs time in the retort for the can with 70% cherry pomace.

All collected data of temperature vs time of the three constant moisture content were entered in the Prop1D software (Prop1D Software, Beck Engineering Consultants Company, [www. BeckEng.com](http://www.BeckEng.com)) and the k_1 and k_2 were calculated and compared with the results for this study showed in Table 4.4. The Prop1D uses a finite difference code for 1-D heat transfer. Results showed good agreement with the values in this study for 70 and 41 % MC (wb). The RMSE for the Prop1D method was much lower than this study, but the experimental time for the Prop1D was also much shorter (about 600 s for 70% MC, wb) to maintain 1D heat transfer.

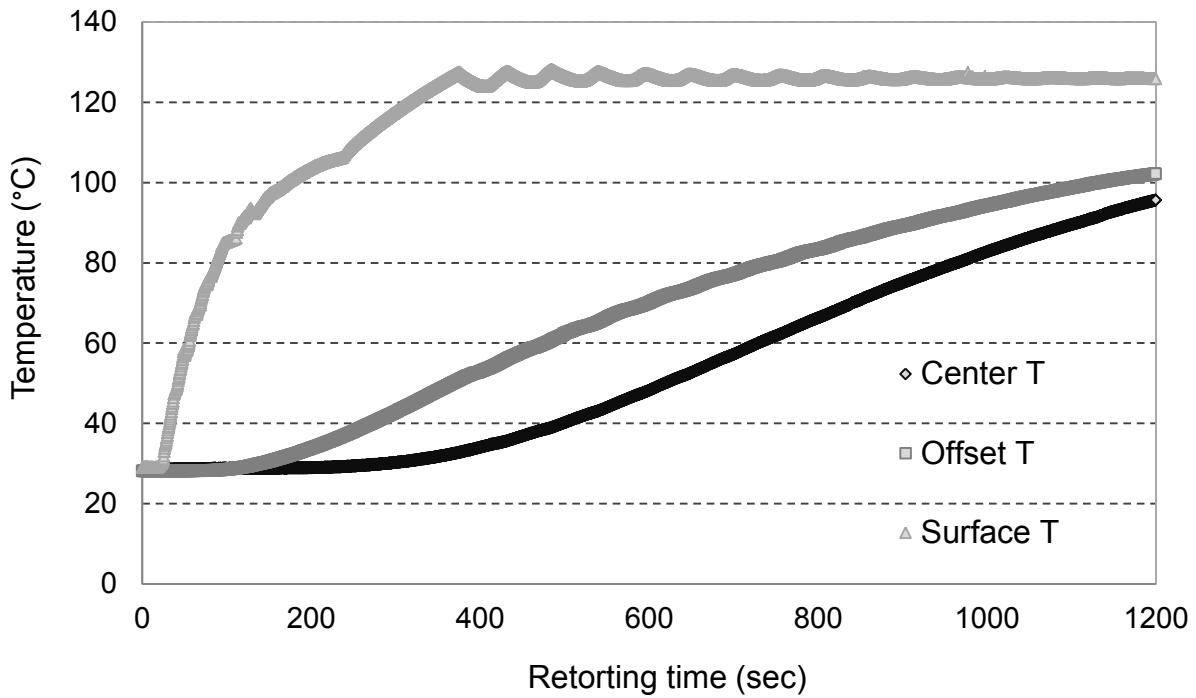


Figure 4.12 Temperature vs. time profile at three location of cherry pomace (70%, wb) in the steel can after retorting at 126.7°C for about 20 min)

Table 4.5 Estimation of thermal conductivity (k(t)) parameters for cherry pomace (90 min retorting): OLS vs.Prop1D method

MC (% ,wb)	k(T) (W m ⁻¹ °C ⁻¹)	k(T) by OLS & sequential	k(T) by Prop1D	RMSE (°C) OLS	RMSE (°C) Prop1D
70	k ₁	0.498	0.502	0.67	1.019
	k ₂	0.559	0.641		
41	k ₁	0.204	0.263	0.95	1.07
	k ₂	0.375	0.382		
25	k ₁	0.149	0.297	4.2	1.92
	k ₂	0.282	0.469		

4.5 Conclusions

- Temperature-dependent specific heat of cherry pomace at three constant moisture contents was determined using the DSC method in a temperature range of 25 to 130 °C the specific heat increased with moisture content and temperature.
- Thermal conductivity values for cherry pomace at three constant moisture contents and temperature range 25 to 125 °C were successfully estimated using OLS and sequential estimation. The values increased with temperature and moisture content.
- Thermal diffusivity increased with temperature and decreased with moisture content (from 25% to 70% moisture) 2.6% and 26 % decrease at 25 °C and 126.7 °C, respectively, due primarily to the significant increase in densities of the pomace.
- This study presents one of the few inverse methods known to estimate temperature-dependent thermal conductivity for solid food products in one experiment at temperature above 100°C in approximately 30 min. This procedure may be used for predicting nutraceutical degradation or microbial inactivation in food processes.

APPENDICES

Appendix B.1 Experimental design and preliminary data

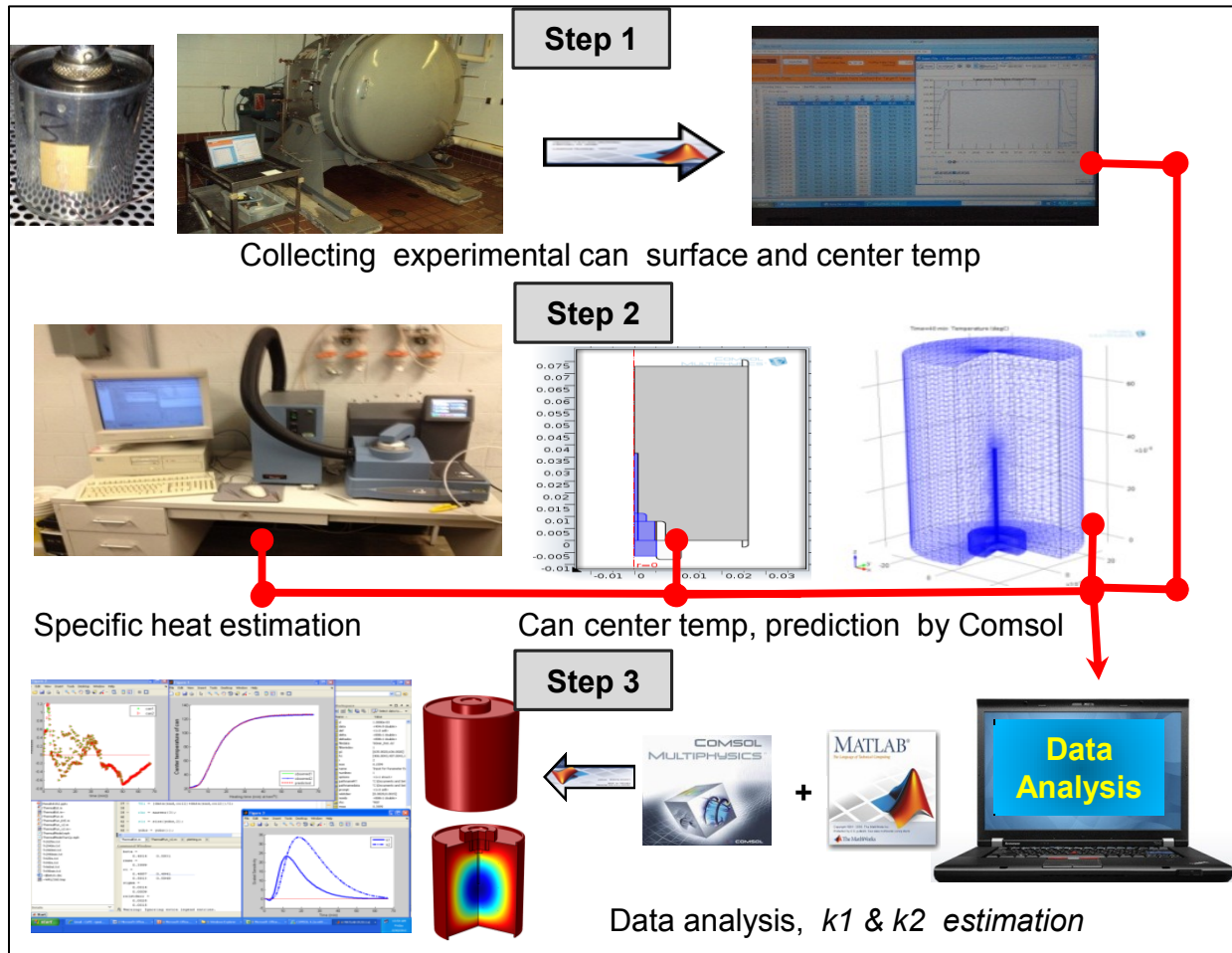


Figure B.1 Process experimental design for thermal properties estimation

Table B.1 Cherry pomace 's bulk density at different Moisture contents

Moisture Content	Weight (g) ^a	MC%	Density ^b			
			kg/m ³	AVG	STDV	SE
25%(wb)	79.73	25	586.3	603	12.7	1.3
	80.3	25	590.4			
	79.53	25	584.8			
	81.32	25	597.9			
	81.3	25	597.8			
	83.11	25	611.1			
	84.44	25	620.9			
	83.4	25	613.2			
	82.6	25	607.4			
	84.3	25	619.9			
41%(wb)	101.99	41	749.9	745	43.3	1.7
	98.77	41	726.3			
	100.12	41	736.2			
	99.24	41	729.7			
	99.61	41	732.4			
	100.3	41	737.5			
	103.73	41	762.7			
	104.3	41	766.9			
	105.2	41	773.5			
	100.5	41	739.0			
70%(wb)	147.55	70	1084.9	1071	106.2	2.0
	147.77	70	1086.5			
	146.48	70	1077.1			
	144.89	70	1065.4			
	144.66	70	1063.7			
	144.49	70	1062.4			
	139.1	70	1022.8			
	146.33	70	1076.0			
	147.7	70	1086.0			
	147.9	70	1087.5			

^a-(10 replicates)

^b-Can effective volume is 136 cm³ (Water replacement)

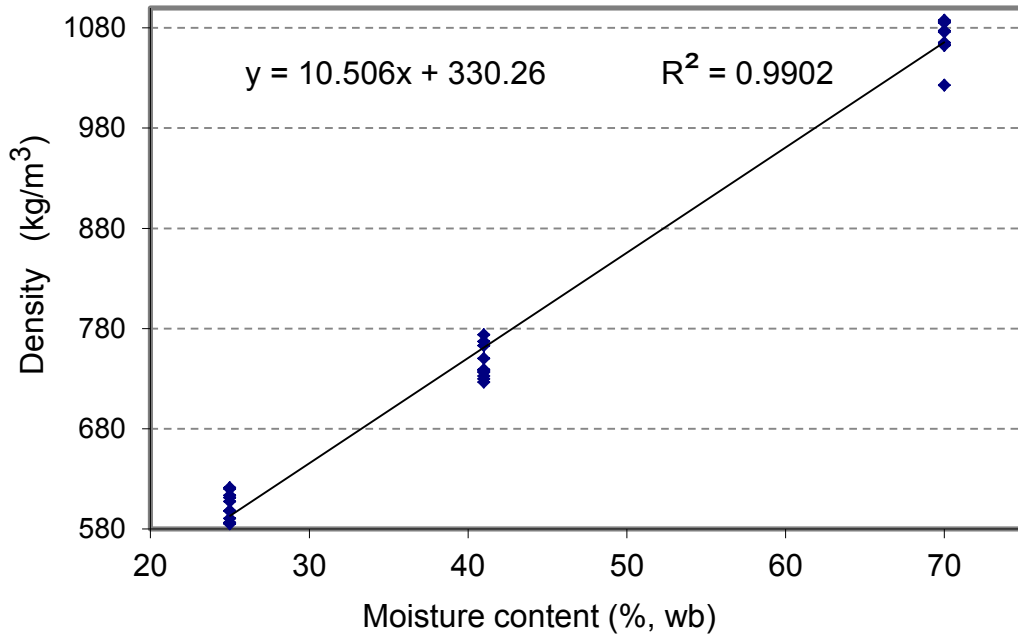


Figure B.2 Cherry pomace 's Bulk density at different Moisture contents

Table B.2 Can Steel (202×214) exact diminutions & (Steel properties (Singh, 2001).

Characteristic	Value	Unit
Inside diameter (ID)	52.40	mm
Outside diameter (OD)	52.62	mm
Steel Thickness (x)	0.22	mm
Radius ($R'=OD/2$)	0.02631	m
Height (H)	0.06724	m
Volume of the can ($\pi R'^2 H$)	0.0001462	m ³
Effective volume (V)	136	cm ³
Height no-edge	67.24	mm
Height + edge	72.65	mm
edge Thickness	1.25	mm
Edge height	2.69	mm
Density (ρ)	7833	Ka/m ³
Specific heat (Cp)	465	J kg ⁻¹ K ⁻¹
Thermal conductivity (k)	54	W m ⁻¹ K ⁻¹

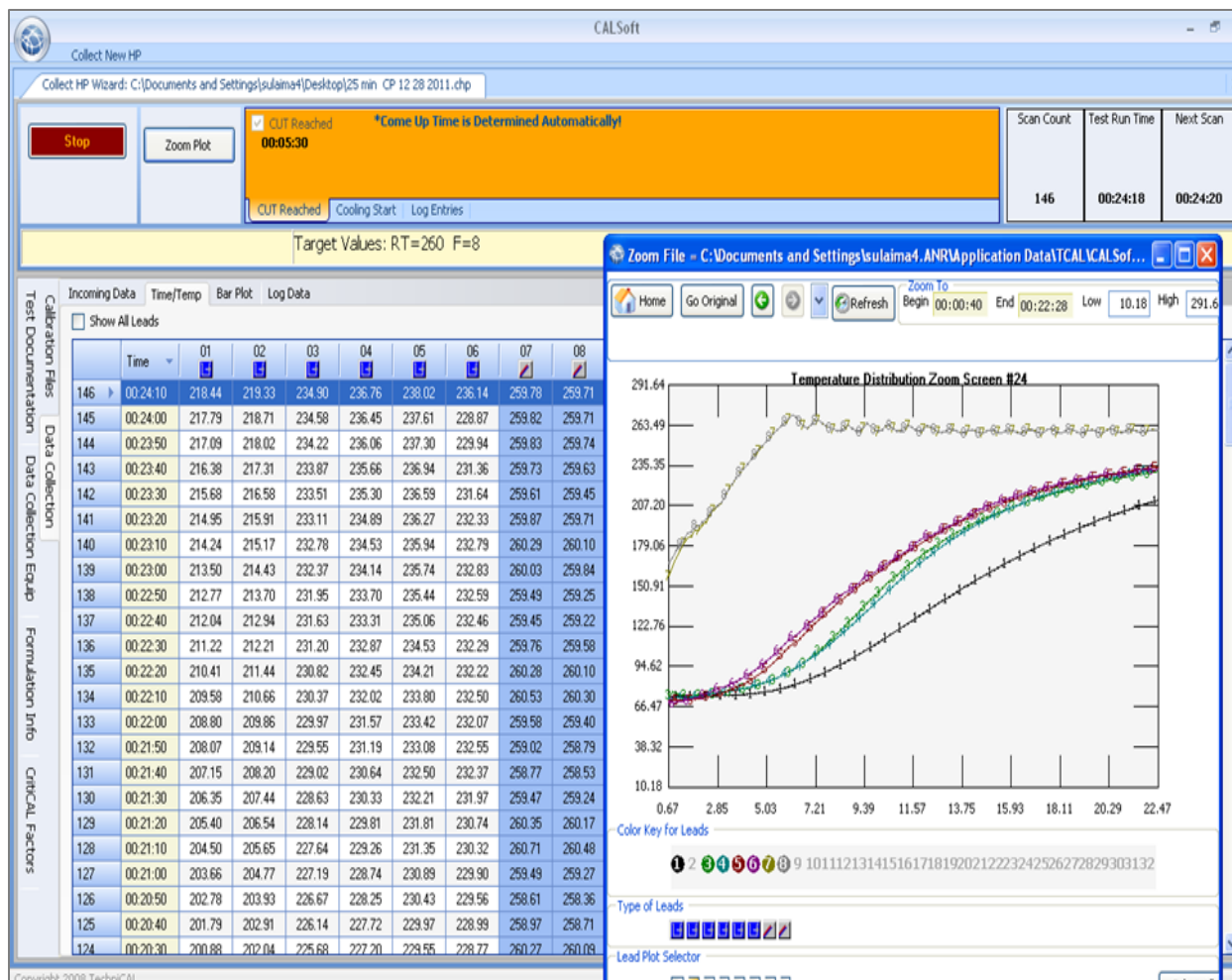


Figure B.3 Gen5 Software view for temperature vs time data collection during retorting. "The text in this figure is not meant to be readable but is for visual reference only".

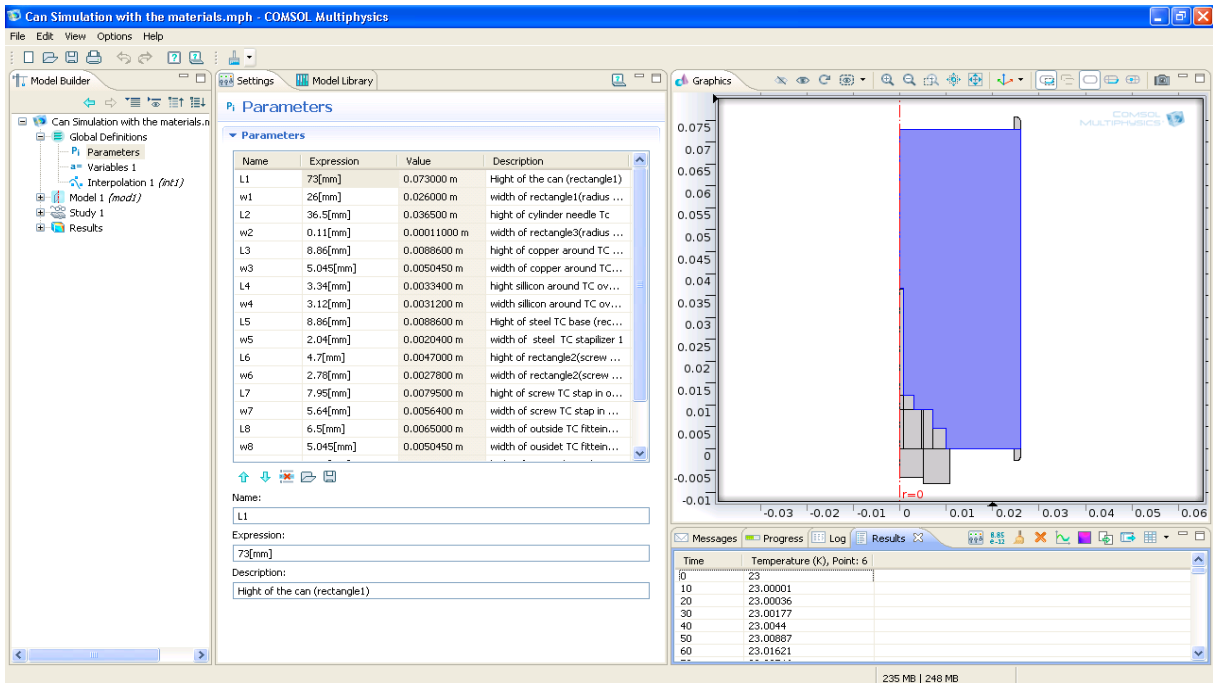


Image 1 .Parameters and geometry

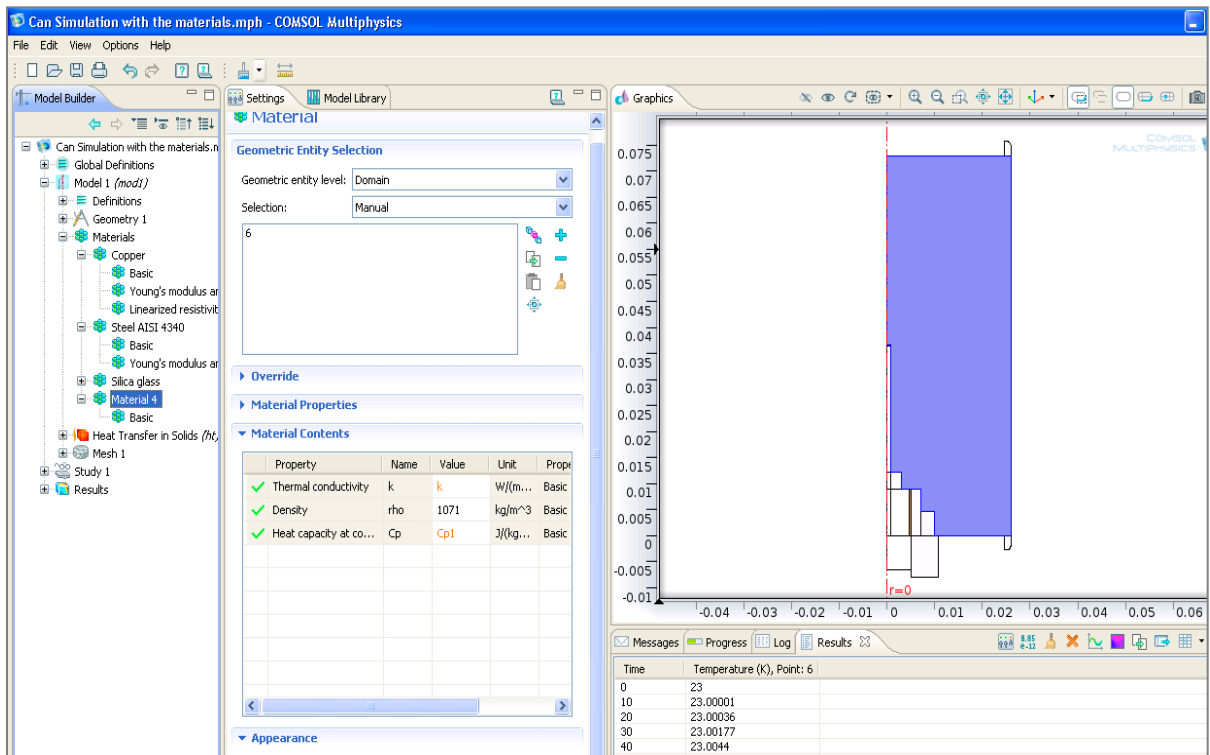


Image 2. Materials

Figure B.4 Images of Comsol simulation Steps of Can Heating. “The text in this figure is not meant to be readable but is for visual reference only”.

Figure B.4 (cont'd)

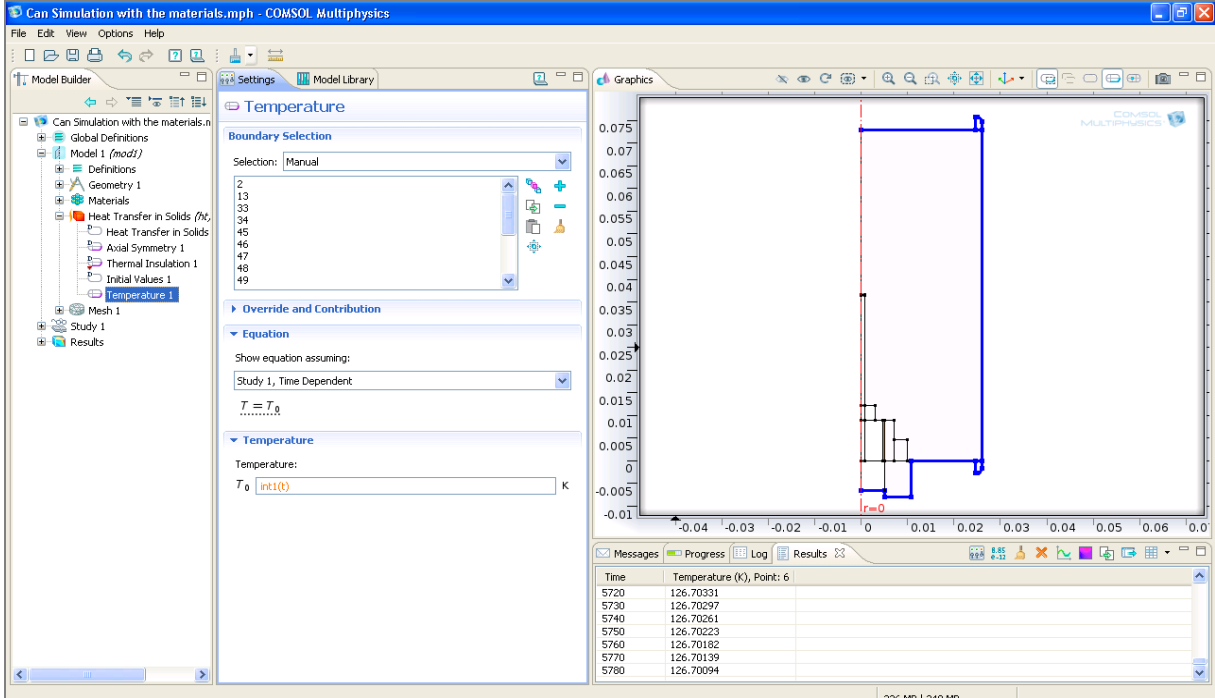


Image 3 .Heat transfer boundary

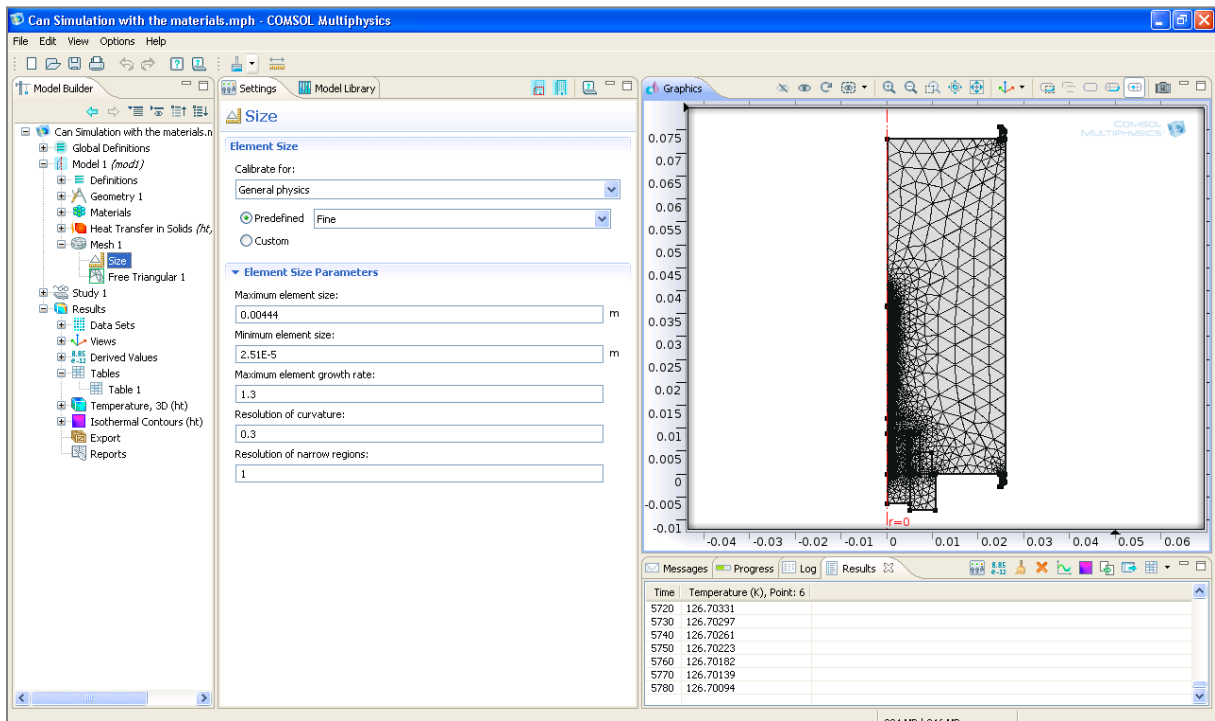


Image 4 Meshing and elements

Figure B.4 (cont'd)

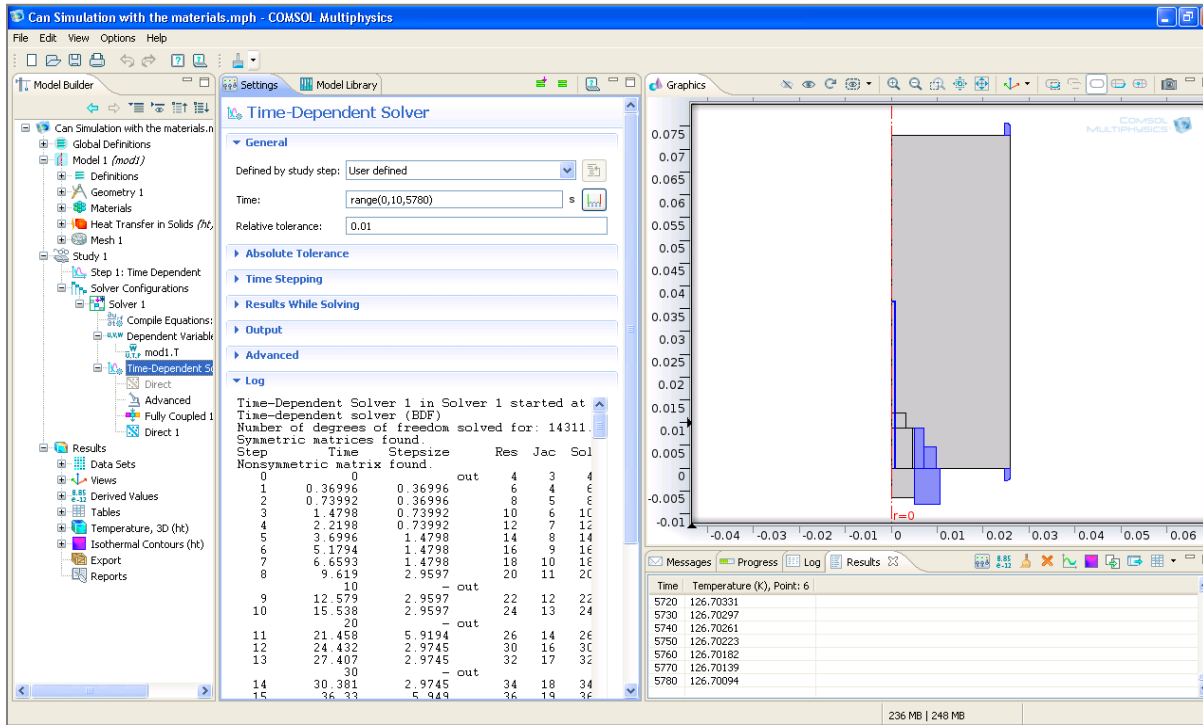


Image 5. Study (Run steps)

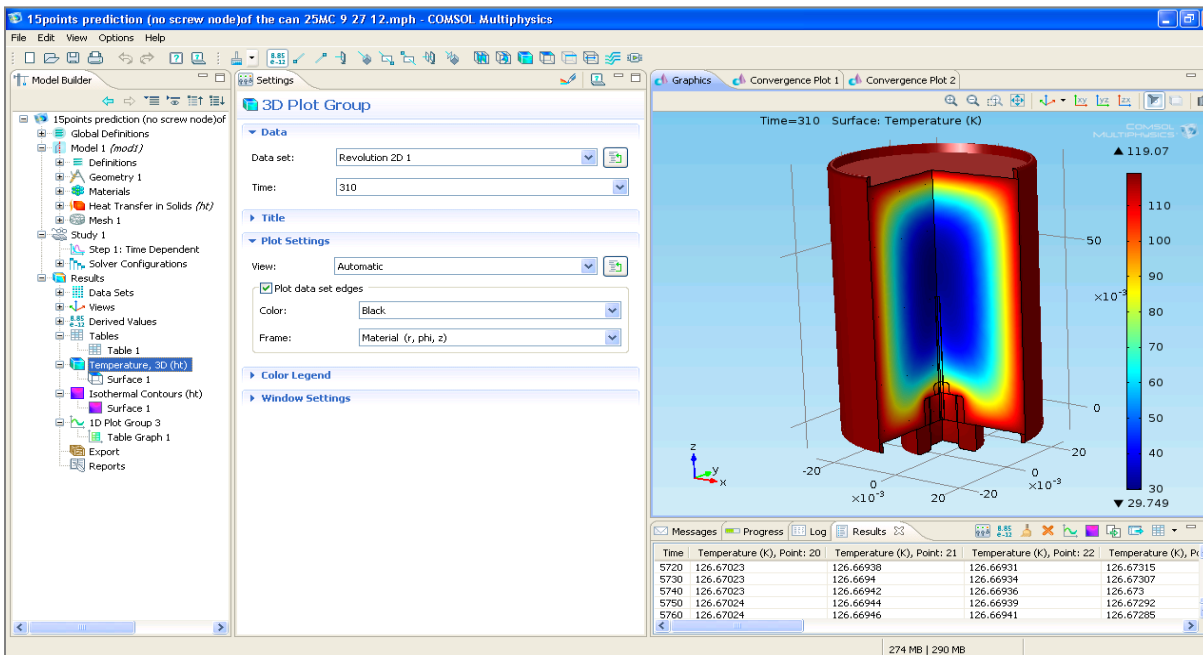


Image 6 Results and predicted data collections

Appendix B.2 Thermal properties determination (DSC)

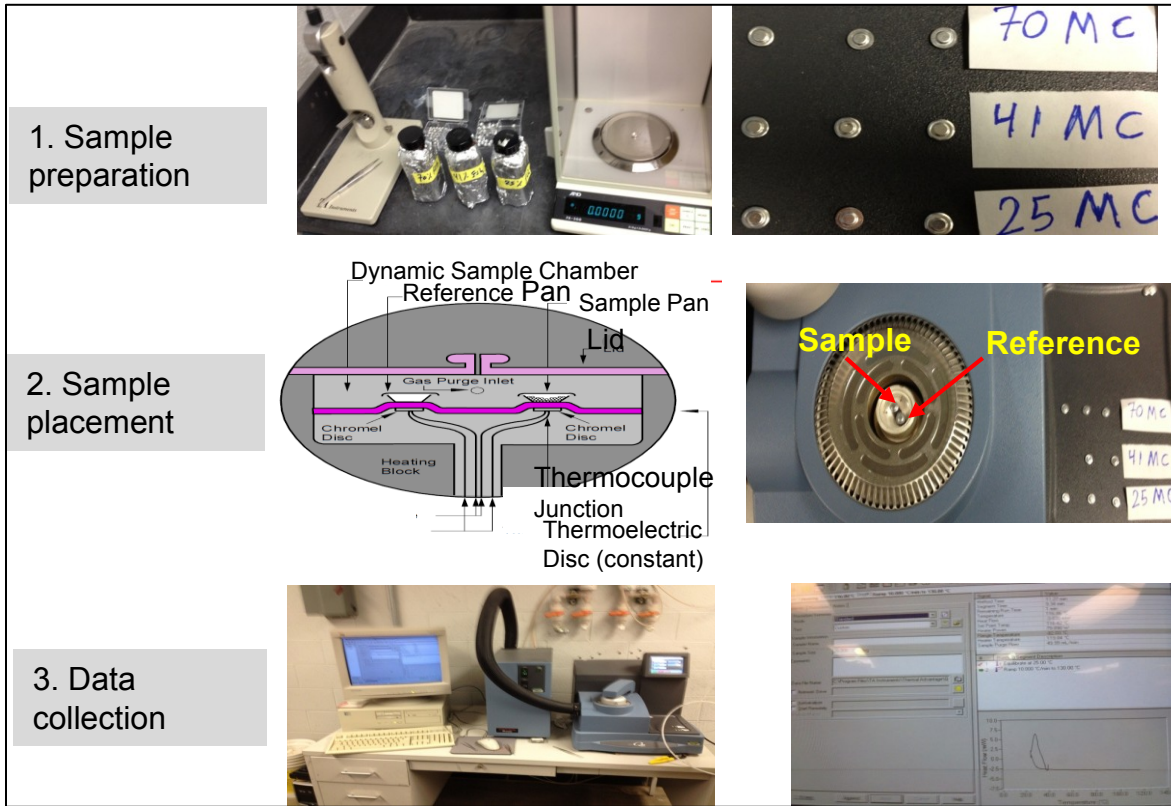


Figure B.5 Steps Cherry pomace's thermal properties measurement using DSC. "The text on the images is not meant to be readable but is for visual reference only.

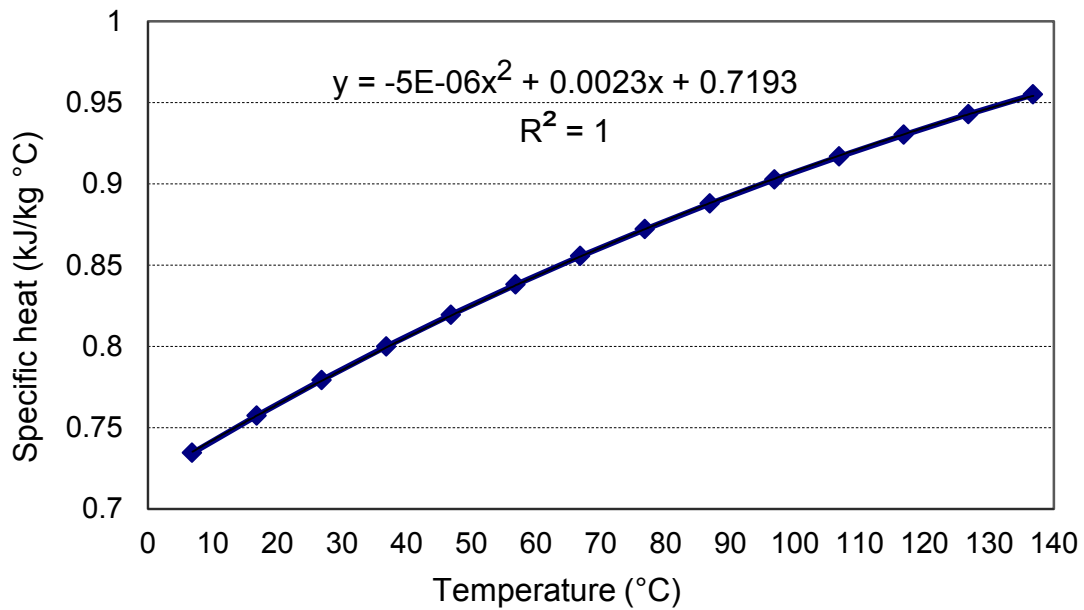


Figure B.6 Sapphire Specific heat capacity

Table B.3 Example Specific heat's (Cp) Excel sheet calculation steps for 70% moisture content (wb) Cherry pomace using DSC method

time min	Heat flow (mW) Spphair (St) and baseline(Bs)			Cp and Calibration constant		Heat flow (mw) Sample			Heat flow Sample-baseline (mw)			Specific heat (Cp) (J kg ⁻¹ °C ⁻¹)			*Statistic	
	St	Bs	Bs-St	Cp _(st)	ks	1	2	3	1	2	3	Cp1	Cp2	Cp3	AVG	STD
25.0	-3.44	0.09	3.53	0.77	0.80	-6.01	-4.83	-4.90	6.09	4.92	4.99	2942	3085	2937	2988	73
25.0	-3.44	0.09	3.53	0.77	0.80	-6.01	-4.84	-4.90	6.10	4.92	4.99	2942	3085	2938		
25.0	-3.44	0.09	3.53	0.77	0.80	-6.01	-4.84	-4.91	6.10	4.92	4.99	2942	3085	2938		
25.1	-3.44	0.09	3.53	0.77	0.80	-6.01	-4.84	-4.91	6.10	4.92	4.99	2943	3086	2802	2944	123
25.1	-3.44	0.09	3.53	0.77	0.80	-6.01	-4.84	-4.91	6.10	4.92	5.00	2943	3086	2803		
25.1	-3.44	0.09	3.53	0.77	0.80	-6.01	-4.84	-4.91	6.10	4.92	5.00	2943	3086	2804		
25.2	-3.44	0.09	3.53	0.77	0.80	-6.01	-4.84	-4.91	6.10	4.93	5.00	2944	3086	2804	2945	122
25.2	-3.44	0.09	3.53	0.77	0.80	-6.02	-4.84	-4.91	6.10	4.93	5.00	2944	3087	2805		
25.2	-3.44	0.09	3.53	0.77	0.80	-6.02	-4.84	-4.91	6.10	4.93	5.00	2945	3087	2806		
25.3	-3.44	0.09	3.53	0.77	0.80	-6.02	-4.84	-4.92	6.10	4.93	5.00	2945	3087	2806	2946	122
25.3	-3.44	0.09	3.53	0.77	0.80	-6.02	-4.84	-4.92	6.11	4.93	5.00	2945	3088	2807		
25.3	-3.45	0.09	3.53	0.77	0.80	-6.02	-4.84	-4.92	6.11	4.93	5.00	2946	3088	2807		
25.4	-3.45	0.09	3.53	0.77	0.80	-6.02	-4.84	-4.92	6.11	4.93	5.00	2946	3088	2807	2947	122
25.4	-3.45	0.09	3.53	0.77	0.80	-6.02	-4.84	-4.92	6.11	4.93	5.01	2946	3088	2807		
25.4	-3.45	0.09	3.53	0.77	0.80	-6.02	-4.84	-4.92	6.11	4.93	5.01	2946	3089	2808		
25.5	-3.45	0.09	3.53	0.77	0.80	-6.02	-4.85	-4.92	6.11	4.93	5.01	2946	3089	2809	2948	121
25.5	-3.45	0.09	3.53	0.77	0.80	-6.02	-4.85	-4.92	6.11	4.93	5.01	2947	3089	2810		
25.5	-3.45	0.09	3.53	0.77	0.80	-6.02	-4.85	-4.93	6.11	4.93	5.01	2947	3090	2810		
25.6	-3.45	0.09	3.54	0.77	0.80	-6.03	-4.85	-4.93	6.11	4.93	5.01	2947	3090	2810	2949	121
25.6	-3.45	0.09	3.54	0.77	0.80	-6.03	-4.85	-4.93	6.11	4.94	5.01	2947	3090	2811		

Table B.3 (cont'd)

25.6	-3.45	0.09	3.54	0.77	0.80	-6.03	-4.85	-4.93	6.11	4.94	5.02	2947	3091	2811		
25.7	-3.45	0.09	3.54	0.78	0.80	-6.03	-4.85	-4.93	6.11	4.94	5.02	2947	3091	2812	2951	120
25.7	-3.45	0.09	3.54	0.78	0.80	-6.03	-4.85	-4.93	6.12	4.94	5.02	2948	3091	2813		
25.7	-3.45	0.09	3.54	0.78	0.80	-6.03	-4.85	-4.93	6.12	4.94	5.02	2948	3091	2814		
25.8	-3.45	0.09	3.54	0.78	0.80	-6.03	-4.85	-4.93	6.12	4.94	5.02	2948	3092	2814	2951	120
25.8	-3.45	0.09	3.54	0.78	0.80	-6.03	-4.85	-4.94	6.12	4.94	5.02	2948	3092	2814		
25.8	-3.45	0.09	3.54	0.78	0.80	-6.03	-4.85	-4.94	6.12	4.94	5.02	2948	3092	2814		
25.9	-3.45	0.09	3.54	0.78	0.80	-6.03	-4.85	-4.94	6.12	4.94	5.02	2948	3092	2815	2952	120
25.9	-3.45	0.09	3.54	0.78	0.80	-6.03	-4.86	-4.94	6.12	4.94	5.02	2949	3092	2815		
25.9	-3.46	0.09	3.54	0.78	0.80	-6.03	-4.86	-4.94	6.12	4.94	5.03	2949	3093	2815		
26.0	-3.46	0.09	3.54	0.78	0.80	-6.04	-4.86	-4.94	6.12	4.94	5.03	2949	3093	2816	2953	120
26.0	-3.46	0.09	3.54	0.78	0.80	-6.04	-4.86	-4.94	6.12	4.94	5.03	2949	3093	2816		
26.0	-3.46	0.09	3.54	0.78	0.80	-6.04	-4.86	-4.94	6.12	4.94	5.03	2950	3093	2816		
26.1	-3.46	0.09	3.54	0.78	0.80	-6.04	-4.86	-4.94	6.12	4.94	5.03	2950	3093	2817	2953	120
26.1	-3.46	0.09	3.54	0.78	0.80	-6.04	-4.86	-4.94	6.12	4.94	5.03	2950	3093	2817		
26.1	-3.46	0.09	3.55	0.78	0.80	-6.04	-4.86	-4.94	6.13	4.95	5.03	2949	3093	2817		
26.2	-3.46	0.09	3.55	0.78	0.80	-6.04	-4.86	-4.95	6.13	4.95	5.03	2949	3093	2817	2953	119
26.2	-3.46	0.09	3.55	0.78	0.80	-6.04	-4.86	-4.95	6.13	4.95	5.03	2950	3093	2817		
26.2	-3.46	0.09	3.55	0.78	0.80	-6.04	-4.86	-4.95	6.13	4.95	5.03	2950	3094	2818		
26.3	-3.46	0.09	3.55	0.78	0.80	-6.04	-4.86	-4.95	6.13	4.95	5.03	2950	3094	2818	2954	119
26.3	-3.46	0.09	3.55	0.78	0.80	-6.04	-4.86	-4.95	6.13	4.95	5.04	2950	3094	2819		

Table B.3 (cont'd)

26.3	-3.46	0.09	3.55	0.78	0.80	-6.04	-4.86	-4.95	6.13	4.95	5.04	2951	3094	2819		
26.4	-3.46	0.09	3.55	0.78	0.80	-6.04	-4.86	-4.95	6.13	4.95	5.04	2951	3094	2819	2955	119
26.4	-3.46	0.09	3.55	0.78	0.80	-6.05	-4.86	-4.95	6.13	4.95	5.04	2951	3094	2819		
26.4	-3.46	0.09	3.55	0.78	0.80	-6.05	-4.87	-4.95	6.13	4.95	5.04	2951	3095	2820		
26.5	-3.46	0.09	3.55	0.78	0.80	-6.05	-4.87	-4.95	6.13	4.95	5.04	2951	3095	2820	2955	119
26.5	-3.47	0.09	3.55	0.78	0.80	-6.05	-4.87	-4.95	6.13	4.95	5.04	2951	3095	2820		
26.5	-3.47	0.09	3.55	0.78	0.80	-6.05	-4.87	-4.96	6.13	4.95	5.04	2951	3095	2820		
26.6	-3.47	0.09	3.55	0.78	0.80	-6.05	-4.87	-4.96	6.13	4.95	5.04	2951	3095	2820	2956	119
26.6	-3.47	0.09	3.55	0.78	0.80	-6.05	-4.87	-4.96	6.14	4.96	5.04	2951	3096	2821		
26.6	-3.47	0.09	3.55	0.78	0.80	-6.05	-4.87	-4.96	6.14	4.96	5.04	2951	3096	2821		
26.7	-3.47	0.09	3.55	0.78	0.80	-6.05	-4.87	-4.96	6.14	4.96	5.05	2951	3096	2822	2957	119
26.7	-3.47	0.09	3.56	0.78	0.80	-6.05	-4.87	-4.96	6.14	4.96	5.05	2951	3096	2822		
26.7	-3.47	0.09	3.56	0.78	0.80	-6.05	-4.87	-4.96	6.14	4.96	5.05	2951	3096	2823		
26.8	-3.47	0.09	3.56	0.78	0.80	-6.05	-4.87	-4.96	6.14	4.96	5.05	2952	3096	2823	2957	118
26.8	-3.47	0.09	3.56	0.78	0.80	-6.05	-4.87	-4.96	6.14	4.96	5.05	2952	3097	2823		
26.8	-3.47	0.09	3.56	0.78	0.80	-6.06	-4.87	-4.97	6.14	4.96	5.05	2952	3097	2824		
26.9	-3.47	0.09	3.56	0.78	0.80	-6.06	-4.88	-4.97	6.14	4.96	5.05	2952	3097	2824	2958	118
26.9	-3.47	0.09	3.56	0.78	0.80	-6.06	-4.88	-4.97	6.14	4.96	5.05	2953	3098	2824		
26.9	-3.47	0.09	3.56	0.78	0.80	-6.06	-4.88	-4.97	6.14	4.96	5.05	2953	3098	2824		
27.0	-3.47	0.09	3.56	0.78	0.80	-6.06	-4.88	-4.97	6.14	4.96	5.06	2953	3098	2825	2959	118
27.0	-3.47	0.09	3.56	0.78	0.80	-6.06	-4.88	-4.97	6.15	4.96	5.06	2953	3098	2825		
27.0	-3.47	0.09	3.56	0.78	0.80	-6.06	-4.88	-4.97	6.15	4.97	5.06	2953	3098	2825		

* Each temperature point done in 9 replicates (average and STDV was calculated)

Table B.4 Thermal properties estimation at two temperatures (25, 126) of cherry pomace $\text{J kg}^{-1} \text{K}^{-1}$

Moisture %,(wb)			Specific heat ($\text{J kg}^{-1} \text{K}^{-1}$)					Thermal Diffusivity (m^2/s)				
	ρ	k	Cp1	Cp2	Cp3	AVG	SE	$\alpha 1$	$\alpha 2$	$\alpha 3$	AVG	SE
Values at 25 °C												
25-MC	603	0.149	1507	1479	1692	1650	34	1.64E-07	1.67E-07	1.46E-07	1.59.E-07	0.033E-07
25-MC			1507	1480	1693			1.64E-07	1.67E-07	1.45E-07		
25-MC			1057	1480	1693			1.64E-07	1.66E-07	1.45E-07		
41-MC	745	0.204	1981	2178	2172	2111	32	1.38E-07	1.25E-07	1.26E-07	1.30.E-07	0.021E-07
41-MC			1981	2179	2173			1.38E-07	1.25E-07	1.26E-07		
41-MC			1982	2180	2173			1.38E-07	1.25E-07	1.26E-07		
70-MC	1071	0.495	2942	3085	2937	2988	24	1.57E-07	1.49E-07	1.57E-07	1.54E-07	0.04E-07
70-MC			2942	3085	2938			1.57E-07	1.49E-07	1.57E-07		
70-MC			2942	3085	2938			1.57E-07	1.49E-07	1.57E-07		
Values at 126 °C												
25-MC	603	0.282	2265	2134	2059	2153	30	2.06E-07	2.19E-07	2.27E-07	2.18E-07	0.03E-07
25-MC			2267	2134	2059			2.06E-07	2.19E-07	2.27E-07		
25-MC			2269	2135	2059			2.06E-07	2.19E-07	2.27E-07		
41-MC	745	0.375	2351	2722	2461	2511	55	2.14E-07	1.85E-07	2.05E-07	2.01E-07	0.04E-07
41-MC			2351	2722	2461			2.14E-07	1.85E-07	2.05E-07		
41-MC			2350	2722	2461			2.14E-07	1.84E-07	2.05E-07		
70-MC	1071	0.559	3402	3314	3029	3248	56	1.53E-07	1.57E-07	1.72E-07	1.61E-07	0.03E-07
70-MC			3402	3314	3028			1.53E-07	1.57E-07	1.72E-07		
70-MC			3402	3314	3028			1.53E-07	1.57E-07	1.72E-07		

Appendix B.3 MATLAB syntax

B.3.1 Script file for nlinfit method

```
% estimating k1 and k2
%% Cleaning
clc
clear all
close all
format compact
global RetortT_file rho siz Tin Tfi %
% data =xlsread('25min_Ret.xls'); % first column time,
%second Temp of 70%MC,
%third Temp for 41%MC, fourth 25%MC, Retort temp
[filedata, pathnamedata, filterindex] = uigetfile( ...
{ '*.xls','Data File (*.xls)'; ...
 '*.txt','Data File (*.txt)'; ...
 '*.xlsx','Data File (*.xlsx)'; ...
 '*.*', 'All Files (*.*)'}, ...
'Pick Retort File', ...
'MultiSelect', 'on');
data =xlsread(filedata);
x=data(:,1);% time (Piasecka, #1707)
% Request for Temperature input in F
prompt = {'Enter 1st Column Number'...
'Enter 2nd Column Number'...
'Enter Product Density'};
name = 'Input for Parameter Estimation';
numlines = 1;
def = {'6','7','603'};% which MC will be estimated,,( clmn1 , clmn 2, density)
options.Resize='on';
options.WindowStyle='normal';
options.Interpreter='tex';
answer=inputdlg(prompt,name,numlines,def,options);

col1 = str2num(answer{1});
col2 = str2num(answer{2});
yobs = [data(:,col1) data(:,col2)];
Tin = (data(1,col1)+data(1,col2))/2;% intial temperature in the two clolomn
Tfi = (data(end,col1)+data(end,col2))/2;% final temperature in the two clolomn
rho = answer{3};% density (kg/m^3)
siz = size(yobs,2);%data in replicta

yobs = yobs(:);
%% Calling surface temperature as boundary condition
```

```

[RetortT, pathnameRT, filterindex] = uigetfile( ...
{ '*.txt','Data File (*.txt)'; ...
 '*.xlsx','Data File (*.xlsx)'; ...
 '*.xls','Data File (*.xls)'; ...
 '*.*', 'All Files (*.*)'}, ...
'Pick Retort Boundary File', ...
'MultiSelect', 'on');
% [cP, pathnamecP, filterindex] = uigetfile( ...
% { '*.txt','Data File (*.txt)'; ...
%   '*.xlsx','Data File (*.xlsx)'; ...
%   '*.xls','Data File (*.xls)'; ...
%   '*.*', 'All Files (*.*)'}, ...
%   'Pick cP File', ...
%   'MultiSelect', 'on');
% cPdata = load(cP);
% cpa = cPdata(1); cpb = cPdata(2); cpc = cPdata(3);
RetortT_file = [pathnameRT RetortT];
% cP_file = [pathnameRT cP];
%% nilinf method
beta0(1)=0.4; % Initial guess value for k1
beta0(2)=0.5; % Initial guess value for k2
[beta,resids,J,COVB,mse] = nlinfit(x,yobs,@ThermalFun_v4,beta0); % inlinfit code
ci=nlparci(beta,resids,J);
[ypred, deltaobs] = nlpredci('ThermalFun_v4',x,beta,resids,J,0.05,'on','observation');
% ypred values
%%
beta % results for estimated k1 & k2
rmse=sqrt(mse)
%% confidence intervals for parameters
ci=nlparci(beta, resids,J) % Confidence intervals values
%% R is the correlation matrix for the parameters, sigma is the standard error vector
[R,sigma]=corrcoef(COVB)
sigma;
relstderr=sigma./beta' %relative standard error for each parameter
%% Plotting Observed vs predicted
x_graph = x./60;% time
yobs1=yobs(1:end/2); % Temperature at center of can 1
yobs2=yobs(end/2+1:end); % Temperature at center of can 2
Ypred=ypred(1:end/2); % predicted Temperature
Figure
hold on
h1(1) = plot(x_graph,yobs1,'-go',
'LineWidth',2,'MarkerEdgeColor','g','MarkerFaceColor','g','MarkerSize',2);
%plot observed Y values at T1

```

```

h1(2) = plot(x_graph,yobs2,'-bs',
'LineWidth',2,'MarkerEdgeColor','b','MarkerFaceColor','b','MarkerSize',2);
%plot observed Y values at T1
h1(3) = plot(x_graph,Ypred,':r*',
'LineWidth',1,'MarkerEdgeColor','r','MarkerFaceColor','y','MarkerSize',4);
% plot predicted Y values at T1
legend(h1,'observed1','observed2','predicted','location','northwest');

xlabel("time(min)",'FontSize',14)
ylabel('Center temperature of can','FontSize',14);
%% Plotting residuals
Figure
hold on
h1(1) = plot(x_graph,resids(1:end/2),'g*');
h1(2) = plot(x_graph,resids(end/2+1:end),'r>');
L4 = ['Heating time (min) at ','tem','^{o}','C'];
xlabel(L4);

ylabel('Residuals','FontSize',14);
legend(h1,'can1','can2','location','northwest');
YLine = [0 0];
XLine = [0 max(x_graph)];
plot (XLine, YLine,'R')

%% Sensitivity coefficient estimation and plotting
beta1 = beta;
d=0.001;
for i=1:length(beta)
if i ==1
betain = [beta1(1)+beta1(1)*d beta1(2)];
elseif i==2
betain = [beta1(1) beta1(2)+beta1(2)*d];
end
yhat{i} = ThermalFun_v4(betain,x);
ysens{i} = (yhat{i}-ypred)/d;
end
% sensitivity coefficient plot
Figure
hold on
ysens1 = ysens{1};
ysens2 = ysens{2};
gca=Figure('Units','inches','Position', [0.5 0.5 6 4]); %[left, bottom, width, height]:
set(gca,'DefaultAxesFontName','Arial','DefaultAxesFontSize',12,'DefaultAxesFontWeight','Normal');

g1(1) = plot(x_graph,ysens1(1:end/2),'b','LineWidth',3);

```

```

g1(2) = plot(x_graph,ysens2(1:end/2),'-b.','LineWidth',3);
YLine = [0 0];
XLine = [0 x_graph(end)];%max()
plot (XLine, YLine,'R');
box on
grid on

legend(g1,'k1','k2','location','best');
xlabel('time(min)','FontSize',14,'fontweight','Normal');
ylabel('Scaled Sensitivity Coefficeints','FontSize',14,'fontweight','Normal');

```

B.3.2 Function file (center can temperature prediction by Comsol)

```

function out = ThermalFun_v4(beta,x)
% Estimating k1 & k2
beta(1)
beta(2)
%global RetortT_file cP_file rho siz cpa cpb cpc Tin Tfi
global RetortT_file rho siz Tin Tfi
import com.comsol.model.*
import com.comsol.model.util.*
model = ModelUtil.create('Model');

fem.const={'x',x,'RetortT_file',RetortT_file,'rho',rho,'Tin',Tin,'Tfi',Tfi};
% RetortT_file= Surface temperature file
% Building can as axisymetric rectangular shape by Comsol
model.param.set('L1', '73[mm]', 'Hight of the can (rectangle1)');
model.param.set('w1', '26[mm]', 'width of rectangle1(radius of can)');
model.param.set('L2', '36.5[mm]', 'hight of cylinder needle Tc');
model.param.set('w2', '0.11[mm]', 'width of rectangle3(radius of TCniddle)');
model.param.set('L3', '8.86[mm]', 'hight of copper around TC base');
model.param.set('w3', '5.045[mm]', 'width of copper around TC base');
model.param.set('L4', '3.34[mm]', 'hight silikon around TC over copper');
model.param.set('w4', '3.12[mm]', 'width silikon around TC over copper');
model.param.set('L5', '8.86[mm]', 'Hight of steel TC base (rectangle2)');
model.param.set('w5', '2.04[mm]', 'width of steel TC stapilizer 1');
model.param.set('L6', '4.7[mm]', 'hight of rectangle2(screw stable TC base)');
model.param.set('w6', '2.78[mm]', 'width of rectangle2(screw stable TC base)');
model.param.set('L7', '7.95[mm]', 'hight of screw TC stap in outside can');
model.param.set('w7', '5.64[mm]', 'width of screw TC stap in outside can');
model.param.set('L8', '6.5[mm]', 'width of outside TC fitteing Silicoun');
model.param.set('w8', '5.045[mm]', 'width of ousidet TC fitteing Silicoun');
model.param.set('L9', '2.75[mm]', 'hight of can sealing edg 1');
model.param.set('w9', '1.35[mm]', 'width ofcan sealing edg 1');
model.modelNode.create('mod1');
model.func.create('int1', 'Interpolation');

```

```

model.func('int1').set('filename',RetortT_file); % surface temperature file
% geometry
model.geom.create('geom1', 2);
model.geom('geom1').axisymmetric(true);
model.geom('geom1').feature.create('r1', 'Rectangle');
model.geom('geom1').feature.create('r2', 'Rectangle');
model.geom('geom1').feature.create('r3', 'Rectangle');
model.geom('geom1').feature.create('r13', 'Rectangle');
model.geom('geom1').feature.create('r4', 'Rectangle');
model.geom('geom1').feature.create('r5', 'Rectangle');
model.geom('geom1').feature.create('r6', 'Rectangle');
model.geom('geom1').feature.create('r7', 'Rectangle');
model.geom('geom1').feature.create('r8', 'Rectangle');
model.geom('geom1').feature.create('r9', 'Rectangle');
model.geom('geom1').feature.create('r10', 'Rectangle');
model.geom('geom1').feature.create('pt1', 'Point');
model.geom('geom1').feature.create('r14', 'Rectangle');
model.geom('geom1').feature.create('fil3', 'Fillet');
model.geom('geom1').feature('r1').set('size', {'w1' 'L1'});
model.geom('geom1').feature('r2').set('pos', {'0.000714' '0'});
model.geom('geom1').feature('r2').set('size', {'w2' 'L2'});
model.geom('geom1').feature('r3').set('pos', {'0' '0'});
model.geom('geom1').feature('r3').set('size', {'w3-0.000381' 'L3'});
model.geom('geom1').feature('r13').set('pos', {'w3-0.000381' '0'});
model.geom('geom1').feature('r13').set('size', {'0.000381' 'L3'});
model.geom('geom1').feature('r4').set('pos', {'0' 'L3'});
model.geom('geom1').feature('r4').set('size', {'w4' 'L4'});
model.geom('geom1').feature('r5').set('pos', {'w3' '0'});
model.geom('geom1').feature('r5').set('size', {'w5' 'L5'});
model.geom('geom1').feature('r6').set('pos', {'w3+w5' '0'});
model.geom('geom1').feature('r6').set('size', {'w6' 'L6'});
model.geom('geom1').feature('r7').set('pos', {'w3' '-0.00795'});
model.geom('geom1').feature('r7').set('size', {'w7' 'L7'});
model.geom('geom1').feature('r8').set('pos', {'0' '-0.0065'});
model.geom('geom1').feature('r8').set('size', {'w8' 'L8'});
model.geom('geom1').feature('r9').set('pos', {'w1-w9' 'L1'});
model.geom('geom1').feature('r9').set('size', {'w9' 'L9'});
model.geom('geom1').feature('r10').set('pos', {'w1-w9' '-0.00275'});
model.geom('geom1').feature('r10').set('size', {'w9' 'L9'});
model.geom('geom1').feature('pt1').set('p', {'0'; '0.0365'});
model.geom('geom1').feature('r14').set('pos', {'0' '0.0365'});
model.geom('geom1').feature('r14').set('size', {'0.000824' '0.00011'});
model.geom('geom1').feature('fil3').set('radius', 'w3/5');
model.geom('geom1').feature('fil3').selection('point').set('r9(1)', [3]);
model.geom('geom1').feature('fil3').selection('point').set('r10(1)', [2]);
model.geom('geom1').run;

```

```

model.variable.create('var1');
% Temperature
model.variable('var1').set('T1', Tin, 'Initial temperature');
model.variable('var1').set('T2', Tfi, 'Final temperature');

% model.variable('var1').set('k2', '0.4[W/(m*K)]', 'Thermal difusivity of T1 to be
evaluated');
model.variable('var1').set('k1',beta (1));
model.variable('var1').set('k2',beta (2));
model.variable.create('var2');
model.variable('var2').model('mod1');
model.variable('var2').set('k', '((T2-T)/(T2-T1))*k1+((T-T1)/(T2-T1))*k2');% model for
estimating k inversly
model.view.create('view2', 3);
% Materials
model.material.create('mat4');
model.material('mat4').selection.set([6]);
model.material.create('mat1');
model.material('mat1').propertyGroup.create('Enu', 'Young"s modulus and Poisson"s
ratio');
model.material('mat1').propertyGroup.create('linzRes', 'Linearized resistivity');
model.material('mat1').selection.set([12]);
model.material.create('mat2');
model.material('mat2').propertyGroup.create('Enu', 'Young"s modulus and Poisson"s
ratio');
model.material('mat2').selection.set([5 7 9 13 14 15 16 17]);
model.material.create('mat3');
model.material('mat3').propertyGroup.create('Enu', 'Young"s modulus and Poisson"s
ratio');
model.material('mat3').propertyGroup.create('RefractiveIndex', 'Refractive index');
model.material('mat3').selection.set([1 2 3 4 8 10 11]);
% heat transfer parameters
model.physics.create('ht', 'HeatTransfer', 'geom1');
model.physics('ht').feature.create('temp1', 'TemperatureBoundary', 1);
model.physics('ht').feature('temp1').selection.set([2 13 33 34 45 46 47 48 50 52 53 54
55 56 57]);
% Mishing
model.mesh.create('mesh1', 'geom1');
model.mesh('mesh1').feature.create('ftri1', 'FreeTri');
model.result.Table.create('tbl1', 'Table');
model.view('view1').axis.set('xmin', '-0.026209384202957153');
model.view('view1').axis.set('xmax', '0.052209384739398956');
model.view('view1').axis.set('ymin', '-0.012134999968111515');
model.view('view1').axis.set('ymax', '0.07993500679731369');

```

% Material for the pomace and thermocouple

```
model.material('mat1').name('Copper');
model.material('mat1').propertyGroup('def').set('relpermeability', {1' 0' 0' 0' 1' 0' 0' 0'
'1'});
model.material('mat1').propertyGroup('def').set('electricconductivity', {5.998e7[S/m] 0'
0' 0' 5.998e7[S/m] 0' 0' 0' 5.998e7[S/m]});
model.material('mat1').propertyGroup('def').set('thermalexpansioncoefficient', {17e-
6[1/K] 0' 0' 0' 17e-6[1/K] 0' 0' 0' 17e-6[1/K]});
model.material('mat1').propertyGroup('def').set('heatcapacity', '385[J/(kg*K)]');
model.material('mat1').propertyGroup('def').set('relpermittivity', {1' 0' 0' 0' 1' 0' 0' 0'
'1'});
model.material('mat1').propertyGroup('def').set('density', '8700[kg/m^3]');
model.material('mat1').propertyGroup('def').set('thermalconductivity', {400[W/(m*K)] 0'
0' 0' 400[W/(m*K)] 0' 0' 0' 400[W/(m*K)]});
model.material('mat1').propertyGroup('Enu').set('youngsmodulus', '110e9[Pa]');
model.material('mat1').propertyGroup('Enu').set('poissonsratio', '0.35');
model.material('mat1').propertyGroup('linzRes').set('rho0', '1.72e-8[ohm*m]');
model.material('mat1').propertyGroup('linzRes').set('alpha', '0.0039[1/K]');
model.material('mat1').propertyGroup('linzRes').set('Tref', '298[K]');
model.material('mat1').propertyGroup('linzRes').addInput('temperature');
```

% Steel

```
model.material('mat2').name('Steel AISI 4340');
model.material('mat2').propertyGroup('def').set('relpermeability', {1' 0' 0' 0' 1' 0' 0' 0'
'1'});
model.material('mat2').propertyGroup('def').set('electricconductivity', {4.032e6[S/m] 0'
0' 0' 4.032e6[S/m] 0' 0' 0' 4.032e6[S/m]});
model.material('mat2').propertyGroup('def').set('thermalexpansioncoefficient', {12.3e-
6[1/K] 0' 0' 0' 12.3e-6[1/K] 0' 0' 0' 12.3e-6[1/K]});
model.material('mat2').propertyGroup('def').set('heatcapacity', '475[J/(kg*K)]');
model.material('mat2').propertyGroup('def').set('relpermittivity', {1' 0' 0' 0' 1' 0' 0' 0'
'1'});
model.material('mat2').propertyGroup('def').set('density', '7850[kg/m^3]');
model.material('mat2').propertyGroup('def').set('thermalconductivity', {44.5[W/(m*K)] 0'
0' 0' 44.5[W/(m*K)] 0' 0' 0' 44.5[W/(m*K)]});
model.material('mat2').propertyGroup('Enu').set('youngsmodulus', '205e9[Pa]');
model.material('mat2').propertyGroup('Enu').set('poissonsratio', '0.28');
model.material('mat3').name('Silica glass');
model.material('mat3').propertyGroup('def').set('relpermeability', {1' 0' 0' 0' 1' 0' 0' 0'
'1'});
model.material('mat3').propertyGroup('def').set('electricconductivity', {1e-14[S/m] 0' 0'
0' 1e-14[S/m] 0' 0' 0' 1e-14[S/m]});
model.material('mat3').propertyGroup('def').set('thermalexpansioncoefficient', {0.55e-
6[1/K] 0' 0' 0' 0.55e-6[1/K] 0' 0' 0' 0.55e-6[1/K]});
model.material('mat3').propertyGroup('def').set('heatcapacity', '703[J/(kg*K)]');
model.material('mat3').propertyGroup('def').set('relpermittivity', {2.09' 0' 0' 0' 2.09' 0'
0' 0' 2.09});
```

```

model.material('mat3').propertyGroup('def').set('density', '2203[kg/m^3]');
model.material('mat3').propertyGroup('def').set('thermalconductivity', {'1.38[W/(m*K)]' '0'
'0' '0' '1.38[W/(m*K)]' '0' '0' '0' '1.38[W/(m*K)]'});
model.material('mat3').propertyGroup('Enu').set('youngsmodulus', '73.1e9[Pa]');
model.material('mat3').propertyGroup('Enu').set('poissonsratio', '0.17');
model.material('mat3').propertyGroup('RefractiveIndex').set('n', {'1.45' '0' '0' '0' '1.45' '0'
'0' '0' '1.45'});
% Pomace materials
model.material('mat4').propertyGroup('def').set('thermalconductivity', {'k' '0' '0' '0' 'k' '0' '0'
'0' 'k'});
model.material('mat4').propertyGroup('def').set('density', rho);

% Polynomial models for Cpo as estimated by DSC (70%, 41% and 25% moisture
% contents)
model.material('mat4').propertyGroup('def').set('heatcapacity', '(-
0.0221*T^2+7.9606*T+2743.3)');
model.material('mat4').propertyGroup('def').set('heatcapacity', '(-
0.0367*T^2+11.373*T+1844.4)');
model.material('mat4').propertyGroup('def').set('heatcapacity', '(-
0.0479*T^2+13.364*T+1209.9)');
% Heat transfer
model.physics('ht').name('Heat Transfer');
model.physics('ht').feature('init1').set('T', 'T1');
% Surface Temperature as heating boundary
model.physics('ht').feature('temp1').set('T0', 'int1(t)');

model.mesh('mesh1').feature('size').set('hauto', 6);
model.mesh('mesh1').run;
% Results
model.result.Table('tbl1').comments('Evaluation of T & k at center (k)');
model.study.create('std1');
model.study('std1').feature.create('time', 'Transient');
model.sol.create('sol1');
model.sol('sol1').study('std1');
model.sol('sol1').attach('std1');
model.sol('sol1').feature.create('st1', 'StudyStep');
model.sol('sol1').feature.create('v1', 'Variables');
model.sol('sol1').feature.create('t1', 'Time');
model.sol('sol1').feature('t1').feature.create('fc1', 'FullyCoupled');
model.sol('sol1').feature('t1').feature.create('d1', 'Direct');
model.sol('sol1').feature('t1').feature.remove('fcDef');
model.result.dataset.create('rev1', 'Revolve2D');
model.result.numerical.create('pev1', 'EvalPoint');
model.result.numerical('pev1').selection.set([6]);
model.result.create('pg1', 'PlotGroup3D');
model.result('pg1').feature.create('surf1', 'Surface');

```

```

model.result.create('pg2', 'PlotGroup2D');
model.result('pg2').feature.create('surf1', 'Surface');
model.study('std1').feature('time').set('tlist',x);
model.study('std1').feature('time').set('rtolactive', true);
model.sol('sol1').feature('st1').name('Compile Equations: Time Dependent');
model.sol('sol1').feature('st1').set('studystep', 'time');
model.sol('sol1').feature('v1').set('control', 'time');
model.sol('sol1').feature('v1').set('notsolmethod', 'sol');
model.sol('sol1').feature('t1').set('tlist', x);
model.sol('sol1').feature('t1').set('maxorder', '2');
model.sol('sol1').feature('t1').set('tstepsbdf', 'strict');
model.sol('sol1').feature('t1').feature('fc1').set('maxiter', '5');
model.sol('sol1').feature('t1').feature('fc1').set('jtech', 'once');
model.sol('sol1').feature('t1').feature('fc1').set('probesel', 'manual');
model.sol('sol1').feature('t1').feature('d1').set('linsolver', 'pardiso');
model.sol('sol1').runAll;
ya = mphinterp(model,'T','coord',[0;0.0365]); % Center can temperature as predicted by
Comsol
out1 = [ya ya];% two cans
out = out1(:); % data of temperature out to MATLAB file for inverse calculations

```

B.3.3 Script file for sequential parameter estimation method

```

% of k1 and k2
global RetortT_file rho siz Tin Tfi seqsort
tol=1e-2;
data =xlsread('90min_Ret.xls');% Expermental data for retorting cherry pomace at 1267
C for 90 min
% MC70 Moisture content
yobs1 = data(:,[1,2]); % choosing column 1&2
yobs2 = data(:,[1,3]);% choosing column 1&3
%MC41 Moisture content
%MC25 Moisture content
%yobs1 = data(:,[1,4]);
%yobs2 = data(:,[1,5]);
x=data(:,1); % time
yobs3=[yobs1;yobs2]; % compining yobs1 &yobs2 in 808*2 matrix
[tT,seqsort]=sortrows(yobs3,1);% sort all data
Ynn=tT(:,2);%temps sorted
siz = size(yobs3,2);
%% density ant T_intial%T_final
prompt = {'Enter Product Density'};
name = 'Input for Parameter Estimation';
numlines = 1;
def = {'1071'};
options.Resize='on';

```

```

options.WindowStyle='normal';
options.Interpreter='tex';
answer=inputdlg(prompt,name,numlines,def,options);
rho = answer{1}; % density
Tin =yobs1(1,2); % average of two cans intial T
Tfi =yobs1(end);% average of two cans Final T
yvals = Ynn;%temps sorted
%% Importing the surfCE T
[RetortT, pathnameRT, filterindex] = uigetfile( ...
{ '*.txt','Data File (*.txt)'; ...
'*.xlsx','Data File (*.xlsx)'; ...
'*.xls','Data File (*.xls)'; ...
'*.*', 'All Files (*.*)'}, ...
'Pick Retort Boundary File', ...
'MultiSelect', 'on');
RetortT_file = [pathnameRT RetortT];% Surface T
beta= [0.4;0.5];% Initial guess
p=length(beta);
Y = yvals;%temps sorted
sX = [length(yvals) length(beta)]; % changed from 1*2 to 2*1

sig = .1*ones(sX(1),1);%

Ratio1 = 1;Ratio2 = 1; Ratio3= 1;
plots=0;
b_old =beta ;
%%
Figure
hold on
set(gca, 'fontsize',14,'fontweight','bold');
while Ratio1 > tol || Ratio2 > tol
P = 100^1*eye(sX(2));
beta0 = b_old;
beta = beta0
ypred = ThermalFun_v2(beta0, x);% predicted center can temperature by Comsol
e = yvals-ypred;
%-----
d=0.001;
for i = 1:p
betain = beta;
betain(i) = beta(i)+beta(i)*d;
yhat{i} = ThermalFun_v2(betain, x);
X{i} = (yhat{i}-ypred)/(beta(i)*d);
end
X1=X{:,1};
for i=2:p

```

```

X1=[X1 X{:,i}]; % changed from 1*2 to 2*1

end
for k = 1:sX(1)
if k == 1
beta = beta0;
end
clear A delta
X1 = [X{:,1} X{:,2}];% changed from 1*2 to 2*1
A(:,k) = P*X1(k,:); %???
delta(k) = sig(k)^2+X1(k,:)*A(:,k);
K(:,k) = A(:,k)/delta(k);
beta = beta + K(:,k)*(e(k)-X1(k,:)*(beta-beta0));
P = P - K(:,k)*A(:,k)';
BBbP{k} = [beta P];
end

h2(1)=plot(plots,b_old(1)/40,'s','MarkerEdgeColor','k','MarkerFaceColor','r','MarkerSize',
10);
h2(2)=plot(plots,b_old(2),'s','MarkerEdgeColor','k','MarkerFaceColor','g','MarkerSize',10)
xlabel('Iteration','FontSize',16,'fontweight','bold');
ylabel('Sequentially Estimated Parameters','FontSize',16,'fontweight','bold');
b_new = BBbP{end};
plots = plots+1;
Ratioall = abs((b_new(:,1)-b_old)./b_old);
Ratio1 = Ratioall(1);
Ratio2 = Ratioall(2);
b_old = b_new(:,1);
end
legend(h2,'par1=Dr/40','par2= (Tinf-Ti)/z');
corrcoef = P(2,1)/(sqrt(P(1,1))*sqrt(P(2,2)));

relerr=stderr./b_old;
n=length(yvals);K=length(beta)+1;
SS=e'*e;
p=length(beta);
mse=SS/(Lyons, #2152);rmse=sqrt(Rms, #1583);
AICc= n*log(SS/n)+2*K+2*K*(K-1)/(n-K-1);
Result = BBbP{end};
hold off

for i = 1:length(BBbP)
BB = BBbP{i};
SeqBeta(:,i) = BB(:,1);
end

```

```

step=0:1:2*length(x)-1;
%% Plotting of sequential estimated  $k_1$  and  $k_2$ 
set(gca, 'fontsize',14,'fontweight','bold');
Figure
h3(1)=plot(step,SeqBeta(1,:),'s','MarkerEdgeColor','b','MarkerFaceColor','r','MarkerSize',10);
legend(h3(1),'k1')
set(gca, 'fontsize',14,'fontweight','bold');
xlabel('step index','FontSize',16,'fontweight','bold');
ylabel('Sequentially Estimated  $k_1$  @21(min)','FontSize',16,'fontweight','bold');

Figure
h3(2) =
plot(step,SeqBeta(2,:),'s','MarkerEdgeColor','k','MarkerFaceColor','beta','MarkerSize',10);
legend(h3(2),'k2')
set(gca, 'fontsize',14,'fontweight','bold');
xlabel('step index','FontSize',16,'fontweight','bold');
ylabel('Sequentially Estimated  $k_2$  @125C','FontSize',16,'fontweight','bold');

```

REFERENCES

REFERENCES

- Abdul Ghani, A.A.G., Farid, M.M., (2006). Sterilization of food in retort pouches. "thermal sterilization of food in cans". Springer, New York, pp. 45-90.
- Archer, D.G., (1993). Thermodynamic properties of synthetic sapphire (Alpha-Al₂O₃), standard reference material 720 and the effect of temperature-scale differences on thermodynamic properties. *Journal of Physical and Chemical Reference Data* 22(6), 1441-1453.
- Bairi, A., Laraqi, N., de Maria, J.M.G., (2007). Determination of thermal diffusivity of foods using 1D Fourier cylindrical solution. *Journal of Food Engineering* 78(2), 669-675.
- Banga, J.R., Alonso, A.A., Gallardo, J.M., Perezmartin, R.I., (1993). Mathematical-modeling and simulation of the thermal-processing of anisotropic and nonhomogeneous conduction-heated canned foods - application to canned tuna. *Journal of Food Engineering* 18(4), 369-387.
- Beck, J.V., Arnold, K.J., (1977). *Parameter estimation in engineering and science*. John Wiley & Sons, New York.
- Beck, J.V., Woodbury, K.A., (1998). Inverse problems and parameter estimation: integration of measurements and analysis. *Measurement Science & Technology* 9(6), 839-847.
- Betta, G., Rinaldi, M., Barbanti, D., Massini, R., (2009). A quick method for thermal diffusivity estimation: Application to several foods. *Journal of Food Engineering* 91(1), 34-41.
- Choi, Y., Okos, M.R., (1986). Effects of temperature and composition on the thermal properties of Foods, . *Food Engineering and Process Application. " Transport Phenomena"*. LeMaguer, M. and Jelen, P, Eds Elsevier. New York. Vol. 1.
- Datta, A.K., (2002b). *Biological and bioenvironmental heat and mass transfer. " governing Equation and Boundary Conditions of Heat transfer"*. Boca Raton, Florida: Taylor & Francis., pp 50-55.
- Donsi, G., Ferrari, G., Nigro, R., (1996). Experimental determination of thermal conductivity of apple and potato at different moisture contents. *Journal of Food Engineering* 30(3-4), 263-268.

- Dutta, S.K., Nema, V.K., Bhardwaj, R.K., (1988). Thermal-Properties of Gram. *Journal of Agricultural Engineering Research* 39(4), 269-275.
- Gill, P., Moghadam, T.T., Ranjbar, a.B., (2010). Differential scanning calorimetry techniques: Applications in biology and nanoscience. *Journal of Biomolecular Techniques* 21, 167-193.
- Gratao, A.C.A., Junior, V.S., Polizelli, M.A., Telis-Romero, J., (2005). Thermal properties of passion fruit juice as affected by temperature and water content. *Journal of Food Process Engineering* 27(6), 413-431.
- Gratzek, J.P., Toledo, R.T., (1993). Solid food thermal-conductivity determination at high-temperatures. *Journal of Food Science* 58(4), 908-913.
- Gupta, M., Yang, J., Roy, C., (2003). Specific heat and thermal conductivity of softwood bark and softwood char particles. *Fuel* 82(8), 919-927.
- Hsu, M.H., Mannapperuma, J.D., Singh, R.P., (1991). Physical and thermal-properties of pistachios. *Journal of Agricultural Engineering Research* 49(4), 311-321.
- Kaletunc, G., (2007). Prediction of specific heat of cereal flours: A quantitative empirical correlation. *Journal of Food Engineering* 82(4), 589-594.
- Magerramov, M.A., Abdulagatov, A.I., Abdulagatov, I.M., Azizov, N.D., (2006a). Thermal conductivity of peach, raspberry, cherry and plum juices as a function of temperature and concentration. *Journal of Food Process Engineering* 29(3), 304-326.
- Magerramov, M.A., Abdulagatov, A.I., Azizov, N.D., Abdulagatov, I.M., (2006b). Thermal conductivity of pear, sweet-cherry, apricot, and cherry-plum juices as a function of temperature and concentration. *Journal of Food Science* 71(5), E238-E244.
- McCune, L.M., Kubota, C., Stendell-Hollis, N.R., Thomson, C.A., (2011). Cherries and health: A review. *Critical Reviews in Food Science and Nutrition* 51(1), 1-12.
- Mishra, D.K., Dolan, K.D., Yang, L., (2008). Confidence intervals for modeling anthocyanin retention in grape pomace during nonisothermal heating. *Journal of Food Science* 73(1), E9-E15.
- Mohamed, I.O., (2009). Simultaneous estimation of thermal conductivity and volumetric heat capacity for solid foods using sequential parameter estimation technique. *Food Research International* 42(2), 231-236.

- Naveh, D., Kopelman, I.J., Pflug, I.J., (1983). The finite-element method in thermal-processing of foods. *Journal of Food Science* 48(4), 1086-1093.
- Pan, Z., Singh, R.P., (2001). Physical and thermal properties of ground beef during cooking. *Lebensmittel-Wissenschaft Und-Technologie-Food Science and Technology* 34(7), 437-444.
- Patras, A., Brunton, N.P., O'Donnell, C., Tiwari, B.K., (2010). Effect of thermal processing on anthocyanin stability in foods; mechanisms and kinetics of degradation. *Trends in Food Science & Technology* 21(1), 3-11.
- Peleg, M., Corradini, M.G., Normand, M.D., (2009). Isothermal and non-isothermal kinetic models of chemical processes in foods governed by competing mechanisms. *Journal of Agricultural and Food Chemistry* 57(16), 7377-7386.
- Rahman, M.S., (1992). Thermal-conductivity of 4 food materials as a single function of porosity and water-content. *Journal of Food Engineering* 15(4), 261-268.
- Singh, P.C., Singh, R.K., Bhamidipati, S., Singh, S.N., Barone, P., (1997). Thermophysical properties of fresh and roasted coffee powders. *Journal of Food Process Engineering* 20(1), 31-50.
- Sweat, V.E., (1975). Modeling the thermal conductivity of meats. *TRANSACTIONS of the ASAE* 18(3), 564-568.
- Sweat, V.E., (1995). Thermal properties of foods. in *engineering properties of foods* (M.A. Rao and S.S. Rizvi). Marcel Dekker Inc New York, NY., 99-138.
- Sweat, V.E., Haugh, C.G., (1974). Thermal-conductivity probe for small food samples. *Transactions of the Asae* 17(1), 56-58.
- Tansakul, A., Lumyong, R., (2008). Thermal properties of straw mushroom. *Journal of Food Engineering* 87(1), 91-98.
- Telejko, T., (2004). Analysis of an inverse method of simultaneous determination of thermal conductivity and heat of phase transformation in steels. *Journal of Materials Processing Technology* 155, 1317-1323.
- Valentas, K.J., Rotstein, E., Singh, P.C., (1997a). *Handbook of food engineering practice. "Thermal and rheological properties of Foodstuffs"*. CRC Press LLC, pp: 425-486.

- Valentas, K.J., Rotstein, E., Singh, P.C., (1997b). Handbook of food engineering practice. "Thermal and rheological properties of Foodstuffs". CRC Press LLC, pp: 427-431.
- Varga, S., Oliveira, J.C., (2000). Determination of the heat transfer coefficient between bulk medium and packed containers in a batch retort. *Journal of Food Engineering* 44(4), 191-198.
- Yang, C.Y., (1998). A linear inverse model for the temperature-dependent thermal conductivity determination in one-dimensional problems. *Applied Mathematical Modelling* 22(1-2), 1-9.
- Yang, W., Sokhansanj, S., Tang, J., Winter, P., (2002). Determination of thermal conductivity, specific heat and thermal diffusivity of storage seeds. *Biosystems Engineering* 82(2), 169-176.
- Zuritz, C.A., Sastry, S.K., McCoy, S.C., Murakami, E.G., Blaisdell, J.L., (1989). A modified fitch device for measuring the thermal-conductivity of small food particles. *Transactions of the Asae* 32(2), 711-718.

CHAPTER 5

OBJECTIVE THREE

Inverse Methods to Estimate Anthocyanin Degradation Kinetic Parameters in
Cherry Pomace During Non-Isothermal Heating

Abstract

Tart cherry pomace is the by-product of cherry juice production. This by-product has high amounts of anthocyanins (ACY), which have health benefits and is used as a natural colorant. The retention of ACY in the pomace was investigated for two retort temperatures 105 and 126.7 °C. Tart cherry pomace was equilibrated to 25, 41, and 70% moisture content (MC) wet basis and heated in sealed 54 × 73 mm cans at 126.7 °C in a steam retort for 25, 40, 60 and 90 min and at 105 °C for 100 and 125 min. ACY retention of 70% pomace decreased with heating time and ranged from 76 % to 10 % for 25 and 90 min heating, respectively at 126.7 °C, and ranged from 60 % to 40 % for 100 and 125 min heating, respectively at 105 °C. Previously estimated thermal properties were used in Comsol software for temperature prediction in the pomace. Time-temperature data were used to estimate the kinetic parameters of the pomace simultaneously by two inverse methods: ordinary least squares and the sequential method. ACY degradation followed a first-order reaction. The rate constant and activation energy for 70% pomace were $k_{115.8^{\circ}\text{C}} = 0.0129 \pm 0.0013 \text{ min}^{-1}$ and $75.7 \pm 10.7 \text{ kJ/mol}$, respectively. The model fit well as shown by RMSE of approximately 9% of initial ACY concentration (about 65 mg/kg db) and relative error of all parameters estimated was less than 24% for all moisture contents.

Keywords: Anthocyanins ; Kinetic parameters ; Cherry pomace ; moisture content

5.1 Introduction

Cherry (*Prunus cerasus* L.) pomace is the solid waste or by-product of cherry juice processing and consists of cherry skin and seeds. It accounts for over 90% of dry matter with high quantity of lignin, cellulose, and dry fiber components (Nawirska A., 2005). Cherries are known to contain substantial quantities of anthocyanins (Wang et al., 1999), which are mainly concentrated in the skins (Chaovanalikit and Wrolstad, 2004; Tomas-Barberan et al., 2001). Anthocyanin stability of black carrots was studied at various solid contents and pHs during both heating, 70–90 °C, and storage at 4–37 °C. Degradation of monomeric anthocyanins increased with increasing solid content during heating, while it decreased during storage (Ahmed et al., 2004; Kirca et al., 2007). The degradation kinetics of anthocyanins in blood orange juice was studied (Kirca and Cemeroglu, 2003). The activation energies for solid content of 11.2 to 69 °Brix were found to be 73.2 to 89.5 kJ/mole. Thermal and moisture effects on grape anthocyanin degradation were investigated using solid media to simulate processing at temperatures above 100 °C (Lai et al., 2009). Anthocyanin degradation followed a pseudo first-order reaction with moisture. Anthocyanins degraded more rapidly with increasing temperature and moisture. The thermal degradation of anthocyanins has been studied in red cabbage (Dyrby et al., 2001), raspberries (Ochoa et al., 1999), pomegranate, grapes (Marti et al., 2002), plum puree (Ahmed and others 2004), blackberries (Wang and Xu, 2007), purple corn cob (Yang et al., 2008) and blueberry (Kechinski et al., 2010).

Kinetic studies for anthocyanins are needed to minimize undesired degradation and to optimize quality of foods. Anthocyanin degradation under isothermal heating (50-90

°C) is reported to follow first order kinetics (Ahmed et al., 2004; Markakis et al., 1957). Degradation of ACY in strawberry paste during high-temperature (80-130°C) high-pressure (up to 700MPa) treatments showed that ACY degradation is increased by both temperature and pressure, with the temperature effect being greatest (Verbeyst et al., 2010). The Effect of water activity on ACY degradation was studied under Non-isothermal heating (100-140 °C) results showed increase in reaction rate constant as water activity decrease (Jimenez et al., 2012)

A higher activation energy implies that a smaller temperature change is needed to degrade a specific compound more rapidly (Cemeroglu et al., 1994) . Studies on ACY extracts from purple-flesh potato and grape showed significantly lower stabilities than ACY in red-flesh potato and purple carrot extracts at 98 °C (Reyes and Cisneros-Zevallos, 2007).

The Arrhenius equation is a common model used to describe the temperature dependence of reaction rate in kinetic problems. Both reaction rate constant (k_r) and activation energy (E_a) are usually estimated from experimental data. These two parameters have strong parameter correlation with each other (Schwaab et al., 2008). Several works suggested the reparameterization of the Arrhenius equation by applying the reference temperature (T_r) in the model (Himmelblau, 1970; Pritchard and Bacon, 1978). Another parameter estimation study established a new approach that was more effective than the standard experimental design criteria in both reducing the uncertainty regions of the parameters and improving the consistency of the estimates (Franceschini and Macchietto, 2008).

Estimating parameters in nonlinear models is complex compared to linear models (Dolan, 2003). However, estimation techniques provide several ways to accurately estimate parameters in non-linear equations if input and the output data are known. A better estimate of a parameter is obtained with prior information of the parameters. In addition, sequential MAP estimation can be used for estimating the parameters in the model simultaneously and sequentially (Beck and Arnold, 1977). A recent example in the food literature of using sequential estimation was done successfully to obtain improved parameter estimates for a generic starch viscosity model (Sulaiman and Dolan, 2013; Sulaiman et al., 2013). Accurate parameter estimates are needed for any food process design and optimization, such as designing drying, extrusion, and other thermal processes for baked goods, confectionaries, breakfast cereals, and other foods containing cherry pomace byproduct. These processes are typically non-isothermal and require nonlinear modeling and estimation of all the parameters simultaneously. Estimating the parameters using all the data simultaneously in a one-step regression has been shown to give better accuracy than estimating the parameters from the same data using two-step regression (Jewell, 2012). Therefore the objectives of this study were to estimate the kinetic parameters for cherry pomace at three constant moisture contents under non-isothermal processing.

5.2 Materials and Methods

5.2.1 Pomace sample preparation

Montmorency cherry pomace was obtained from Cherry Growers Inc., (Grawn, Michigan, U.S.A.). The moisture content (MC) of the samples was measured using a Sartorius Moisture Analyzer – MA30 (Sartorius AG, Goettingen, Germany). The initial

MC of cherry pomace was 70% (wet basis, control). Two additional samples with MC of 41 and 25% (MC-41 and MC-25) were prepared using a pilot-scale cabinet dryer (Proctor and Schwartz Inc., Philadelphia, Penn, U.S.A.) at $50 \pm 2^\circ\text{C}$. Pomace samples MC-70, MC-41, and MC-25 represent pomace with 70, 41, and 25% MC, respectively. Each of the three cherry pomace samples were filled and sealed under vacuum (20-mm Hg) in 202 × 214 steel cans (54-mm diameter and 73-mm height) and heated at 126.7°C , for heating time intervals (0, 25, 40, 60 and 90 min) using a rotary steam retort (FMC Steritort Laboratory Sterilizer, Madera, Calif, U.S.A.) and at 105°C for 100 and 125 min. Each can was fitted with a needle thermocouple (Ecklund-Harrison Technologies Inc., Fort Myers, Florida, U.S.A.) to measure the center temperature. The time-temperature profile of retorting process (samples and retort) is shown in Figure 5.1. Experimental design showed in Appendix C.1, Figure C.1.

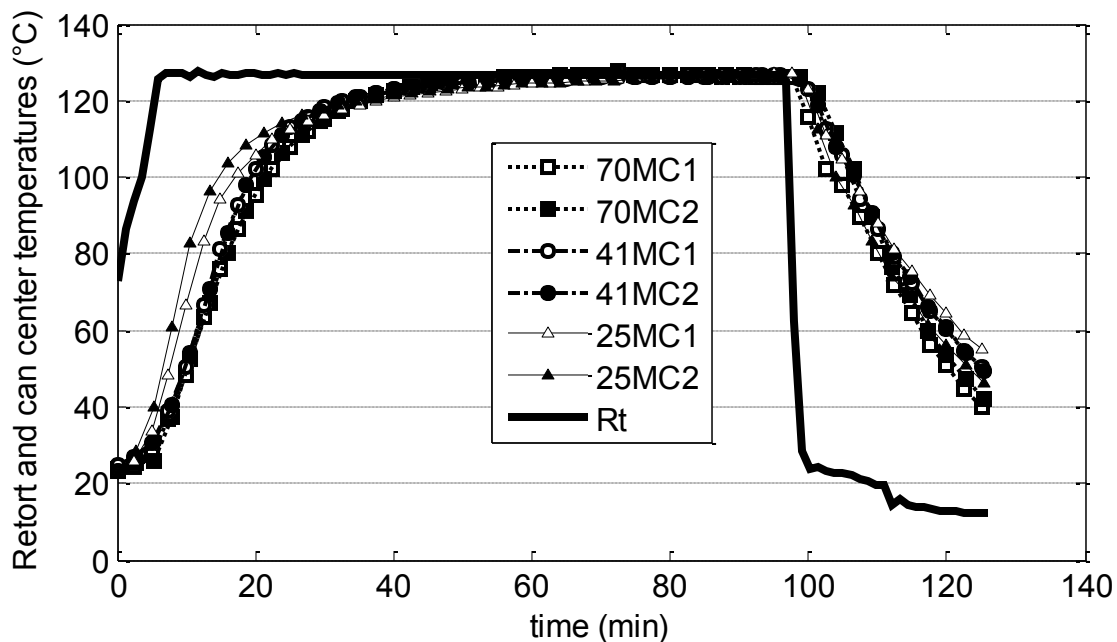


Figure 5.1 Can-center temperature profile of cherry pomace in a rotary steam retort at 126.7 °C for 90 min after 10 min come-up-time. (Rt=Retort temperature; MC-70, MC-41, and MC-25 represent cherry pomace with 70, 41, and 25% moisture (wb), respectively).

5.2.2 Anthocyanins extraction

Anthocyanins (ACY) from pomace samples were extracted using the method of Chaovanalikit and Wrolstad (2004) with some modification. Briefly, fresh and heat-treated samples of cherry pomace were dried (41°C) and then ground using a coffee grinder (Krupps, Medford, Mass, U.S.A.) to a coarse-particle size powder. Ground pomace (20g) was suspended in 80 mL of acetone stock solution (70% aqueous acetone, 0.01% hydrochloric acid, and 30% distilled water). The pomace slurry was stored overnight (-20°C) in sealed glass jars, and wrapped in aluminum foil to protect the sample from light, to achieve an equilibrium state. The slurry was filtered through Whatman number 4 filter paper (Whatman Inc., Clifton, New Jersey, U.S.A.) using a Buchner funnel (under vacuum), followed by a wash with 50 mL of stock buffer. The

filtrate was mixed with 40 mL of chloroform and stored overnight. The supernatant was collected and used for the determination of monomeric anthocyanin content.

5.2.3 Monomeric anthocyanin content determination

The total monomeric anthocyanin content was determined using the pH differential assay (Rodriguez-Saona et al., 1999). Specific volume of the supernatant was dissolved in potassium chloride buffer (KCl, 0.025 M, pH 1.0) and sodium acetate ($\text{CH}_3\text{CO}_2\text{Na}_3 \cdot \text{H}_2\text{O}$, 0.4 M, pH 4.5) and allowed to equilibrate, with a predetermined dilution factor. The absorbance of each equilibrated sample of extracted ACY was then measured at 510nm and 700nm for haze correction, using a Genesys 5 spectrophotometer (Spectronic Instruments, Rochester, NY, USA) and 1 cm path-length cells were used for spectral measurements. ACY contents was calculated, as cyanidin 3-glucoside equivalent (Lee et al., 2005), and reported as mg/kg (dry-basis).

5.2.4 Mathematical Modeling

5.2.4.1 Estimation the kinetic parameters

The heating was assumed to be axisymmetric in the can. Gauss-Legendre quadrature was used to choose a total of 15 points in half of the can (Figure 5.2). Gauss-Legendre quadrature was chosen as the integration method because it is the most accurate of all numerical integration techniques for a given number of points (Chapra, 2011) . The point locations were normalized with r/R' , z/H , where R' and H were the can's radius and height, respectively. Comsol was used to compute $T(r, t, z)$ at the 15 points, using the can dimensions based on all estimated thermal properties from chapter 4 (density, specific heat and thermal conductivity), the measured dynamic

surface temperature (T_s), as the boundary heat source for all processes, and the uniform initial temperature of the pomace at room temperature.

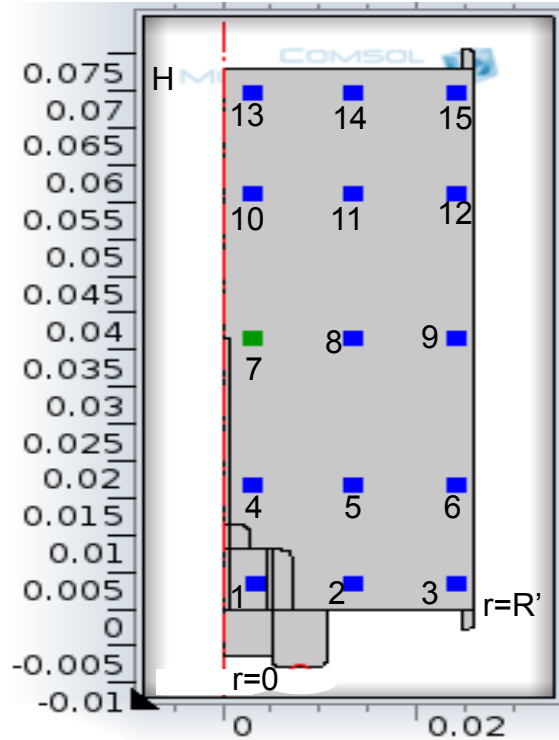


Figure 5.2 Location of the 15 Gauss-Legendre points in the half-can based on axisymmetric heating.

In this study the reaction is following a first order reaction:

$$\frac{dC}{dt} = -kC \quad (5.1)$$

Integration of equation (5.1) with integration limits gives:

$$\int_{C_0}^{C(t)} \frac{dC}{C} = \int_0^t -k dt \quad (5.2)$$

When k is a function of temperature and moisture content, Eq. (5.2) is written as follows:

$$\int_{C_0}^{C(t)} \frac{dC}{C} = \int_0^t -k(T, MC) dt \quad (5.3)$$

Where $k(T, MC)$ is the reaction rate, which follows Arrhenius temperature dependence, and includes the moisture content term, assumed to be exponential (Lai et al., 2009):

$$k(T, MC) = -k_r \exp \left[\frac{-Ea}{R} \left(\frac{1}{T(r, z, t)} - \frac{1}{T_r} \right) + b(MC - MC_r) \right] \quad (5.4)$$

k_r is the rate constant at reference temperature (T_r) and at reference moisture content (MC_r). Substituting Eq. (5.4) in Eq.(5.3), and integrating the left side yields:

$$\ln C(t) - \ln C_0 = -k_r \int_0^t e^{\left[\frac{-Ea}{R} \left(\frac{1}{T(r, z, t)} - \frac{1}{T_r} \right) + b(MC - MC_r) \right]} dt \quad (5.5)$$

Because moisture content is not a function of time in this study the MC term will be outside the integral, yielding:

$$\ln C(t) - \ln C_0 = k_r e^{b(MC - MC_r)} \int_0^t e^{\left[\frac{-Ea}{R} \left(\frac{1}{T(r, z, t)} - \frac{1}{T_r} \right) \right]} dt \quad (5.6)$$

Let the time temperature history equal $\Psi(t)$:

$$\psi(t) = \int_0^t e^{\left[\frac{-Ea}{R} \left(\frac{1}{T(r, z, t)} - \frac{1}{T_r} \right) \right]} dt \quad (5.7)$$

Then by solving for C(t) in Eq. 5.4 yields:

$$C(t) = C_0 e^{\left[-kr\psi(t)e^{(b(MC - MC_r))} \right]} \quad (5.8)$$

Equation (5.8) was predicted the degradation of ACY at any chosen point inside the cylinder during heating for a constant MC and time temperature history ($\psi(t)$). Because ACY concentration cannot be measured at an infinitely small point, we must continue to develop the equation for mass-average ACY concentration, which can be measured experimentally. To compute mass-average ACY in the can ($\bar{C}(t)$) the point concentrations ($C(t)$) should be integrated over the can:

$$\psi(t) = \frac{\int_0^H \int_0^{R'} C(t) \times 2\pi r dr dz}{\int_0^H \int_0^{R'} 2\pi r dr dz} \quad (5.9)$$

Substituting $C(t)$ from Eq. (5.8) into Eq. (5.9) yields:

$$\bar{C}(t) = \frac{2\pi C_0 \int_0^H \int_0^{R'} e^{-kr\psi(t)e^{(b(MC - MC_r))}} r dr dz}{2\pi \times \frac{R'^2}{2} \times H} \quad (5.10)$$

Normalizing, $r^*=r/R'$ and $z^*=z/H$, the final form of Eq. (5.10) will be

$$\bar{C}(t) = 2C_0 \int_0^1 \int_0^1 e^{-kr\psi(t)e^{(b(MC - MC_r))}} r^* dr^* dz^* \quad (5.11)$$

Equation (5.11) is the equation that was used in this study for calculation of predicted mass-average ACY concentration as function of moisture content and time-temperature history.

5.2.4.2 Arrhenius Reference Temperature

The importance of the reference temperature T_r is that it controls the correlation coefficient between the rate constant (kr) and activation energy (E_a). As the correlation coefficient is minimized, the confidence interval for kr is also minimized, Datta (1993), allowing estimation of both parameters simultaneously. The optimum T_r was found iteratively by holding T_r at different fixed values, estimating the parameters for Eq. 5.11, plotting the correlation coefficient and choosing the T_r where the correlation was nearly zero (Dolan et al., 2013; Schwaab et al., 2008).

The estimation was done with a numerical procedure in MATLAB (Appendix C.3, at C.3.1 –C.3.2). An initial guess of parameters, model equations, and experimental data (ACY concentration at two retorting temperature, Table 5.1) collected on time and temperature of the sample were entered into the program. Nonlinear regressions, using the `nlinfit` function in MATLAB (Appendix C.3, at C 3.4), were used to estimate the parameters. Finding the optimum reference temperature which lead to uncorrelated model parameters involved a number of steps: after an initial parameter estimates with initial guess of reference temperature, the reference temperatures was allowed to vary and then the new covariance matrix of the parameter estimates was recalculated for each new reference temperature .

5.2.4.3 Moisture content Constant

The moisture content of the pomace samples is constant during this non-isothermal process. The moisture content parameter b in Eq.(5.6), was estimated by applying the slope method,Lai et al. (2009). The reaction rate constant kr values at each

sample of cherry pomace (25, 41 and 70%) were used for b value estimation. Readjusting Eq. (5.6) by setting $T=Tr$, yields:

$$k(MC) = kr \exp(b(MC - MC_r)) \quad (5.12)$$

Using log to linearize Eq. 5.12, linear regression for Eq.(5.12), will give the slope which equal to the parameter of moisture constant (b).

5.2.5 Parameter Estimation Techniques

5.2.5.1 Sensitivity Coefficient Plot

The sensitivity coefficient (X_{ij}), where i is the time index, and j is the parameter index, indicates how sensitive the dependent variable is to a parameter β_j , is formed by taking the first derivative of a dependent variable with respect to a specific parameter. The parameters in the model can be estimated most accurately when its X_{ij} is maximized (Beck and Arnold, 1977). Estimation of kinetic parameters for non-isothermal food processes using nonlinear parameter estimation has been discussed by (Dolan, 2003). To place the X_{ij} on the same scale, we used a scaled sensitivity coefficient (X'_{ij}). The scaled sensitivity coefficient plots are helpful in determining which parameters can be estimated most accurately, and which parameters are most important in the model. Here, we determined the sensitivity coefficient (X_{ij}) of parameter (β) using the finite difference method of forward difference approximation (Beck and Arnold, 1977) for each parameter as presented in Eq.(5.13). The $\delta\beta_j$ is some relatively small quantity and is given as Eq.(5.13). The scaled sensitivity coefficients shown in Eq. (5.14) were

computed using MATLAB (Appendix C.3, at C.3.3). To have a sensitivity coefficient plot, we must have independent variable input and approximate value of parameters:

$$\frac{\partial \bar{C}(i)}{\partial \beta_i} \approx X_{ij} = \frac{\bar{C}(b_1, \dots, b_j, + db_j, \dots, b_p) - \bar{C}(b_1, \dots, b_j, \dots, b_p)}{\partial b_j} \quad (5.13)$$

$$\partial b_i = 0.001 b_i$$

$$X'_{ij} = \beta_j \frac{\partial \bar{C}(i)}{\partial \beta_i} = \frac{\bar{C}(b_1, \dots, b_j, + db_j, \dots, b_p) - \bar{C}(b_1, \dots, b_j, \dots, b_p)}{0.001} \quad (5.14)$$

5.2.5.2 Ordinary Least Squares (OLS) Estimation Procedure

The kinetic parameters (Ea , kr) and initial concentration of ACY (C_0) in Equation (5.11) were estimated with the inverse problem method using MATLAB with Comsol. The MATLAB function “nlinifit” (Appendix C.3, at C.3.4) was used to minimize the sum of squares:

$$SS = \sum_i \left[(\bar{C}_{obs})_i - (\bar{C}_{prd})_i \right]^2 \quad (5.15)$$

The 95% asymptotic confidence intervals (ci) of the parameters and the correlation coefficient matrix of parameters were also computed in MATLAB (Dolan et al., 2007; Mishra et al., 2008). Estimated parameters are significant when the ci does not contain zero.

5.2.5.3 Sequential Estimation Procedure

The second method used to estimate model parameters is the sequential method. Parameter values are updated in sequential estimation as experimental data of time and temperature are added. The sequential method shows the changes in the values of parameters being estimated until they reach a steady value.

Non-linear Maximum A Posteriori (MAP) sequential estimation procedure given in (Beck and Arnold, 1977 p. 277) was used to find parameters in Eq.(5.16). The MAP equation is shown in Eq.(5.17)

$$b_{MAP} = \mu_{\beta} + P_{MAP} X^T \psi^{-1} (Y - X \mu_{\beta}) \quad (5.16)$$

$$P_{MAP} = (X^T \psi^{-1} X + V_{\beta}^{-1})^{-1} \quad (5.17)$$

Eq.(5.16) and Eq. (5.17). are in matrix format, where b_{MAP} is the matrix (px1) vector parameter to be estimated; μ_{β} is matrix (px1) vector with prior information on the parameters; P_{MAP} is the covariance vector matrix of parameters (pxp) which gives information about the variance (on the diagonal) and covariance (correlation between parameter) on off-diagonal elements; X is the sensitivity coefficient matrix (npx); ψ is covariance matrix (nxn) of errors, and Y is the measurement (nx1) vector and V is covariance matrix of μ_{β} .

Sequential parameter estimation gives more insight into the estimation process. Improvement in the estimation can easily be seen as the parameter is estimated and plotted at each datum addition (Mohamed, 2009). Under sequential estimation we expect the parameters to approach a constant as the number of observations increases. MATLAB programming was used to conduct the sequential estimation (Appendix C.3, at C.3.5). The sequential estimation was done by sorting on predicted ACY concentration, rather than time. The reason for choosing this type of sort was that there were two retort temperatures. Therefore, time of heating was not the only determining factor of the anthocyanin retention. Different combinations of time and temperature affected

ACY concentration. To account for two retort temperatures, the ACY concentration, starting at the highest concentration and proceeding to the lowest, was used as the sort.

5.3 Results and discussion

5.3.1 Anthocyanin (ACY) degradation

Initial average ACY content in the control cherry pomace (MC-70) was 65.4 mg/kg (dry-basis). Thermal treatment in the rotary steam retort at 126.7 °C for 90 min degraded the ACY to a mean of 6.6 mg/kg. This process reduced the ACY to a mean of 5.2 mg/kg for MC-41 and 0 mg/kg for MC-25 pomace. The second heat treatment 105 °C (100 and 125 min) degraded the ACY to means of 22.5 ±2.2 mg/kg in MC-70, 12.5 ±2.3 mg/kg in MC-41 and to 12.1 ±0.76 mg/kg in MC-25 at 125 min retorting time, as shown in Table 5.1. Thus this study showed greater ACY loss with increasing temperature history on the cherry pomace. Similar observations were reported in study for black carrots at different solids contents at 70 to 90°C, degradation of ACY increased with increasing solid content during heating Kirca et al. (2007). Non-isothermal heating of grape pomace in wheat flour (with loss in moisture during heating, which is a main difference with this study) up to 105 and 145°C showed also degradation of ACY as temperature and moisture increased, Lai et al. (2009)

Table 5.1 Cherry pomace ACY concentration after retorting at two different temperatures for different times

time (min)	Retorting Temperature					
	126.7°C			105°C		
	Cherry pomace Moisture contents (MC %, wb)					
	70-MC	41-MC	25-MC	70-MC	41-MC	25-MC
0	57.89	44.6	37.27	65.43 [#]	54.58 [#]	51.86 [#]
0	59.70	59.33	57.89	65.43	54.58	51.86
0	78.70	59.79	60.42	65.43	54.58	51.86
25	37.99	40.48	28.22	NA	NA	NA
25	44.32	32.20	31.12	NA	NA	NA
25	47.04	30.82	29.33	NA	NA	NA
40	19.00	22.08	14.47	NA	NA	NA
40	37.99	12.88	28.58	NA	NA	NA
40	36.18	32.20	25.69	NA	NA	NA
60	28.04	17.48	21.35	NA	NA	NA
60	19.00	19.78	17.37	NA	NA	NA
60	24.42	14.72	8.32	NA	NA	NA
90	1.81	5.98	0.00	NA	NA	NA
90	10.85	9.66	0.00	NA	NA	NA
90	7.24	0.00	0.00	NA	NA	NA
100	NA	NA	NA	37.88 [*]	33.24 [*]	25.48 [*]
100	NA	NA	NA	43.62 [*]	39.71 [*]	42.34 [*]
100	NA	NA	NA	43.62 [*]	33.30 [*]	45.38 [*]
125	NA	NA	NA	24.11 [*]	11.58 [*]	12.74 [*]
125	NA	NA	NA	25.44 [*]	16.91 [*]	10.58 [*]
125	NA	NA	NA	18.17 [*]	9.23 [*]	12.97 [*]

[#]. is an average of values of zero time left side

^{*}. Values were corrected from lower values due to effect of storage. Corrected values = $(C_t/C_0)_{105^\circ\text{C}} \times (C_0)_{127^\circ\text{C}}$. Raw data $C_{t105^\circ\text{C}}$ are shown in Appendix C.1, (Table C.3).

5.3.2 Reference Temperature Plot

The reference temperature at each pomace moisture content of pomace samples was estimated: The correlations of parameters with reference temperature T_r are illustrated in Figure 5.3. For both heating temperature (126.7°C and 105°C), the T_r values were found as 115.1, 115.1 and 115.8°C for 25, 41 and 70% MC (wb) , respectively based on the parameter correlation between kr and E_a nearly equal to zero (Figure 5.3). This value 115.8 °C of T_r , which is close to maximum heating temperature of 126.7°C Datta (1993), was used for the next estimation for all parameters for the all moisture contents of cherry pomace samples. Figure 5.3 is similar in principle to results shown by Dolan et al. (2013), Sulaiman and Dolan (2013), and (Sulaiman et al., 2013)

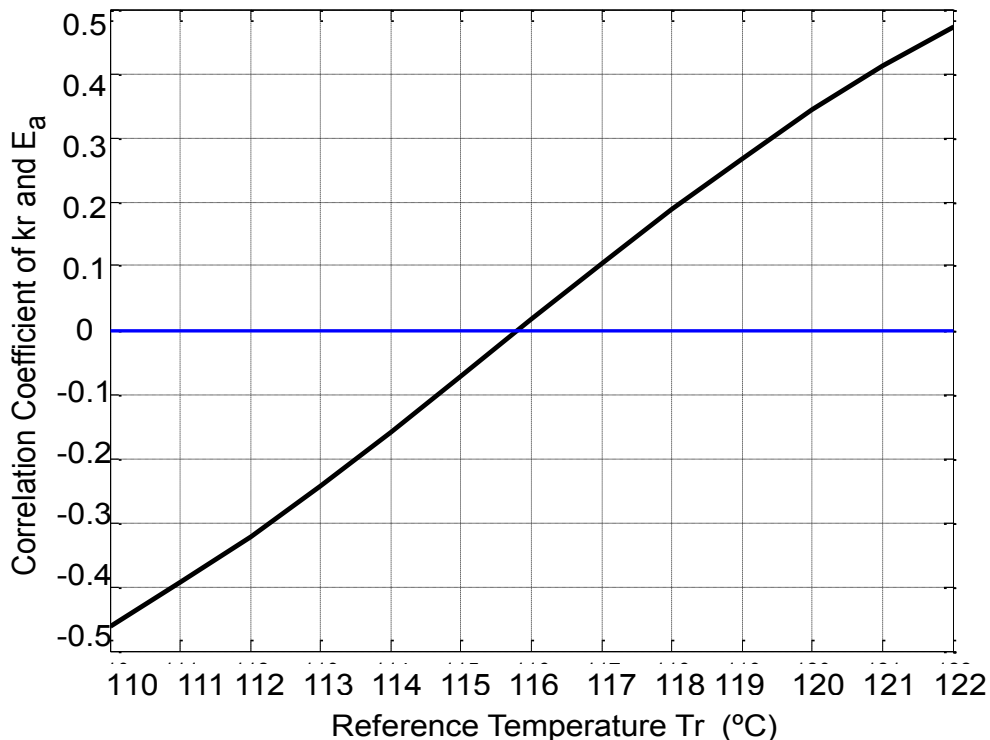


Figure 5.3 Correlation coefficient of parameters kr and E_a as a function of the reference temperature T_r (for ACY degradation under retorting process)

5.3.3 Scaled Sensitivity Coefficient Plot

Sensitivity coefficient analysis helps to know whether or not the parameters are linearly dependent or independent of each other, and which parameters will have the smallest relative error. The three parameters (C_o , kr and E_a) in Eq. (5.11) were uncorrelated, which means they could be estimated separately. Figure 5.4 shows the scaled sensitivity coefficient plots. The absolute value of the scaled sensitivity coefficient plots for reaction rate constant ($X'_{kr115.8^\circ\text{C}}$) at both retorting temperatures (127°C and 105°C) are larger than the size of X'_{E_a} at the two retort temperatures (Figure 5.4). Therefore, the parameter $kr_{115.8}$ was estimated with more accuracy than the parameter E_a (see relative errors in Table 5.2). However, Figure 5.4 shows that the absolute value of X'_{E_a} at 105°C is about 10, which larger than the value at 127°C, which was about 6. These two plots indicated that at least two experiments with two different retort temperatures are needed to estimate the parameter E_a with high accuracy. The most accurate parameter was C_o , which has smallest relative error (Table 5.2).

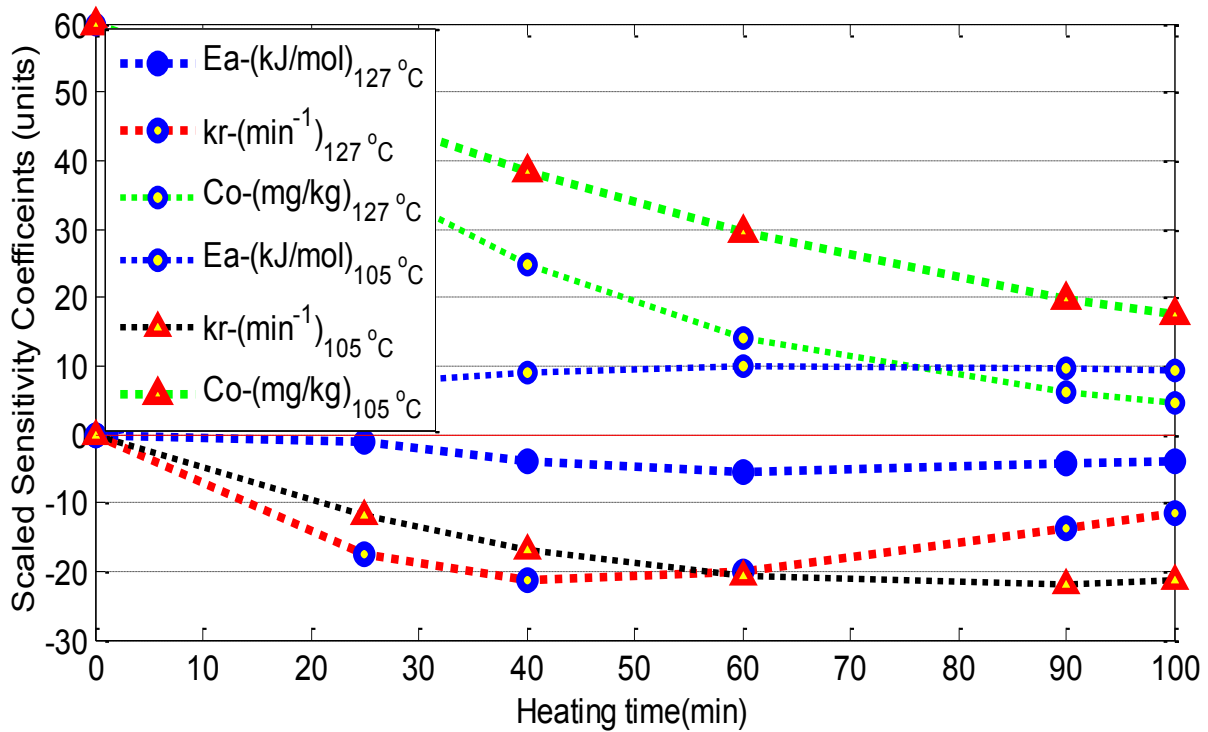


Figure 5.4 Scaled sensitivity coefficient plots of the three parameters at retort temperatures 105°C and 127°C, using initial parameter values of $E_a = 45\text{kJ/mol}$, $kr_{115.8^\circ\text{C}} = 0.019\text{ min}^{-1}$ and $C_0 = 60\text{ mg/kg}$.

5.3.4 Parameter Estimation using Ordinary Least Squares

Estimated parameters for the cherry pomace ACY samples at three constant moisture contents in Eq. (5.11) are shown in Table 5.2. Since the most important parameters are the Arrhenius parameters, Tr was established where the correlation coefficient between kr and E_a was nearly zero. The confidence intervals and the percentage relative errors of the estimated parameters are given in Table 5.2. In general, the confidence interval and the relative errors are small.

Table 5.2 Kinetic parameter estimates of ACY degradation in cherry pomace at three constant moisture contents after retorting processing

MC %(wb)	OLS estimates Ea (kJ/mol) kr (min ⁻¹) Co (mg/kg,db)	relative error (%)	CI (95%)		RMSE (mg/kg)
70	75.7 ±10.7 0.0129 ±0.0013 65.256 ±2.72	14.2 9.8 4.2	53400 0.01034 59.59	97930 0.0156 70.92	7.02
41	69.66 ±12.7 0.01417 ±0.0016 54.5 ±2.77	18.3 11.4 5.1	43071 0.01079 48.66	96265 0.0176 60.25	7.00
25	77.8 ±17.9 0.0134 ±0.0022 51.65 ±3.62	23.0 16.4 7.0	40201 0.00877 44.05	115580 0.0180 59.26	9.15

Table 5.2 shows the results of parameters estimated at three constant moisture contents of pomace. For 70% pomace ACY, the root mean square error (RMSE) is about 7% of the total scale of about 65 as also shown in Figure 5.5, which indicates a good fit. The lowest relative error was with the initial concentration parameter (Co), equal to about 5% average for all moistures (Table 5.2), which means it was the easiest parameter to be estimated as indicated by the scaled sensitivity coefficient plot (Figure 5.4). Also as predicted by Figure 5.4, the largest relative error was in E_a (Table 5.2) of 14 to 23%. All parameters were significant, as shown by the 95% CIs not containing zero.

Table 5.3 shows a comparison of the kinetic parameter values of ACY in literature and in this study. Similar materials with similar moisture content (41%) were compared. The activation energies were similar, while the rate constant in this study was lower. It is

not clear why anthocyanins in cherry pomace would thermally degrade more slowly than anthocyanins in grape pomace. The rate constant (Mishra, 2008) was $k_{r115.8^{\circ}\text{C}} = 0.0823 \text{ min}^{-1}$, Lai et al. (2009) was 0.0795 min^{-1} and Verbeyst et al. (2010) was 0.0472 min^{-1} (all converted from Table 5.3 using Arrhenius equation) versus 0.0142 min^{-1} in this study. The activation energy values in the previous three studies, ranging from 65 to 75 kJ/mole, were very close values in comparison with this study as shown in Table 5.3. Lai (2009) used the extruder to heat the sample to about 140°C under atmospheric pressure, which means the moisture content decreased with time, and the data were corrected for this change. In this study the heating was under constant pressure and constant moisture content.

. In the latest two studies (Lai et al., 2009; Mishra et al., 2008) the parameters were estimated using OLS only, while in this study sequential estimation was also used where the parameters were estimated at each experimental step.

Table 5.3 Summary of published kinetic parameters of anthocyanin degradation by thermal treatments using 1st – order model

Material	Processing Temp, (°C)	Method	ΔE (kJ/mol)	k_{Tr} (min ⁻¹)	Tr °C	References
Cherry pomace (41% MC, wb)	105, 126.7	nonlinear regression	69.66	0.01416	115.8	This study
Grape pomace in wheat flour(30% MC)	100	minimizing SS of residual	75.3	0.0075	80	(Lai et al., 2009)
Grape pomace (42%MC,wb)	126.7	nonlinear regression	65.32	0.0607	110	(Mishra et al., 2008)
Purple-flesh potato	25,50,80,98	Arrhenius model	72.49	7.3×10^{-3}	98	(Reyes and Cisneros-Zevallos, 2007)
Grape		,forward problem	75.03	5.8×10^{-3}	98	
Purple carrot		,forward problem	81.34	2.4×10^{-3}	98	
blackcurrant juice	110;10;140	minimizing SSE of C/C ₀ values	81.51	0.017	110	(Harbourne et al., 2008)
			91.09	0.165	140	
Blackberry juice (65°Brix)	5,25,37	Arrhenius model	75.5	0.0591	37	(Wang and Xu, 2007)
		,forward problem		0.0216	25	
Strawberry paste	80-130	n/a	63.3	0.0351	110	(Verbeyst et al., 2010)
Sour cherry juice	50,60,70,80	Arrhenius model	75.9	9.8×10^{-4}	80	(Cemeroglu et al., 1994)
45°Brix			,forward problem	80.1	1.62×10^{-3}	
71° Brix	50,60,70,80	,forward problem				

The correlation matrix of parameters for Eq. (5.11) is presented in Table 5.4. The correlation between the parameters was very low indicating that the parameters will be more independent and can be estimated better. At all three moisture contents the correlations between E_a and $kr_{115.8^\circ\text{C}}$ was nearly zero, resulting in the lowest relative error for kr . The correlations among the other parameters were not high (Table 5.4).

Table 5.4 Correlation matrices Table of the kinetics parameters of Eq.(5.11).

MC(wb)	E_a	kr	C_o	
70%	1	SYMMETRIC		E_a
	-0.063	1		kr
	-0.073	0.574	1	C_o
41%	1	SYMMETRIC		E_a
	-0.0038	1		kr
	-0.023	0.549	1	C_o
25%	1	SYMMETRIC		E_a
	-0.00043	1		kr
	-0.031	0.564	1	C_o

Predicted and observed ACY mass average in cherry pomace vs. heating times (126.7°C and 105°C) was plotted for both retorting temperatures. The plot showed good fit with small confidence intervals as shown in Figure 5.5. The Figure shows also the 95% confidence (CB) and prediction band (PB) for 126.7°C, the CB shows the region where 95% of regression lines are expected to be. The PB shows the region where 95% of the data are expected to be. The figure showed that most of the data are in the CB region which indicated good fit.

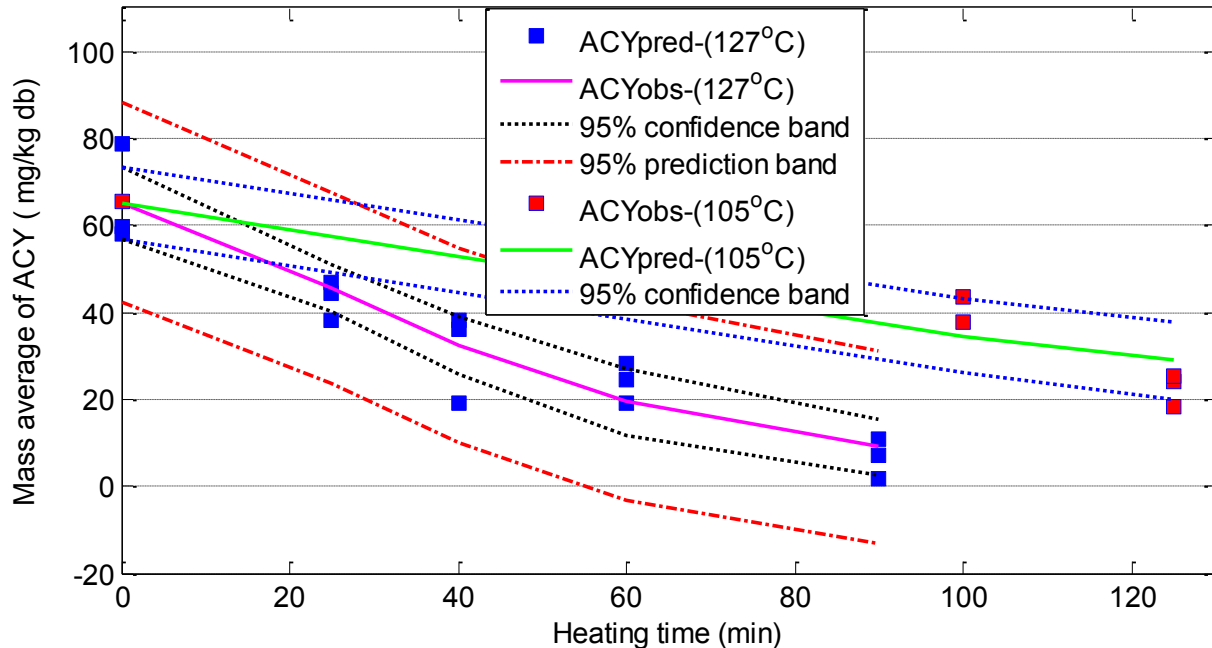


Figure 5.5 Plot of observed and predicted with confidence intervals of ACY values in cherry pomace (MC-70, wb) after retorting at 126.7°C and 105°C for different times. Prediction bands for 105°C are not shown, for clarity.

Residuals for prediction of ACY values were small, as shown in Figure 5.6. Residuals were larger during the 0 min and after 40 min heating at 126.7 °C, showing some difficulty in fitting. At other heating times the residuals were additive and variance constant and the mean is close to zero (-0.071), which confirms a good fit of the equation used for estimating the degradation parameters of ACY in cherry pomace. For retorting at 105°C residuals also showed a good fit, with slightly larger residual at 125 min heating (Figure 5.6). The residual histogram (Figure 5.7) shows that the residuals were nearly normally distributed.

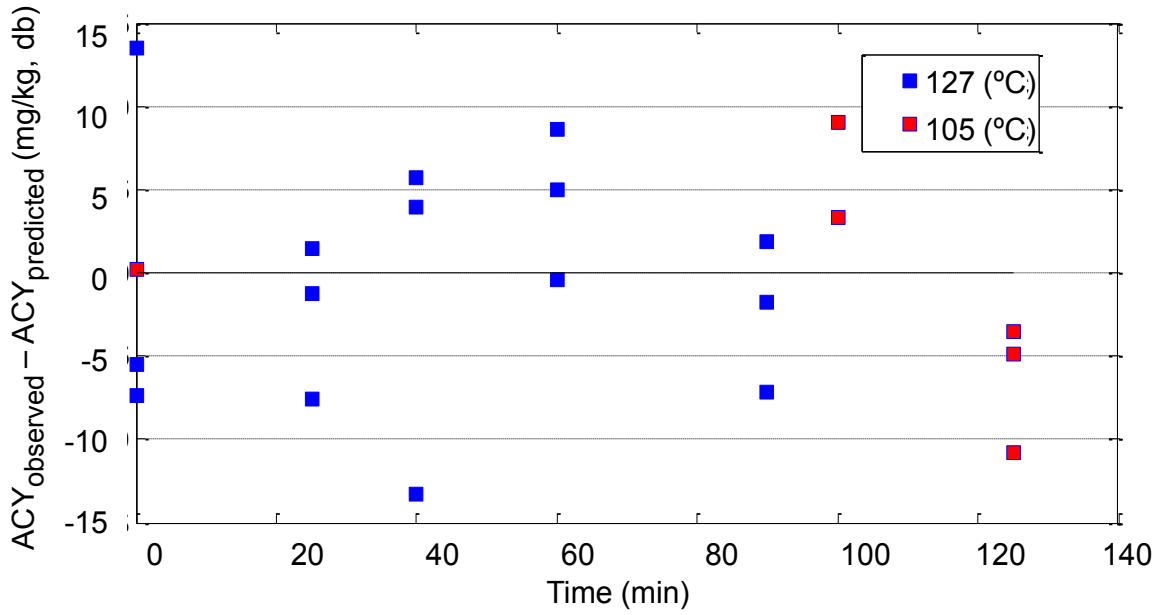


Figure 5.6 Residual scatter plot of mass average of ACY in cherry pomace (MC-70) heated at retort temperatures(126.7°C &105°C).

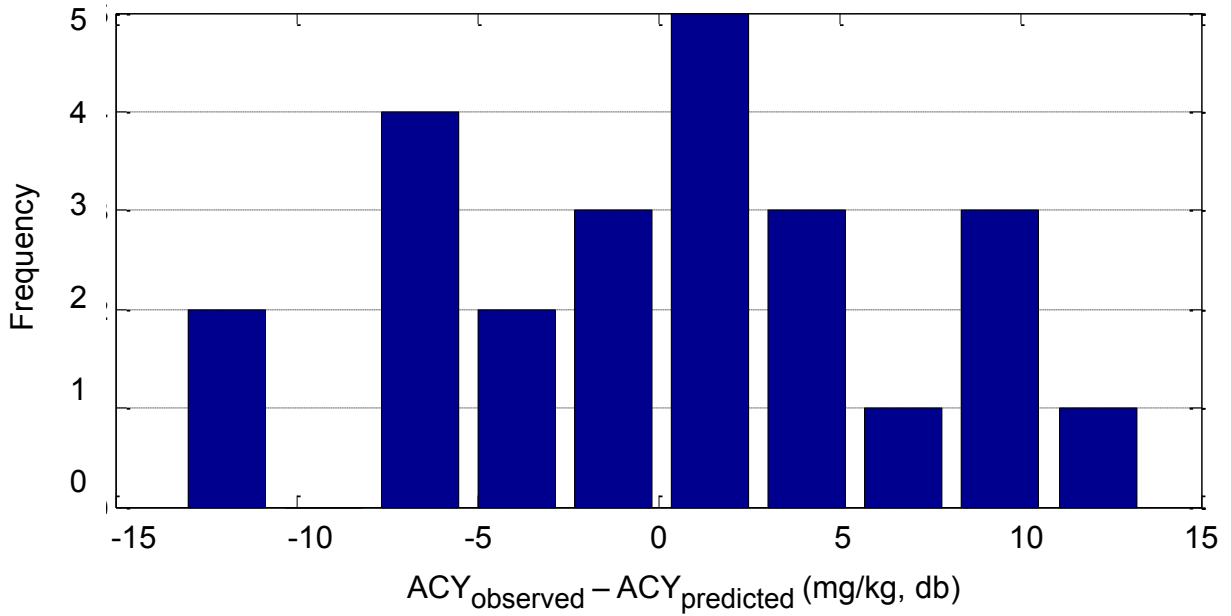


Figure 5.7 Plots of frequency versus difference between observed and predicted ACY in cherry pomace (MC-70).

5.3.4.1 Moisture content constant estimation

From reaction rate constant values in Table 5.2 the moisture content parameter was estimated by applying the linear regression for Eq. (5.4). The result (Appendix C.1, Figure C.1.4) indicated that there was no significant effect of moisture content on the ACY rate constant or activation energy during the retorting process ($p=0.65$, $R^2=0.28$).

5.3.5 Sequential Parameter Estimation

The sequentially estimated parameter values of E_a , kr , and C_o were 75665 J/g mol, 0.01294 min^{-1} and 65.25 (Figure. 5.8 to Figure.5.10). The parameters E_a and $kr_{115.8^\circ\text{C}}$ reached a constant when the last three data points were added (Figure. 5.8 and Figure.5.9), showing that almost all the data were needed for accurate estimation. The final values for the parameters results are, as expected, very similar to the OLS results given in Table 5.2 for the model. For the model studied, sequential results are the best possible estimates, where the three parameters reach nearly a constant value by the end of the experiment.

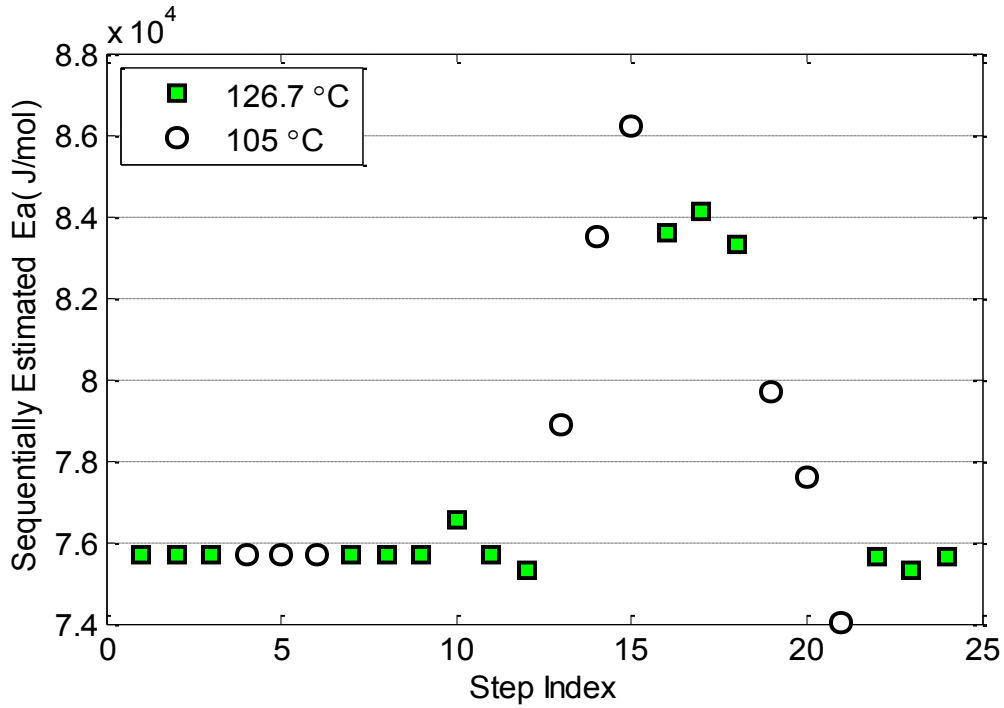


Figure 5.8 Sequentially estimated parameter of activation energy (E_a).

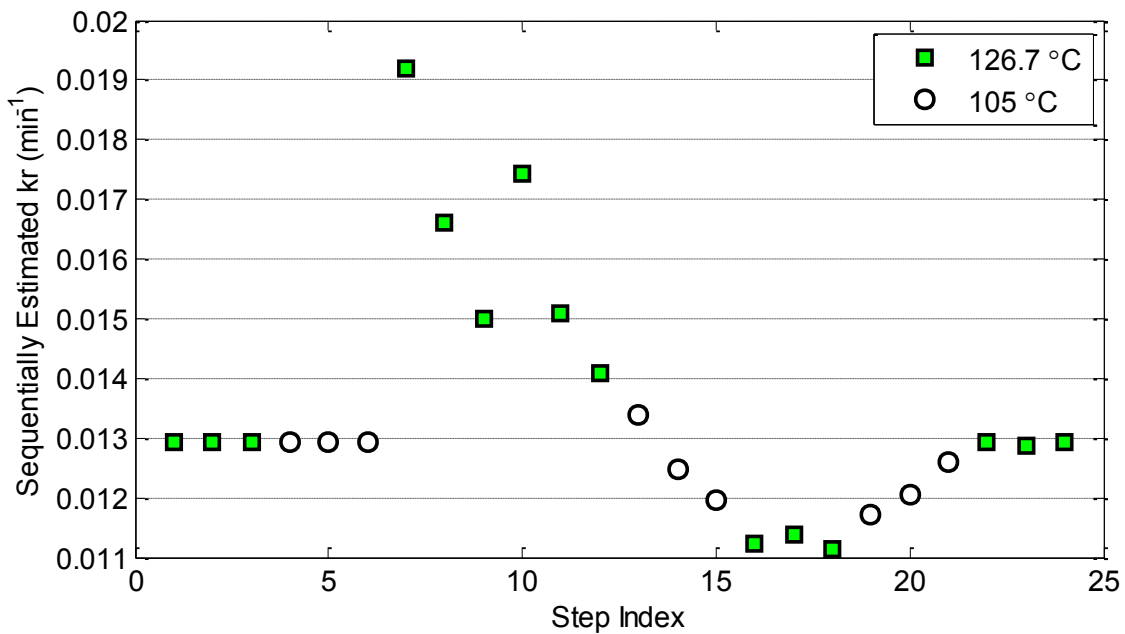


Figure 5.9 Sequentially estimated parameter of reaction rate ($k_{r115.8^\circ\text{C}}$) (min^{-1}).

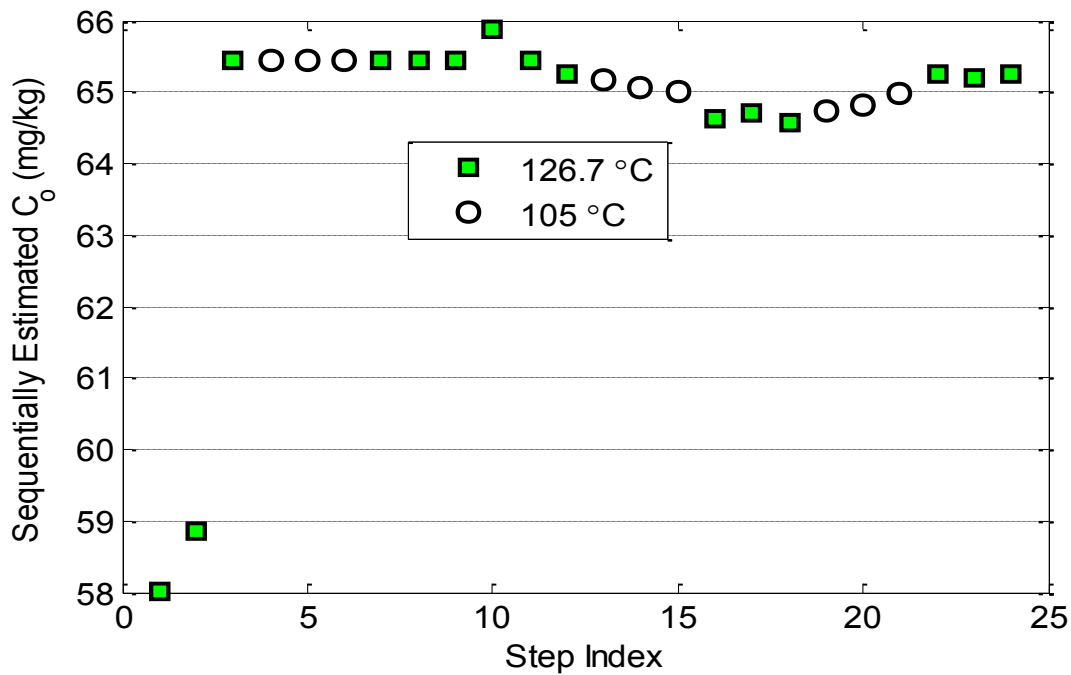


Figure 5.10 Sequentially estimated parameter of Initial concentration (C_0)

5.4 Conclusions

1. This study shows innovative data efficient methods to estimate the kinetic parameters for cherry pomace ACY degradation at two different retorting temperatures. These methods can be used to estimate other kinetic parameters for non-isothermal conditions.
2. A minimum of two retort temperatures are needed to estimate E_a accurately, because scaled sensitivity coefficient for E_a for only one retort temperature is small.
3. There was no significant effect of moisture content on the rate constant in this study.
4. Relative errors of the kinetic parameters were under 24%.
5. For future studies the parameter accuracy may be increased by applying optimal experimental design to determine the best times and temperatures to collect data.

APPENDICES

Appendix C.1 Experimental design and preliminary data

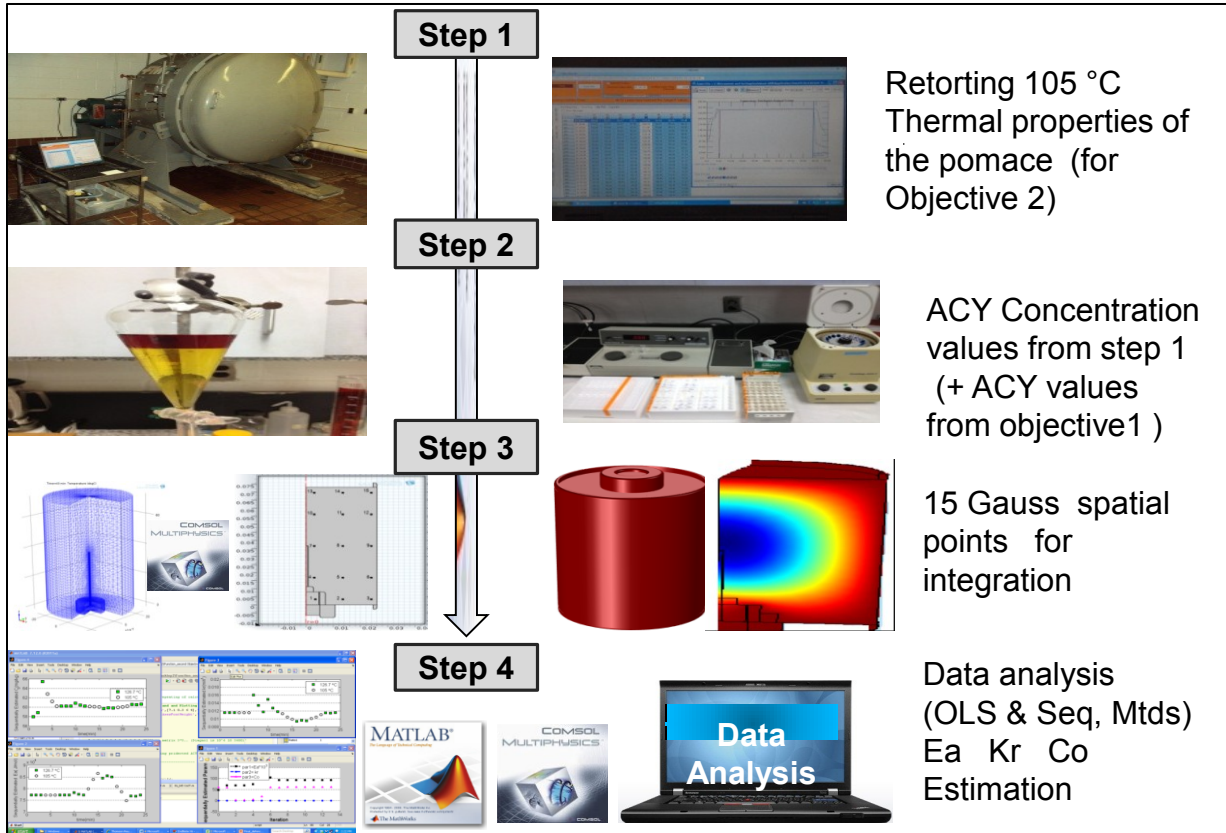


Figure C.1 Process experimental design for kinetic parameter estimation

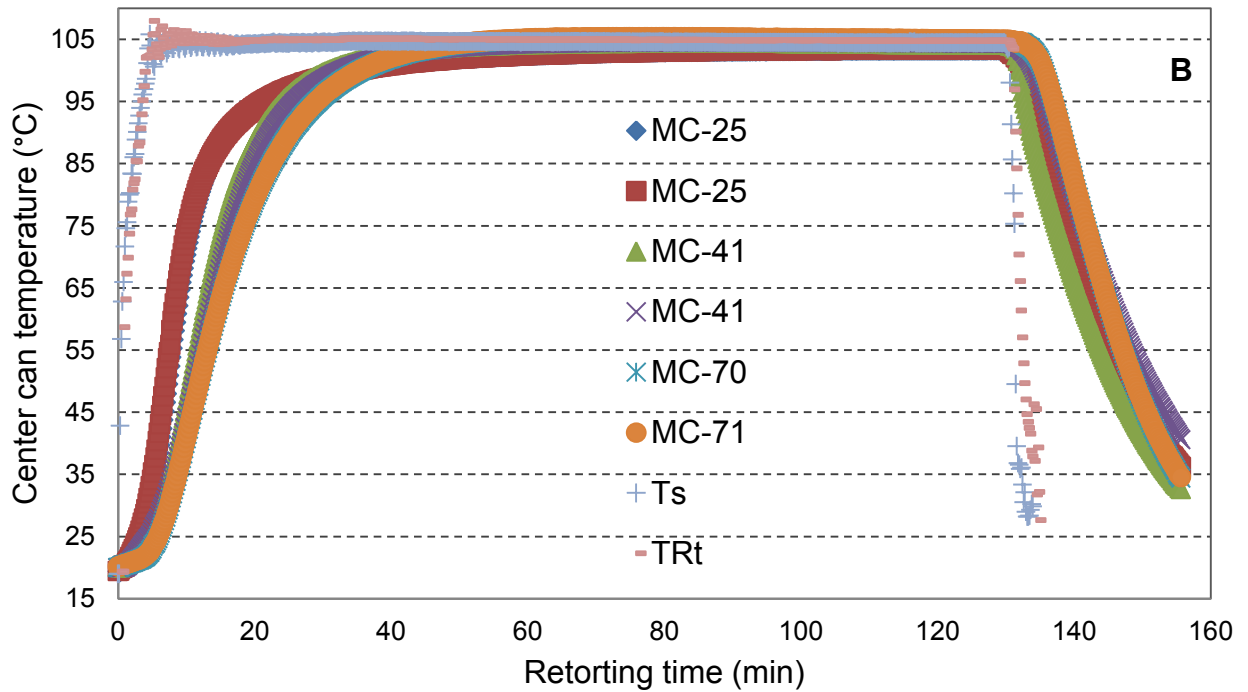
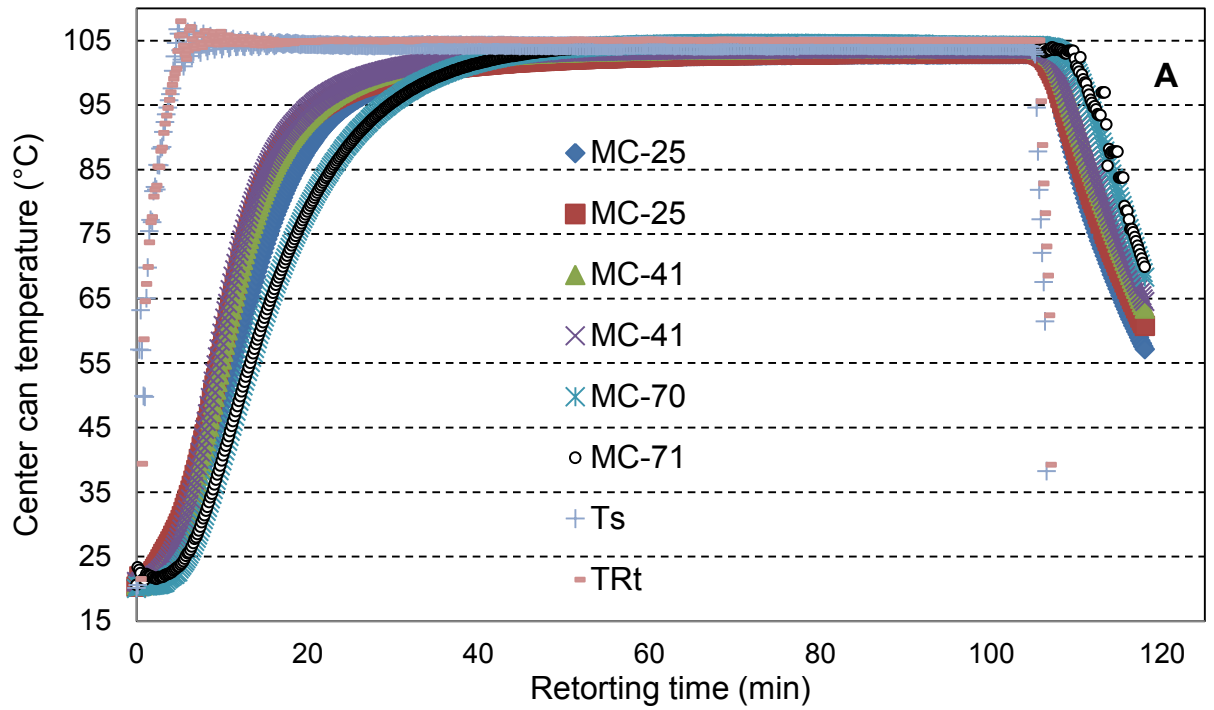


Figure C.2 Can-center temperature profile of cherry pomace in a retort at 105 °C for 100 min (A) and 125 min (B) (TRt=Retort temperature, Ts= can surface temperature; 70%, 41%, and 25% MC represent the pomace with 70, 41, and 25% moisture (wb), respectively).

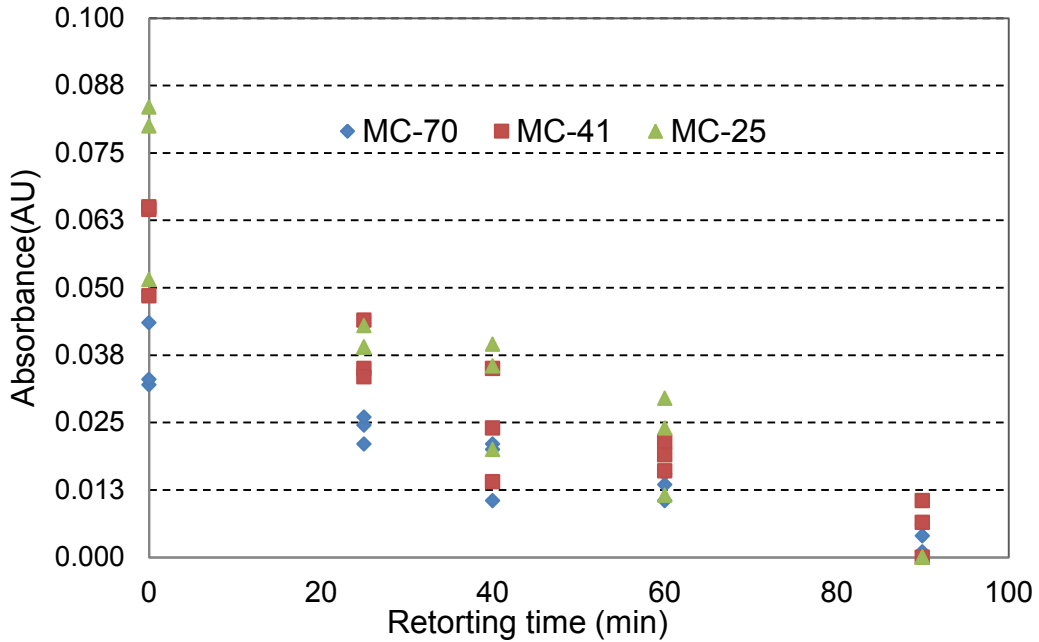


Figure C.3 Absorbance versus Retorting time of Cherry pomace ACY's extractions at three constant moisture content (wb) heated at 126.7°C

Table C.1 Absorbance versus Retorting time of Cherry pomace ACY's extractions at three constant moisture content heated at 126.7°C

time(min)	Absorbance(AU)			Standard deviation		
	MC-70	MC-41	MC-25	MC-70	MC-41	MC-25
0	0.0320	0.0485	0.0515	0.0064	0.0094	0.0176
0	0.0330	0.0645	0.0800			
0	0.0435	0.0650	0.0835			
25	0.0210	0.0440	0.0390	0.0026	0.0057	0.0023
25	0.0245	0.0350	0.0430			
25	0.0260	0.0335	0.0390			
40	0.0105	0.0240	0.0200	0.0058	0.0105	0.0103
40	0.0210	0.0140	0.0395			
40	0.0200	0.0350	0.0355			
60	0.0155	0.0190	0.0295	0.0025	0.0028	0.0092
60	0.0105	0.0215	0.0240			
60	0.0135	0.0160	0.0115			
90	0.0010	0.0065	0	0.0025	0.0053	0
90	0.0060	0.0105	0			
90	0.0040	0.0000	0			

Table C.2 Cherry pomace's ACY concentration after retorting at two different temperatures for different times

Concentration of ACY (mg/kg) dry basis						
time(min)	Temperature 127 °C			Temperature 105 °C		
	MC-70	MC-41	MC-25	MC-70	MC-41	MC-25
0	65.4 ±6.7	54.8 ±5.1	51.9 ±5.9	65.4 ±6.7	54.8 ±5.1	51.9 ±5.9
25	43.1 ±2.7	34.5 ±3.0	29.2 ±1.0	NA	NA	NA
40	31.1 ±6.1	22.3 ±5.6	22.9 ±4.3	NA	NA	NA
60	23.8 ±2.6	17.3 ±1.5	15.7 ±3.9	NA	NA	NA
90	6.6 ±2.6	5.2 ±2.8	0	NA	NA	NA
100	NA	NA	NA	41.7 ±1.9	35.3 ±2.1	37.7 ±6.1
125	NA	NA	NA	22.5 ±2.2	12.5 ±2.3	12.1 ±0.76

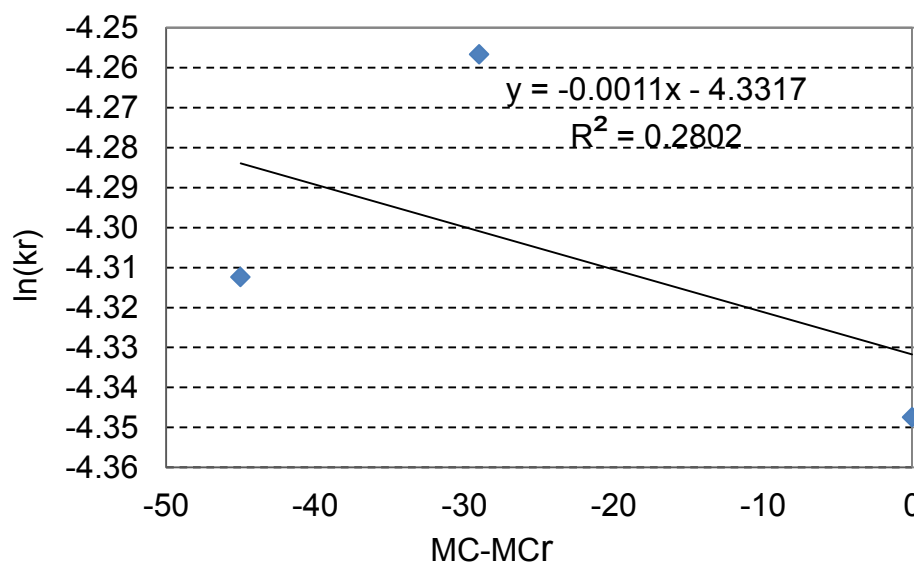


Figure C.4 Slope method for estimate the moisture constant (b) for the retorted cherry pomace samples ACY concentration

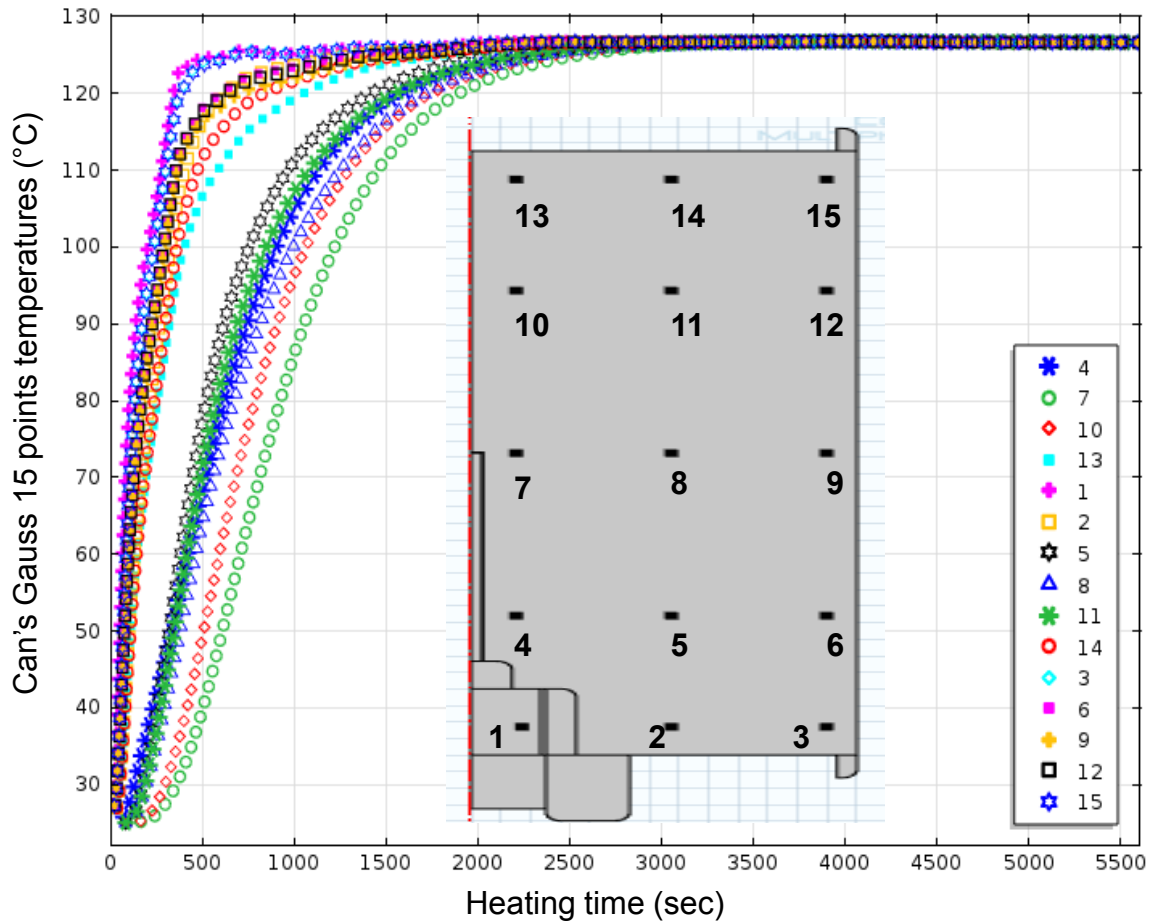


Figure C.5 Plot of gauss points in the can with cherry pomace 70% MC (wb), predicted by Comsol. "The text in this figure is not meant to be readable but is for visual reference only".

Appendix C.2 Predicted Temperatures data by Comsol software

Table C.3 Part of predicted temperatures (°C) data at 15 gauss points (Pts) in the can for Cherry pomace (70% MC, wb) at 126.7°C Retort Temperature).

time min	Pt 1	Pt 2	Pt 3	Pt 4	Pt 5	Pt 6	Pt 7
0.0	25.2	25.0	25.0	25.0	25.0	25.0	25.0
0.2	27.6	25.3	26.3	25.0	25.0	26.1	25.0
0.3	28.5	25.8	27.2	25.0	25.0	26.8	25.0
0.5	32.0	26.4	29.2	25.0	25.0	28.5	25.0
0.7	39.0	27.8	33.3	25.1	25.0	31.9	25.0
0.8	47.2	30.2	39.1	25.2	25.0	36.7	25.0
1.0	54.8	33.3	45.4	25.3	25.0	41.8	25.0
1.2	61.6	36.9	51.5	25.6	25.1	46.9	25.0
1.3	67.5	40.6	57.4	25.9	25.2	51.7	25.0
1.5	72.8	44.5	62.8	26.4	25.4	56.2	25.0
1.7	77.0	48.2	67.5	26.9	25.6	60.2	25.0
1.8	80.4	51.8	71.6	27.5	25.9	63.8	25.0
2.0	83.4	55.2	75.3	28.2	26.4	67.0	25.0
2.2	86.1	58.4	78.6	29.0	26.9	70.0	25.0
2.3	88.5	61.4	81.5	29.7	27.6	72.6	25.0
2.5	90.5	64.3	84.2	30.5	28.3	75.1	25.1
2.7	92.4	66.9	86.6	31.4	29.2	77.3	25.1
2.8	94.1	69.4	88.7	32.2	30.1	79.4	25.1
3.0	95.6	71.8	90.7	33.0	31.1	81.3	25.2
3.2	97.0	74.0	92.5	33.8	32.2	83.1	25.3
3.3	98.3	76.1	94.1	34.7	33.4	84.8	25.3
3.5	99.4	78.0	95.6	35.5	34.6	86.3	25.4
3.7	100.4	79.8	97.0	36.4	35.9	87.7	25.6
3.8	101.3	81.6	98.1	37.2	37.2	88.9	25.7
4.0	102.6	83.3	99.5	38.1	38.5	90.4	25.9
4.2	104.0	84.9	101.0	39.0	39.9	91.8	26.1
4.3	105.6	86.6	102.5	39.8	41.3	93.4	26.3
4.5	107.2	88.2	104.1	40.7	42.7	94.9	26.5
4.7	108.9	89.9	105.7	41.6	44.1	96.6	26.8
4.8	110.5	91.6	107.3	42.6	45.5	98.2	27.1
5.0	112.1	93.2	108.9	43.5	46.9	99.8	27.5
5.2	113.6	94.9	110.5	44.5	48.3	101.3	27.8
5.3	115.1	96.5	112.1	45.4	49.7	102.9	28.2
5.5	116.5	98.1	113.6	46.4	51.1	104.4	28.6
5.7	117.8	99.7	115.0	47.5	52.5	105.8	29.1
5.8	118.9	101.1	116.3	48.5	53.9	107.1	29.6
6.0	120.0	102.6	117.5	49.5	55.3	108.4	30.1
6.2	120.9	103.9	118.6	50.6	56.7	109.5	30.6

Table C.3, (Cont'd)

6.3	121.7	105.3	119.6	51.6	58.1	110.6	31.2
6.5	122.3	106.5	120.4	52.7	59.5	111.6	31.8
6.7	122.8	107.6	121.2	53.8	60.9	112.4	32.4
6.8	123.2	108.7	121.8	54.8	62.3	113.2	33.0
7.0	123.5	109.7	122.4	55.9	63.6	113.9	33.7
7.2	123.7	110.6	122.8	57.0	65.0	114.5	34.3
7.3	123.8	111.4	123.1	58.1	66.3	115.0	35.0
7.5	123.8	112.2	123.4	59.1	67.6	115.4	35.7
7.7	123.8	112.8	123.5	60.2	68.9	115.8	36.5
7.8	123.6	113.4	123.6	61.3	70.2	116.0	37.2
8.0	123.5	113.9	123.6	62.3	71.5	116.3	38.0
8.2	123.4	114.4	123.6	63.3	72.7	116.5	38.8
8.3	123.3	114.9	123.6	64.3	74.0	116.7	39.6
8.5	123.1	115.2	123.6	65.4	75.2	116.9	40.4
8.7	123.0	115.6	123.5	66.4	76.3	117.0	41.3
8.8	123.0	115.9	123.6	67.3	77.5	117.2	42.1
9.0	123.1	116.2	123.6	68.3	78.6	117.4	43.0
9.2	123.2	116.6	123.7	69.3	79.7	117.6	43.8
9.3	123.3	116.8	123.8	70.2	80.8	117.9	44.7
9.5	123.5	117.1	123.9	71.2	81.8	118.1	45.6
9.7	123.6	117.4	124.0	72.1	82.8	118.4	46.5
9.8	123.8	117.7	124.1	73.0	83.8	118.6	47.4
10.0	123.9	118.0	124.3	74.0	84.7	118.9	48.3
10.2	124.1	118.3	124.4	74.9	85.7	119.1	49.2
10.3	124.3	118.6	124.6	75.8	86.6	119.4	50.1
10.5	124.4	118.9	124.7	76.6	87.5	119.6	51.0
10.7	124.6	119.1	124.8	77.5	88.3	119.8	51.9
10.8	124.7	119.4	125.0	78.4	89.2	120.1	52.9
11.0	124.8	119.6	125.1	79.2	90.0	120.3	53.8
11.2	124.8	119.9	125.2	80.1	90.8	120.5	54.7
11.3	124.9	120.1	125.2	80.9	91.5	120.6	55.6
11.5	124.9	120.3	125.3	81.7	92.3	120.8	56.5
11.7	124.9	120.5	125.3	82.5	93.0	120.9	57.5
11.8	124.9	120.6	125.4	83.3	93.7	121.0	58.4
12.0	124.9	120.8	125.4	84.1	94.4	121.2	59.3
12.2	124.9	120.9	125.4	84.9	95.1	121.2	60.2
12.3	124.8	121.1	125.3	85.6	95.8	121.3	61.1
12.5	124.8	121.2	125.3	86.4	96.4	121.4	61.9
12.7	124.7	121.3	125.2	87.1	97.0	121.4	62.8
12.8	124.6	121.4	125.1	87.8	97.6	121.4	63.7
13.0	124.4	121.4	125.0	88.5	98.2	121.4	64.6
13.2	124.3	121.5	124.9	89.2	98.8	121.4	65.5
13.3	124.3	121.6	124.9	89.9	99.4	121.5	66.3
13.5	124.3	121.7	124.9	90.5	99.9	121.6	67.2
13.7	124.3	121.8	124.9	91.2	100.5	121.6	68.0

Table C.3, (Cont'd)

13.8	124.3	121.8	124.9	91.8	101.0	121.7	68.9
14.0	124.4	121.9	124.9	92.4	101.5	121.8	69.7
14.2	124.4	122.0	125.0	93.1	102.0	121.9	70.5
14.3	124.5	122.1	125.0	93.7	102.5	122.0	71.3
14.5	124.5	122.2	125.0	94.2	103.0	122.0	72.1
14.7	124.6	122.2	125.0	94.8	103.4	122.1	73.0
14.8	124.7	122.3	125.1	95.4	103.9	122.2	73.7
15.0	124.7	122.4	125.1	96.0	104.3	122.3	74.5
15.2	124.8	122.5	125.2	96.5	104.7	122.4	75.3
15.3	124.9	122.6	125.2	97.1	105.2	122.5	76.1
15.5	124.9	122.7	125.2	97.6	105.6	122.6	76.8
15.7	125.0	122.8	125.3	98.1	106.0	122.7	77.6
15.8	125.1	122.8	125.4	98.6	106.4	122.8	78.3
16.0	125.2	122.9	125.4	99.1	106.7	122.9	79.1
16.2	125.2	123.0	125.5	99.6	107.1	123.0	79.8
16.3	125.3	123.1	125.5	100.1	107.5	123.1	80.5
16.5	125.3	123.2	125.5	100.6	107.8	123.1	81.2
16.7	125.3	123.2	125.5	101.0	108.2	123.2	81.9
16.8	125.3	123.3	125.6	101.5	108.5	123.2	82.6
17.0	125.3	123.3	125.6	101.9	108.8	123.3	83.3
17.2	125.3	123.4	125.5	102.4	109.1	123.3	83.9
17.3	125.2	123.4	125.5	102.8	109.5	123.4	84.6
17.5	125.2	123.5	125.5	103.2	109.8	123.4	85.3
17.7	125.2	123.5	125.5	103.6	110.1	123.4	85.9
17.8	125.2	123.6	125.5	104.0	110.4	123.4	86.5
18.0	125.2	123.6	125.5	104.4	110.7	123.5	87.2
18.2	125.2	123.7	125.5	104.8	110.9	123.5	87.8
18.3	125.2	123.7	125.5	105.2	111.2	123.6	88.4
18.5	125.2	123.7	125.5	105.6	111.5	123.6	89.0
18.7	125.2	123.8	125.5	105.9	111.8	123.6	89.6
18.8	125.2	123.8	125.5	106.3	112.0	123.7	90.2

Table C.3, (Cont'd)

time min	Pt 8	Pt 9	Pt 10	Pt 11	Pt 12	Pt 13	Pt 14	Pt 15
0.0	25.0	25.2	25.0	25.0	25.0	25.5	25.1	25.0
0.2	25.0	26.1	25.0	25.0	26.1	25.2	25.3	26.3
0.3	25.0	26.8	25.0	25.0	26.8	25.8	25.7	27.2
0.5	25.0	28.5	25.0	25.0	28.4	26.6	26.4	29.2
0.7	25.0	31.9	25.0	25.0	31.9	27.9	27.8	33.3
0.8	25.0	36.7	25.0	25.0	36.7	30.0	30.0	39.1
1.0	25.0	41.8	25.0	25.0	41.8	33.0	33.0	45.4
1.2	25.1	46.8	25.0	25.1	46.9	36.2	36.3	51.5
1.3	25.2	51.6	25.0	25.2	51.7	39.7	39.7	57.4
1.5	25.3	56.2	25.0	25.3	56.2	43.1	43.2	62.8
1.7	25.5	60.2	25.0	25.5	60.2	46.3	46.6	67.5
1.8	25.7	63.7	25.1	25.8	63.8	49.4	49.8	71.6
2.0	26.0	67.0	25.1	26.1	67.0	52.4	52.8	75.3
2.2	26.4	69.9	25.1	26.5	70.0	55.1	55.7	78.6
2.3	26.9	72.6	25.2	27.1	72.6	57.6	58.4	81.5
2.5	27.5	75.0	25.3	27.7	75.1	60.0	61.0	84.2
2.7	28.1	77.3	25.4	28.4	77.3	62.2	63.4	86.6
2.8	28.8	79.3	25.6	29.2	79.4	64.2	65.6	88.7
3.0	29.5	81.2	25.8	30.0	81.3	66.2	67.8	90.7
3.2	30.3	82.9	26.0	31.0	83.1	68.0	69.8	92.5
3.3	31.1	84.6	26.2	32.0	84.7	69.7	71.7	94.1
3.5	32.0	86.0	26.5	33.0	86.2	71.2	73.5	95.6
3.7	32.9	87.4	26.9	34.1	87.6	72.7	75.3	96.9
3.8	33.9	88.6	27.2	35.2	88.9	74.1	76.9	98.0
4.0	34.8	90.0	27.7	36.4	90.3	75.5	78.5	99.4
4.2	35.8	91.4	28.1	37.5	91.8	77.0	80.1	100.9
4.3	36.8	92.9	28.6	38.8	93.3	78.4	81.7	102.4
4.5	37.8	94.4	29.1	40.0	94.8	79.8	83.3	103.9
4.7	38.8	96.0	29.7	41.2	96.4	81.2	84.9	105.5
4.8	39.8	97.6	30.3	42.5	98.0	82.6	86.5	107.2
5.0	40.9	99.1	30.9	43.7	99.6	84.1	88.1	108.7
5.2	41.9	100.6	31.6	45.0	101.2	85.6	89.7	110.3
5.3	42.9	102.1	32.3	46.3	102.7	87.0	91.3	111.9
5.5	44.0	103.6	33.1	47.5	104.2	88.5	92.8	113.4
5.7	45.0	104.9	33.8	48.8	105.6	89.9	94.3	114.8
5.8	46.1	106.2	34.6	50.1	106.9	91.2	95.8	116.0
6.0	47.1	107.4	35.5	51.4	108.1	92.5	97.2	117.2
6.2	48.2	108.5	36.3	52.6	109.3	93.7	98.5	118.3
6.3	49.2	109.5	37.2	53.9	110.3	94.9	99.8	119.3
6.5	50.3	110.5	38.1	55.2	111.3	96.0	101.0	120.2
6.7	51.3	111.3	39.0	56.4	112.1	97.1	102.1	120.9
6.8	52.4	112.0	39.9	57.7	112.9	98.1	103.2	121.6
7.0	53.5	112.6	40.9	59.0	113.6	99.0	104.2	122.1

Table C.3, (Cont'd)

7.2	54.5	113.2	41.8	60.2	114.1	99.9	105.1	122.5
7.3	55.6	113.7	42.8	61.5	114.6	100.7	105.9	122.8
7.5	56.6	114.0	43.8	62.7	115.1	101.4	106.7	123.1
7.7	57.6	114.4	44.8	63.9	115.4	102.1	107.4	123.2
7.8	58.7	114.6	45.8	65.1	115.6	102.7	108.0	123.3
8.0	59.7	114.8	46.9	66.3	115.9	103.2	108.6	123.3
8.2	60.7	115.0	47.9	67.5	116.1	103.8	109.1	123.3
8.3	61.7	115.1	49.0	68.7	116.3	104.2	109.6	123.3
8.5	62.7	115.3	50.0	69.8	116.4	104.7	110.0	123.3
8.7	63.7	115.4	51.1	70.9	116.5	105.1	110.4	123.2
8.8	64.7	115.5	52.1	72.0	116.7	105.5	110.9	123.2
9.0	65.6	115.7	53.2	73.1	116.9	105.9	111.3	123.3
9.2	66.6	115.9	54.2	74.2	117.1	106.3	111.6	123.3
9.3	67.5	116.1	55.3	75.2	117.4	106.7	112.0	123.4
9.5	68.4	116.3	56.4	76.2	117.6	107.1	112.4	123.5
9.7	69.3	116.5	57.4	77.2	117.8	107.6	112.8	123.6
9.8	70.2	116.8	58.5	78.2	118.1	108.0	113.1	123.8
10.0	71.0	117.0	59.5	79.2	118.3	108.4	113.5	123.9
10.2	71.9	117.3	60.6	80.1	118.6	108.8	113.8	124.1
10.3	72.7	117.5	61.6	81.0	118.8	109.2	114.2	124.2
10.5	73.5	117.7	62.6	81.9	119.1	109.6	114.5	124.4
10.7	74.3	117.9	63.6	82.8	119.3	110.0	114.8	124.5
10.8	75.1	118.2	64.7	83.6	119.5	110.3	115.2	124.6
11.0	75.9	118.4	65.7	84.4	119.7	110.7	115.5	124.7
11.2	76.7	118.5	66.6	85.2	119.9	111.1	115.8	124.8
11.3	77.5	118.7	67.6	86.0	120.1	111.4	116.0	124.9
11.5	78.2	118.8	68.6	86.8	120.2	111.7	116.3	125.0
11.7	78.9	119.0	69.5	87.5	120.3	112.0	116.6	125.0
11.8	79.7	119.1	70.5	88.3	120.5	112.3	116.8	125.0
12.0	80.4	119.2	71.4	89.0	120.6	112.6	117.0	125.0
12.2	81.1	119.3	72.3	89.7	120.7	112.9	117.2	125.0
12.3	81.8	119.4	73.2	90.4	120.7	113.1	117.4	125.0
12.5	82.5	119.4	74.1	91.1	120.8	113.4	117.6	125.0
12.7	83.2	119.5	75.0	91.8	120.8	113.6	117.7	124.9
12.8	83.8	119.5	75.9	92.4	120.8	113.8	117.9	124.8
13.0	84.5	119.5	76.8	93.0	120.8	114.0	118.0	124.7
13.2	85.1	119.5	77.6	93.7	120.8	114.2	118.1	124.6
13.3	85.8	119.6	78.4	94.3	120.9	114.4	118.3	124.6
13.5	86.4	119.6	79.3	94.9	121.0	114.6	118.4	124.6
13.7	87.0	119.7	80.1	95.5	121.1	114.8	118.5	124.6
13.8	87.6	119.8	80.9	96.0	121.1	115.0	118.7	124.6
14.0	88.2	119.9	81.6	96.6	121.2	115.2	118.8	124.7
14.2	88.8	120.0	82.4	97.1	121.3	115.4	119.0	124.7
14.3	89.4	120.1	83.2	97.6	121.4	115.6	119.1	124.7
14.5	89.9	120.2	83.9	98.2	121.5	115.8	119.2	124.7

Table C.3, (Cont'd)

14.7	90.5	120.3	84.6	98.7	121.6	116.0	119.3	124.8
14.8	91.1	120.4	85.4	99.2	121.7	116.2	119.5	124.8
15.0	91.6	120.5	86.1	99.6	121.8	116.4	119.6	124.8
15.2	92.1	120.6	86.8	100.1	121.9	116.6	119.7	124.9
15.3	92.7	120.7	87.5	100.6	121.9	116.8	119.9	124.9
15.5	93.2	120.8	88.1	101.1	122.1	117.0	120.0	125.0
15.7	93.7	120.9	88.8	101.5	122.2	117.2	120.1	125.1
15.8	94.2	121.0	89.4	101.9	122.3	117.3	120.3	125.1
16.0	94.7	121.2	90.1	102.4	122.4	117.5	120.4	125.2
16.2	95.2	121.3	90.7	102.8	122.5	117.7	120.5	125.3
16.3	95.7	121.4	91.3	103.2	122.5	117.9	120.7	125.3
16.5	96.2	121.4	91.9	103.6	122.6	118.0	120.8	125.3
16.7	96.6	121.5	92.5	104.0	122.7	118.2	120.9	125.3
16.8	97.1	121.6	93.1	104.4	122.7	118.3	121.0	125.3
17.0	97.6	121.6	93.7	104.8	122.8	118.5	121.1	125.3
17.2	98.0	121.7	94.2	105.1	122.8	118.6	121.1	125.3
17.3	98.4	121.8	94.8	105.5	122.9	118.7	121.2	125.3
17.5	98.9	121.8	95.3	105.9	122.9	118.9	121.3	125.3
17.7	99.3	121.8	95.8	106.2	122.9	119.0	121.4	125.3
17.8	99.7	121.9	96.4	106.5	123.0	119.1	121.5	125.3
18.0	100.1	121.9	96.9	106.9	123.0	119.2	121.6	125.3
18.2	100.6	122.0	97.4	107.2	123.0	119.4	121.6	125.3
18.3	101.0	122.1	97.9	107.5	123.1	119.5	121.7	125.3
18.5	101.4	122.1	98.4	107.9	123.1	119.6	121.8	125.3
18.7	101.8	122.2	98.9	108.2	123.2	119.7	121.8	125.3
18.8	102.1	122.2	99.3	108.5	123.2	119.8	121.9	125.3

Table C.4 Part of predicted temperatures (°C) data at 15 gauss points (Pts) in the can for Cherry pomace (70% MC, wb) (105 °C Retort Temp).

time min	Pt 1	Pt 2	Pt 3	Pt 4	Pt 5	Pt 6	Pt 7
0.0	25.2	25.0	25.0	25.0	25.0	25.0	25.0
0.4	27.6	25.3	26.3	25.0	25.0	26.1	25.0
0.7	28.5	25.8	27.2	25.0	25.0	26.8	25.0
0.9	32.0	26.4	29.2	25.0	25.0	28.5	25.0
1.0	39.0	27.8	33.3	25.1	25.0	31.9	25.0
1.1	47.2	30.2	39.1	25.2	25.0	36.7	25.0
1.1	54.8	33.3	45.4	25.3	25.0	41.8	25.0
1.1	61.6	36.9	51.5	25.6	25.1	46.9	25.0
1.2	67.5	40.6	57.4	25.9	25.2	51.7	25.0
1.2	72.8	44.5	62.8	26.4	25.4	56.2	25.0
1.3	77.0	48.2	67.5	26.9	25.6	60.2	25.0
1.4	80.4	51.8	71.6	27.5	25.9	63.8	25.0
1.4	83.4	55.2	75.3	28.2	26.4	67.0	25.0
1.5	86.1	58.4	78.6	29.0	26.9	70.0	25.0
1.6	88.5	61.4	81.5	29.7	27.6	72.6	25.0
1.7	90.5	64.3	84.2	30.5	28.3	75.1	25.1
1.7	92.4	66.9	86.6	31.4	29.2	77.3	25.1
1.8	94.1	69.4	88.7	32.2	30.1	79.4	25.1
1.9	95.6	71.8	90.7	33.0	31.1	81.3	25.2
2.0	97.0	74.0	92.5	33.8	32.2	83.1	25.3
2.0	98.3	76.1	94.1	34.7	33.4	84.8	25.3
2.1	99.4	78.0	95.6	35.5	34.6	86.3	25.4
2.2	100.4	79.8	97.0	36.4	35.9	87.7	25.6
2.3	101.2	81.5	98.1	37.2	37.2	88.9	25.7
2.4	101.7	83.1	99.0	38.1	38.5	89.9	25.9
2.5	102.0	84.5	99.8	39.0	39.9	90.8	26.1
2.5	102.2	85.8	100.3	39.8	41.3	91.6	26.3
2.6	102.6	87.0	101.0	40.7	42.6	92.4	26.5
2.7	103.0	88.1	101.5	41.5	44.0	93.1	26.8
2.8	103.5	89.1	102.1	42.4	45.4	93.8	27.1
2.9	103.9	90.1	102.7	43.3	46.8	94.6	27.5
3.0	104.4	91.1	103.2	44.1	48.2	95.3	27.8
3.1	104.7	91.9	103.6	45.0	49.5	95.8	28.2
3.2	104.7	92.7	103.9	45.9	50.9	96.3	28.6
3.3	104.5	93.4	104.0	46.8	52.2	96.6	29.1
3.4	104.3	94.0	104.1	47.7	53.5	96.9	29.6
3.5	104.1	94.5	104.0	48.5	54.8	97.1	30.1

Table C.4, (Cont'd)

3.6	103.7	94.9	103.9	49.4	56.0	97.2	30.6
3.7	103.5	95.3	103.8	50.3	57.2	97.3	31.2
3.8	103.2	95.7	103.7	51.2	58.4	97.3	31.7
3.9	103.0	96.0	103.5	52.0	59.6	97.4	32.3
4.0	103.0	96.3	103.5	52.9	60.7	97.6	33.0
4.1	103.1	96.5	103.5	53.7	61.8	97.7	33.6
4.2	103.2	96.8	103.5	54.6	62.9	97.9	34.3
4.3	103.3	97.1	103.6	55.4	63.9	98.1	34.9
4.3	103.5	97.4	103.7	56.2	64.9	98.4	35.6
4.4	103.5	97.6	103.8	57.1	65.9	98.6	36.3
4.5	103.6	97.9	103.8	57.9	66.8	98.8	37.0
4.6	103.5	98.1	103.9	58.7	67.7	98.9	37.8
4.7	103.5	98.3	103.9	59.5	68.6	99.1	38.5
4.8	103.5	98.5	103.9	60.3	69.5	99.2	39.2
4.9	103.5	98.7	103.9	61.1	70.3	99.3	40.0
5.0	103.5	98.9	103.9	61.9	71.1	99.4	40.8
5.1	103.5	99.1	103.9	62.6	71.9	99.6	41.5
5.2	103.5	99.2	103.9	63.4	72.6	99.7	42.3
5.3	103.5	99.4	104.0	64.1	73.4	99.8	43.1
5.4	103.6	99.6	104.0	64.9	74.1	99.9	43.8
5.5	103.6	99.7	104.0	65.6	74.8	100.0	44.6
5.6	103.6	99.9	104.0	66.3	75.5	100.2	45.4
5.7	103.7	100.0	104.1	67.0	76.1	100.3	46.1
5.8	103.7	100.1	104.1	67.7	76.8	100.4	46.9
5.9	103.8	100.3	104.1	68.4	77.4	100.5	47.7
6.0	103.8	100.4	104.2	69.1	78.0	100.6	48.4
6.1	103.8	100.5	104.2	69.8	78.6	100.7	49.2
6.2	103.9	100.6	104.2	70.4	79.1	100.8	50.0
6.3	103.9	100.8	104.3	71.1	79.7	100.9	50.7
6.4	103.9	100.9	104.3	71.7	80.2	101.0	51.5
6.4	103.9	101.0	104.3	72.3	80.8	101.1	52.2
6.5	104.0	101.1	104.3	72.9	81.3	101.2	52.9
6.6	104.0	101.2	104.4	73.5	81.8	101.3	53.7
6.7	104.0	101.3	104.4	74.1	82.3	101.4	54.4
6.8	104.1	101.4	104.4	74.7	82.8	101.5	55.1
6.9	104.1	101.5	104.4	75.3	83.2	101.5	55.8
7.0	104.1	101.6	104.4	75.8	83.7	101.6	56.5
7.1	104.1	101.7	104.5	76.4	84.1	101.7	57.3
7.2	104.1	101.8	104.5	76.9	84.5	101.8	58.0
7.3	104.2	101.8	104.5	77.4	85.0	101.9	58.6
7.4	104.2	101.9	104.5	77.9	85.4	101.9	59.3

Table C.4, (Cont'd)

7.5	104.2	102.0	104.5	78.4	85.8	102.0	60.0
7.6	104.2	102.1	104.5	78.9	86.2	102.1	60.7
7.7	104.2	102.2	104.6	79.4	86.6	102.1	61.3
7.8	104.3	102.2	104.6	79.9	86.9	102.2	62.0
7.9	104.3	102.3	104.6	80.4	87.3	102.3	62.6
8.0	104.3	102.4	104.6	80.8	87.7	102.3	63.3
8.1	104.3	102.4	104.6	81.3	88.0	102.4	63.9
8.1	104.3	102.5	104.6	81.7	88.3	102.4	64.6
8.2	104.4	102.6	104.6	82.2	88.7	102.5	65.2
8.3	104.4	102.6	104.7	82.6	89.0	102.5	65.8
8.4	104.4	102.7	104.7	83.0	89.3	102.6	66.4
8.5	104.4	102.7	104.7	83.4	89.6	102.6	67.0
8.6	104.4	102.8	104.7	83.8	89.9	102.7	67.6
8.7	104.4	102.8	104.7	84.3	90.2	102.8	68.2
8.8	104.5	102.9	104.7	84.6	90.5	102.8	68.8
8.9	104.5	103.0	104.7	85.0	90.8	102.9	69.3
9.0	104.5	103.0	104.7	85.4	91.1	102.9	69.9
9.1	104.5	103.1	104.8	85.8	91.4	103.0	70.5
9.2	104.5	103.1	104.8	86.2	91.7	103.0	71.0
9.3	104.5	103.2	104.8	86.5	92.0	103.0	71.6
9.4	104.5	103.2	104.8	86.9	92.2	103.1	72.1
9.5	104.6	103.2	104.8	87.2	92.5	103.1	72.6
9.6	104.6	103.3	104.8	87.6	92.7	103.2	73.1
9.7	104.6	103.3	104.8	87.9	93.0	103.2	73.7
9.8	104.6	103.4	104.8	88.2	93.2	103.3	74.2
9.8	104.6	103.4	104.8	88.6	93.5	103.3	74.7
9.9	104.6	103.5	104.8	88.9	93.7	103.3	75.2
10.0	104.6	103.5	104.9	89.2	93.9	103.4	75.6
10.1	104.6	103.5	104.9	89.5	94.1	103.4	76.1
10.2	104.7	103.6	104.9	89.8	94.3	103.4	76.6
10.3	104.7	103.6	104.9	90.0	94.5	103.5	77.1
10.4	104.7	103.6	104.9	90.3	94.7	103.5	77.5
10.5	104.7	103.7	104.9	90.6	94.9	103.5	78.0
10.6	104.7	103.7	104.9	90.9	95.1	103.6	78.4
10.7	104.7	103.7	104.9	91.2	95.4	103.6	78.9
10.8	104.7	103.8	104.9	91.4	95.5	103.6	79.3
10.9	104.7	103.8	104.9	91.7	95.7	103.7	79.7
11.0	104.7	103.8	104.9	91.9	95.9	103.7	80.2
11.1	104.7	103.9	104.9	92.2	96.1	103.7	80.6
11.2	104.8	103.9	104.9	92.5	96.3	103.8	81.0
11.3	104.8	103.9	104.9	92.7	96.5	103.8	81.4

Table C.4, (Cont'd)

11.4	104.8	103.9	104.9	92.9	96.6	103.8	81.8
11.5	104.8	104.0	105.0	93.2	96.8	103.8	82.2
11.5	104.8	104.0	105.0	93.4	97.0	103.9	82.6
11.6	104.8	104.0	105.0	93.6	97.1	103.9	83.0
11.7	104.8	104.0	105.0	93.8	97.3	103.9	83.4
11.8	104.8	104.1	105.0	94.0	97.4	103.9	83.7
11.9	104.8	104.1	105.0	94.2	97.6	104.0	84.1
12.0	104.8	104.1	105.0	94.4	97.7	104.0	84.5
12.1	104.8	104.1	105.0	94.6	97.8	104.0	84.8
12.2	104.8	104.2	105.0	94.8	98.0	104.0	85.1
12.3	104.8	104.2	105.0	95.0	98.1	104.1	85.5
12.4	104.9	104.2	105.0	95.2	98.2	104.1	85.8
12.5	104.9	104.2	105.0	95.4	98.3	104.1	86.1
12.6	104.9	104.2	105.0	95.5	98.5	104.1	86.5
12.7	104.9	104.2	105.0	95.7	98.6	104.1	86.8
12.8	104.9	104.3	105.0	95.9	98.7	104.2	87.1
12.9	104.9	104.3	105.0	96.1	98.8	104.2	87.4
13.0	104.9	104.3	105.0	96.2	99.0	104.2	87.7
13.1	104.9	104.3	105.0	96.4	99.1	104.2	88.0
13.2	104.9	104.3	105.0	96.6	99.2	104.2	88.3
13.2	104.9	104.4	105.0	96.7	99.3	104.3	88.6
13.3	104.9	104.4	105.0	96.9	99.4	104.3	88.9
13.4	104.9	104.4	105.0	97.1	99.5	104.3	89.2
13.5	104.9	104.4	105.0	97.2	99.6	104.3	89.5
13.6	104.9	104.4	105.0	97.4	99.7	104.3	89.8
13.7	104.9	104.4	105.0	97.5	99.8	104.3	90.0
13.8	104.9	104.4	105.0	97.6	99.9	104.4	90.3
13.9	104.9	104.5	105.0	97.8	100.0	104.4	90.6
14.0	104.9	104.5	105.1	97.9	100.1	104.4	90.8
14.1	105.0	104.5	105.1	98.0	100.2	104.4	91.1
14.2	105.0	104.5	105.1	98.2	100.3	104.4	91.3
14.3	105.0	104.5	105.1	98.3	100.4	104.4	91.5
14.4	105.0	104.5	105.1	98.4	100.5	104.4	91.8
14.5	105.0	104.5	105.1	98.5	100.5	104.4	92.0
14.6	105.0	104.5	105.1	98.6	100.6	104.5	92.2
14.7	105.0	104.6	105.1	98.7	100.7	104.5	92.4
14.8	105.0	104.6	105.1	98.9	100.8	104.5	92.7
14.9	105.0	104.6	105.1	99.0	100.9	104.5	92.9
15.0	105.0	104.6	105.1	99.1	100.9	104.5	93.1
15.0	105.0	104.6	105.1	99.2	101.0	104.5	93.3
15.1	105.0	104.6	105.1	99.3	101.1	104.5	93.5

Table C.4, (Cont'd)

15.2	105.0	104.6	105.1	99.4	101.2	104.5	93.8
15.3	105.0	104.6	105.1	99.5	101.2	104.6	94.0
15.4	105.0	104.6	105.1	99.6	101.3	104.6	94.2
15.5	105.0	104.7	105.1	99.7	101.4	104.6	94.4
15.6	105.0	104.7	105.1	99.8	101.5	104.6	94.5
15.7	105.0	104.7	105.1	99.9	101.5	104.6	94.7
15.8	105.0	104.7	105.1	100.0	101.6	104.6	94.9
15.9	105.0	104.7	105.1	100.1	101.7	104.6	95.1
16.0	105.0	104.7	105.1	100.2	101.7	104.6	95.3
16.1	105.0	104.7	105.1	100.3	101.8	104.6	95.5
16.2	105.0	104.7	105.1	100.4	101.8	104.7	95.6
16.3	105.0	104.7	105.1	100.5	101.9	104.7	95.8
16.4	105.0	104.7	105.1	100.6	102.0	104.7	96.0
16.5	105.0	104.7	105.1	100.6	102.0	104.7	96.1
16.6	105.0	104.7	105.1	100.7	102.1	104.7	96.3
16.7	105.0	104.8	105.1	100.8	102.1	104.7	96.4
16.8	105.1	104.8	105.1	100.9	102.2	104.7	96.6
16.8	105.1	104.8	105.1	100.9	102.2	104.7	96.7
16.9	105.1	104.8	105.1	101.0	102.3	104.7	96.9
17.0	105.1	104.8	105.1	101.1	102.3	104.7	97.0
17.1	105.1	104.8	105.1	101.2	102.4	104.7	97.2
17.2	105.1	104.8	105.1	101.2	102.4	104.7	97.3
17.3	105.1	104.8	105.1	101.3	102.5	104.8	97.5
17.4	105.1	104.8	105.1	101.4	102.5	104.8	97.6
17.5	105.1	104.8	105.1	101.4	102.6	104.8	97.7
17.6	105.1	104.8	105.1	101.5	102.6	104.8	97.9
17.7	105.1	104.8	105.1	101.6	102.7	104.8	98.0
17.8	105.1	104.8	105.1	101.6	102.7	104.8	98.1
17.9	105.1	104.8	105.1	101.7	102.8	104.8	98.3
18.0	105.1	104.9	105.1	101.8	102.8	104.8	98.4
18.1	105.1	104.9	105.1	101.8	102.8	104.8	98.5
18.2	105.1	104.9	105.1	101.9	102.9	104.8	98.6
18.3	105.1	104.9	105.1	101.9	102.9	104.8	98.7
18.4	105.1	104.9	105.1	102.0	103.0	104.8	98.8
18.5	105.1	104.9	105.1	102.1	103.0	104.8	99.0
18.6	105.1	104.9	105.1	102.1	103.0	104.8	99.1
18.6	105.1	104.9	105.1	102.2	103.1	104.9	99.2
18.7	105.1	104.9	105.1	102.2	103.1	104.9	99.3
18.8	105.1	104.9	105.1	102.3	103.1	104.9	99.4

Table C.4, (Cont'd)

time min	Pt' 8	Pt 9	Pt 10	Pt 11	Pt 12	Pt 13	Pt 14	Pt15
0.0	25.0	25.2	25.0	25.0	25.0	25.5	25.1	25.0
0.4	25.0	26.1	25.0	25.0	26.1	25.2	25.3	26.3
0.7	25.0	26.8	25.0	25.0	26.8	25.8	25.7	27.2
0.9	25.0	28.5	25.0	25.0	28.4	26.6	26.4	29.2
1.0	25.0	31.9	25.0	25.0	31.9	27.9	27.8	33.3
1.1	25.0	36.7	25.0	25.0	36.7	30.0	30.0	39.1
1.1	25.0	41.8	25.0	25.0	41.8	33.0	33.0	45.4
1.1	25.1	46.8	25.0	25.1	46.9	36.2	36.3	51.5
1.2	25.2	51.6	25.0	25.2	51.7	39.7	39.7	57.4
1.2	25.3	56.2	25.0	25.3	56.2	43.1	43.2	62.8
1.3	25.5	60.2	25.0	25.5	60.2	46.3	46.6	67.5
1.4	25.7	63.7	25.1	25.8	63.8	49.4	49.8	71.6
1.4	26.0	67.0	25.1	26.1	67.0	52.4	52.8	75.3
1.5	26.4	69.9	25.1	26.5	70.0	55.1	55.7	78.6
1.6	26.9	72.6	25.2	27.1	72.6	57.6	58.4	81.5
1.7	27.5	75.0	25.3	27.7	75.1	60.0	61.0	84.2
1.7	28.1	77.3	25.4	28.4	77.3	62.2	63.4	86.6
1.8	28.8	79.3	25.6	29.2	79.4	64.2	65.6	88.7
1.9	29.5	81.2	25.8	30.0	81.3	66.2	67.8	90.7
2.0	30.3	82.9	26.0	31.0	83.1	68.0	69.8	92.5
2.0	31.1	84.6	26.2	32.0	84.7	69.7	71.7	94.1
2.1	32.0	86.0	26.5	33.0	86.2	71.2	73.5	95.6
2.2	32.9	87.4	26.9	34.1	87.6	72.7	75.3	96.9
2.3	33.9	88.6	27.2	35.2	88.8	74.1	76.9	98.0
2.4	34.8	89.6	27.7	36.4	89.9	75.3	78.3	98.9
2.5	35.8	90.4	28.1	37.5	90.7	76.5	79.6	99.6
2.5	36.8	91.1	28.6	38.7	91.5	77.5	80.9	100.2
2.6	37.8	91.9	29.1	40.0	92.3	78.5	82.0	100.8
2.7	38.8	92.6	29.7	41.2	93.0	79.4	83.1	101.4
2.8	39.8	93.2	30.3	42.4	93.7	80.3	84.2	101.9
2.9	40.8	93.9	30.9	43.6	94.4	81.2	85.2	102.5
3.0	41.8	94.6	31.6	44.9	95.1	82.0	86.1	103.0
3.1	42.8	95.1	32.3	46.1	95.7	82.8	87.0	103.4
3.2	43.8	95.5	33.0	47.3	96.1	83.4	87.8	103.7
3.3	44.8	95.7	33.8	48.5	96.4	84.1	88.5	103.8
3.4	45.7	96.0	34.6	49.7	96.6	84.6	89.1	103.9
3.5	46.7	96.1	35.4	50.9	96.8	85.1	89.7	103.8
3.6	47.6	96.1	36.2	52.0	96.9	85.6	90.2	103.7

Table C.4, (Cont'd)

3.7	48.5	96.2	37.1	53.2	97.0	86.0	90.6	103.6
3.8	49.5	96.2	37.9	54.3	97.0	86.3	91.0	103.4
3.9	50.4	96.3	38.8	55.4	97.1	86.7	91.3	103.3
4.0	51.2	96.4	39.7	56.4	97.2	87.0	91.7	103.2
4.1	52.1	96.5	40.6	57.5	97.4	87.3	92.1	103.2
4.2	53.0	96.7	41.5	58.5	97.6	87.7	92.4	103.3
4.3	53.8	96.8	42.4	59.5	97.8	88.1	92.7	103.3
4.3	54.6	97.1	43.4	60.4	98.0	88.4	93.1	103.4
4.4	55.4	97.2	44.3	61.4	98.2	88.8	93.4	103.5
4.5	56.2	97.4	45.2	62.3	98.4	89.1	93.7	103.6
4.6	57.0	97.5	46.1	63.2	98.5	89.5	94.0	103.6
4.7	57.7	97.6	47.0	64.0	98.7	89.8	94.3	103.6
4.8	58.4	97.7	48.0	64.9	98.8	90.1	94.6	103.6
4.9	59.2	97.8	48.9	65.7	98.9	90.4	94.8	103.6
5.0	59.9	97.9	49.8	66.5	99.0	90.7	95.1	103.6
5.1	60.6	98.0	50.7	67.3	99.1	91.0	95.3	103.6
5.2	61.3	98.1	51.6	68.0	99.2	91.3	95.5	103.7
5.3	61.9	98.2	52.4	68.8	99.3	91.5	95.8	103.7
5.4	62.6	98.3	53.3	69.5	99.5	91.8	96.0	103.7
5.5	63.3	98.5	54.2	70.2	99.6	92.1	96.2	103.7
5.6	63.9	98.6	55.0	70.9	99.7	92.3	96.4	103.8
5.7	64.5	98.7	55.9	71.5	99.8	92.6	96.6	103.8
5.8	65.2	98.8	56.7	72.2	99.9	92.9	96.8	103.8
5.9	65.8	98.9	57.5	72.8	100.0	93.1	97.0	103.9
6.0	66.4	99.0	58.3	73.5	100.1	93.4	97.2	103.9
6.1	67.0	99.1	59.1	74.1	100.2	93.6	97.3	103.9
6.2	67.5	99.2	59.9	74.6	100.3	93.8	97.5	104.0
6.3	68.1	99.3	60.7	75.2	100.4	94.1	97.7	104.0
6.4	68.7	99.4	61.5	75.8	100.5	94.3	97.8	104.0
6.4	69.3	99.5	62.2	76.4	100.6	94.5	98.0	104.0
6.5	69.8	99.6	63.0	76.9	100.7	94.7	98.2	104.1
6.6	70.4	99.7	63.7	77.4	100.8	94.9	98.3	104.1
6.7	70.9	99.8	64.4	78.0	100.9	95.1	98.5	104.1
6.8	71.4	99.9	65.1	78.5	101.0	95.4	98.6	104.1
6.9	71.9	99.9	65.8	79.0	101.1	95.5	98.7	104.2
7.0	72.5	100.0	66.5	79.5	101.1	95.7	98.9	104.2
7.1	73.0	100.1	67.2	79.9	101.2	95.9	99.0	104.2
7.2	73.5	100.2	67.9	80.4	101.3	96.1	99.1	104.2
7.3	73.9	100.3	68.5	80.9	101.4	96.3	99.3	104.3
7.4	74.4	100.4	69.1	81.3	101.4	96.5	99.4	104.3
7.5	74.9	100.4	69.8	81.8	101.5	96.6	99.5	104.3

Table C.4, (Cont'd)

7.6	75.4	100.5	70.4	82.2	101.6	96.8	99.6	104.3
7.7	75.8	100.6	71.0	82.6	101.7	97.0	99.8	104.3
7.8	76.3	100.7	71.6	83.0	101.7	97.1	99.9	104.4
7.9	76.8	100.7	72.2	83.4	101.8	97.3	100.0	104.4
8.0	77.2	100.8	72.8	83.8	101.9	97.5	100.1	104.4
8.1	77.6	100.9	73.4	84.2	101.9	97.6	100.2	104.4
8.1	78.1	100.9	73.9	84.6	102.0	97.8	100.3	104.4
8.2	78.5	101.0	74.5	85.0	102.0	97.9	100.4	104.4
8.3	78.9	101.1	75.0	85.3	102.1	98.0	100.5	104.5
8.4	79.3	101.1	75.5	85.7	102.1	98.2	100.6	104.5
8.5	79.7	101.2	76.1	86.0	102.2	98.3	100.7	104.5
8.6	80.1	101.3	76.6	86.4	102.3	98.5	100.8	104.5
8.7	80.5	101.3	77.1	86.7	102.3	98.6	100.8	104.5
8.8	80.9	101.4	77.6	87.1	102.4	98.7	100.9	104.5
8.9	81.3	101.5	78.1	87.4	102.4	98.9	101.0	104.5
9.0	81.7	101.5	78.6	87.7	102.5	99.0	101.1	104.6
9.1	82.1	101.6	79.1	88.1	102.5	99.1	101.2	104.6
9.2	82.5	101.7	79.5	88.4	102.6	99.2	101.3	104.6
9.3	82.8	101.7	80.0	88.7	102.6	99.3	101.4	104.6
9.4	83.2	101.8	80.5	89.0	102.7	99.5	101.4	104.6
9.5	83.6	101.8	80.9	89.3	102.7	99.6	101.5	104.6
9.6	83.9	101.9	81.3	89.6	102.8	99.7	101.6	104.6
9.7	84.3	101.9	81.8	89.9	102.8	99.8	101.7	104.6
9.8	84.6	102.0	82.2	90.2	102.9	99.9	101.7	104.7
9.8	84.9	102.0	82.6	90.4	102.9	100.0	101.8	104.7
9.9	85.3	102.1	83.0	90.7	102.9	100.1	101.9	104.7
10.0	85.6	102.1	83.4	91.0	103.0	100.2	101.9	104.7
10.1	85.9	102.2	83.8	91.2	103.0	100.3	102.0	104.7
10.2	86.2	102.2	84.2	91.5	103.1	100.4	102.1	104.7
10.3	86.5	102.3	84.5	91.7	103.1	100.5	102.1	104.7
10.4	86.8	102.3	84.9	91.9	103.1	100.6	102.2	104.7
10.5	87.1	102.4	85.3	92.2	103.2	100.7	102.2	104.7
10.6	87.4	102.4	85.6	92.4	103.2	100.7	102.3	104.7
10.7	87.7	102.5	86.0	92.7	103.3	100.8	102.3	104.8
10.8	88.0	102.5	86.3	92.9	103.3	100.9	102.4	104.8
10.9	88.3	102.6	86.7	93.1	103.3	101.0	102.5	104.8
11.0	88.6	102.6	87.0	93.3	103.4	101.1	102.5	104.8
11.1	88.9	102.7	87.4	93.6	103.4	101.2	102.6	104.8
11.2	89.2	102.7	87.7	93.8	103.4	101.3	102.6	104.8
11.3	89.4	102.7	88.0	94.0	103.5	101.3	102.7	104.8
11.4	89.7	102.8	88.3	94.2	103.5	101.4	102.7	104.8

Table C.4, (Cont'd)

11.5	90.0	102.8	88.6	94.4	103.5	101.5	102.8	104.8
11.5	90.2	102.9	88.9	94.6	103.6	101.6	102.8	104.8
11.6	90.5	102.9	89.2	94.8	103.6	101.6	102.9	104.8
11.7	90.7	102.9	89.5	95.0	103.6	101.7	102.9	104.8
11.8	91.0	103.0	89.8	95.1	103.6	101.8	103.0	104.8
11.9	91.2	103.0	90.1	95.3	103.7	101.8	103.0	104.9
12.0	91.4	103.1	90.3	95.5	103.7	101.9	103.0	104.9
12.1	91.7	103.1	90.6	95.7	103.7	101.9	103.1	104.9
12.2	91.9	103.1	90.8	95.8	103.7	102.0	103.1	104.9
12.3	92.1	103.2	91.1	96.0	103.8	102.1	103.1	104.9
12.4	92.3	103.2	91.3	96.1	103.8	102.1	103.2	104.9
12.5	92.5	103.2	91.6	96.3	103.8	102.2	103.2	104.9
12.6	92.7	103.3	91.8	96.4	103.8	102.2	103.2	104.9
12.7	93.0	103.3	92.0	96.6	103.9	102.3	103.3	104.9
12.8	93.2	103.3	92.3	96.8	103.9	102.3	103.3	104.9
12.9	93.4	103.4	92.5	96.9	103.9	102.4	103.4	104.9
13.0	93.6	103.4	92.8	97.1	103.9	102.4	103.4	104.9
13.1	93.8	103.4	93.0	97.2	104.0	102.5	103.4	104.9
13.2	94.0	103.5	93.2	97.4	104.0	102.5	103.5	104.9
13.2	94.2	103.5	93.4	97.5	104.0	102.6	103.5	104.9
13.3	94.4	103.5	93.6	97.6	104.0	102.6	103.5	104.9
13.4	94.6	103.5	93.9	97.8	104.0	102.7	103.6	104.9
13.5	94.7	103.6	94.1	97.9	104.1	102.7	103.6	104.9
13.6	94.9	103.6	94.3	98.0	104.1	102.8	103.6	105.0
13.7	95.1	103.6	94.5	98.2	104.1	102.8	103.6	105.0
13.8	95.3	103.7	94.6	98.3	104.1	102.9	103.7	105.0
13.9	95.5	103.7	94.8	98.4	104.1	102.9	103.7	105.0
14.0	95.6	103.7	95.0	98.5	104.2	103.0	103.7	105.0
14.1	95.8	103.7	95.2	98.6	104.2	103.0	103.8	105.0
14.2	95.9	103.8	95.4	98.8	104.2	103.0	103.8	105.0
14.3	96.1	103.8	95.5	98.9	104.2	103.1	103.8	105.0
14.4	96.3	103.8	95.7	99.0	104.2	103.1	103.8	105.0
14.5	96.4	103.8	95.9	99.1	104.2	103.1	103.8	105.0
14.6	96.6	103.8	96.0	99.2	104.3	103.2	103.9	105.0
14.7	96.7	103.9	96.2	99.3	104.3	103.2	103.9	105.0
14.8	96.8	103.9	96.3	99.4	104.3	103.2	103.9	105.0
14.9	97.0	103.9	96.5	99.5	104.3	103.3	103.9	105.0
15.0	97.1	103.9	96.6	99.6	104.3	103.3	104.0	105.0
15.0	97.3	104.0	96.8	99.7	104.3	103.3	104.0	105.0
15.1	97.4	104.0	97.0	99.8	104.4	103.4	104.0	105.0
15.2	97.6	104.0	97.1	99.9	104.4	103.4	104.0	105.0

Table C.4, (Cont'd)

15.3	97.7	104.0	97.3	100.0	104.4	103.4	104.0	105.0
15.4	97.8	104.0	97.4	100.1	104.4	103.5	104.1	105.0
15.5	98.0	104.1	97.5	100.2	104.4	103.5	104.1	105.0
15.6	98.1	104.1	97.7	100.3	104.4	103.5	104.1	105.0
15.7	98.2	104.1	97.8	100.3	104.4	103.6	104.1	105.0
15.8	98.3	104.1	97.9	100.4	104.5	103.6	104.1	105.0
15.9	98.5	104.1	98.1	100.5	104.5	103.6	104.2	105.0
16.0	98.6	104.2	98.2	100.6	104.5	103.7	104.2	105.0
16.1	98.7	104.2	98.3	100.7	104.5	103.7	104.2	105.0
16.2	98.8	104.2	98.4	100.8	104.5	103.7	104.2	105.0
16.3	98.9	104.2	98.5	100.8	104.5	103.7	104.2	105.0
16.4	99.0	104.2	98.7	100.9	104.5	103.8	104.3	105.1
16.5	99.1	104.2	98.8	101.0	104.5	103.8	104.3	105.1
16.6	99.2	104.3	98.9	101.0	104.5	103.8	104.3	105.1
16.7	99.3	104.3	99.0	101.1	104.6	103.8	104.3	105.1
16.8	99.4	104.3	99.1	101.2	104.6	103.8	104.3	105.1
16.8	99.5	104.3	99.2	101.2	104.6	103.9	104.3	105.1
16.9	99.6	104.3	99.3	101.3	104.6	103.9	104.3	105.1
17.0	99.7	104.3	99.4	101.4	104.6	103.9	104.4	105.1
17.1	99.8	104.4	99.5	101.5	104.6	103.9	104.4	105.1
17.2	99.9	104.4	99.6	101.5	104.6	104.0	104.4	105.1
17.3	100.0	104.4	99.7	101.6	104.6	104.0	104.4	105.1
17.4	100.1	104.4	99.8	101.7	104.6	104.0	104.4	105.1
17.5	100.2	104.4	99.9	101.7	104.7	104.0	104.4	105.1
17.6	100.3	104.4	100.0	101.8	104.7	104.1	104.4	105.1
17.7	100.4	104.4	100.1	101.8	104.7	104.1	104.5	105.1
17.8	100.5	104.5	100.2	101.9	104.7	104.1	104.5	105.1
17.9	100.6	104.5	100.3	102.0	104.7	104.1	104.5	105.1
18.0	100.6	104.5	100.4	102.0	104.7	104.1	104.5	105.1
18.1	100.7	104.5	100.4	102.1	104.7	104.1	104.5	105.1
18.2	100.8	104.5	100.5	102.1	104.7	104.2	104.5	105.1
18.3	100.9	104.5	100.6	102.2	104.7	104.2	104.5	105.1
18.4	100.9	104.5	100.7	102.2	104.7	104.2	104.5	105.1
18.5	101.0	104.5	100.8	102.3	104.7	104.2	104.6	105.1
18.6	101.1	104.6	100.8	102.3	104.7	104.2	104.6	105.1
18.6	101.2	104.6	100.9	102.4	104.8	104.3	104.6	105.1
18.7	101.2	104.6	101.0	102.4	104.8	104.3	104.6	105.1
18.8	101.3	104.6	101.1	102.5	104.8	104.3	104.6	105.1

Appendix C.3 MATLAB syntaxes

C.3.1 Script file for reference temperature determination

```
%for cherry pomace retorting
% Retorting at 126.7 and 105 C for three MC( 70 41 and 25 %)
%% cleaning work space
clc
clear
close all
format compact
format shortG
%% PLOT OF Tr VS Correlation for E and kr ( estimated parameter)
% TrV = 110:2:130; % for starting evaluation
TrV = 110:1:120; % for getting the exact Tr
for i = 1:length(TrV);
    Tr = TrV(i);
    corr(i) = Call_calcC2Tr(Tr); % script File of kr and E estimation convert to Function
file, which will
% call the function file for all 15 points in the can for each MC
% for ACY degradation data after Diff retorting times at Two RT temp
end
%% Plot to read the exact Tr
Figure
hold on
set(gca, 'fontsize',18,'fontweight','bold');
h = plot(TrV,corr,'-k', 'linewidth',2.5);
xlabel('Reference Temperature \it{T_r} , \rm\bf(^oC)','FontSize',16,'fontweight','bold');
ylabel('Correlation Coefficient of \it{k_r} and \it{E}','FontSize',16,'fontweight','bold');
plot([min(TrV),max(TrV)],[0,0], 'R','linewidth',2)
grid on
```

C.3.2 Function file-1 and 2

```
% ( was Script file for E kr and Co estimation)
function corrkE=Call_calcC2Tr(Tr);
format compact
format shortG
%% Read in ACY concentration data
ACY =xlsread('ACY_con1.xls'); % 1st column time(min); each column onwards would
represent ACY conc in (mg/L,db)...
%(example: for 3 Moisture contents there would be three column..each column
representing a specific MC ( MC-70 , MC-41, MC-25)
% ht=ACY(:,1); %Retoorting time in in Mint
```

```

ACY1=[ACY(:,2);ACY(:,5)] ; % ACY concentration (mg/L,db) for MC-70
ACY1=ACY1(isfinite(ACY1)); % Command to take out all ANN ( no data) in the vector)
and combine it
% ACY2=[ACY(:,3);ACY(:,6)]; % ACY concentration (mg/L,db) for MC-41
% ACY3=[ACY(:,4);ACY(:,4)] % ACY concentration (mg/L,db) for MC-25
% ht=1;
%% Initial parameter guesses
E=50000; % initial guess activation energy %Ea must be in j/mol
kr=0.05; % initial guess kinetic degradation constant %kr must be in min^-1
Co= 60; % initial guess of ACY initial concentration
beta0(1)=E; %initial guess
kfactor=exp((-beta0(1)/8.314)*(1/(Tr+273.15)-1/(122.5+273.15)));
beta0(2)=kr*kfactor; %initial guess
beta0(3)=Co; %initial guess
% beta0(4)=m; %initial guess
beta=beta0; %set beta=to the initial guesses
%% Read in prediction 15 points data by Comsol foe each time and each MC two temp
126.7
global Prd_points3 Prd_points4 % for script and function file ,
Prd_points3 = xlsread('points70MC2.xls','90min');% all predicted temperature data with
time at 15 gauss points in the can
time=[0,181,271,391,571,631,781]; % steps heating times by Retort in Excel sheet (0 25
40 60 90 100 125 min) all + 5min come up time
% for j = 1:length(ht);
%% Read in prediction 15 points data by Comsol foe each time and each MC temp 105
Prd_points4 = xlsread('points70MC1.xls','90min');% all predicted data with time
time=[0,181,271,391,571,631,781]; % steps heating times by Retort in Excel sheet (0 25
40 60 90 100 125 min) all + 5min come up time
%% nlinfit returns parameters, residuals, Jacobean (sensitivity %coefficient matrix),
%covariance matrix, and mean square error.
timec=[0 0 0 25 25 25 40 40 40 60 60 60 90 90 90 0 0 0 100 100 100 125 125 125];
x1 =1:length(timec);
timec=timec';
x1=x1';
x1(1,2)=Tr;
ACY1=ACY1;
[beta,resids,J,COVB,mse] = nlinfit(x1,ACY1,'calcC2Tr',beta0); % calling second
function file with Trapz and gauss integration
beta;
rmse=sqrt(mse);
%% confidence intervals for parameters
ci=nlparci(beta, resids,J);
%% R is the correlation matrix for the parameters, sigma is the standard error vector

```

```

[R,sigma]=corr cov(COVB);
sigma;
R;
relstderr=sigma./beta'; %relative standard error for each parameter
corrkE=R(2,1); % correlation matrix for E and kr
end
%%Function file-2
%integration ACY over the 15 points in the can
function C70= calcC2Tr(beta,x)
global Prd_points3 Prd_points4
ht=[181,271,391,571,631,781]; % heating times by Retort
Rg = 8.314 ; % gas constant
Tr = x(1,2)+273.15; % reference temperature Tr
count=1;
psiall=zeros(1,15);
for m=1:2; % retort Temp loop data 15 points 2 files ( two Tretort)
    for j = 1:length(ht); % heating times , [25 40 60 90 100 125]
        if j==1
            psiall(count,:)=0;
            count=count+1;
        end
        %Trapezoid method
        for i=1:15; % loop for the Temp data for 15 points in the can
            if m==1
                intgrnd1 = exp(-(beta(1)/Rg)*( 1./(Prd_points3(1:ht(j),i+1)+273.15) - 1/Tr));
                % previous line for integration the
                % Eq.. Psi=exp(-E/R*((1/(T(r,z,t)))-(1/Tr))
                timex = Prd_points3(1:ht(j),1)./60;
                psia(i)=trapz(timex,intgrnd1);% Trapz Integration of Psi @ 127 C
            elseif m==2
                intgrnd2 = exp(-(beta(1)/Rg)*( 1./(Prd_points4(1:ht(j),i+1)+273.15) - 1/Tr));
                timex = Prd_points4(1:ht(j),1)./60;
                psia(i)=trapz(timex,intgrnd2);% Trapz Integration of Psi@105 C
            end
        end
        psiall(count,:)=psia;
        count=count+1;
    end
end
end
% psiall=psiall';
% psiall(2:5,:)=psiall(1:4,:);
% psiall(1,:)=0;

```

```

% Gauss method
wr=[5/9 8/9 5/9]; %Gauss nodes weight values 3 points
wz=[0.2369268850 0.4786286705 0.5688888889 0.4786286705 0.2369268850]; %z
direction
r=[0.11270167,0.5,0.8872983]; %points nodes values for 0 to 1 dimintion r direction
for k=1:14; % values of ACY at zero and Retorting times ( 0 25 40 60 90 100 125)
    ct=1;
    Csum=0;
    for j=1:5; % weight values at 5 points (z direction)
        for i=1:3; % radius values 3 points ( r direction)
            Csum=Csum+wr(i)*wz(j)*exp(-beta(2)*psiall(k,ct))*r(i);
            % for Eq.. ACY(C)=exp(-kr*(exp(-E/R*((1/(T(r,z,t)))-(1/Tr))))*rdr
            ct=ct+1;
        end
    end
    C(k)=beta(3)*Csum/2;
    % for Eq.. ACY(t)=Acy(0)*exp(-kr*(exp(-E/R*((1/(T(r,z,t)))-(1/Tr))))*rdr
    C70(3*(k-1)+1:3*(k-1)+3)=C(k);
end
C70=C70'; %values of predicted ACY values at all times two cans ( all data +ANN)
C70=[C70(1:15);C70(22:24);C70(37:42)]; % to take only rows with data and combine
them in vector 24by1, from 42by1 which have ann data
end

```

C.3.3 Script file scaled sensitivity coefficients

```

%for the two retorting temperature % For invers problem estimation
% Retorting Process at 126.7 C and 105 C
%% Clean Up and organizing cell
clc
clear
close all
format compact
format shortG
%% Read in prediction 9 points data by Comsol foe each time and each MC temp 105
Prd_points3 = xlsread('points70MC2.xls','90min');% all predicted data with time
time=[0,181,271,391,571,631];
% for j = 1:length(ht);
% timet = Prd_points(1:time(j),1)./60;
% end
%% Read in prediction 9 points data by Comsol foe each time and each MC temp 127
Prd_points4 = xlsread('points70MC1.xls','90min');% all predicted data with time

```

```

time=[0,181,271,391,571,631];
% for j = 1:length(ht);
% timet = Prd_points(1:time(j),1)./60;
% end
%% Scale Sensitivity Coefficient
beta=[45000; 0.019; 60];
x1 =1:36;
timec=[0 0 0 25 25 25 40 40 40 60 60 60 90 90 90 100 100 100 0 0 0 25 25 25 40 40 40
60 60 60 90 90 90 100 100 100];
timec=timec';
x1=x1';
ypred=calcC2T(beta,x1)
beta1 = beta;
% Sensitivity Coefficient
d=0.001;
for i=1:length(beta)
    if i ==1
        betain = [beta1(1)+beta1(1)*d beta1(2) beta1(3)];
    elseif i==2
        betain = [beta1(1) beta1(2)+beta1(2)*d beta1(3)];
    elseif i==3
        betain = [beta1(1) beta1(2) beta1(3)+beta1(3)*d];
    end
    yhat{i} = calcC2T(betain,x1);
    ysens{i} = (yhat{i}-ypred)/d;
end
%% sensitivity coefficient plot
set(Figure,'Units','inches','Position',[7.1 0.3 6 4],'DefaultAxesFontName','Arial', ...
'DefaultAxesFontSize',12,'DefaultAxesFontWeight','Normal');
hold on
set(gca, 'YGrid', 'on', 'XGrid','off');
ysens1 = ysens{1};
ysens2 = ysens{2};
ysens3 = ysens{3};
%g1(1) = plot(x_graph,ysens{1},'-','LineWidth',2);
%g1(2) = plot(x_graph,ysens{2},':','LineWidth',2);
plot(timec(1:18),ysens1(1:18),'bo','lineWidth',3,'MarkerEdgeColor','b','MarkerFaceColor'
,'b','MarkerSize',6);
plot(timec(1:18),ysens2(1:18),'ro','lineWidth',3,'MarkerEdgeColor','b','MarkerFaceColor',
'y','MarkerSize',6);
plot(timec(1:18),ysens3(1:18),'go','lineWidth',2,'MarkerEdgeColor','b','MarkerFaceColor'
,'y','MarkerSize',6);

```

```

plot(timec(19:36),ysens1(19:36),':bo','lineWidth',2,'MarkerEdgeColor','b','MarkerFaceColor','y','MarkerSize',6);
plot(timec(19:36),ysens2(19:36),':k^','lineWidth',2,'MarkerEdgeColor','r','MarkerFaceColor','y','MarkerSize',6);
plot(timec(19:36),ysens3(19:36),':g^','lineWidth',3,'MarkerEdgeColor','r','MarkerFaceColor','y','MarkerSize',6);
box on
YLine = [0 0];
XLine = [0 timec(length(timec))];%max()
plot (XLine, YLine,'R');
legend('Ea -127 ^oC','kr-127 ^oC','Co-127 ^oC','Ea-105 ^oC','kr105 ^oC','Co105 ^oC','location','best');
xlabel('time(min)','FontSize',14,'fontweight','Normal');
ylabel('Scaled Sensitivity Coefficeints','FontSize',14,'fontweight','Normal');

```

C.3.4 Script file for nlinfit method

% for kr, E , and Co of Cherry pomace

% Retorting Process at 126.7 C and 105 C

%% Clean Up and organizing cell

clc

clear

close all

format compact

format shortG

%% Read in ACY concentration data

ACY =xlsread('ACY_con1.xls'); % 1st column time(min); each column onwards would represent ACY conc in (mg/L,db)...

%(example: for 3 Moisture contents there would be three column..each column representing a specific MC (MC-70 , MC-41, MC-25)

ACY1=[ACY(:,2);ACY(:,5)]; % ACY concentration (mg/L,db) for MC-70 at 127 C and 105 , respectively

ACY1=ACY1(isfinite(ACY1)); % organizing all data one collomn 24 rows

% ACY2=[ACY(:,3);ACY(:,6)]; % ACY concentration (mg/L,db) for MC-41

% ACY3=[ACY(:,4);ACY(:,4)] % ACY concentration (mg/L,db) for MC-25

% ht=1;

%% Initial parameter guesses

E=50000; % initial guess activation energy %Ea must be in j/mol

kr=0.05; % initial guess kintek degradation constant %kr must be in min⁻¹

Co= 60; % initial guess of ACY initial concentration

beta0(1)=E; %initial guess

beta0(2)=kr; %initial guess

beta0(3)=Co; %initial guess

beta=beta0; %set beta=to the initial guesses

```

%% Read in prediction 15 points data by Comsol for each time and each MC temp
126.7 C
global Prd_points3 Prd_points4 % to connect data from script file with function file
Prd_points3 = xlsread('points70MC2.xls','90min');% all predicted data with time
%% Read in prediction 15 points data by Comsol for each time and each MC temp 105
C
Prd_points4 = xlsread('points70MC1.xls','90min');% all predicted data with time
time=[0,181,271,391,571,631,781];
%% nlinfit returns parameters, residuals, Jacobean (sensitivity %coefficient matrix),
timec=[0 0 0 25 25 25 40 40 40 60 60 60 90 90 90 0 0 0 100 100 100 125 125 125]; %
heating time at the two temp
x1 =1:length(timec);
timec=timec';
x1=x1';
[beta,resids,J,COVB,mse] = nlinfit(x1,ACY1,'calcC2T',beta0);
beta % results of estimation
rmse=sqrt(mse)
%% confidence intervals for parameters
ci=nlparci(beta, resids,J)
%% R is the correlation matrix for the parameters, sigma is the standard error vector
[R,sigma]=corrcoef(COVB);
sigma
R
relstderr=sigma./beta' %relative standard error for each parameter
%% Confidence and prediction intervals for the dependent variable
% nonlinear regression confidence intervals-- 'on' means simultaneous
% bounds; 'off' is for non-simultaneous bounds; must use 'curve' for
% regression line, 'observation' for prediction interval
[ypred, delta] = nlpredci('calcC2T',x1,beta,resids,J,0.05,'on','curve'); %confidence band
for regression line
[ypred, deltaob] = nlpredci('calcC2T',x1,beta,resids,J,0.05,'on','observation');%prediction
band for individual points
% ypred
%simultaneous confidence bands for regression line
CBu=ypred+delta;
CBl=ypred-delta;
% simultaneous prediction bands for regression line
PBu=ypred+deltaob;
PBl=ypred-deltaob;
%% Plot Pred vs Obs of ACY
set(Figure,'Units','inches','Position',[0.1 0.4 6 4],'DefaultAxesFontName','Arial', ...
'DefaultAxesFontSize',12,'DefaultAxesFontWeight','Normal');
hold on

```

```

h1(1)=plot(timec(1:15),ypred(1:15),'-b','Markerfacecolor','b'); %predicted y values
h1(2)=plot(timec(1:15),ACY1(1:15),'square','Markerfacecolor','r');
set(gca,'YGrid','on','XGrid','off');
box on;
xlabel('time (min)','FontSize',14,'fontweight','Normal');
ylabel('ACYpred-ACYobs','FontSize',14,'fontweight','Normal');
title('ACYoobs vs ACYprd @127C')
legend('pred','obs','location','best');
hold on
%% Output --CIs and PIs
%plot Cobs, Cpred line, confidence band for regression line
hold on
h1(3) = plot(timec(1:15),CBu(1:15),'--g','LineWidth',2);
plot(timec(1:15),CBI(1:15),'--g','LineWidth',2);
hold on
%plot prediction band for regression line
h1(4) = plot(timec(1:15),PBu(1:15),'-.r','LineWidth',2);
plot(timec(1:15),PBI(1:15),'-.r','LineWidth',2);
legend('ACYpred','ACYobs','CB','PB','location','best')

%% residual scatter plot
set(Figure,'Units','inches','Position',[0.5 0.6 6 4],'DefaultAxesFontName','Arial', ...
'DefaultAxesFontSize',12,'DefaultAxesFontWeight','Normal');
hold on
plot(timec(1:24), resid(1:24), 'square','Markerfacecolor','b');
YLine = [0 0];
XLine = [0 max(timec)];
plot(XLine, YLine,'k'); %plot a straight red line at zero
set(gca,'YGrid','on','XGrid','off');
box on;
ylabel('Observed ACY - Predicted ACY','fontsize',14,'fontweight','Normal');
xlabel('time (min)','fontsize',14,'fontweight','Normal');
%% residuals histogram--same as dfittool, but no curve fit here
[n1, timecout] = hist(resid(1:24),10); %10 is the number of bins
set(Figure,'Units','inches','Position',[0.5 0.6 6 4],'DefaultAxesFontName','Arial', ...
'DefaultAxesFontSize',12,'DefaultAxesFontWeight','Normal');
hold on
set(gca,'YGrid','on','XGrid','off');
box on;
bar(timecout, n1) % plots the histogram
xlabel('Y_{observed} - Y_{predicted}','fontsize',14,'fontweight','Normal');
ylabel('Frequency','fontsize',14,'fontweight','Normal');

```

%% Function file for estimating SSC and for inlinfit to estimate E kr and Co for ACY degradation

```

function C70= calcC2T(beta,x)
global Prd_points3 Prd_points4
ht=[181,271,391,571,631,781];
% j=1:length(ht);
R = 8.314 ; % gas constant
Tr = 114.9+273.15 ; % temp reference ,Tr
count=1;
psiall=zeros(1,15);
for m=1:2;% retort Temp data 15 pints 2 files
    for j = 1:length(ht); % heating times , [25 40 60 90 100 125]
        if j==1
            psiall(count,:)=0;
            count=count+1;
        end
        % TRAPZ method
        for i=1:15; % Temp data for 15 points in the can
            if m==1
                intgrnd1 = exp(-(beta(1)/R)*( 1./(Prd_points3(1:ht(j),i+1)+273.15) - 1/Tr));
                timex = Prd_points3(1:ht(j),1)./60;
                psia(i)=trapz(timex,intgrnd1);% Trapz Integration of Psi @ 127 C

            elseif m==2
                intgrnd2 = exp(-(beta(1)/R)*( 1./(Prd_points4(1:ht(j),i+1)+273.15) - 1/Tr));
                timex = Prd_points4(1:ht(j),1)./60;
                psia(i)=trapz(timex,intgrnd2);% Trapz Integration of Psi@ 105 C
            end
        end
        psiall(count,:)=psia;
        count=count+1;
    end
end
% psia
end
end
% xlswrite('Ssiall_ACy70.xls', psia);
% psiall=psiall;
% psiall(2:5,:)=psiall(1:4,:);
% psiall(1,:)=0;
% Gauss method
wr=[5/9 8/9 5/9]; %Gauss nodes weight values 3 points
wz=[0.2369268850 0.4786286705 0.5688888889 0.4786286705 0.2369268850]; %z
direction
r=[0.11270167,0.5,0.8872983]; %points nodes values for 0 to 1 dimintion r direction

```

```

for k=1:14; %#ok<*ALIGN> % heating time ( 0 25 40 60 90 100 125 )
    ct=1;
    Csum=0;
    for j=1:5; % weight values at 15 points (z direction)
        for i=1:3; % radius values ( r direction
            Csum=Csum+wr(i)*wz(j)*exp(-beta(2)*psiall(k,ct))*r(i);
            ct=ct+1;
        end
    end
    C(k)=beta(3)*Csum/2;
    C70(3*(k-1)+1:3*(k-1)+3)=C(k); % makes triplicate
end
C70=C70'; %values of predicted ACY values at all times two cans ( all data +ANN)
% xlswrite('ACy70prd.xls', C70);
C70=[C70(1:15);C70(22:24);C70(37:42)]; % to take only rows with data and combine
them in vector 24by1, from 42by1 which have ann datae
end

```

C.3.5 Script file for sequential parameter estimation method

```

%, kr, E , and Co of Cherry pomace 70- MC
%% Sequential Parameter Estimation for kr, E , Co and b of Cherry pomace 70% MC
% Retorting Process at 126.7 C and 105 C
%% Clean up and organizing
clc
clear
close all
format compact
format shortG
%% Read in ACY concentration data
ACY =xlsread('ACY_con1.xls'); % 1st column time(min); each column onwards would
represent ACY conc in (mg/kg,db)...
%(example: for 3 Moisture contents there would be three column..each column
%representing a specific MC ( MC-70 , MC-41, MC-25)...
% Columns 2 3 and 4 for ( Acy at 127C), and columns 5 6 and 7 for Acy ( at 105 C)
% Calling each pomace's ACY concentration at specific Moisture contents.
ACY1=[ACY(:,2);ACY(:,5)] ; % ACY concentration (mg/L,db) for MC-70
ACY1=ACY1(isfinite(ACY1)); % to clear all empty cells
% ACY2=[ACY(:,3);ACY(:,6)]; % ACY concentration (mg/L,db) for MC-41
% ACY1=ACY1(isfinite(ACY1));
% ACY3=[ACY(:,4);ACY(:,4)] % ACY concentration (mg/L,db) for MC-25
% ACY1=ACY1(isfinite(ACY1));
n=length(ACY1);
siz = size(ACY1,1);

```

```

%% Initial parameter guesses
E/R=40000/8.314; % initial guess activation energy %Ea must be in J/mol
kr=0.05; % initial guess kintek degradation constant %kr must be in min^-1
Co= 60; % initial guess of ACY initial concentration (mg/kg)
% m=0.5; % initial guess of MC parameter
beta0(1)=E; %initial guess
beta0(2)=kr; %initial guess
beta0(3)=Co; %initial guess
beta=beta0; %set beta=to the initial guesses
beta=beta';
beta0=beta0';
%% Read in prediction 15 points data by Comsol for each time and each MC temp
126.7 C
global Prd_points3 Prd_points4 seqsort
Prd_points3 = xlsread('points70MC2.xls','90min');% all predicted Gauss temperature
data with time
%% Read in prediction 15 points data by Comsol foe each time and each MC temp 105
Prd_points4 = xlsread('points70MC1.xls','90min');
% time=[0,181,271,391,571,631,781]; % steps at Excel file for each time
%% Heating time at Retort
timec=[0 0 0 25 25 25 40 40 40 60 60 60 90 90 90 0 0 0 100 100 100 125 125 125];
x=1:length(timec);
timec=timec';
x=x';
%% Estimating the ACy predicted Concentration
% For estimation the ACY predicted based of the 15 Temperature Gauss points
ypred =calcC2T(beta0, x);
% for Indicating the Retort temperature of the Figures
ypredRT=[ypred 127*ones(length(ypred),1)];
ypredRT(16:24,2)=105;
% for arranging the ACY pred from high to low
[tT,seqsort]=sortrows(ypredRT,-1);
Ynn=ACY1(seqsort);%ACY cons sorted
p=length(beta);% all initial gess parameters
yvals=Ynn;
Y = yvals;
sX = [length(yvals) length(beta)]; % changed from 1*2 to 2*1
sig = 8*ones(sX(1),1);% making vector 1colomn by 24 raws( 1*0.1)
Ratio1 = 1;Ratio2 = 1; Ratio3= 1;
plots=0;
b_old =beta ;
tol=1e-4; % For Iteration limit for repeating of calculation
set(Figure,'Units','inches','Position',[7.1 0.3 6 4],'DefaultAxesFontName','Arial', ...

```

```

'DefaultAxesFontSize',12,'DefaultAxesFontWeight','Normal');
hold on
% while Ratio1 > tol || Ratio2 > tol
Ratioall=1;
while Ratioall > tol
%   P = 10000^2*eye(sX(2));
P=[10^6.5 0 0;0 10 0;0 0 60^2];% matrix 3*3.. (Diagnol is 10^6 10 3600)'
beta0 = b_old;
beta = beta0;
ypred =calcC2Ts(beta0, x);% Calling predicted ACY consc, by Comsol prediction
using Gauss 15 points in the can
e = yvals-ypred;
d=0.001; %
for i = 1:p
betain = beta;
betain(i) = beta(i)+beta(i)*d;
yhat(Reyes and Cisneros-Zevallos) = calcC2Ts(betain, x);
X(Yang et al.) = (yhat(Yang et al.)-ypred)/(beta(i)*d);
end
X1=X{:,1};
for i=2:p
X1=[X1 X{:,i}]; % changed from 1*2 to 2*1
end
for k = 1:sX(1)
if k == 1
beta = beta0;
end
clear A delta
A(:,k) = P*X1(k,:);
delta(k) = sig(k)^2+X1(k,:)*A(:,k);
K(:,k) = A(:,k)/delta(k);
beta = beta + K(:,k)*(e(k)-X1(k,:)*(beta-beta0));
P = P - K(:,k)*A(:,k)';
BBbP{k} = [beta P];
end
% Iteration plots for all three parameters
h2(1)=plot(plots,b_old(1)/1e2,':ks','lineWidth',3,'MarkerEdgeColor','k','MarkerFaceColor','k','MarkerSize',3);
h2(2)=plot(plots,b_old(2),'-
.bo','lineWidth',3,'MarkerEdgeColor','b','MarkerFaceColor','b','MarkerSize',3);
h2(3)=plot(plots,b_old(3),'-
m^','lineWidth',3,'MarkerEdgeColor','m','MarkerFaceColor','m','MarkerSize',3);
% plot(plots,b_old(4),'s','MarkerEdgeColor','k','MarkerFaceColor','k','MarkerSize',5);

```

```

xlabel('Iteration','FontSize',14,'fontweight','Normal');
ylabel('Sequentially Estimated Parameters','FontSize',14,'fontweight','Normal');
b_new = BBbP{end};
plots = plots+1;
% Ratioall = abs((b_new(:,1)-b_old)./b_old);
Ratioall = max(abs((b_new(:,1)-b_old)./b_old));
% Ratio1 = Ratioall(1);
% Ratio2 = Ratioall(2);
b_old = b_new(:,1);
end
set(gca, 'YGrid', 'on', 'XGrid', 'off');
legend(h2,'par1=Ea*10^{3}','par2= kr','par3=Co','Location','Best');
corrcoef = P(2,1)/(sqrt(P(1,1))*sqrt(P(2,2)));
% [R,sigma]=corrcoef(P);
% relerr=stderr./b_old
n=length(yvals);K=length(beta)+1;
SS=e*e;
p=length(beta);
mse=SS/(n-p);rmse=sqrt(mse)
AICc= n*log(SS/n)+2*K+2*K*(K-1)/(n-K-1);
% Data estimated for each parameter
Result = BBbP{end};
hold off
for i = 1:length(BBbP)
    BB = BBbP{i};
    SeqBeta(:,i) = BB(:,1);
end
% Plotting the Sequential Estimation for Each parameter
%% 1. Plot for Activation Energy (Ea) ( J/mol)
step=1:n;
set(Figure,'Units','inches','Position',[0.1 0.4 6 4],'DefaultAxesFontName','Arial', ...
'DefaultAxesFontSize',12,'DefaultAxesFontWeight','Normal');
hold on
for i=1:24;
    if tT(i,2)==127;
        h3(1)=plot(i,SeqBeta(1,i)*8.314,'-
rs','LineWidth',1.5,'MarkerEdgeColor','k','MarkerFaceColor','g','MarkerSize',8);
        elseif tT(i,2)==105;
            h3(2)=plot(i,SeqBeta(1,i)*8.314,'-
ro','lineWidth',1.5,'MarkerEdgeColor','k','MarkerFaceColor','w','MarkerSize',8);
        end
    end
end
h3(3)=plot(step,SeqBeta(1,:)*8.134,'-k','lineWidth',2);

```

```

set(gca, 'YGrid', 'on', 'XGrid', 'off');
legend(h3, '126.7 \circC', '105 \circC', 'Ea (J/mol)', 'location', 'northWest');
box on
ylabel('Sequentially Estimated E ( J/mol)', 'FontSize', 14, 'fontweight', 'Normal');
xlabel('step Index', 'FontSize', 14, 'fontweight', 'Normal');
%% 2. Plot for Reaction rate (kr) ( min^-1)
set(Figure, 'Units', 'inches', 'Position', [7.3 3.3 6 4], 'DefaultAxesFontName', 'Arial', ...
'DefaultAxesFontSize', 12, 'DefaultAxesFontWeight', 'Normal');
hold on
for i=1:24;
    if tT(i,2)==127;
        h3(1)=plot(i, SeqBeta(2,i), '-
.ks', 'lineWidth', 1.5, 'MarkerEdgeColor', 'k', 'MarkerFaceColor', 'g', 'MarkerSize', 8);
        elseif tT(i,2)==105;
            h3(2)=plot(i, SeqBeta(2,i), '-
.ro', 'lineWidth', 1.5, 'MarkerEdgeColor', 'k', 'MarkerFaceColor', 'w', 'MarkerSize', 8);
        end
    end
h3(3)=plot(step, SeqBeta(2,:), '-k', 'lineWidth', 2);
set(gca, 'YGrid', 'on', 'XGrid', 'off');
legend(h3, '126.7 \circC', '105 \circC', 'kr (min^{-1})', 'location', 'northeast');
box on
xlabel('step Index', 'FontSize', 12, 'fontweight', 'Normal');
ylabel('Sequentially Estimated kr(min^{-1})', 'FontSize', 12, 'fontweight', 'Normal');

%% 3. Plot for Reaction rate (Co) ( mg/kg)
set(Figure, 'Units', 'inches', 'Position', [0.1 3.2 6 4], 'DefaultAxesFontName', 'Arial', ...
'DefaultAxesFontSize', 12, 'DefaultAxesFontWeight', 'Normal');
hold on
for i=1:24;
    if tT(i,2)==127;
        h3(1)=plot(i, SeqBeta(3,i), 'ks', 'lineWidth', 1.5, 'MarkerEdgeColor', 'k', 'MarkerFaceColor', 'g', '
MarkerSize', 10);
        elseif tT(i,2)==105;
            h3(2)=plot(i, SeqBeta(3,i), 'ro', 'lineWidth', 1.5, 'MarkerEdgeColor', 'k', 'MarkerFaceColor', 'w', '
MarkerSize', 10);
        end
    end
h3(3)=plot(step, SeqBeta(3,:), '-k', 'lineWidth', 2);
set(gca, 'YGrid', 'on', 'XGrid', 'off');
legend(h3, '126.7 \circC', '105 \circC', 'C_{\text{ito}}(mg/kg)', 'location', 'best');
box on
xlabel('step Index', 'fontname', 'Arial', 'FontSize', 14, 'fontweight', 'Normal');

```

```
ylabel('Sequentially Estimated  
C_{\text{ito}}(mg/kg)', 'fontname', 'Arial', 'FontSize', 14, 'fontweight', 'Normal');
```

```
%% Function 1 for seq script file to estimate ACY predicted data (Seq Sorted data)
```

```
%% Function 1 for estimating ACY predicted data (Seq Sorted data)
```

```
% Trapezoidal and Gauss Integration for the can
```

```
function C70= calcC2Ts(beta,x)
```

```
%for sequential
```

```
global Prd_points3 Prd_points4 seqsort
```

```
ht=[181,271,391,571,631,781];
```

```
R = 8.314 ; % gas constant
```

```
Tr = 114.9+273.15 ; % temp reference ,Tr
```

```
count=1;
```

```
psiall=zeros(1,15);
```

```
for m=1:2;% retort Temp data 15 pints 2 files
```

```
for j = 1:length(ht); % heating times , [25 40 60 90 100 125]
```

```
if j==1
```

```
psiall(count,:)=0;
```

```
count=count+1;
```

```
end
```

```
for i=1:15; % Temp data for 15 points in the can
```

```
if m==1
```

```
intgrnd1 = exp(-(beta(1))*( 1./(Prd_points3(1:ht(j),i+1)+273.15) - 1/Tr));
```

```
timex = Prd_points3(1:ht(j),1)./60;
```

```
psia(i)=trapz(timex,intgrnd1);% Trapz Integration of Psi @ 127 C
```

```
elseif m==2
```

```
intgrnd2 = exp(-(beta(1))*( 1./(Prd_points4(1:ht(j),i+1)+273.15) - 1/Tr));
```

```
timex = Prd_points4(1:ht(j),1)./60;
```

```
psia(i)=trapz(timex,intgrnd2);% Trapz Integration of Psi@ 105 C
```

```
end
```

```
en
```

```
psiall(count,:)=psia;
```

```
count=count+1;
```

```
end
```

```
end
```

```
% Gauss method
```

```
wr=[5/9 8/9 5/9]; %Gauss nodes weight values 3 points
```

```
wz=[0.2369268850 0.4786286705 0.5688888889 0.4786286705 0.2369268850];
```

```
%z direction
```

```
r=[0.11270167,0.5,0.8872983]; %points nodes values for 0 to 1 dimintion r direction
```

```
for k=1:14; %#ok<*ALIGN> % heating time ( 0 25 40 60 90 100 125 )
```

```
ct=1;
```

```

Csum=0;
for j=1:5; % weight values at 15 points (z direction)
    for i=1:3; % radius values ( r direction
        Csum=Csum+wr(i)*wz(j)*exp(-beta(2)*psiall(k,ct))*r(i);
        ct=ct+1;
    end
end
end
C(k)=beta(3)*Csum/2;
C70(3*(k-1)+1:3*(k-1)+3)=C(k); % makes triplicate
end
C70=C70';
% xlswrite('ACy70prd.xls', C70);
C70=[C70(1:15);C70(22:24);C70(37:42)];
C70=C70(seqsort);
end

```

REFERENCES

REFERENCES

- Ahmed, J., Shivhare, U.S., Raghavan, G.S.V., (2004). Thermal degradation kinetics of anthocyanin and visual colour of plum puree. *European Food Research and Technology* 218(6), 525-528.
- Beck, J.V., Arnold, K.J., (1977). *Parameter estimation in engineering and science*. John Wiley & Sons, New York.
- Cemeroglu, B., Velioglu, S., Isik, S., (1994). Degradation kinetics of anthocyanins in sour cherry juice and concentrate. *Journal of Food Science* 59(6), 1216-1218.
- Chaovanalikit, A., Wrolstad, R.E., (2004). Total anthocyanins and total phenolics of fresh and processed cherries and their antioxidant properties. *Journal of Food Science* 69(1), C67-C72.
- Chapra, S.C., (2011). *Applied numerical methods W/MATLAB: for Engineers & Scientists* McGraw-Hill Science/Engineering/Math; 2 edition, 426-444.
- Datta, A.K., (1993). Error estimates for approximate kinetic parameters used in food literature. *Journal of Food Engineering* 18(2), 181-199.
- Dolan, K.D., (2003). Estimation of kinetic parameters for nonisothermal food processes. *Journal of Food Science* 68(3), 728-741.
- Dolan, K.D., Valdramidis, V.P., Mishra, D.K., (2013). Parameter estimation for dynamic microbial inactivation: which model, which precision? *Food Control* 29(2), 401-408.
- Dolan, K.D., Yang, L., Trampel, C.P., (2007). Nonlinear regression technique to estimate kinetic parameters and confidence intervals in unsteady-state conduction-heated foods. *Journal of Food Engineering* 80(2), 581-593.
- Dyrby, M., Westergaard, N., Stapelfeldt, H., (2001). Light and heat sensitivity of red cabbage extract in soft drink model systems. *Food Chemistry* 72(4), 431-437.
- Franceschini, G., Macchietto, S., (2008). Novel anticorrelation criteria for model-based experiment design: Theory and formulations. *Aiche Journal* 54(4), 1009-1024.

- Harbourne, N., Jacquier, J.C., Morgan, D.J., Lyng, J.G., (2008). Determination of the degradation kinetics of anthocyanins in a model juice system using isothermal and non-isothermal methods. *Food Chemistry* 111(1), 204-208.
- Himmelblau, D.M., (1970). *Process analysis by statistical methods*. New York: Wiley., (pp. 148-149, 186-201).
- Jewell, K., (2012). Comparison of 1-step and 2-step methods of fitting microbiological models. *International Journal of Food Microbiology* 160(2), 145-161.
- Jimenez, N., Bohuon, P., Dornier, M., Bonazzi, C., Perez, A.M., Vaillant, F., (2012). Effect of water activity on anthocyanin degradation and browning kinetics at high temperatures (100-140 degrees C). *Food Research International* 47(1), 106-115.
- Kechinski, C.P., Guimaraes, P.V.R., Norena, C.P.Z., Tessaro, I.C., Marczak, L.D.F., (2010). Degradation kinetics of anthocyanin in blueberry juice during thermal treatment. *Journal of Food Science* 75(2), C173-C176.
- Kirca, A., Cemeroglu, B., (2003). Degradation kinetics of anthocyanins in blood orange juice and concentrate. *Food Chemistry* 81(4), 583-587.
- Kirca, A., Ozkan, M., Cemeroglu, B., (2007). Effects of temperature, solid content and pH on the stability of black carrot anthocyanins. *Food Chemistry* 101(1), 212-218.
- Lai, K.P.K., Dolan, K.D., Ng, P.K.W., (2009). Inverse method to estimate kinetic degradation parameters of grape anthocyanins in wheat flour under simultaneously changing temperature and moisture. *Journal of Food Science* 74(5), E241-E249.
- Lee, J., Durst, R.W., Wrolstad, R.E., (2005). Determination of total monomeric anthocyanin pigment content of fruit juices, beverages, natural colorants, and wines by the pH differential method: Collaborative study. *Journal of Aoac International* 88(5), 1269-1278.
- Markakis, P., Livingston., G., Fellers., C., (1957). Quantitative aspects of strawberry-pigment degradation. *Food Research* 22, 117-130.
- Marti, N., Perez-Vicente, A., Garcia-Viguera, C., (2002). Influence of storage temperature and ascorbic acid addition on pomegranate juice. *Journal of the Science of Food and Agriculture* 82(2), 217-221.
- Mishra, D.K., Dolan, K.D., Yang, L., (2008). Confidence intervals for modeling anthocyanin retention in grape pomace during nonisothermal heating. *Journal of Food Science* 73(1), E9-E15.

- Mohamed, I.O., (2009). Simultaneous estimation of thermal conductivity and volumetric heat capacity for solid foods using sequential parameter estimation technique. *Food Research International* 42(2), 231-236.
- Nawirska A. , K.M., (2005). Dietary fibre fractions from fruit and vegetable processing waste. *Journal of Food Chemistry* 91, 221–225.
- Ochoa, M.R., Kessler, A.G., Vullioud, M.B., Lozano, J.E., (1999). Physical and chemical characteristics of raspberry pulp: Storage effect on composition and color. *Food Science and Technology-Lebensmittel-Wissenschaft & Technologie* 32(3), 149-153.
- Pritchard, D.J., Bacon, D.W., (1978). Prospects for reducing correlations among parameter estimates in kinetic-models. *Chemical Engineering Science* 33(11), 1539-1543.
- Reyes, L.F., Cisneros-Zevallos, L., (2007). Degradation kinetics and colour of anthocyanins in aqueous extracts of purple- and red-flesh potatoes (*Solanum tuberosum* L.). *Food Chemistry* 100(3), 885-894.
- Rodriguez-Saona, L.E., Wrolstad, R.E., Pereira, C., (1999). Glycoalkaloid content and anthocyanin stability to alkaline treatment of red-fleshed potato extracts. *Journal of Food Science* 64(3), 445-450.
- Schwaab, M., Lemos, L.P., Pinto, J.C., (2008). Optimum reference temperature for reparameterization of the Arrhenius equation. Part 2: Problems involving multiple reparameterizations. *Chemical Engineering Science* 63(11), 2895-2906.
- Sulaiman, R., Dolan, K.D., (2013). Effect of amylose content on estimated kinetic parameters for a starch viscosity model. *Journal of Food Engineering* 114(1), 75-82.
- Sulaiman, R., Dolan, K.D., Mishra, D.K., (2013). Simultaneous and sequential estimation of kinetic parameters in a starch viscosity model. *Journal of Food Engineering* 114(3), 313-322.
- Tomas-Barberan, F.A., Gil, M.I., Cremin, P., Waterhouse, A.L., Hess-Pierce, B., Kader, A.A., (2001). HPLC-DAD-ESIMS analysis of phenolic compounds in nectarines, peaches, and plums. *Journal of Agricultural and Food Chemistry* 49(10), 4748-4760.
- Verbeyst, L., Oey, I., Van der Plancken, I., Hendrickx, M., Van Loey, A., (2010). Kinetic study on the thermal and pressure degradation of anthocyanins in strawberries. *Food Chemistry* 123(2), 269-274.

Wang, H.B., Nair, M.G., Strasburg, G.M., Chang, Y.C., Booren, A.M., Gray, J.I., DeWitt, D.L., (1999). Antioxidant and antiinflammatory activities of anthocyanins and their aglycon, cyanidin, from tart cherries (vol 62, pp 296, 1999). *Journal of Natural Products* 62(5), 802-802.

Wang, W.D., Xu, S.Y., (2007). Degradation kinetics of anthocyanins in blackberry juice and concentrate. *Journal of Food Engineering* 82(3), 271-275.

Yang, Z.D., Han, Y.B., Gu, Z.X., Fan, G.J., Chen, Z.G., (2008). Thermal degradation kinetics of aqueous anthocyanins and visual color of purple corn (*Zea mays* L.) cob. *Innovative Food Science & Emerging Technologies* 9(3), 341-347.

CHAPTER 6

Overall Conclusions and Recommendations

6.1 Summary and Conclusions

The goal of the work was to estimate the kinetic parameters of anthocyanin degradation in cherry pomace under non-isothermal heat treatments at three constant moisture contents. The three moistures were fresh pomace (70%MC) high moisture, and dried pomace (41% and 25%) as low-moisture product, was determined. The following were the specific objectives: (a) To measure the color changes and estimate the color kinetic parameters and correlation between red color and ACY degradation under different times of heating. (b) To estimate the temperature-dependent thermal properties (thermal conductivity and specific heat) of the pomace in a wide dynamic temperature range (25 -130 °C) under nonisothermal heating; (c) To estimate the kinetic parameters of ACY degradation under this process.

The novel contributions of this study were as follows:

1. Presents one of the few inverse methods known to estimate temperature dependent thermal conductivity for solid food products in one experiment at temperature above 100 C in approximately 30 min.
2. The scaled sensitivity coefficients plots helped determine optimal experimental design to estimate which kinetic parameters in the model were most important.
3. The sequential method was used to estimate both thermal properties and kinetic degradation parameters in solid foods during dynamic heating at temperatures greater than 100°C. The sequential results showed that all parameters approached a constant before the end of the experiment, indicating that the model was appropriate for the data.

Overall, the extent of color degradation increased with heating time. A significant decrease in Hunter color L , a , b and Chroma values was observed at each heating time. Loss of color due to heat treatment followed zero-order kinetics. Higher ACY degradation was observed with increasing heating time for all pomace samples at different moisture contents. Significant effect of moisture content on cherry pomace thermal conductivity as function of temperature was observed more at high temperatures. There was no significant effect of moisture content on the rate constant in this study. Relative errors of the kinetic parameters were under 24%.

For cherry pomace at 70% MC the following equation was established:

1. ACY and red color correlation:

$$\frac{ACY_t}{ACY_0} = 1.8929 \left(\frac{a}{a_0} \right) - 0.9522$$

2. Specific heat as function of temperature:

$$C_{p(70MC)} = 2743.3 + 7.9606 \times T - 0.0221 \times T^2$$

3. Temperature dependent thermal conductivity at 70% moisture:

$$k(T) = \left(\frac{(T_2 - T)}{(T_2 - T_1)} \times 0.498 + \frac{(T - T_1)}{(T_2 - T_1)} \times 0.559 \right)$$

4. Kinetic parameters of ACY degradation:

$$\bar{C}(t) = 65.25 \times \exp \left[-0.0129 \times \int_0^t e^{\left[\frac{-75665}{R} \left(\frac{1}{T(r,z,t)} - \frac{1}{115.8} \right) \right]} dt \right]$$

6.2 Recommendations for Future Research

The following topics are recommended for future research:

1. Run the non-isothermal heating at three or more different retort temperatures for more accuracy of estimation of activation energy.
2. Accuracy of parameters estimates may be increased by applying optimal experimental design to determine the best times and temperatures to collect data.
3. Apply the method to estimate thermal properties in a food solid to microbial inactivation experiments, where the heating rates in the solid will be different, depending on the position in the solid.